ISSN : 2349-6495(P) | 2456-1908 (O)

International Journal of Advanced Engineering Research and Science

(IJAERS)

An Open Access Peer Reviewed International Journal

Journal DOI: 10.22161/ijaers

Issue DOI: 10.22161/ijaers.4.9

AI PUBLICATIONS

Vol.- 4| Issue - 9 | Sept, 2017

editor@ijaers.com | http://www.ijaers.com/

FOREWORD

I am pleased to put into the hands of readers Volume-4; Issue-9: 2017 (Sept, 2017) of **"International Journal of Advanced Engineering Research and Science (IJAERS) (ISSN: 2349-6495(P)| 2456-1908(O)" ,** an international journal which publishes peer reviewed quality research papers on a wide variety of topics related to Science, Technology, Management and Humanities. Looking to the keen interest shown by the authors and readers, the editorial board has decided to release print issue also, but this decision the journal issue will be available in various library also in print and online version. This will motivate authors for quick publication of their research papers. Even with these changes our objective remains the same, that is, to encourage young researchers and academicians to think innovatively and share their research findings with others for the betterment of mankind. This journal has DOI (Digital Object Identifier) also, this will improve citation of research papers.

I thank all the authors of the research papers for contributing their scholarly articles. Despite many challenges, the entire editorial board has worked tirelessly and helped me to bring out this issue of the journal well in time. They all deserve my heartfelt thanks.

Finally, I hope the readers will make good use of this valuable research material and continue to contribute their research finding for publication in this journal. Constructive comments and suggestions from our readers are welcome for further improvement of the quality and usefulness of the journal.

With warm regards.

Dr. Swapnesh Taterh
Editor-in-Chief
Date: Oct, 2017

Editorial/ Reviewer Board

Vol-4, Issue-9, September 2017

Sr No.	Detail with DOI
1	***Implementation of Fuzzy Sugeno Method for Power Efficiency*** **Author:** *Riza Alfita, Durrotul Mamluah, Miftachul Ulum, Rosida Vivin Nahari* **DOI:** *10.22161/ijaers.4.9.1* **Page No:** *001-005*
2	***High Performance Smart Temperature Sensor Using Voltage Controlled Ring Oscillator*** **Author:** *Praveen Kumar Sharma, Gajendra Sujediya* **DOI:** *10.22161/ijaers.4.9.2* **Page No:** *006-009*
3	***The "Light Clocks" Thought Experiment and the "Fake" Lorentz Transformations*** **Author:** *Carmine Cataldo* **DOI:** *10.22161/ijaers.4.9.3* **Page No:** *010-013*
4	***Considerations on the Lift Force*** **Author:** *Osvaldo Missiato, Celso Luis Levada, Oswaldo Melo Souza Filho, Alexandre Luis Magalhães Levada* **DOI:** *10.22161/ijaers.4.9.4* **Page No:** *014-017*
5	***Adherence to Gluten Free Diet in Pakistan-Role of Dietitian*** **Author:** *Sumaira Nasim, Zainab Hussain* **DOI:** *10.22161/ijaers.4.9.5* **Page No:** *018-021*
6	***Software Cost Estimation using Single Layer Artificial Neural Network*** **Author:** *Shaina Arora, Nidhi Mishra* **DOI:** *10.22161/ijaers.4.9.6* **Page No:** *022-026*
7	***Sound Intensity Measuring Instrument Based on Arduino Board with Data Logger System*** **Author:** *Intan Nurjannah, Drs. Alex Harijanto, Drs. Bambang Supriadi* **DOI:** *10.22161/ijaers.4.9.7* **Page No:** *027-035*
8	***Study on Impact of Microstructure and Hardness of Aluminium Alloy After Friction Stir Welding*** **Author:** *Gosula Suresh* **DOI:** *10.22161/ijaers.4.9.8* **Page No:** *036-039*
9	***Experimental Research on Performances of Air Turbines for a Fixed Oscillating Water Column-Type Wave Energy Converter*** **Author:** *Tengen Murakami, Yasutaka Imai, Shuichi Nagata, Manabu Takao, Toshiaki Setoguchi* **DOI:** *10.22161/ijaers.4.9.9* **Page No:** *040-047*

10	***On the Schwarzschild Solution: a Review*** ***Author:*** *Carmine Cataldo* ***DOI:*** *10.22161/ijaers.4.9.10* ***Page No:*** *048-052*
11	***Assessment of Factors Responsible for the Choice of Contractors' Prequalification Criteria for Civil Engineering Project: Consultants' Perspective*** ***Author:*** *Akinmusire Adeleye Ola, Alabi Olumuyiwa Michael, Olofinsawe Moses Akinloye* ***DOI:*** *10.22161/ijaers.4.9.11* ***Page No:*** *053-062*
12	***The Tendency of Development and Application of Service Robots for Defense, Rescue and Security*** ***Author:*** *Isak Karabegovic, Milena Dukanovic* ***DOI:*** *10.22161/ijaers.4.9.12* ***Page No:*** *063-068*
13	***Computational Performances and EM Absorption Analysis of a Monopole Antenna for Portable Wireless Devices*** ***Author:*** *Mohammed Shamsul Alam* ***DOI:*** *10.22161/ijaers.4.9.13* ***Page No:*** *069-072*
14	***Nonlinear Dynamic Analysis of Cracked Beam on Elastic Foundation Subjected to Moving Mass*** ***Author:*** *Nguyen Thai Chung, Le Pham Binh* ***DOI:*** *10.22161/ijaers.4.9.14* ***Page No:*** *073-081*
15	***Data Acquisition and Processing of Hartha Formation in the east Baghdad oil field, Central of Iraq*** ***Author:*** *Salman Z. Khorshid, Falih M. Duaij, Hayder H. Majeed* ***DOI:*** *10.22161/ijaers.4.9.15* ***Page No:*** *082-089*
16	***Trend Analysis of Landcover/ Landuse Change in Patani L.G.A, Delta State Nigeria*** ***Author:*** *Ojiako J.C, Igbokwe E.C* ***DOI:*** *10.22161/ijaers.4.9.16* ***Page No:*** *090-093*
17	***Characterization of polygalacturonases produced by the endophytic fungus Penicillium brevicompactum in solid state fermentation - SSF*** ***Author:*** *Sideney Becker Onofre, Ivan Carlos Bertoldo, Dirceu Abatti, Douglas Refosco, Amarildo A. Tessaro, Alessandra B. Tessaro* ***DOI:*** *10.22161/ijaers.4.9.17* ***Page No:*** *094-102*
18	***Seismic stratigraphy study of the East Razzaza in Jurassic- Cretaceous succession- Central Iraq*** ***Author:*** *Layalen H. Ali, Salman Z. khorshid , Ghazi H.AL.Sharaa* ***DOI:*** *10.22161/ijaers.4.9.18* ***Page No:*** *103-108*

https://dx.doi.org/10.22161/ijaers.4.9.1 *ISSN: 2349-6495(P) | 2456-1908(O)*

Implementation of Fuzzy Sugeno Method for Power Efficiency

Riza Alfita[1], Durrotul Mamlu'ah[2], Miftachul Ulum[3], Rosida Vivin Nahari [4]

[1]Department of Engineering, Trunojoyo University, , Indonesia
Email: yogya_001@yahoo.co.id
[2]Department of Engineering, Trunojoyo University, Indonesia
Email: dumalulu22@gmail.com
[3]Department of Engineering, Trunojoyo University, , Indonesia
Email: mif_ulum21@yahoo.com
[4]Department of Engineering, Trunojoyo University, , Indonesia
Email: rosida_vn@yahoo.com

Abstract— *Energy is one of the basic needs for human being. One of the most vital energy sources is electricity. Electricity is a type of energy that sustains survival of human being, more particularly in industrial sector. Efficiency in industrial sector refers to a state where electricity is used to as little as possible to produce the same amount of product. The case study was conducted in marine commodity sector, anchovy and jellyfish supplier. The supplier was classified as SME that installed 33,000 VA electric powers (B2). The data were in the form of energy consumption intensity (ECI) and specific energy consumption (SEC) to determine the energy efficiency level. The objective of the study was to classify the efficiency level of electricity consumption using Sugeno Fuzzy method. The findings of the study were 1) the average ECI between January, 2016 and April, 2017 was 1,949 kWh/m2; it was classified as efficient; 2) the average SEC at the same period was 126,108 kWh/ton; it was classified as excessive. Sugeno Fuzzy logic was implemented to determine efficiency level of electricity in this company. Based on the average ECI and SEC, the electricity consumption of the company was categorized as excessive with FIS Sugeno output of 0.803.*

Keywords— Electrical Power, Efficiency, Fuzzy Sugeno, ECI, SEC

I. INTRODUCTION

Energy is one of the basic needs for human being. One of the most vital energy sources is electricity. Electricity is a type of energy that sustains survival of human being, more particularly in industrial sector. Efficiency in industrial sector refers to a state where electricity is used to as little as possible to produce the same amount of product. The case study was conducted in marine commodity sector, anchovy and jellyfish supplier. The supplier was classified as SME that installed 33,000 VA electric powers (B2). In 2015, the marine commodity supplier consumed 14,534 kWh of electricity and produced 133,460 kilograms of anchovy and jellyfish.

This study described the use of electricity during production, the energy consumption intensity (ECI) and specific energy consumption (SEC) to determine efficiency level of electricity. The findings were efficiency level of electricity consumption in the company (marine commodity supplier) as well as to evaluate whether or not Sugeno FIS algorithm was applicable in this case study. The supplier may use the findings to evaluate how much electricity they use during production, maintenance and for operating their electrical appliances.

II. METHODOLOGY

Electrical Energy

Electrical energy is type of energy generated from the flow of electrical charges. Energy is ability to do an activity or apply certain power to move an object. In terms of electrical energy, force is the attraction of electricity or repulsion between charged particles. Electrical energy can be either potential energy or energy, which is usually stored as potential energy, stored in relative positions of charged particles or electric fields.

Charged particles moves through wires or other media called current or electricity. In addition, there is static electricity, which results from an imbalance or separation of positive and negative charges on an object. Static electricity is a form of electrical potential energy. If enough charge accumulates, electrical energy can be released to form sparks (or even lightning), which have electrical kinetic energy.

Energy Consumption Intensity (ECI)

Energy Consumption Intensity (ECI) is the division between energy consumption and total area of a building (SNI 03-6196, 2000). Energy consumption refers to the amount of energy consumption of both electrical energy and other energy sources in one building within one year.

https://dx.doi.org/10.22161/ijaers.4.9.1 *ISSN: 2349-6495(P) | 2456-1908(O)*

Electricity consumption for one year (KWH / year) is obtained from electricity bill, while other energy consumption is obtained from records of fuel consumption or consumption of other energy sources.

Energy Consumption Intensity (ECI) is term used to describe the amount of energy used per square meter of gross total area of a building within certain period of time (per year or per month).

$$\text{ECI}\left(\frac{kWh}{m^2}\right) = \frac{\text{total energy consumption } (kWh)}{\text{total area of a building } (m^2)}$$

Specific Energy Consumption

Specific energy consumption (SEC) is the amount of energy used for production. These elements are used to measure specific energy consumption (SEC) of an industry.

1. Energy consumption of an industry for certain period of time (kWh/period of time, GJ/period of time)
2. Total production for certain period of time (ton/period)

The following equation can be used to measure the specific energy consumption (SEC) of an industry.

$$\text{SEC} = \frac{\text{total energy consumption } (kWh)}{\text{total production } (ton)} \quad (2)$$

Fuzzy Sugeno

Sugeno Fuzzy method is fuzzy inference method for rules represented in the form IF-THEN, where system output (consequently) is not in the form of fuzzy set, but rather a constant or a linear equation. This method was introduced by Takagi-Sugeno Kang in 1985. [6] Sugeno model uses the Singleton membership function, membership function of which membership degree is 1 on a single crisp value and 0 on another crisp value.

Zero-Order Sugeno Fuzzy Model

In general, the equation for the zero-order Sugeno Fuzzy model is IF (x1 is A1) • (x2 is A2) • (x3 is A3) • ... .. • (XN iS AN) THEN z = k. A1 is the set of Ith fuzzy as antecedent and k is a constant as a consequence. Advantage of the Sugeno-type FIS is zero-order is often sufficient for various modeling purposes. [7].

III. RESULT AND IMPLEMENTATION

Data Management

This study uses Fuzzy Logic, particularly Fuzzy Inference System (FIS) with zero-order Sugeno Method. Fuzzy logic is often used to calculate vague score. In accordance to the Fuzzy Logic theory, the theory requires input score, input variable and linguistic variable. This study involves various processes or stages of the zero-order Sugeno method, from the start until the end. The stages are as follow:

A. Preparation

Prior to ECI and SEC data input to Sugeno FIS method, the researchers should do these steps.

1. Calculating ECI and SEC score

Table 1 described the 2015 ECI and SEC score of the marine commodity supplier.

Table 1. 2015 ECI and SEC of the Company

No	Month	ECI (kWh/m^2)	SEC (kWh/ton)
1	January	3,504	125,824
2	February	4,574	110,997
3	March	5,522	97,637
4	April	1,880	107,033
5	May	1,864	106,955
6	June	1,249	85,853
7	July	2,125	111,385
8	August	2,078	118,159
9	September	1,419	97,652
10	October	4,762	111,935
11	November	3,793	122,810
12	December	1,438	100,892
Total		**34,207**	**108,932**
Minimum		**1,249**	**85,853**
mean		**2,851**	**108,094**
Maximum		**5,522**	**125,824**

2. Classifying the ECI and SEC variables

Having obtained the ECI and SEC scores, the following stage was to classify ECI and SEC variables. Standardized ECI for non air conditioned room from the Department of Education and Culture was used as reference for ECI variable classification since the supplier did not use any air conditioner. Table 2 described the criteria for the ECI variable.

Table 2 ECI Variable Criteria

Kriteria	Range of ECI
Very efficient	0,84 s/d 1,67
efficient	1,67 s/d 2,50
Excessive	2,50 s/d 3,34
Really Excessive	3,34 s/d 4,17

Table 3.SEC Variable Criteria

Kriteria	Range of SEC
very good	≤ 85,853
good	85,853 s/d 108,094
poor	108,094 s/d 125,824
Very poor	≥ 125,824

Data Input Process

The ECI and SEC were used as the input for the Sugeno

https://dx.doi.org/10.22161/ijaers.4.9.1 *ISSN: 2349-6495(P) | 2456-1908(O)*

FIS method. The input was conducted manually into the system. Both data were used as the required parameter to determine how much electricity the company used.

Sugeno Fuzzy Process

In using the FIS sugeno method required some process done, namely the formation of membership functions for input variables, formation of combination rules (fuzzyfikasi), and affirmation (defuzzyfikasi).

There were several steps in the Sugeno FIS method, namely membership function for the input variable, fuzzyfication and defuzzyfication.

1. Membership Function

   Based on the literature related to fuzzy membership function and the criteria of ECI and SEC in Table 2 and 3, the membership function for ECI variable was as follow (Figure 1).

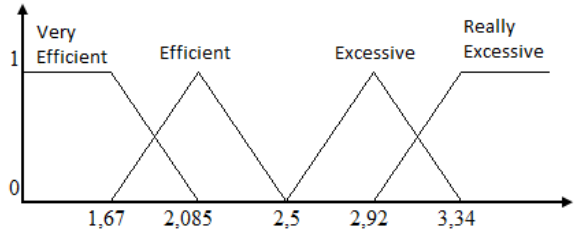

Fig 1. Membership Function of ECI Variable

   Meanwhile, Figure 2 described the membership function for SEC variable.

Fig 2. Membership Function of SEC Variable

2. Combination and Weighting

   Table 4 described the combination used in this study.

Table 4. Combination for Electricity Consumption

No	Input		Output
	ECI	**SEC**	**Electricity Consumption**
1	Very efficient	Very good	Very efficient
2	Very efficient	good	efficient
3	Very efficient	poor	quite efficient
4	Very efficient	Very poor	quite Excessive
5	efficient	Very good	efficient
6	efficient	good	quite efficient
7	efficient	poor	quite Excessive
8	efficient	Very poor	Excessive
9	Excessive	Very good	quite efficient
10	Excessive	good	quite Excessive
11	Excessive	poor	Excessive
12	Excessive	Very poor	Excessive
13	Really Excessive	Very good	quite Excessive
14	Really Excessive	good	Excessive
15	Really Excessive	poor	Excessive
16	Really Excessive	Very poor	Really Excessive

3. Defuzzyfication

   To determine electricity consumption in the company, combination of the two variables as described in Table 4 was the requirement. The following formula was used to determine the output.

$$Z = \frac{\alpha_1(w_1) + \alpha_2(w_2) + \alpha_3(w_3) + \ldots + \alpha_n(w_n)}{\alpha_1 + \alpha_2 + \alpha_3 + \ldots + \alpha_n}$$

Description:

Z = weighted average output and the constant (k),

α = α-predicate = minimum score from the n^{th} fuzzyfication

W = Weights for each determination in the fuzzyfication

Based on the rules in Table 4 and the calculation of Z score after calculating the average weighting, it was confirmed the criteria described in Table 5 should be used to determine the electricity consumption

Table 5 Criteria for Electricity Consumption

Kriteria	Range
Very efficient	$Z \leq 0.25$
efficient	$0.25 < Z \leq 0.375$
quite efficient	$0.375 < Z \leq 0.5$
quite Excessive	$0.5 < Z \leq 0.625$
Really Excessive	$0.625 < Z \leq 0.875$
quite Excessive	$0.875 < Z \leq 1$

Result

This stage is the last stage, which displays the results of the processing of two input data into FIS sugeno method in the form of Z value and grouped according to criteria according to table 5. Manual calculation for sample training data from CV. Mahera 2015 in determining the

https://dx.doi.org/10.22161/ijaers.4.9.1 *ISSN: 2349-6495(P) | 2456-1908(O)*

use of electricity with two variables of ECI and SEC is as in table 6 below:

Table 6. Final Result of Training Data 2015 by Calculating Manual of FIS Sugeno Method

Month	ECI (kWh/ m^2)	SEC (kWh/ ton)	FIS Manual	Electricity Consumption
Jan	3,504	125,824	1	Really Excessive
Feb	4,574	110,997	0,875	Excessive
Mar	5,522	97,637	0,875	Excessive
Apr	1,880	107,033	0,4375	Quite Efficient
May	1,864	106,955	0,4375	Quite Efficient
Jun	1,249	85,853	0,25	Sangat Efficient
Jul	2,125	111,385	0,625	Quite Excessive
Aug	2,078	118,159	0,75	Excessive
Sep	1,419	97,652	0,375	Efficient
Oct	4,762	111,935	0,875	Excessive
Nov	3,793	122,810	0,9375	Really Excessive
Dec	1,438	100,892	0,375	Efficient

The last stage referred to describing the result of processing two inputs into the Sugeno FIS method. The result was Z score which was later classified based on the criteria described in Table 5. Table 6 described manual data analysis for electricity consumption in CV. Mahera in 2015 using two variables, ECI and SEC.

Table 6. The 2015 Training Data Result using Sugeno FIS Manual Calculation

System Implementation

Figure 3 described the real implementation in the matlab.

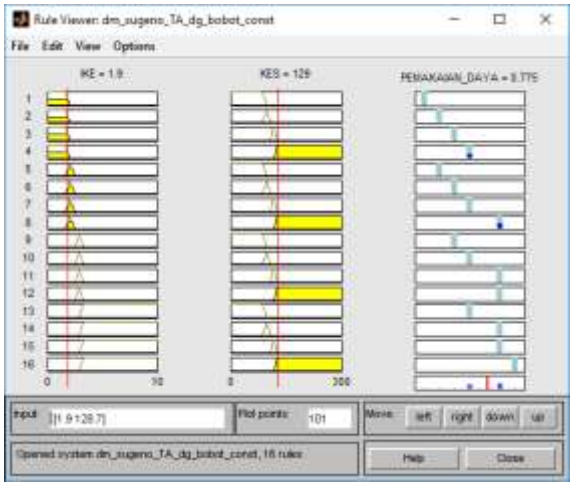

Fig 3. FIS Implementation using Matlab

Figure 3 showed that when user entered the ECI of 1.9 kWh/m2 and SEC of 129 kWh/ton, the electricity consumption (output) was 0.775, which was categorized as excessive. To replace the input, the user put a score on the input column between brackets ([ECI SEC]) and pressed the enter button. The program would automatically display the output. Another method was to shift the red line in the ECI and/or SEC variables in order to automatically change the electricity consumption score.

Analysis of the Test Result

Based on the testing using matlab in Table 7, the Sugeno FIS method was able to provide satisfying results or expected outcome.

IV. CONCLUSION

Based on the data related to the system implementation and testing obtained from the company between January, 2015 to April 2017, the average Energy Consumption Intensity (ECI) for January, 2016 to April 2017 is 1.949 kWh/m2; the score is categorized as efficient. On the other hand, the average of Specific Energy Consumption (SEC) from January, 2016 to April, 2017 is 126.108 kWh/ton; it is categorized as excessive.

Based on the average of ECI and SEC between January, 2016 and April, 2017, the consumption of electricity in CV. Mahera is categorized as excessive with the Sugeno FIS output 0.803. The Fuzzy logic with the zero-order Sugeno method is applicable for determining efficiency level of electricity consumption in a company. The efficiency level is shown based on the result of processing, analysis, and accuracy testing of the data obtained from the company.

REFERENCES

[1] Raharjo, B.A. (2014) "Studi Analisis Konsumsi dan Penghematan Energi di PT. P.G. Krebet Baru I", Tugas Akhir Teknik Elektro, Universitas Brawijaya, Malang.

[2] Harmoko, I. W., & Nazori, A. Z., (2014) "Prototipe Model Prediksi Peluang Kejadian Hujan Menggunakan Metode Fuzzy Logic Tipe Mamdani dan Sugeno", Jurnal TELEMATIKA MKOM, Vol. 5, 1.

[3] Eugene. C, Hanapi, & Gunawan. Drs. Ir., (1993). Mesin dan Rangkaian Listrik, Edisi Keenam, ITB, Bandung.

[4] Wahid, A., (2014) "Analisis Kapasitas dan Kebutuhan Daya Listrik untuk Menghemat Penggunaan Energi Listrik di Fakultas Teknik Universitas Tanjungpura", Jurnal Teknik Elektro Universitas Tanjungpura, Vol. 2, 1.

[5] Laksono, H.D., & Arief, A., (2013) "Penggunaan Logika Fuzzy Clustering untuk Peramalan

https://dx.doi.org/10.22161/ijaers.4.9.1 *ISSN: 2349-6495(P) | 2456-1908(O)*

Kebutuhan Energi Listrik Jangka Panjang di Provinsi Sumatera Barat", Jurnal Teknologi Informasi & Pendidikan. Vol 6.

[6] Santosa, H., (2014) "Aplikasi Penentuan Tarif Listrik Menggunakan Metode Fuzzy Sugeno", Jurnal Sistem Informasi Bisnis. Vol 01.

[7] Naba, Agus. Dr. Eng., (2009) Belajar Cepat Fuzzy Logic Menggunakan MATLAB, Andi Offset, Yogyakarta.

[8] Takagi, T., & Sugeno, M. (1985). Fuzzy identification of systems and its applications to modeling and control. IEEE transactions on systems, man, and cybernetics, (1), 116-132.

[9] Melin, P., Mancilla, A., Lopez, M., & Mendoza, O. (2007). A hybrid modular neural network architecture with fuzzy Sugeno integration for time series forecasting. Applied Soft Computing, 7(4), 1217-1226.

[10] Li, H., Wang, J., Du, H., & Karimi, H. R. (2017). Adaptive Sliding Mode Control for Takagi-Sugeno Fuzzy Systems and Its Applications. IEEE Transactions on Fuzzy Systems.

[11] Pak, J. M., Ahn, C. K., Lee, C. J., Shi, P., Lim, M. T., & Song, M. K. (2016). Fuzzy horizon group shift FIR filtering for nonlinear systems with Takagi–Sugeno model. Neurocomputing, 174, 1013-1020.

[12] Jia, Q., Chen, W., Zhang, Y., & Li, H. (2015). Fault reconstruction and fault-tolerant control via learning observers in Takagi–Sugeno fuzzy descriptor systems with time delays. IEEE Transactions on industrial electronics, 62(6), 3885-3895

[13] Hassan, L. H., Moghavvemi, M., Almurib, H. A., & Muttaqi, K. M. (2016, October). Damping of low-frequency oscillations using Takagi-Sugeno Fuzzy stabilizer in real-time. In Industry Applications Society Annual Meeting, 2016 IEEE (pp. 1-7). IEEE.

[14] Talla, J., Streit, L., Peroutka, Z., & Drabek, P. (2015). Position-based TS fuzzy power management for tram with energy storage system. IEEE Transactions on Industrial Electronics, 62(5), 3061-3071.

[15] Kumar, A., Jones, D. D., Meyer, G. E., & Hanna, M. A. (2015). A Fuzzy Inference System (FIS) and Dimensional Analysis for Predicting Energy Consumption and Mean Residence Time in a Twin-Screw Extruder. Journal of Food Process Engineering, 38(2), 125-134.

https://dx.doi.org/10.22161/ijaers.4.9.2 *ISSN: 2349-6495(P) | 2456-1908(O)*

High Performance Smart Temperature Sensor Using Voltage Controlled Ring Oscillator

Praveen Kumar Sharma[1], Gajendra Sujediya[2]

[1]Research Scholar, Department of ECE, Rajasthan Institute of Engineering and Technology, Jaipur, India
[2]Assistant Professor, Department of ECE, Rajasthan Institute of Engineering and Technology, Jaipur, India

Abstract— *In the broadest definition, a* ***sensor*** *is an electronic component, module, or subsystem whose purpose is to detect events or changes in its environment and send the information to other electronics, frequently a computer processor. Temperature is most-measured process variable in the industrial automation. The most commonly, temperature sensor was used to convert the temperature value to the electrical value. The temperature sensors are the key to read the temperatures correctly and to control the temperature in the industrials applications. Such "smart" temperature sensors combine a sensor and interface electronics on the single chip, and are preferably manufactured in a low-cost standard CMOS process.*

Keywords—CMOS, Sensor, Temperature.

I. INTRODUCTION

Temperature sensors are widely applied in measurement, instrumentation, and control systems. In many applications, it would be attractive to use the temperature sensors which generate a readily interpretable temperature reading in the digital format.

Temperature is unique of the supreme significant important physical quantities and is almost common in our day-to-day life and which is autonomous of the amount of material i.e. temperature is having intensive property. CMOS temperature sensor which is designed using self-bias differential voltage controlled ring oscillator at 180 nm TSMC CMOS technology to achieve low jitter operation. Temperature sensor and its various components Used VCRO has full range voltage controllability along with a wide tuning range from 185 MHz to 810 MHz, and with free running frequency of 93 MHz. Power dissipation of Voltage controlled ring oscillator at 1.8V power supply is 438.91µW.There are different types of smart sensors used in many fields of the industry like, biomedical application, control systems, security systems etc. These Microsystems combine sensing, accuracy and signal processing in a microscopic scale. Examples of smart sensors include

- Temperature sensors
- Pressure sensors
- Accelerometer sensors
- Optical sensors
- Humidity sensors
- Gas sensors

II. TEMPRATURE SENSOR

Temperature is one of the most important fundamental physical quantities that are a measure of hotness and coldness on a numerical scale. Temperature sensors are widely used in measurement, instrumentation, and control systems. In many applications, it would be attractive to use the temperature sensors which produce readily interpretable temperature reading in the digital format [2]. Such "smart" temperature sensors combine a sensor and interface electronics on the single chip, and are preferably manufactured in a low-cost standard CMOS process. Block diagram and Circuit diagram for temperature sensor is shown below in fig 2.1.

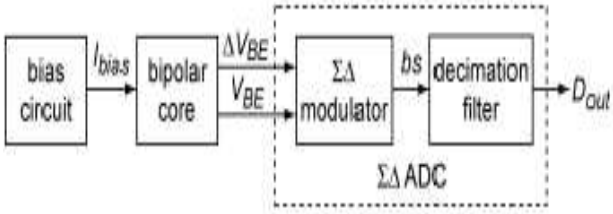

FIG 2.1 (A) BASIC BLOCK DIAGRAM OF TEMPERATURE SENSOR

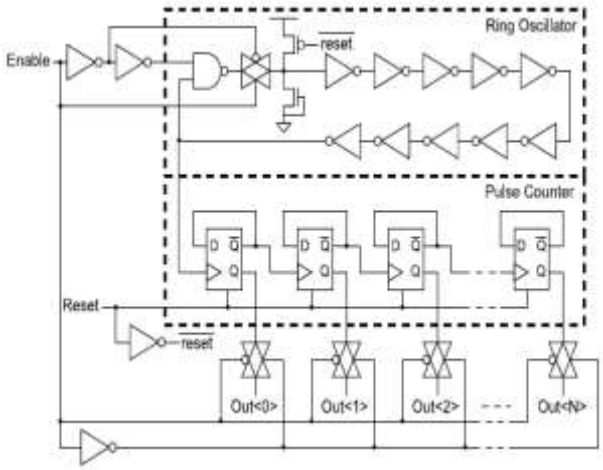

FIG 2.1 (B) SCHEMATIC OF TEMPERATURE SENSOR COMPONENT

https://dx.doi.org/10.22161/ijaers.4.9.2 *ISSN: 2349-6495(P) | 2456-1908(O)*

It consist ring oscillator [1], transmission gate and pulse counter circuit. Pulse counter circuit is designed using d flip flop. The oscillation period (1/*f*) is converted in to a number of oscillations by applying enable signal of fixed pulse width (PW), and the number of oscillations is stored in the counter to produce the digital output [3]

III. VOLTAGE CONTROLLED RING OSCILLATOR

The voltage controlled ring oscillator is used to generate a signal of specific frequency. This VCO is designed using self-bias differential ring oscillator as shown in figure 3.1. A ring oscillator device is composed of odd number of NOT gates and whose output is oscillates between the two voltage levels, representing logic '1' and logic '0'.

In this figure 3.1, the MOSFETs M7 and M13 operate as inverter while MOSFETs M2 and M18 operate as current sources. The current sources are used to limit the current available to the inverter or it can be said that the inverter is starved for the current. So this type of oscillator is called current starved voltage controlled oscillator. Here the drain currents of MOSFETs M1 and M12 are the same and are set by the input control voltage. The other transistors are added just to form the 5-stages of ring oscillator because the 5-stage ring oscillator gives better VCO characteristic and frequency range.

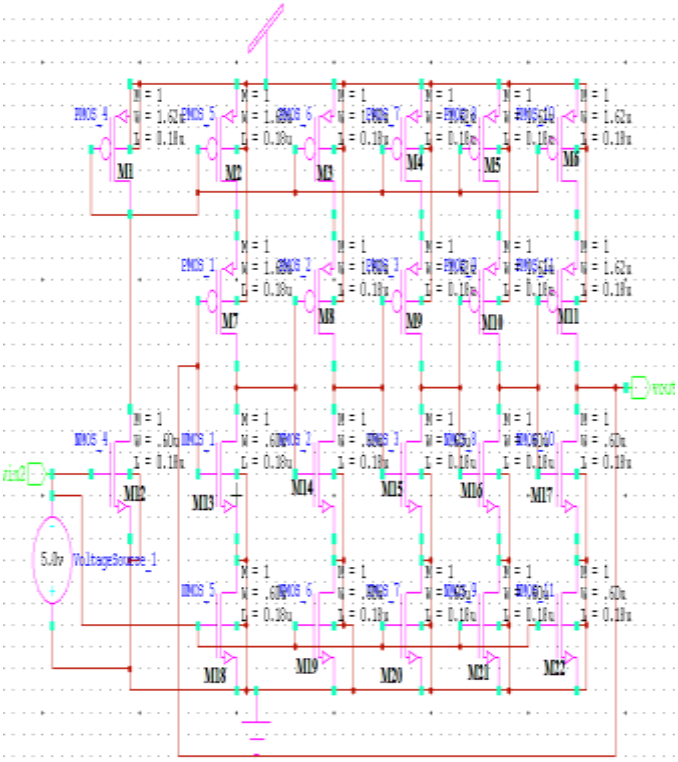

Fig 3.1: Voltage Controlled Ring Oscillator

This VCO characteristic also depends on the width and length parameters. So the width and length of each MOSFET is chosen very carefully according to the used technology. Specification table for ring oscillator is shown in table 3.1. Length and width of MOS transistor is set according to technology.

Table 3.1: Specification for Ring Oscillator

S.No.	Parameter	Values	
1.	Technology	180nm	
2.	Threshold Voltage	0.37V	
3.	Minimum Operating Voltage	1.8 V	
4.	NMOS	Length=0.18u	Width=0.60u
5.	PMOS	Length=0.18u	Width=1.62u

IV. TEMPERATURE SENSOR COMPONENT AND SENSOR

The temperature sensor component is shown in fig 4.1. It consists of a ring oscillator and a pulse counter circuit. The oscillation period (1/*f*) of voltage controlled ring counter is converted to a number of oscillations by applying enable signal of fixed pulse width, and the number of oscillations is stored in the counter to produce the digital output. Additional circuitry between the enable input and the ring oscillator is used to remove synchronization problem, and the sensor outputs are connected to transmission gates to avoid unnecessary toggling [4]. The reason of synchronization problem is the oscillator frequency which is temperature-dependent [6].

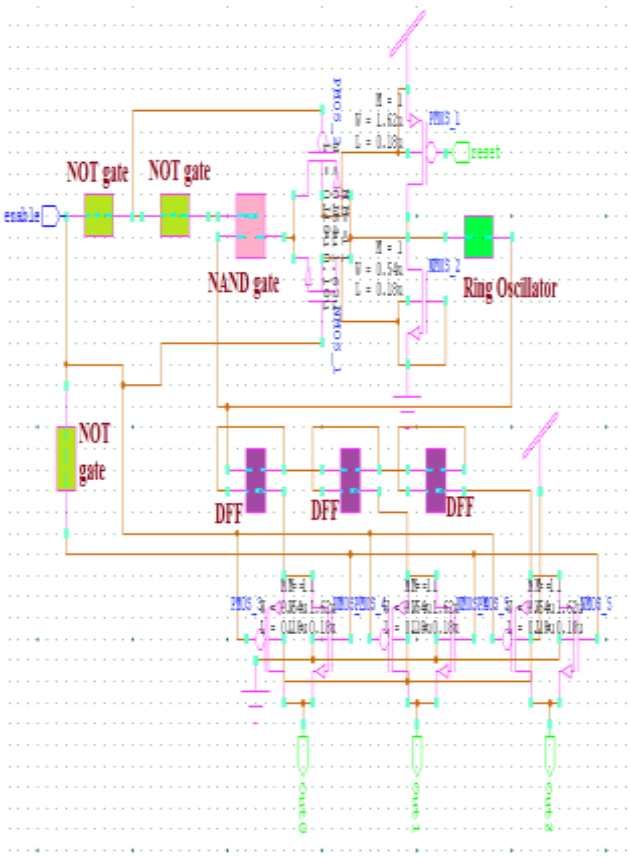

Fig 4.1: Temperature Sensor component

https://dx.doi.org/10.22161/ijaers.4.9.2 *ISSN: 2349-6495(P) | 2456-1908(O)*

The complete diagram of temperature sensor contains two temperature sensor components, level shifter, two buffers, two comparator circuit, three XOR gate and one AND gate. Temperature sensor component is used to take readings simultaneously at given temperature readings V_{KT} and operating voltage (V_{OP}) of system. These readings ($T_{KT,t}$ and $V_{OP,t}$) is taken at time t. Low-voltage up level shifters convert the lower voltage, taken from output of temperature sensor component 1 to higher voltage. Comparator compares each temperature reading with previous temperature reading to produce output [5]. Previous temperature readings are stored in buffer circuit. The two comparator outputs are then passed into an XOR gate circuit, which determines if the temperature(V_{KT}) sense by temperature sensor component 1, depends at operating voltage V_{OP} (same as V_{OP}) of temperature sensor component 2 or not. If both V_{KT} and V_{OP} are same then XOR gate gives logic zero output and if different then gives logic '1' output. Circuit diagram of temperature sensor is shown in fig 4.2.

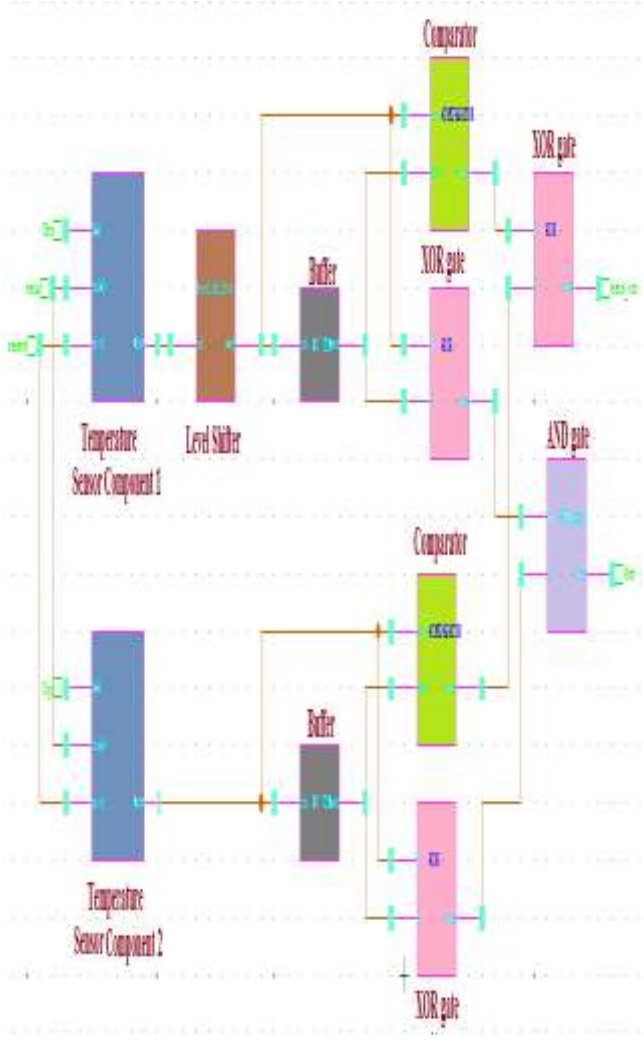

Fig 4.2: Temperature Sensor

V. RESULT AND ANALYSIS

Delay and power dissipation of temperature sensor component is given in table 5.1.

Table 5.1: Delay & Power Dissipation at different V_{DD} of sensor Component

Vdd(V)	Delay (nS)	Power Dissipation (mW)
1.8	1.528	2.1465
1.6	3.442	1.437
1.4	5.379	0.810
1.2	6.962	0.548
1.0	8.047	0.263

Table 5.2: Delay and Power Dissipation of Temperature sensor at different Temperature

Temperature (ºC)	Delay (nS)	Power Dissipation (mW)
27	7.656	80.88
37	6.923	83.235
47	5.357	89.56
57	3.514	102.35

Table 5.3: Delay and Power dissipation of Temperature sensor at different V_{TH}

V_{DD} (V)	Delay (nS)	Power Dissipation (mW)
0.37	7.656	80.88
0.47	9.534	76.475
0.57	10.916	65.32
0.67	12.546	60.44

VI. CONCLUSION

A voltage controlled ring oscillator-based CMOS temperature sensor has been designed at 180 nm CMOS TSMC technology. The proposed temperature sensor occupies smaller silicon area with higher resolution than the conventional temperature sensor based on band gap reference. Various parameters like delay and power dissipation of other circuits are also calculated with respect to different power supply & threshold voltages. Result shows that speed and power dissipation of circuit are directly proportional to power supply voltage. Power dissipation and delay of VCRO based temperature sensor at 5V power supply is 80.88mW and 7.656 nS respectively.

REFERENCES

[1] Shruti Suman, Prof. B.P. Singh, "Ring Oscillator Based Cmos Temperature Sensor Design", International Journal of Scientific & Technology, ISSN 2277-8616, Volume 1, Issue 4, May 2012.

https://dx.doi.org/10.22161/ijaers.4.9.2 *ISSN: 2349-6495(P) | 2456-1908(O)*

[2] David Wolpert, And Paul Ampadu, "Exploiting Programmable Temperature Compensation Devices To Manage Temperature-Induced Delay Uncertainty", IEEE Transactions On Circuits And Systems—I Regular Papers, Vol. 59, No. 4, April 2012.

[3] Sunghyun Park, Changwook Min and Seong Hwan Cho, "A 95nW Ring Oscillator-based Temperature Sensor for RFID Tags in 0.13¹m CMOS", IEEE International Symposium on Circuits and Systems, 2009.

[4] Poorvi Jain and Pramod Kumar Jain, "Design and Implementation of CMOS Temperature Sensor", International Journal of Current Engineering and Technology, Vol.4, No.2 (April 2014).

[5] Eran Socher, Salomon Michel Beer, and Yael Nemirovsky, "Temperature Sensitivity of SOI-CMOS Transistors for Use in Uncooled Thermal Sensing" , IEEE Transactions on Electron Devices, Vol. 52, No. 12, December 2005.

[6] Xuan Zhang and Alyssa B. Apsel, "A Low-Power, Process-and-Temperature-Compensated Ring Oscillator with Addition-Based Current Source", IEEE Transactions on Circuits and Systems, 2010.

https://dx.doi.org/10.22161/ijaers.4.9.3 *ISSN: 2349-6495(P) | 2456-1908(O)*

The "Light Clocks" Thought Experiment and the "Fake" Lorentz Transformations

Carmine Cataldo

Independent Researcher, PhD in Mechanical Engineering, Battipaglia (SA), Italy
Email: catcataldo@hotmail.it

Abstract**—***In this paper an alternative version of the well-known "light clocks" experiment is discussed. The so-called Lorentz transformations, backbone of the Special Relativity theory, are herein deduced by resorting to the above-mentioned experiment, albeit with a different meaning. Time dilation and length contraction are not considered as being real phenomena. Time, in fact, is peremptorily postulated as being absolute. Nonetheless, this strong assumption does not imply that instruments and devices of whatever kind, finalized to measure time, are not influenced by motion. In particular, although the "light clock" in the mobile frame ticks, so to say, more slowly than the one at rest, it can be easily shown how no time dilation actually occurs. The apparent length contraction is considered as being nothing but a banal consequence of a deceptive time measurement.*

Keywords—Lorentz Transformations, Special Relativity, Light Clocks, Absoluteness of Time.

I. INTRODUCTION

Firstly, it is fundamental to underline how time is considered as being absolute. Such an assumption, that could undoubtedly sound very anachronistic, does not imply that instruments and devices of whatever kind, finalized to measure time, are not influenced by motion and gravity [1] [2] [3]. Space is herein considered as being flat. The speed of light is considered as being constant and independent of the motion of the source.

Let's consider two "light clocks", initially at rest. At the beginning, the origins of the corresponding frames of reference, denoted by *O* and *O'*, are coincident. The homologous axes are parallel. We have two light sources, placed in *O* and *O'*, and two corresponding receivers, placed in *R* and *R'*, along the axes *y* and *y'* respectively. The distances between the sources and the corresponding receivers, identifiable with the heights of the clocks, are constant and equal to each other. Consequently, *R* and *R'* coincide when the frames are still at rest. When *t=0*, the clock whose frame is centered in O' starts moving rightwards, along *x* and *x'*, with a constant speed, denoted by *v*, whose value cannot equate that of light. The motion consists in a simple translation. Simultaneously, both the sources are switched on: light is propagated along any direction, with a constant speed denoted by *c*.

Let's now suppose that when *t=T* a light signal is simultaneously received in *R* and *R'*. We contemplate two paradoxical scenarios.

The first scenario is qualitatively depicted in *Figure 1*.

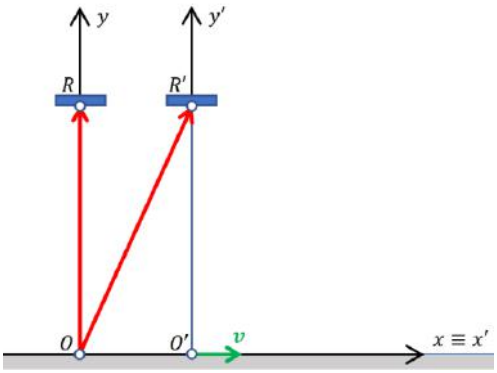

Figure 1. Variable Speed of Light

When t=T, denoting with *l* the height of the clocks, we can write the following:

$$\overline{OR} = \overline{O'R'} = l = cT \tag{1}$$

$$\overline{OO'} = vT \tag{2}$$

For the signal to be simultaneously received in *R* and *R'*, light should travel, along the linear path bordered by *O* and *R'*, with a greater speed whose value, denoted by *c'*, should be provided by the following relation:

$$c' = \frac{\overline{O'R'}}{T} = \frac{\sqrt{\overline{OR'}^2 + \overline{OO'}^2}}{T} = \sqrt{c^2 + v^2} \tag{3}$$

Obviously, such a scenario would clearly contradict the hypothesis according to which the speed of light is constant. In this case, in fact, the speed of the light signal would depend on the motion of the source. Consequently, at least as far as the above-mentioned explanation is concerned, the signal cannot be simultaneously received.

The second scenario is qualitatively depicted in *Figure 2*.

https://dx.doi.org/10.22161/ijaers.4.9.3 *ISSN: 2349-6495(P) | 2456-1908(O)*

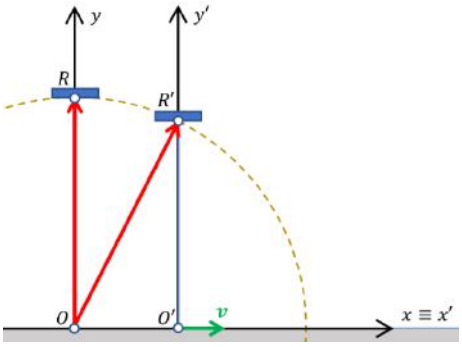

Figure 2. Variable "Light Clock" Height

This time, for the signal to be simultaneously received in *R* and *R'*, the mobile device should undergo a contraction along the direction orthogonal to the one along which the motion takes place.

If we denote with γ the so-called Lorentz factor [4] [5], the reduced height of the mobile "light clock" would be provided by the following relation:

$$\overline{O'R'} = \sqrt{\overline{OR'^2} - \overline{OO'^2}} = \overline{OR'}\sqrt{1-\left(\frac{v}{c}\right)^2} = \frac{\overline{OR'}}{\gamma} \qquad (4)$$

Very evidently, the scenario just imagined would clearly contradict the hypothesis according to which the heights of the clocks must remain constant. According to Special Relativity [6], in fact, the so-called "Lorentzian" contraction should exclusively occur along the direction of the motion. Consequently, once again, we cannot accept the possibility that the signal may be simultaneously received in *R* and *R'*. At this point, we are forced to admit that the signal must be received in *R* first, and then in *R'*.

Let's now investigate the real scenario.

On this purpose, we can suppose that when $t=T'$ the signal is received in *R'*. The signal that followed the path bordered by *O* and *R* was previously received in *R* when $t=T$, with $T<T'$.

The real scenario in qualitatively depicted in *Figure 3*.

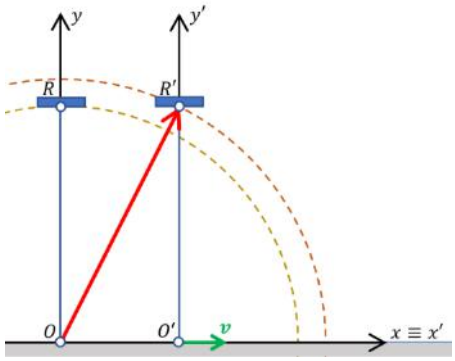

Figure 3. Real Scenario

Exploiting *Figure 3*, we can easily write the following:

$$\overline{OO'} = vT' \qquad (5)$$

$$\overline{OR'} = cT' \qquad (6)$$

$$cT = l = \sqrt{\overline{OR'^2} - \overline{OO'^2}} = cT'\sqrt{1-\left(\frac{v}{c}\right)^2} \qquad (7)$$

$$\frac{T'}{T} = \frac{1}{\sqrt{1-\left(\frac{v}{c}\right)^2}} = \gamma \qquad (8)$$

In theory, the phenomenon just analysed can recur indefinitely: suffice it to think that, for example, the receivers can consist in, and the sources can be replaced by, a couple of mirrors. Obviously, the measuring of the time elapsed clearly depends on the number of oscillations.

Consequently, although time keeps on being absolute, we can state that its measurement depends on the state of motion. In other terms, if we denote with t_f the measurement, that coincides with the absolute one, of the time elapsed in the frame at rest, and with t_m the measurement of the time elapsed in the mobile frame, we can write:

$$t_f = \gamma t_m \qquad (9)$$

II. THE "FAKE" TRANSFORMATIONS

Let's suppose that, at $t=0$, the mobile frame starts moving rightward with a constant speed equal to *v*.

Simultaneously, a light signal is sent from a generic point denoted by *P*.

The scenario is qualitatively depicted in *Figure 4*.

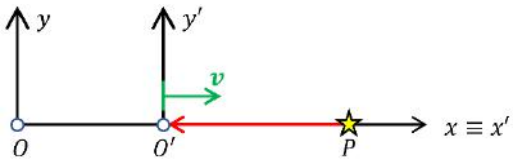

Figure 4. Direct Transformations

If we denote with $t_{m,a}$ the time actually elapsed when the signal is received in *O'*, and with t_m the corresponding time measurement provided by the mobile light clock, we have:

$$\overline{OO'} = vt_{m,a} \qquad (10)$$

$$t_m = \frac{t_{m,a}}{\gamma} \qquad (11)$$

$$\overline{OO'} = \gamma v t_m \qquad (12)$$

https://dx.doi.org/10.22161/ijaers.4.9.3 *ISSN: 2349-6495(P) | 2456-1908(O)*

If we denote with $x_{m,a}$ the absolute distance between *O'* and *P*, as soon as the signal is received in *O'*, and x_m the corresponding measurement deduced by exploiting the mobile clock, we have:

$$x_{m,a} = \overline{O'P} = ct_{m,a} \tag{13}$$

$$x_m = ct_m = \frac{ct_{m,a}}{\gamma} \tag{14}$$

$$\overline{O'P} = ct_{m,a} = \gamma x_m \tag{15}$$

If we denote with x_f the distance, absolute by definition, between *P* and *O*, we can write:

$$x_f = \overline{OP} = \overline{O'P} + \overline{OO'} = \gamma(x_m + vt_m) = \frac{x_m + vt_m}{\sqrt{1-\left(\frac{v}{c}\right)^2}} \tag{16}$$

If we denote with t_f the time actually elapsed between the signal emission and the moment it is received in *O*, we can evidently write:

$$t_f = \frac{x_f}{c} \tag{17}$$

Moreover, very banally, from *(14)* we obtain:

$$t_m = \frac{x_m}{c} \tag{18}$$

From *(16)*, *(17)*, and *(18)*, we have:

$$t_f = \frac{\frac{x_m}{c} + v\frac{t_m}{c}}{\sqrt{1-\left(\frac{v}{c}\right)^2}} = \frac{t_m + \frac{vx_m}{c^2}}{\sqrt{1-\left(\frac{v}{c}\right)^2}} \tag{19}$$

From *(16)* and *(19)*, if we replace x_f with *x*, x_m with *x'*, t_f with *t*, and t_m with *t'*, we obtain the underlying well-known relations, that represent the so-called direct Lorentz Transformations [4] [5]:

$$x = \frac{x' + vt'}{\sqrt{1-\left(\frac{v}{c}\right)^2}} \tag{20}$$

$$t = \frac{t' + \frac{vx'}{c^2}}{\sqrt{1-\left(\frac{v}{c}\right)^2}} \tag{21}$$

Let's now suppose that at *t=0* the mobile frame starts moving leftward with a constant speed equal to *v*. Simultaneously, once again, a light signal is sent from a point P.

This time, very evidently, the signal reaches *O* first.

The scenario is qualitatively depicted in *Figure 5*.

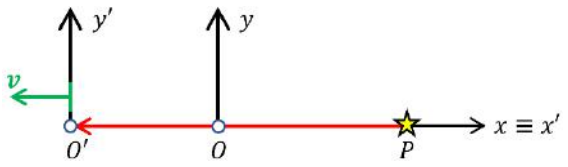

Figure 5. Inverse Transformations

At this point, maintaining the notation and exploiting the same line of reasoning we have followed in order to deduce the direct transformations, we can write:

$$x_f = \overline{OP} = \overline{O'P} - \overline{OO'} = \gamma(x_m - vt_m) = \frac{x_m - vt_m}{\sqrt{1-\left(\frac{v}{c}\right)^2}} \tag{22}$$

$$t_f = \frac{\frac{x_m}{c} - v\frac{t_m}{c}}{\sqrt{1-\left(\frac{v}{c}\right)^2}} = \frac{t_m - \frac{vx_m}{c^2}}{\sqrt{1-\left(\frac{v}{c}\right)^2}} \tag{23}$$

In order to deduce the inverse transformations in their usual form, we have to replace, this time, x_m with *x*, t_m with *t*, x_f with *x'* and t_m with *t'*.

From *(22)* and *(23)* we obtain:

$$x' = \frac{x - vt}{\sqrt{1-\left(\frac{v}{c}\right)^2}} \tag{24}$$

$$t' = \frac{t - \frac{vx}{c^2}}{\sqrt{1-\left(\frac{v}{c}\right)^2}} \tag{25}$$

The replacements we have carried out in order to deduce the inverse transformations can be easily legitimised by means of a simple observation: as far as the scenario depicted in *Figure 5* is concerned, the frame at rest receives the signal in advance with respect to the mobile one.

Consequently, it is as if the frame at rest were in motion towards the emission point.

It is worth underlining that, at this point, we can easily deduce a shorter and more elegant version of the transformations by exploiting the hyperbolic functions.

Let's carry out the following position:

$$\frac{v}{c} = \tanh\varphi \tag{26}$$

From the previous identity we can banally deduce the so-called boost parameter:

$$\varphi = \tanh^{-1}\left(\frac{v}{c}\right) \tag{27}$$

https://dx.doi.org/10.22161/ijaers.4.9.3 *ISSN: 2349-6495(P) | 2456-1908(O)*

From *(26)* we immediately obtain:

$$\gamma = \frac{1}{\sqrt{1-\left(\frac{v}{c}\right)^2}} = \frac{1}{\sqrt{1-\tanh^2\varphi}} = \cosh\varphi \qquad (28)$$

At this point, for example, the inverse transformations can be rewritten as follows:

$$x' = x\cosh\varphi - ct\frac{v}{c}\cosh\varphi = x\cosh\varphi - ct\sinh\varphi \qquad (29)$$

$$ct' = ct\cosh\varphi - x\frac{v}{c}\cosh\varphi = -x\sinh\varphi + ct\cosh\varphi \qquad (30)$$

Finally, from the previous two relations we can immediately obtain the well-known underlying form:

$$\begin{pmatrix} x' \\ ct' \end{pmatrix} = \begin{pmatrix} \cosh\varphi & -\sinh\varphi \\ -\sinh\varphi & \cosh\varphi \end{pmatrix}\begin{pmatrix} x \\ ct \end{pmatrix} \qquad (31)$$

III. BRIEF CONCLUSIONS

The Lorentz Transformations are herein deduced by exploiting the well-known "light clocks" thought experiment. As provocatively suggested by the title, we highlight some contradictions that arise from hypothesizing that the above-mentioned devices, coherently with the well-known hypotheses under which the experiment is commonly carried out, could receive the light signals simultaneously. It is worth underlining how, in the light of some noteworthy criticisms concerning Special Relativity [7] [8], we have elsewhere carried out a further alternative deduction of the Lorentz Transformations [9], by hypothesizing a closed Universe, belonging to the so called oscillatory class [10] [11], globally flat, characterized by four spatial dimensions [12].

REFERENCES

[1] Cataldo, C. (2017). On the Absoluteness of Time. Applied Physics Research, 9(3), 46-49. https://doi.org/10.5539/apr.v9n3p46

[2] Cataldo, C. (2017). A short discussion on the Gravitational Redshift in the light of an alleged local variability of the Planck Constant. Journal of Applied Mathematics and Physics, 5, 1001-1008. https://doi.org/10.4236/jamp.2017.55087

[3] Cataldo, C. (2017). Gravity and the Absoluteness of Time: a simple qualitative model. App. Phys. Res., 9(2), 42-52. http://dx.doi.org/10.5539/apr.v9n3p46

[4] Lorentz, H. A. (1904). Electromagnetic Phenomena in a System Moving with Any Velocity Smaller than That of Light. Proceed. of the Roy. Netherlands Acad. of Arts and Sciences, 6, 809-831. Retrieved from http://www.dwc.knaw.nl/DL/publications/PU00014148.pdf

[5] Lorentz, H. A. (1909). The Theory of Electrons and Its Applications to the Phenomena of Light and Radiant Heat. Teubner. Retrieved from https://archive.org/details/electronstheory00lorerich

[6] Einstein, A. (1916). Relativity: The Special and General Theory (translated by R. W. Lawson, 1920). Henry Holt and Company, New York. Retrieved from https://archive.org/details/cu31924011804774

[7] Di Mauro, P., & Notarrigo, S. (1995). Critica delle usuali derivazioni delle trasformazioni di Lorentz. Com. al LXXXI Cong. Naz. SIF, Perugia. Retrieved from http://www.lascuolaitalica.it/pubbl12.htm

[8] Ghosal, S. K., Nandi, K. K., & Chakraborty, P. (1991). Passage from Einsteinian to Galilean Relativity and Clock Synchrony. Zeitschrift für Naturforschung, 46a, 256-258. Retrieved from http://www.degruyter.com/downloadpdf/j/zna.1991.46.issue-3/zna-1991-0307/zna-1991-0307.xml

[9] Cataldo, C. (2016). Faster than Light: again on the Lorentz Transformations. Applied Physics Research, 8(6), 17-24. http://dx.doi.org/10.5539/apr.v8n6p17

[10] Harrison, E. R. (1967). Classification of Uniform Cosmological Models. Monthly Notices of the Royal Astronomical Society, 137, 69-79. https://doi.org/10.1093/mnras/137.1.69

[11] Cataldo, C. (2017). From the Oscillating Universe to Relativistic Energy: a Review. Journal of High Energy Physics, Gravitation and Cosmology, 3, 68-77. http://dx.doi.org/10.4236/jhepgc.2017.31010

[12] Cataldo, C. (2017). From General Relativity to A Simple-Harmonically Oscillating Universe, and Vice-Versa: a Review. Applied Physics. Research, 9(1), 86-92. http://dx.doi.org/10.5539/apr.v9n1p86

https://dx.doi.org/10.22161/ijaers.4.9.4 *ISSN: 2349-6495(P) | 2456-1908(O)*

Considerations on the Lift Force

Osvaldo Missiato[1], Celso Luis Levada[2], Oswaldo Melo Souza Filho[3], Alexandre Luis Magalhâes Levada[4]

[1]Faculdades Integradas Einstein de Limeira, SP
[2]Fundação Hermínio Ometo Uniararas, SP
[3]Academia da Força Aérea, Pirassununga, SP
[4]UFSCAR – São Carlos- Brazil

Abstract— *Many authors at criticizing the conventional explanation of aerodynamic lift based on Bernoulli's law commit the same mistake laying within the scope of mechanics and ignoring the effects of viscosity in the generation of forces. Because it is an irreversible process, we affirm that it is not possible to generate lift without increasing entropy. And for an increase of entropy it must be considered the viscosity and vorticity.*

Keywords— viscosity, vorticity, lifting, entropy.

I. INTRODUCTION

The Lift force (L) is an extraordinary force, especially when trying to understand how it is possible for an aircraft, such as an Airbus, to take off and fly so smoothly. The lift force is the component of the aerodynamic force acting in the direction perpendicular to the air flow. The other component of aerodynamic force is the drag that acts against the body's motion. Both depend on pressure distributions and shear stresses (FOX and McDONALD(4), 2001; ANDERSON(2), 2001).

The Lift force L can be represented by:

$$L = CL\, \rho\, v^2\, S / 2,$$

where CL is the lift coefficient, determined for each wing profile and which varies according to the angle of attack, ρ is the specific mass of air; S is the projected area over the plane perpendicular to the wind direction and v is the wind speed relative to the aerodynamic profile (relative wind).

II. CIRCULATION, VORTICITY AND TURBULENCE

ALLEN(1) (1982) comments that when an ideal flow is produced around a cylinder such that all flow lines are concentric circles, the observed motion is defined as circulation. According to other authors, circulation is a mathematical concept applied to the flow of fluids: the scalar product line integral of velocity v with the line element $d\boldsymbol{l}$ (WELTNER(6) et al). If this integration is carried out along a closed path and is not null, its value is the circulation, Γ, this is é:

$$\Gamma = \oint \boldsymbol{v}.d\boldsymbol{l}\ .$$

Considering this constant magnitude throughout the flow region of an ideal flow, the velocity is inversely proportional to the radius, that is

$$v = \Gamma/2\pi r$$

If the flow of circulation around the cylinder is superimposed by a linear flow on the cylinder, a holding force is produced perpendicular to the direction of flow. Vortex is a portion of the fluid in rotational motion and vorticity, ω, is the measure of the rotational motion of a small element of fluid whose numerical value is equal to twice the value of the mean angular velocity, this is

$$\omega = 2<\Omega>$$

In vector terms, vorticity is defined as the rotational velocity vector, such that

$$\boldsymbol{\omega} = \nabla x \boldsymbol{v}.$$

Vorticity also appears in turbulence which is a flow of a fluid characterized by chaotic and stochastic property changes. The turbulence translates into the irregular fluctuation of velocity that overlaps with that of the flow (ALLEN(1), 1982) and will not be discussed in this work.

There are authors who present circulation as the cause of the velocity distribution around the wing, but others consider it only a mathematical description of velocity distribution, but not an explanation of the phenomenon.

KUTTA E JOUKOWSKI (cited by WELTNER(5) et al, 2001) showed separately that the circulation Γ and the support L are related.

The formula of the support they found, called the Kutta-Joukowski theorem, is thus written:

$$L = \rho v \Gamma\ ,$$

where v is the relative wind speed or the undisturbed flow, ρ is the specific mass of the air and L is the lift per unit length (L / l).

Note that without circulation there is no support and that to have circulation there must be viscosity! The idea is more or less equivalent to walking: to go forward you have to push the floor back.

According WU(14) the viscous origin of circulation theory has been recognized for a long time, mainly because of the research of Von Karman, Millikan, Howardh, Sears etc, who have recognized some aspects of the viscous phenomena that produce circulation.

https://dx.doi.org/10.22161/ijaers.4.9.4 *ISSN: 2349-6495(P) | 2456-1908(O)*

III. THE CAUSE OF LIFT FORCE

ANDERSON[2] (2001) in Fundamentals Aerodynamics writes on p. 294: "We emphasize that the resulting aerodynamic force in a body immersed in a flow is due to the net effect of the integration of pressure distributions and shear stresses on the surface of the body. Furthermore, we note that such support on an airfoil surface is primarily due to the distribution of surface pressure and that shearing has virtually no effect on the support. It is easy to see why. Consider, for example, a standard airfoil. Remember that the pressure acts normal to the surface, and for these support surfaces the direction of this normal pressure is essentially vertically, that is, in the direction of the lift. In contrast, the shear acts tangentially to the surface, and for these support surfaces the direction of this tangential shear stress is mainly in the horizontal direction, ie the direction of drag. Thus, pressure is the dominant element for lift generation and shear stress has an insignificant effect on lift ".

However, if we lived in a perfectly invested world the surface of an airfoil would not produce lift. Certainly, the presence of viscosity is the fundamental reason why we have the support. Viscosity produces the circulation and this generates the support according to the Kutta-Joukowski theorem. This seems strange, even contradictory, taking into account what the author said about the insignificance of shear in the generation of support. What happens then?

The answer is that in real life, this is the way that nature has found to make the flow smoother on the trailing edge, that is, it is the mechanism nature uses to not give infinite speed at the trailing edge. Nature imposes Kutta's condition through viscosity (ANDERSON [2]).

Thus, we are brought to the most ironic situation that may seem, ie, the calculation of the pressure distribution on the surface generates support, although the sustenance cannot exist in a world invested by the conditions of Kutta. Following the conditions of Kutta, we can say that without viscosity we cannot have sustentation, for having no circulation. Another important observation to be made is that without power, no lift can be generated.

IV. LUDWIG PRANDTL'S LIMIT LAYER THEORY

The physical effects, which involved the uncovered support force, from the beginning of the last century were of fundamental importance in the development of flight theory, especially from the boundary layer theory formulated by Ludwig Prandtl in a seminal lecture Delivered at the Heidelberg mathematical congress in 1904 and titled, "On the Motion of a Fluid with Too Little Attrition." Prandtl notes that for a given flow, the classical fluid theory could be applied in a very narrow region, called the boundary layer, adjacent to the wall where the viscous effects should be considered (outside the boundary layer the potential flow applies). Prandtl made some simplifications of the Navier-Stokes equations, and analyzed the part of the flow at which the viscosity is significant. By better understanding the technical details of the boundary layer one can then deal with such difficult problems as the separation of flows and the physical mechanisms behind the Kutta condition.

We must not forget that the boundary layer is the region of the flow where the fluid interacts mechanically and thermally with the solid. Therefore, the recognition of the existence of the boundary layer constituted in the first pass for the understanding of the mechanism of friction in the wall and heat exchange, hence the entropy variations (FREIRE[6]).

It is also observed that for high Reynolds numbers the shear layer must be very thin, that is, when the flows happen to large Reynolds numbers, the viscous effects are only of great importance in the region of the boundary layer.

The literature on boundary layer and support is vast and numerous authors discuss the theme, for example, PRANDTL[10], SCHLICHTING and GERSTEN[13], MUNSON[8]et al). We can deduce that a body immersed in the flowing stream of a fluid experiences forces and moments resulting from this interaction (MUNSON [8] et al).

The characteristic of the flow around a body depends on several parameters such as body shape, velocity, orientation and properties of the fluid flowing on the body. The most important parameters to describe the air flow over a body are: the Reynolds number and the Mach number.

In the region of the boundary layer, a shear stress τ acts. For a Newtonian fluid, τ is directly proportional to the velocity gradient, du/dy, and the coefficient of proportionality μ represents the dynamic viscosity of the fluid, which depends on the temperature.

The viscosity of the air causes the particles near the aerodynamic profile to adhere so that the velocity of these particles tends to zero. Moving away from the adhesion region, the particles are braked due to the friction between them, but with much less intensity.

The further away from the surface of the airfoil, the greater the velocity of the air particles, so that at a certain distance the stream maintains the same relative wind speed.

According to OLIVEIRA[9], the vortices are characterized by high-velocity circular flow with a high kinetic energy load, so they can transfer some of this energy to the "boundary layer", avoiding their early stagnation and separation.

https://dx.doi.org/10.22161/ijaers.4.9.4 *ISSN: 2349-6495(P) | 2456-1908(O)*

This transfer of energy to the "boundary layer" allows an increase in the angle of attack and, consequently, of the lift, without the airplane entering into "loss", but at the expense of an increased drag force.

When boundary layer separation occurs, the flow is very turbulent and there is even reversal of flow direction, causing a drastic decrease in lift force, increased drag, and loss of control and stability.

TOWNSEND (cited by LAMESA e SOARES [7]) Suggested that the vorticity of the mean flow and the energy content of turbulent motions are due to coherent anisotropic swirls, also called attached eddies.

These are involved by a fluid containing swirls of scales much smaller, statistically isotropic.

Numerous field and laboratory experiments conducted over the last three decades suggest that organized and coherent eddies are responsible for most heat transfer and momentum in boundary layer (C_L) flows.

It is also found that, superimposed on these coherent movements, there are less organized whirlwinds on a small scale.

V. FINAL CONSIDERATIONS

For ROSA[9], the viscosity is responsible for the generation of vorticity in the region of the boundary layer and this is due to the non-slip of the fluid in the contours of the body.

Vorticity is concentrated in the boundary layer being subject to both viscosity diffusion and convection, by the action of the inertia forces of the flow according to the vorticity transport equation:

$$(D\boldsymbol{\omega}/Dt) = (\boldsymbol{\omega}.\nabla)\,V + \upsilon\,\nabla^2\,\boldsymbol{\omega},$$

where $\boldsymbol{\omega}$ is the vorticity, υ is the kinematic viscosity, V is the velocity of the fluid, the term $(\boldsymbol{\omega}.\nabla)V$ represents the convection and the term $\upsilon\nabla^2\boldsymbol{\omega}$ represents the diffusion.

The thickness of the boundary layer can be used as a measure of diffusion of the vorticity in the flow. Large boundary layer thicknesses indicate that vorticity has had time to diffuse, while small thicknesses indicate that convection of vorticity is more important, not allowing time for diffusion.

The entropy variation can be due to conduction heat flux, viscous dissipation, other heat sources and other irreversibilities. For the support problem, we are interested in verifying the variation of the entropy due to the viscous dissipation.

A mechanical friction process to convert the mechanical energy of motion into thermal energy tends to a heating, that is, tends to increase the temperature.

We can say that energy dissipated by friction because it is an irreversible process leads to an increase in entropy. On the other hand, the increase in entropy is also related to circulation, yy means of the equation:

$$(d\Gamma/dt) = -\oint(dp/\rho),$$

and the relationship

$$T\,dS = cp\,dT - (dp/\rho g).$$

offering as a result, (DOMMASCH [3]):

$$(d\Gamma/dt) = g\oint TdS,$$

where Γ é is the circulation, T is the temperature, S is the entropy, cp is the specific heat at constant pressure, p is the pressure, g is the acceleration of gravity and ϱ is the specific mass.

Hence, if there is no variation in the entropy, there is no variation in the circulation. Therefore, the rotational motion is a result of a change in entropy unless the flow is isothermal.

The particular case of this variation is null, that is, $(d\Gamma/dt)=0$ constitutes Kelvin's theorem, treated in the book Dynamics of Fluids of HUGLES[12].

According to the condition of Kutta and with the Kutta-Joukowski theorem to have sustentation it is necessary that there be viscosity and circulation.

Therefore, to sustain in an airfoil it is necessary that an increase in entropy occurs, which can be seen by the previous result of DOMMASCH[3].

Thus, if there is no variation in entropy, there is no change in circulation. In an invincible, purely mechanical world, there would be no point in speaking of irreversibility (a thermodynamic result), for there would be no friction, no heat, and therefore no drag and no Lift.

Finally one could inquire that being an irreversible process the temperature should increase on the surface of the body.

It should not be forgotten, however, that the body is in relative motion and that in this case it tends to cool because of movement.

REFERENCES

[1] ALLEN, J.E. *Aerodynamics, the science of air in motion*, 2aedição, New York: Granada Publishing, 1982.

[2] ANDERSON J.R., John D. *Fundamentals of Aerodynamics*. McGraw-Hill, Third Edition, 2001.

[3] DOMMASCH, Daniel O. *Principles of Aerodynamics*. London: Sir Isaac Pitman & Sons, LTD., 1953.

[4] FOX, R,.W e McDONALD, A.T. Introduction to Fluid Mechanics, 5nd ed. Rio de Janeiro: Ed. LTC, 2001.

[5] WELTNER, K.; SUNDBERG, M.I.; ESPERIDIÃO, A.S. and MIRANDA, P. Supplemental Fluid Dynamics and wing Lift, Brazilian Journal of Physics Teaching, vol. 23, n. 4, São Paulo, 2001.

[6] FREIRE, A.P. S., Turbulence and its historical development, available in

https://dx.doi.org/10.22161/ijaers.4.9.4 *ISSN: 2349-6495(P) | 2456-1908(O)*

www.fem.unicamp.br/~im450/palestras&artigos/Cap2-APSilvaFreire.pdf, access in 20/05/2015

[7] LAMESA, J.E. E SOARES, J. Spectral study of the surface boundary layer, Brazilian Congress of Meteorology of 2006, available in www.cbmet.com/cbm-files/12-pdf, access 12/07/2014

[8] MUNSON, B. R.; YOUNG D. F., OKIISHI, T. H. Fundamentals of Fluid Mechanics. 4th Edition, São Paulo: Publisher Edgard Blucher 2004.

[9] OLIVEIRA, P.M., Aerodynamic Lift, the physical mechanism, text available on the site www.scribd.com/doc/.../Sustentacao-Aerodinamica, access 30/05/2015.

[10] PRANDTL, L. *Essentials of Fluid Dynamics: with applications to Hydraulics, Aeronautics, Metereology and other subjects*. London and Glasgow: Blackie and Son Limited, 1953.

[11] ROSA, E.S. Differential form of conservation and transport equations, available in www.femunicamp.br/textos.../aula-1.doc, access in 10/08/2015

[12] HUGHES, W.F., "Fluid Dynamics", Publisher McGraw-Hill of Brazil Ltda, Schaum collection, 1974.

[13] SCHLICHTING, H. e GERSTEN, K. *Boundary-Layer Theory*. New York: McGraw-Hill, 1979.

[14] WU, J.C., *AIAA Journal*, vol.19, nº 4, April 1981.

https://dx.doi.org/10.22161/ijaers.4.9.5 *ISSN: 2349-6495(P) | 2456-1908(O)*

Adherence to Gluten Free Diet in Pakistan-Role of Dietitian

Sumaira Nasim[1]*, Zainab Hussain[2]

[1]M.Sc Human Nutrition (Pakistan) and MPH (Australia), RD
[2]Diet Consultant at SFC, Tabba Heart Institute (THI), Pakistan

WHAT IS CELIAC DISEASE?

Celiac disease (CD) is a common multi-system autoimmune disease, affecting approximately 1% of people worldwide [1]. Predisposed individuals develop an immune response to gluten, a protein found in the cereal grains: wheat, barley and rye. Autoimmune intestinal damage is the cardinal feature of celiac disease, and typically involves villous atrophy, crypt hyperplasia, and increased intraepithelial lymphocytes [2]. Symptoms may be subclinical, varying from gastrointestinal upset to severe malabsorption [3,4]. Skin, nervous system, and multisystem involvement is also recognized. Strict avoidance of gluten-containing foods can reverse both enteric and extra-intestinal manifestations of the disease.

PREVELANCE OF CELIAC DISEASE IN THE WORLD:

In many developed countries like UK and Australia, dietitians are specialized in food allergies; thus being able to educate and conduct research in this field and can facilitate in shopping skills, cooking skills and in modifying recipes. Celiac disease has been reported from North and South America, Europe, Australia, Africa, Middle East, Iran and India. Although the exact prevalence of celiac disease in Pakistan is not known, it is felt to be a common disorder present in all four provinces.

INTERNATIONAL CELIAC DAY:

16th May is International Celiac disease day. Nutritionists and Dietitians can arrange seminars, talk shows such events that are aimed at raising awareness of celiac disease and its symptoms amongst medical professionals and the general public.

WHAT TO DO WHEN SUFFERING FROM CELIAC DISEASE?

One of the safest solution identified till date is lifelong exclusion of food items containing gluten but this exclusion is a challenge for people suffering from celiac disease and their family members. Although straightforward in principle, strict avoidance of gluten is challenging in practice.These problems are further aggravated due to lack of awareness among public and even health professionals. Moreover, many people with celiac disease might also suffer from other autoimmune diseases, for example if the person is suffering from Type 1 diabetes along with the celiac disease, it might lead to further reduction in food choices. Additionally, in certain life stages it can be more difficult to follow gluten free diet such as teenage and pregnancy. Here the role of dietitians and nutritionists step in providing updated knowledge and skills regarding what to eat in this phase. Moreover, dietitian involvement was recommended in the National Institutes of Health (NIH) Consensus Development Conference on celiac disease (2004).[5]

While a gluten-free diet continues to be the best solution for full-blown celiac disease, an autoimmune condition brought on by exposure to gluten, some enzyme supplements may reduce negative reactions for those with mild gluten intolerance. There are no supplements that cure celiac disease or reverse gluten intolerance. But a specific type of enzyme can help enhance the breakdown and digestion of gluten.

DPP IV-Since gluten is made up of a combination of proteins, a combination of enzymes may help to break it down. DPP IV, short for dipeptidyl peptidase IV, is an enzyme blend designed to break down bonds that hold gluten proteins together, and thus to enhance their digestion. Products containing DPP IV are ideal for targeting hidden sources of gluten, whether from restaurant meals or accidental cases of cross-contamination. And if you don't have celiac disease, DPP IV can help reduce symptoms from that occasional splurge on gluten-containing foods; although, again, the enzymes are intended as more of an insurance against accidental gluten ingestion.[7]

WHAT CELIAC PATIENTS SHOULD CONSUME OR AVOID?

Individuals with celiac disease should not consume any of the following gluten containing grains; Wheat (including atta, maida, sooji), Barley, Rye , Triticale (a cross between wheat and rye).However, the following foods are safe for

https://dx.doi.org/10.22161/ijaers.4.9.5 *ISSN: 2349-6495(P) | 2456-1908(O)*

patients with celiac disease if free from gluten contamination; Rice, corn (makai), Millett (bajra), Lentils and Pulses (daal), Oats (only if pure and uncontaminated), Nuts and seeds, All fruits and vegetables, Milk and dairy products, All types of meats, Eggs, Salt, pepper, turmeric and other spices, Water, tea, fruit juices and most other beverages.[6]

In Pakistan, the staple diet is chapatti or roti mainly made of wheat which is rich source of gluten. In some parts of Pakistan, there is custom of consuming oat (Joe) roti. Though oat does not contain gluten, however, milling process takes place in same area, thus chances of cross contamination and therefore isrestricted for coeliac patients.For example, the preparation of corn flour on the same machine that makes wheat flour (atta) may lead to cross contamination with gluten. Therefore, corn flour made on such a machine will not be safe and even a small amount of gluten can lead to problems.

IMPORTANCE OF DIETITIANS IN PROMOTING TECHNOLOGY TO PROVIDE KNOWLEDGE ON CELIAC DISEASE TO PATIENTS:

We are living in an era of modern technology and use of it in healthcare is on rise. So in addition to development of print material, dietitians can create awareness for patients on the use of websites of containing information on celiac disease such as Dietitian Association of Australia and British Dietetic Association. Similarly, nowadays apps on Android phones are available for gluten free diet. However, the limitation of such websites and Apps is that it provides information regarding western foods, thus limited implication in Pakistan.

Also the use of technology can save patients time and money. Dietitians and Nutritionists can develop awareness how to use this technology. Moreover, there is extreme shortage of dietitians in Pakistan, especially in rural areas and this shortage can be overcome by the use of technology as internet is available even in remote areas of Pakistan. The dietitians can also suggest patients and family members to join facebook page and share their stories and experiences to help other patients suffering from the same disease. They can also share recipes and these activities can reduce sense of isolation among patients.

In this manner, nutritionist and dietitians in Pakistan can help transform scientific knowledge into practical information.

- **SHOPPING SKILLS:**

It is important to prefer fresh fruits and vegetables.Frozen and canned fruits, Dried fruits (dates) and vegetables can be preferred if they are not dusted with oat flour. Fresh meat, fish, and poultry, Meat marinades and flavorings, Tofu can also be taken if they donot contain any seasoning made with wheat derivatives. Milk, buttermilk, cream Milk, buttermilk, cream Most yogurt (plain, fruited or flavored) Cheese, plain Cream cheese, cottage cheese are all open for patients with celiac disease but be careful with Malted milk Cheese sauces, cheese spreads, flavored cheeses. Flavored teas and coffees, herbal teas, and non-dairy beverages may contain barley malt flavoring or barley malt extract and should be carefully seen. Cocoa drinks may contain malt or malt flavoring (e.g., Ovaltine is NOT gluten free). Honey, jams, jellies, marmalade, molasses, corn syrup, maple syrup, sugar are all safe.

Though in Pakistan, processed food consumption is quite less as compared to western countries, thus majority of Pakistani population do not have good label reading skills. In western countries, most of the food items are packed and government regulatory agencies are quite strict in meeting standard of food labels. However, in Pakistan it is general observation that people are not consuming much packed food, secondly, there is no strict rules and monitoring by any regulatory organization. Thus, chances of consuming hidden sources of gluten can be high.

- **COOKING SKILLS:**

In Pakistan, we have helpers at home doing house chores. Therefore, in addition to family members, it is important to train them and explain in local terms regarding potential sources of gluten and signs of coeliac disease. Prior menu planning is important in order to avoid last moment hassles. This includes advance grocery shopping, involvement of all family members in menu planning and cooking steps.

- **COOKING GADGETS:**

It is better to have separate rolling pin and board and toaster, if not possible, gluten free chapatti and bread should be cooked/toasted first. After using for regular bread, clean well toaster. Similarly, gluten free meals should be prepared first.

- **MENU PLANNING:**

The best approach can be to involve family members in menu planning. This can reduce the sense of isolation among such people, for example, one day all family members may consume gluten free diet.

- **DINE OUT:**

Dine out can be the most challenging as nowadays due to aggressive marketing strategies, there is great trend of dine out in Pakistan. On other hand, hardly any restaurant is offering gluten free diet.

https://dx.doi.org/10.22161/ijaers.4.9.5 *ISSN: 2349-6495(P) | 2456-1908(O)*

ORGANISATIONS FOR CELIAC DISEASE AWARENESS:

In developed countries such as UK and Australia, there are non-profit associations facilitating people suffering from celiac diseaseas well as health professionals collaborating with food industry and supporting researches conducted on celiac patients. Similarly, "PAKISTAN CELIAC SOCIETY" is working for such patients and their family members in Pakistan.

GLUTEN FREE DIET AT EDUCATIONAL INSTITUTE:

Parents should inform the teachers and administered staff regarding food allergy of their child. In Pakistani culture, many parents feel ashamed to disclose illness especially for female child. Thus, it is important to minimize stigma associated with celiac disease. The child should also be counselled to avoid sharing his/her lunch. The parents should be encouraged to give homemade lunch to their children. Nutritionist can provide recipes and useful websites for healthy lunch options to the mothers. Another tip for improving diet consultation can be "Emphasize what to eat rather than what not to eat".

Though few food industries and bakeries provide gluten-freeproducts in Pakistan, however, such products are expensive and available on few leading grocery stores and there is lack of awareness among the people that such products are available. The dietitians can develop collaborations with food industry and involve in gluten free products. Similarly, they can develop awareness via social media such as Facebook, blogs or writing articles for general public in Newspaper. Similarly, there is trend of morning shows, where nutritionist can openly allow mothers to ask queries regarding celiac disease.

MANAGING CELIAC DISEASE WITH OTHER CO-MORBIDS:

As celiac disease is an auto immune disease, there are chances ofdeveloping other autoimmune diseases as well. For instance, such patients especially children with coeliac disease might suffer from Type 1 diabetes or multiple sclerosis. It is common observation that family members are trying to cure Type 1 in similar way as Type 2 diabetes among elderly patients in family members. The dietitians can develop awareness that apart from dietary management of two auto immune diseases, the child needs balance diet for proper growth and development. Thus regular consultation and monitoring of growth is an essential part of disease management. Unfortunately, there is lack of awareness and such child suffer from severe nutritional deficiencies.

Similarly, secondary lactose intolerance is also common among such patients. In such cases, local greens (Sagg), oranges, dried figs (Injeer) and nuts can be alternate source of calcium.

In rare cases, gluten free diet does not mean zero gluten. According to FDA, 20PPM is allowed, in layman language it is 20g/kg of flour. Additionally many non-food items and medicines contain gluten. Common examples are glue, Play-Doh, multivitamins, over the counter medicine and lipsticks and toothpaste. Thus it is important for people suffering from coeliac disease to develop habit of label reading on medicines as well. Again dietitians can play an important role in developing awareness for such things. It is important to differentiate between terms Gluten free, reduced gluten and low gluten products. According to Coeliac UK, that there is no term as "No-Gluten containing ingredients".

CHALLENGES TO FACE WHILE PREPARING GLUTEN FREE PRODUCTS:

A great challenge Pakistanis face while preparing gluten free products is to prepare food on events such as weddings, Eid and other social gatherings. Vermicelli (Siwayyan), Nihari, drumsticks, can be hidden source of gluten. Sometimes, ketchup, mayonnaise, salad dressings, white pepper and even toothpaste can contain hidden gluten. Gluten may also be present in gravies thickened with flour or in those flavored with soy sauce or malt vinegar. Soy sauce is a common ingredient in many marinades and sauces served in restaurants and sold in grocery stores. Sausages, meatloaf, meatballs, and other ground meats often contain wheat-based fillers. Breadcrumbs may be added to hamburger patties to bind the meat and improve texture. Many vegetarian meat alternatives, such as veggie burgers and vegetarian sausages, are made with seitan, also known as wheat gluten. Others are made with gluten-containing flours or breadcrumbs that act as binders. And while tofu in its unadulterated form is gluten free, the fried tofu served in restaurants may be fried in a gluten-containing batter or marinated in a soy sauce that contains wheat. Whole potatoes found in the produce department in supermarkets are gluten free, but potato chips and fries can be hidden sources of gluten. Potato chips may be seasoned with malt vinegar or contain wheat starch. Even if patient choose any item which is apparently gluten free, however there is high chance of cross contamination.

CODE WORDS FOR HIDDEN GLUTEN

Clients and patients who must eliminate gluten from their

https://dx.doi.org/10.22161/ijaers.4.9.5 *ISSN: 2349-6495(P) | 2456-1908(O)*

diets not only must become aware of the many foods in which gluten can hide, but they also must learn the names of ingredients that masquerade as gluten on ingredient lists. Code words such as "fried," "coated," "crispy," or "crusted" should raise a red flag, alerting clients that the food may contain gluten, Begun says, noting that these descriptors in particular may indicate the food is coated in a breading or gluten-containing flour before its fried.

CONCLUSION:

There is strong need of Multidisciplinary approach, which includes, doctors, dietitians, media and food industry to check for minor details when giving gluten free diet. In Pakistan, there are registered dietitians working in different hospital settings. There is need to train health professionals especially doctors and nutritionist regarding updated knowledge and skills to follow gluten free diet. Group education sessions can be conducted for parents and care givers, especially those who have family history of celiac disease, school teachers and food industry.

REFERENCES

[1] Green P.H.R., Cellier C. Celiac disease. N. Engl. J. Med. 2007;357:1731–1743. doi: 10.1056/NEJMra071600.

[2] Oberhuber G., Granditsch G., Vogelsang H. The histopathology of coeliac disease: Time for a standardized report scheme for pathologists. Eur. J. Gastroenterol. Hepatol. 1999;11:1185–1194. doi: 10.1097/00042737-199910000-00019.

[3] Corazza G.R., Frisoni M., Treggiari E.A., Valentini R.A., Filipponi C., Volta U., Gasbarrini G. Subclinical celiac sprue. Increasing occurrence and clues to its diagnosis. J. Clin. Gastroenterol. 1993;16:16–21. doi: 10.1097/00004836-199301000-00006.

[4] Ciacci C., Cirillo M., Sollazzo R., Savino G., Sabbatini F., Mazzacca G. Gender and clinical presentation in adult celiac disease. Scand. J. Gastroenterol. 1995;30:1077–1081. doi: 10.3109/00365529509101610

[5] NIH Consensus Development Conference on Celiac Disease. U.S. Department of Health and Human Services; Bethesda, MD, USA: 2004. http://www.celiac.com.pk/images/brochure-en.pdf

[6] Tweed, V. (2015, July 01). Gluten-Free Enzymes. Retrieved July 14, 2017, from https://www.betternutrition.com/checkout/gluten-free-enzymes

https://dx.doi.org/10.22161/ijaers.4.9.6 *ISSN: 2349-6495(P) | 2456-1908(O)*

Software Cost Estimation using Single Layer Artificial Neural Network

Shaina Arora[1], Nidhi Mishra[2]

[1]Assistant Professor (CSE) AIET, Jaipur, India
{shaina.arora22@gmail.com}
[2]Associate Professor(CSE),Poornima University,Jaipur,India
{nidhi.mishra@poorinma.edu.in}

Abstract— *The most challenging task of software project management is the cost estimation. Cost estimation is to accurately assess required assets and schedules for software improvement ventures and it includes a number of things under its wide umbrella, for example, estimation of the size of the software product to be produced, estimation of the effort required, and last but not the least estimating the cost of the project. The overall project life cycle is impacted by the accurate prediction of the software development cost. The COCOMO model makes employments of single layer feed forward neural system while being actualized and prepared to utilize the perceptron learning algorithm. To test and prepare the system the COCOMO dataset is actualized. This paper has the goal of creating the quantitative measure in not only the current model but also in our proposed model.*

Keywords— Software Cost Estimation, COCOMO, Artificial Neural Network, Feed Forward Neural Network, Magnitude Relative Error.

I. INTRODUCTION

Estimation of required assets and calendar should be possible through precise cost estimation. Talking about the parameters, the exactness of the product advancement and the precision of the administration choices both are interrelated. The exactness of the previous is dependent on the precision of the last mentioned in terms of relying that is the former will rely on the latter. There are number of parameters for example improvement time, effort estimation and group, and for the calculation of each one of the models is required. For estimation of software cost effort estimation technique used most popular COCOMO model. What is unique about COCOMO model is that it makes use of mathematical formula to analyze project cost effort estimation. The paper based on COCOMO model is making use of single layer neural network technique using perception algorithm.

II. COCOMO

The Constructive Cost Model or better known as the COCOMO model, first presented by Dr. Barry Boehm in 1981 surpassed all the software development practices that took place in those days. Software development techniques have been undergoing many changes and evolving since those days. The COCOMO model can be sub-divided in following models based on the type of application [12].

A. Basic COCOMO

Project Qualities details are not needed to implements parameterized equation of basic COCOMO model.

Person Month=a (KLOC) b (1)

Development Time =2.5*PM c (2)

Three modes of progress of projects are there, on which all the three parameters depend, namely a, b and c.

B. Intermediate COCOMO

According to basic COCOMO model there is no provision to do software development. To add the accuracy in basic COCOMO model there is 15 cost drivers provided by Boehm. Cost driver can be classified into

Table.1: Cost Drivers

Cost Drivers			
Product Attributes	Computer Attributes	Personnel Attributes	Project Attributes
RELY DATA CPLX	TIME STOR VIRT TURN	ACAP AEXP PCAP VEXP LEXP	MODP TOOLS SCED

1. Product attributes
   - Required software reliability or better known as RELY
   - Database size or better known as DATA
   - Product complexity or better known as CPLX
2. Computer attributes
   - Execution time constraint or better known as TIME
   - Main storage constraint or better known as STOR
   - Virtual machine volatility or better known as VIRT
   - Computer turnaround time or better known as TURN

https://dx.doi.org/10.22161/ijaers.4.9.6 *ISSN: 2349-6495(P) | 2456-1908(O)*

3. Personnel attributes
   - Analyst capability or better known as ACAP
   - Application experience or better known as AEXP
   - Programmer capability or better known as PCAP
   - Virtual machine experience or better known as VEXP
   - Programming language experience or better known as LEXP
4. Project attributes
   - Modern programming practices or better known as MODP
   - Use of software tools or better known as TOOLS
   - Required development schedule or better known as SCED [12].

III. ARTIFICIAL NEURAL NETWORK

An Artificial Neural Network (ANN) is nonlinear information (signal) processing devices, which are built from interconnected elementary processing devices called neurons. An Artificial Neural Network (ANN) is an information-processing model that is stimulated by the way biological nervous systems, such as the brain, process information. The key element of this paradigm is the novel structure of the information processing system. It is composed of a large number of highly interconnected processing elements (neurons) working in unification to resolve specific tribulations [15].

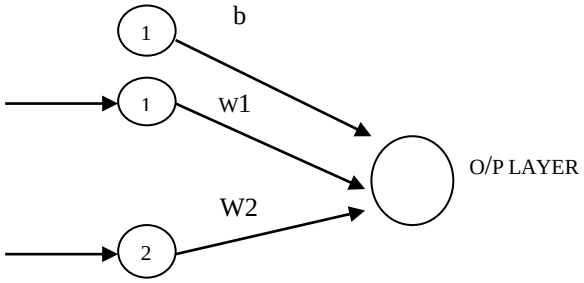

Fig.1: A Simple Artificial Neural Net

Figure 1 shows a simple artificial neural network with two inputs neurons (1, 2) and one output neuron (O). The interconnected weights are given by w1 and w2. There always exists a common bias of '1'. The input neurons are connected to the output neurons through weighted interconnections. This is a single layer network because it has only one layer of interconnections between the input and the output neurons. This network perceives the input signal received and performs the classification [15].

IV. RELATED WORK

Researchers in effort estimation models have developed multiple software's. Artificial neural network is capable for generating good information and modeling complex non-linear relationships. For the calculation of software effort estimation researchers all across the world have used the artificial neural network approach. Moreover, Boehm's COCOMO dataset is also used. N.Tadayon[9] reports the use of neural network with a back propagation. Anupma Kaushik[12] also research on multilayer neural network using perceptron learning algorithm. COCOMO [8] is the most effective and widely used software for effort estimation model, which arranges beneficial expert knowledge. For getting appropriate calculations COCOMO model is one of the most imperative tools, that produces capacity for developing effort estimation models with better analytical accuracy. In this paper, single layer feed forward neural network using perceptron learning algorithm and COCOMO data set have been used. Using this approach, an effort estimation model for software cost evaluation has been proposed.

V. PROPOSED NEURAL NETWORK MODEL

In proposed system Single Layer ANN used to calculate the software cost estimation. For this 16 input parameters are taken which includes 15 Effort Multiplier (EM) and one bias weight (b). First we calculate the net input output (sum of the product of each input neuron to their corresponding weight) after this applies identity activation function get estimated output.

A. Estimated Effort

The System is implemented with the help of single layer artificial neural network and trained using the perceptron leaning algorithm. The COCOMO dataset is used to train to test the network.

$$Sum = sum + EM_i * W_i$$

$$O_{est} = b + Sum;$$

$$MRE = ((oact - oest) / oact) * 100;$$

Here

O_{est} is the estimated effort,

Wi effort multiplier weight,

MRE is magnitude relative error,

O_{act} actual effort

It describes about experimenting networks and calculating new set of weight.

B. Flow Chart of System Implementation

https://dx.doi.org/10.22161/ijaers.4.9.6 *ISSN: 2349-6495(P) | 2456-1908(O)*

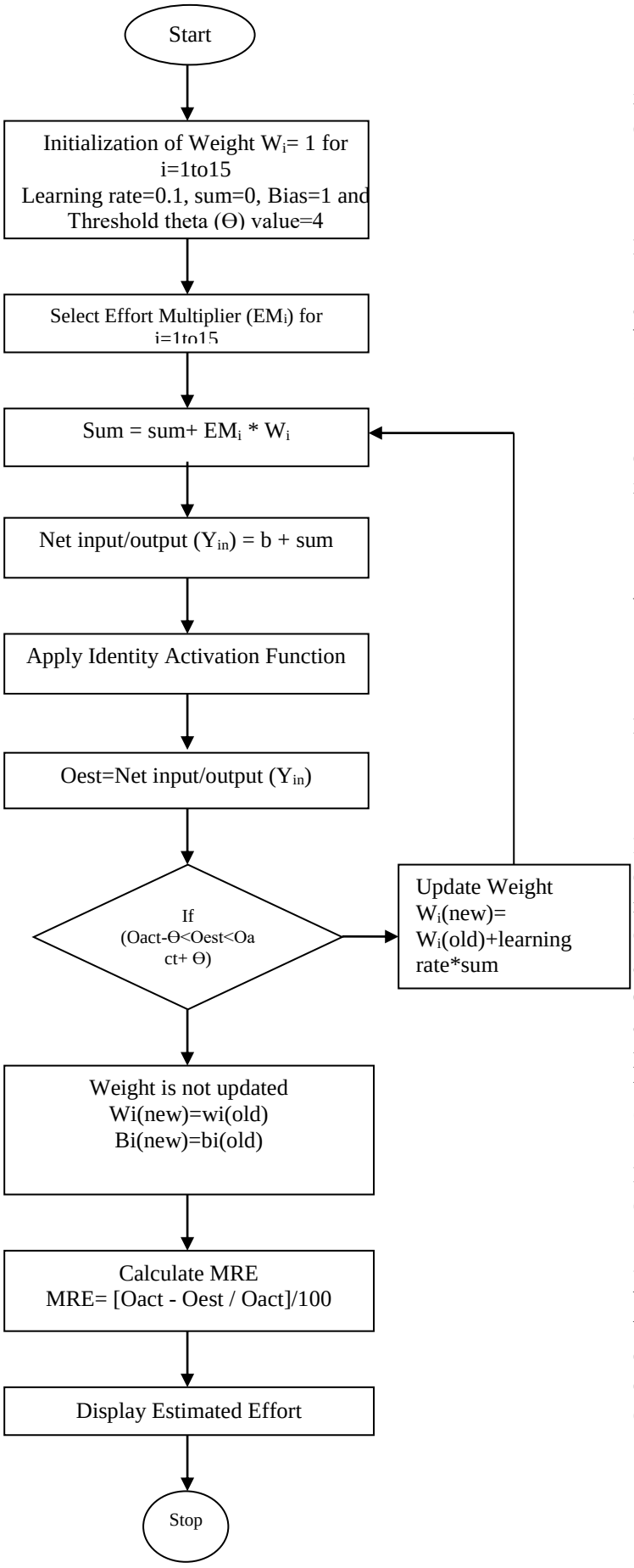

C. Steps Followed for Proposed Model

Step1. Initialize the bias(b=1), weights(Wi=1 for i=1to15),set learning rate (lrnrate=0.1) and Threshold theta (Θ) value=4.

Step2. Execute steps 3-9 until stopping condition is false.

Step3. Execute step 4-8 for each training pair.

Step4. Total Number of inputs 16 in which Total Effort Multiplier 15 and One Bias.

Step5. Calculate the response of each unit

a) Calculate Sum of total input using Sum = sum+ EMi * Wi

b) Calculate Net input output using Net input/output (Yin) = b + sum

Step6. Apply identity activation function and calculate estimated output i.e effort using Oest=Net input/output(Yin)

Step7. if (Oact-Θ<Oest<Oact+ Θ).

Step 8 Weights are not updated. Go to step 10

Step9. Else Weights and Bias are updated

Wi(new)= Wi(old)+learning rate*sum

b(new)=b(old)+learning rate*Oact

Step9. Repeat step 5 to 7.

Step10. Calculate Magnitude Relative Error (MRE)

MRE = ((Oact - Oest) / Oact)*100

Step 11: Stop.

VI. EVALUATION CRITERIA AND RESULTS

In this area, we depict the procedure utilized for figuring endeavors and the outcomes get when actualizing proposed neural system model to the COCOMO information set [14]. COCOMO information set is open source cost evaluating apparatus which comprises of 63 undertakings. The tool does the logical appraisal among the exactness of the assessed exertion with the genuine exertion. For examining programming exertion estimation we have calculated error using Magnitude of Relative Error (MRE) which is

Characterized as :-

MRE= (actual effort-estimated effort/actual effort)*100 (3)

20 experimental values have been shown in table 2 which were tested. Actual effort of the model has been compared with these values. The comparison reflects us about the efficiency of our network. Table 3 contains the estimated effort, actual effort and Mean Magnitude of Relative Error (MRE) values for 20 experimented projects.

https://dx.doi.org/10.22161/ijaers.4.9.6 *ISSN: 2349-6495(P) | 2456-1908(O)*

Table.2: Assessment of Calculated Effort

Project No.	Actual Effort	Estimated Effort using Proposed Model
P1	113	110.5
P2	293	289.7
P3	132	128.3
P4	60	56.6
P5	16	15.6
P6	04	0.8
P7	22	21.06
P8	25	21.1
P9	6.1	4.8
P10	320	316.5
P11	1150	1147.2
P12	299	297.58
P13	252	248.4
P14	118	116.1
P15	90	87.2
P16	30	28.8
P17	48	44.8
P18	390	387.8
P19	77	73.7
P20	9.4	6.4

Table.3: Assessment of MRE (Magnitude Relative Error)

Project No.	Actual Effort	Our Proposed Model	MRE using our Proposed Model (%)
P1	113	110.5	2.7
P2	293	289.7	1.1
P3	132	128.3	2.8
P4	60	56.6	5.8
P5	16	15.6	2.7
P6	04	0.8	79
P7	22	21.06	3.6
P8	25	21.1	15.6
P9	6.1	4.8	40.9
P10	320	316.5	1.1
P11	1150	1147.2	0.2
P12	299	297.58	1.2
P13	252	248.4	1.4
P14	118	116.1	3.3
P15	90	87.2	2.6
P16	30	28.8	3.9
P17	48	44.8	6.7
P18	390	387.8	0.8
P19	77	73.7	4.3
P20	9.4	6.4	31.9

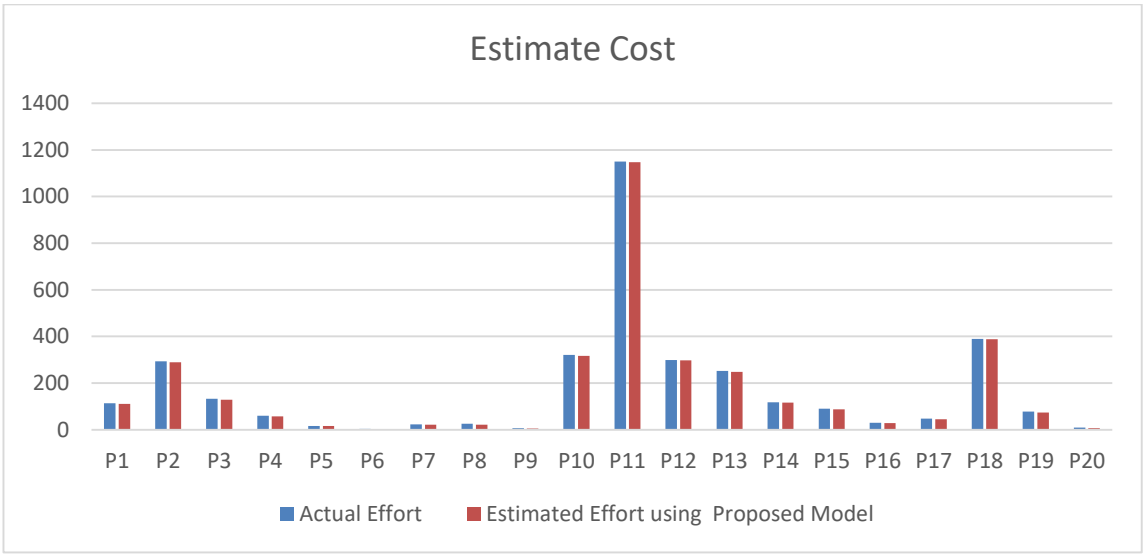

Actual Effort

Estimated Effort using Proposed Model

Fig.2: Graphical Representation of Calculated Effort

Table 2, Table 3 and Figure 2 shows that the described neural network model gives the most proficient effort estimation results as compared to other models.

https://dx.doi.org/10.22161/ijaers.4.9.6 *ISSN: 2349-6495(P) | 2456-1908(O)*

VII. CONCULSION

Having a dependable and precise estimate of software development has never been an easy task and this is where has always lied the problem for many scholarly and industrial conglomerates since ages. Talking about anticipating the future programming shows how a cost estimation model is built based on single layer artificial neural network. The neural network that is used to estimate the software improvement effort is single layer feed forward network with identity activation function. Accurate value is attained through neural network. In future, for software cost estimation we will put our focus on neuro fuzzy approach.

ACKNOWLEDGMENT

I would like to express my deep gratitude and thanks to Dr Nidhi Mishra, Associate Professor, Department of Computer Engineering, Poornima University, IT Developer Devesh Arora and Prof Pramod Choudhry for giving me an opportunity to work under his guidance for preparing the paper.

Finally thanks to my family members Mr. Gopal Das (Father), Anju Arora (Mother), Abhishek(Brother), Shivani, Neeraj Munjal, my friend Hridya Narang and Sumit Sharma for their constant encouragement and support throughout the research.

REFERENCES

[1] Reddy Ch., KVSVN Raju.: A Concise Neural Network Model for Estimating Software Effort International Journal of Recent Trends in Engineering, Issue. 1, Volume 1 (2009).

[2] Bayindir, Colak R., Sagiroglu I., Kahraman S., H.T.:Application of Adaptive Artificial Neural Network Method to Model the Excitation Currents of Synchronous Motors, 11th International Conference on in Machine Learning and Applications (ICMLA) , vol 2, pp.498-502, (2012).

[3] Kumari S.: Performance Analysis of the Software Cost Estimation Methods A Review, International Journal of Advanced Research in Computer Science and Software Engineering, Issue 7,vol 3,(2013).

[4] Sharma T..: Statistical Analysis of various models of Software Cost Estimation International Journal of Engineering Research and Applications (IJERA),Issue 3,vol 2,pp.683-685, (2012)

[5] Kaushik A., Soni A.K, Soni R.: A Simple Neural Network Approach to Software Cost Estimation, Global Journal of Computer Science and Technology Neural & Artificial Intelligence, Issue 1, vol 13, Version 1.0,(2013)

[6] Hamza H., Kamel, Shams A., K.: Software Effort Estimation Using Artificial Neural Networks A Survey of the Current Practices, Tenth International Conference on Information Technology: New Generations (ITNG), pp.731-733, 15-17, (2013).

[7] Krenke A., Bešter J., Kos A..: Introduction to the Artificial Neural Networks, Methodological Advances and Biomedical Applications,(2011)

[8] Sharma T.: A Comparative study of COCOMO II and Putnam models of Software Cost Estimation, International Journal of Scientific & Engineering Research , Issue 11,vol 2, (2011).

[9] Tadayon N.: Neural Network Approach for Software Cost Estimation, IEEE International Conference on Information Technology: Coding and Computing (ITCC'05), vol 2 ,pp 815-818,4-6,(2005).

[10] Mukherjee S.: Optimization of Project Effort Estimate Using Neural Network IEEE International Conference on Advanced Communication Control and Computing Technologies, pp 406-410,(2014).

[11] Jodpimai, P., Lursinsap P., C.: Estimating Software Effort with Minimum Features Using Neural Functional Approximation in International Conference on Computational Science and Its Applications (ICCSA), pp.266-273, 23-26 (2010)

[12] Kaushik A., Chauhan A., Mittal D.,: COCOMO Estimates Using Neural Networks, International Journal if Intelligent Systems and Applications (IJISA), vol 4, No.9, (2012)

[13] Ghose, M.K., Bhatnagar, Bhattacharjee R., V.: Comparing some neural network models for software development effort prediction, National Conference on Emerging Trends and Applications in Computer Science (NCETACS), pp.1-4, 4-5 (2011).

[14] http://promise.site.uottawa.ca/SERepository/datasets/cocomo81.arff

[15] Andrej Krenke, Janez Bešter, Andrej Kos, "Introduction to the Artificial Neural Networks", Methodological Advances and Biomedical Applications, April 11, 2011.

https://dx.doi.org/10.22161/ijaers.4.9.7 *ISSN: 2349-6495(P) | 2456-1908(O)*

Sound Intensity Measuring Instrument Based on Arduino Board with Data Logger System

Intan Nurjannah, Drs. Alex Harijanto, M.Si., Drs. Bambang Supriadi, M.Sc.

Faculty of Teacher Training and Education, University of Jember, Kalimantan Street No.37, Bumi Tegalboto, Jember, East Java, Indonesia 68121

***Abstract*—** *The government set the average sound intensity in the morning and evening around the non-noise places of worship is 55 dB. Measuring instrument the intensity of sounds around places of worship during the day and night is needed to record data during the day and night. Arduino board is a combination of hardware and software with low resource requirements, which allows user to interact with objects (physical quantities) in the vicinity. Keyes- 037 microphone sound sensor module is a high-sensitivity sound detector. SKU-316412 is a data logging system equipped with an SD card interface for memory cards capable of storing 32 MB to 8 GB of data. The arduino and it's both modules can be assembled into a measuring instrument and sound recording intensity to be placed in the desired places.*

***Keywords*— Sound Intensity, Noise Level, Sound Level Meter, Arduino, Microphone Sound Sensor, Data Logger System.**

I. INTRODUCTION

Environmental health is an important factor in this life. In line with the population grows rapidly, unbalanced in the environment increased too. Environmental health can be disturbed by the existence of environmental pollution or so-called pollution. Pollution can be categorized into 4 kinds, namely: air pollution, water pollution, soil pollution, and sound pollution. Sound pollution or we can call it noise is an unwanted noise and may interfere with human hearing[1].

Noise can occur in various places. For example the noise that occurs in places of worship. Noise in the place of worship can be affected by several factors, such as: the busy traffic of vehicles on the highway near by the mosque, the number of people who pass around the mosque, and sound system with a loud voice placed in the mosque. Excessive intensity of this sound can certainly distrub the concentration of worshipers in performing worship. The level of sound intensity can be measured using a measuring instrument called Sound level meter.

Along with the development of the electronics worlds that is growing rapidly, created a digital technology—that became the beginning of the creation of sophisticated devices called microcontrollers. The most popular and widely used microcontroller brand in the world today is the arduino microcontroller. Arduino is designed to facilitate the use of electronic devices in various fields. Based on this, an SLM has been created with an Arduino board based data logger system, which can retrieve and store data within a predetermined time. The main components of SLM consists of sound sensor, devices for display, and system data logger. The captured data can be stored automatically in the system data logger, which consists of SD module and SD card.

II. MAJOR HEADING

1. Sound

Sound is a series of waves propagating from the source of vibration as a result of changes in density and also air pressure[2]. Sound can defined as mechanical vibration waves in air or in solids which in the process produce sound and can be heard by the human ear in normal circumstances ranging from 20-20.000 Hz[3].

There are two aspects of the sound heard by the human ear. This aspect is loudness and altitude. Loudness is related to energy in sound waves. The pitch of the sound states whether the sound is high like the sound of a flute and a violin, or whether the sound is low as the sound of a bass and a drum. Physical quantity that determines altitude is frequency. Human ear hearing range is between 20 Hz to 20,000 Hz. A tendency that the more aged a person, then the person is increasingly unable to hear sounds with high frequency[4].

1.1 Intensity and Sound Intensity Level

Sound intensity is the energy carried by sound waves per unit of time through the change of each unit area. Intensity is comparable with the amplitude of the wave and has a unit of Watt/meter^2 (W/m^2)[5]

$$I = P/A \qquad (1)$$

It is known that the human ear is sensitive with various intensities of sound. Thus a logarithmic intensity scale (β) is used, which is defined by the equation:

$$\beta = (10\ \text{dB}) \log \frac{I}{I_0}$$

https://dx.doi.org/10.22161/ijaers.4.9.7 *ISSN: 2349-6495(P) | 2456-1908(O)*

in this equation, I0 is the specified reference noise intensity of 10^{-12} W/m^2, based on a minimum human hearing threshold of 1000 Hz. The sound intensity level is expressed in decibels (dB). The value of one decibel is equal to $\frac{1}{10}$ bel[6].

The intensity and intensity levels for a number of common sounds are known as follows:

Table.1: Several levels of intensity and intensity levels of sound[7]

The Source of Sound	The Intensity Levels	Intensity of Sound
Jet plane at a distance of 30	140	100
Threshold of pain	120	1
Loud rock concert indoors	120	1
Sirine at a distance of 30 m	100	1×10^{-2}
The interior of the car,	75	3×10^{-5}
Busy road traffic	70	1×10^{-5}
Ordinary conversations,	65	3×10^{-6}
Slow radio	40	1×10^{-8}
Whisper	20	1×10^{-10}
Leaf rustling	10	1×10^{-11}
Hearing limit	0	1

1. Noise

Noise can be defined as an undesired sound where its duration, intensity, and quality lead to various impacts on the physiology or psychological of humans and other creatures[8].

There are various sources of noise. Source of noise based on its location is divided into two, such as[9]:

a. An interior noise source is sourced from humans, household appliances, or building machines.

b. Outdoor noise is a noisy source derived from traffic, transportation, industry, mechanical tools seen in buildings, buildings, road works, sports activities and others outdoors or buildings. The main effect of noise is on the senses of the listener, where the damage that occurs consists of: 1) Temporary loss of hearing and can be recovered if the noise can be avoided, 2) People become immune to noise, 3) Buzzing ears, and 4) Settled and not recovered. In addition, noise also causes loss of concentration and increased fatigue at low sound frequencies. While at high frequency can cause misinterpretation when talking to others[10].

At the noise measurement, an instrument called a sound level meter is used. This tool is used to measure noise between 30-130 dB and from frequency 20-20.000 Hz. Sound Level Meter is used to measure the level of sound intensity. The parts consist of microphones, amplifiers, some types of circuits, and a calibration of measurements into decibels[11].

Fig.1: Sound level meter[12]

2. Microcontroller

Spesifically, it can be said that a microcontroller is a digital electronics device that has input, output, and controlled programs that can be written and deleted in a special way. In terms of its use, the microcontroller system is more widely used in deterministic applications. It means that this system is used for certain purposes only, such as a PID controller on industrial instrumentation, data communication controller on distributed control system, and so on[13].

The application of microcontroller among others in the following fields:

a. Automotive: engine control unit, air bag, speedometer, and alarm security system

b. Household and office supplies: remote control, washing machine, and microwave

c. Controlling equipment in the industry

d. Robotics

The most widely used microcontroller is an 8 bit microcontroller, with the brand Motorolla 68HC05/11, Intel 8051, Microchip PIC 16, and which is very popular recently from the Atmel AVR family[14].

3. Arduino Board

Arduino is an open source electronic board, based on flexible and easy-to-use software and hardware, aimed at artists, designers, electronics enthusiasts, and anyone interested in creating interactive objects or environments[15].

Fig.2: Arduino IDE Software

Arduino/Genuino Uno is a microcontroller board based

https://dx.doi.org/10.22161/ijaers.4.9.7 ISSN: 2349-6495(P) | 2456-1908(O)

on ATmega328P, which has 14 digital input/output pins (6 of which can be used as PWM output), 6 analog inputs, 16 MHz crystal oscillator, USB connection, power jack, ICSP header, and button Reset. Detail arduino uno can be seen in Table 2, with the following specifications:

Table.2: Specification arduino uno

Part	Spesification
Mikrocontroller	ATmega328P
Operated voltage	5V
Input voltage	7-12V
Input voltage (limit)	6-20V
Pin digital I/O	14 (provide 6 PWM output)
Pin PWM digital I/O	6
Analog pins input	6
DC current per I/O pin	20 mA
DC current for 3.3V pin	50 mA
Flash Memori	32 KB (ATmega328P) that 0.5 KB used by
SRAM	2 KB (ATmega328P)
EEPROM	1 KB (ATmega328P)
Time velocity	16 MHz
LED_BUILTIN	13
Length	68.6 mm
Width	53.4 mm
Weight	25 g

Fig.3: Arduino uno ATmega328P

4. Sound Sensor

Sound sensor usually used for detecting noise in surrounding environment. Arduino can collect the output signal from the sensor and run it simultaneously. Sound sensor can be used to create multiple interactive works such as "clap and ringer" to find lost keys or create a remote control if a buzzer is added. This sensor works by analyzing the sound. Specification tool as follows[16]:

a. Voltage source: 3.3V to 5V
b. Function: Detects the intensity of the sound quickly
c. Interface: Analog
d. Size: 22 x 32 mm (0.87 x 1.26 inches)

Fig.4: Analog sound sensor type KY-037[17]

5. LED (*Light Emitting Diode*)

Diode is a simple component made of semiconductor materials. Silicon is the most of the materials that used to make diode. Diodes are composed of material relations of type P and type N. These PN junctions only
carry current if given a forward bias voltage, by means of the P type material (as anode) connected to the positive terminal of the power supply, while the N type material (as the cathode) is connected to the negative terminal of the power supply. This characteristic PN junction causes the diode to be used as a current rectifier[18].

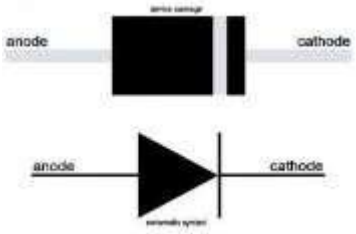

Fig.5: LED shape and emblem (Light Emitting Diodes)[19].

*Fig.6: LED (Light Emitting Diode)[20].*LED pole installation should not be inverted because if it is reversed, LED will not turn on. If higher current flowing on the LED, the brighter light will be generated. However, the allowed current ranges between 20 mA - 40 mA and a voltage of 1.6 Volt - 3.5 Volt according to the resulting color character. Here is a working voltage on an LED, based on the resulting color[21]:

1. Infrared : 1.6 V
2. Red : 1.8 V - 2.1 V
3. Orange : 2.2 V
4. Yellow : 2.4 V

https://dx.doi.org/10.22161/ijaers.4.9.7 *ISSN: 2349-6495(P) | 2456-1908(O)*

5. Green : 2.6 V
6. Blue : 3.0 V - 3.5 V
7. White : 3.0 V - 3.6 V
8. Ultraviolet : 3.5 V

7. LCD (Liquid Crystal Display)

LCD (Liquid Crystal Display) is an electronic device that has been configured in a plastic or glass container so as to provide the appearance of dots, lines, symbols, letters, numbers, and images. LCD is divided into two kinds based on the shape and appearance, namely Text-LCD and Graphic-LCD. Display on Text-LCD in the form of letters and numbers. While the shape of the display on the Graphic-LCD in the form of dots, lines, and images[22].

LCD function to display a value of the detection by the sensor, display text, or display the menu in the microcontroller application. LCD used in this research is a type of LCD M1632. The M1632 LCD is an LCD module with a 16 x 2 line display with low power consumption[23].

Fig.7: LCD Display[24]

8. Micro SD Module

SD module or SD Card Shield is a module used to send data to SD card. Pinout from SD module can be connected to arduino and other microcontroller, so it is useful to increase data storage and data logger (data logger system). This module can be directly connected to the arduino. The specialty of this SD module is[25]:

a. There are modules for standard SD card and micro SD (TF) cards
b. There is a switch to select a flash card slot
c. Can be connected directly to arduino
d. Can be used for other microcontoller

Micro SD Module suitable with TF SD card (used in mobile phone) and it is the smallest card in the market. SD module can be used for various applications such as data logger, audio, video, and graphics. This module will greatly expand the arduino capacity with small memory usage. This module has SPI interface and 5V power supply in accordance with arduino UNO/Mega. SD Card Shield or SD Module is the solution to send data to SD card. The features of this Micro SD Module are[26]:

a. Working on voltage : 5V
b. Size : 20 x 28mm (0.79 x 1.10 ")
c. Interface : SPI
d. Suitable used for : MicroSD(TF)

Fig.8: SD module type SKU-316412[27]

9. Micro SD

One example of external memory is the SD Card. SD Card is one part to compile a data logger system.

We can store long-term data on SD card. Comparison of storage capacity on arduino and SD card chips is very much different. An arduino chip has a permanent storage EEPROM that has a capacity of only a few hundred bytes, very small if we compared it with the capacity of data that can fit an SD card of several gigabytes. The price of SD card is very cheap and easy to obtain in various electronics stores. SD card is the right choice for long- term data storage with large capacity[28].

Fig.9: SD card [29]

10. Resistors

In a circuit of electronics, resistor has various functions, such as current limiting, voltage dividers, and current measurements. Each electronics component has a maximum current limit that can pass through it. Current limiting resistors are used to prevent excessive current damage. Examples of resistors as current limiting are used in LED current limiters[30].

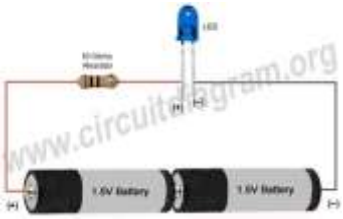

Fig.10: Resistor circuit as LED current limiter[31]

The resistor value as LED current limiter can be used using the following formula:

$$R = \frac{V_c - V_L}{i} \quad (3)$$

where R is the resistor value (Ω), V_C is the source voltage (volts), V_{LED} is the voltage reducing by the LED (volt),

https://dx.doi.org/10.22161/ijaers.4.9.7 *ISSN: 2349-6495(P) | 2456-1908(O)*

and *i*is the ideal current required by the LED (20-40 mA)[32].

III. METHODOLOGY

1. Place and Time of Research

The process of planning, designing tools, and taking data are located at the author's residence, at the Advanced Physics Laboratory in Physics FKIP University of Jember (UNEJ), and in Sunan Kalijaga Mosque Jember. The research will be conducted in the even semester of the academic year 2016/2017.

2. Tools and Components

It takes some tools and equipment components to make SLM design. The required tools and components are listed in Table 3 below:

Table.3: Tools and Components

No.	Component Type	Spesifications	Total
1.	*Sound Level Meter* (type SL-	30-130 dB	1
2.	Arduino uno	-	1
3.	*Sound sensor* type KY-038	-	1
4.	SD *Module* tipe SKU-316412	-	1
5.	SD *Card*	8 GB	1
6.	LED	Output colors: red, yellow, and	3
7.	LCD	16 x 2	1
8.	Trimpot	1KΩ	1
9.	*Power Bank*	*Output voltage* 5V	1
10.	Resistor	330 Ω	3
11.	Jumper cable	*male to male* dan *female to male*	sufficiently
12.	*Project Board*	-	1
13.	Length meter	-	1
14.	Solder	-	1
15.	Lead	50 cm	1

(Source: author)Basic Concepts of System Design

The design of this tool is determined by measuring the level of sound intensity with a distance of few meters from the sound source with a different state of time and atmosphere, utilizing SLM factory production as calibrator and sound sensor as sound source input controlled by arduino uno microcontroller, with output display on LED , LCD, and data logger.

3. The Descriptions of System Work

Broadly, the designed of Sound Level Meter (SLM) equipped with data logger system based on arduino board is made to measure the level of sound intensity in a place, so that the noise level in that place can be detected and impact on the increased comfort in our activity and reduce damage hearing due to excessive exposure to noise.

The design of this tool begins with try to understand of indoor sound acoustics, with different air temperatures, and predetermined spacing. The tool is calibrated using SLM factory production as a calibrator. Then, the results analyzed and processed into tabel and observational charts.

4. System Block Scheme

The design of diagram block is shown in the following figure:

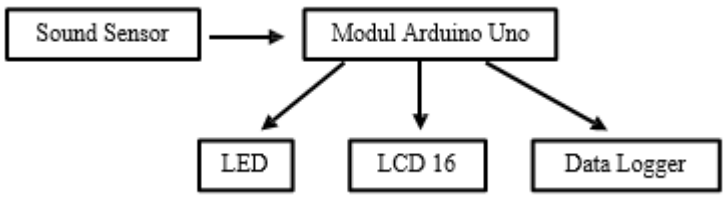

Fig.11: Block diagram of the tool design

5. Design of circuit tools

Draw a set of tools in the following drawings:

https://dx.doi.org/10.22161/ijaers.4.9.7 ISSN: 2349-6495(P) | 2456-1908(O)

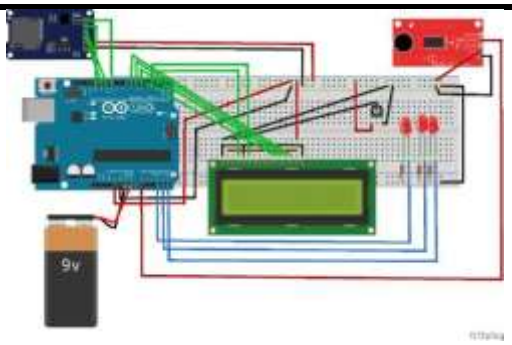

Fig.12: Design tool

6. Data retrieval

There are 2 kinds of data taken. The first data is assembled assembly calibration data compared to SLM production factory. The second data is a sample of data measuring the intensity of sound at Sunan Kalijaga Mosque
in Jember during the day and night. Data are placed in Table 4 and Table 5.

IV. RESULT AND DISCUSSION

In this chapter will be discussed about the results of calibration of SLM tools of researchers design with SLM production factory. In addition, we also discussed the sample data taken at the Sunan Kalijaga Mosque during the day and night, as described in the methodology chapter.

1. Tool Circuit

Sound Level Meter with Arduino Board based on Data Logger system has been created, with the following series:

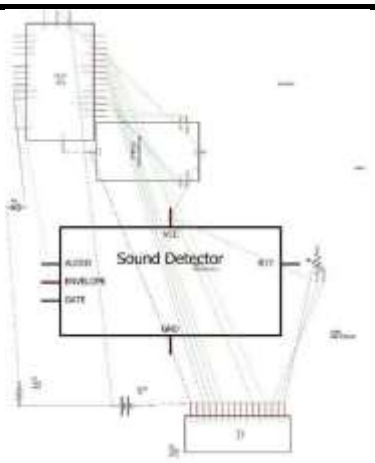

Fig.13: Tool circuit made with Fritzing software[33]

2. SLM Calibration Results Researcher Design with Standard SLM Calibrator

The SLM accuracy test of the research design is done by calibrating the measuring result using the calibrator of SLM DEK-O type SL-130. Demonstrated graph of normality as follows:

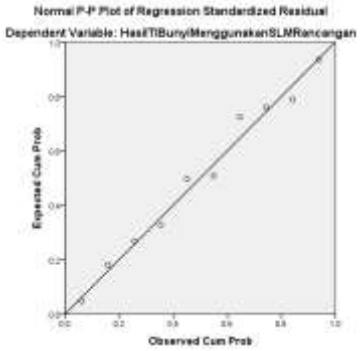

Fig.14: Normalized graph from data

The output from both device were normalized to measure the sound intensity level.
Below is a calibration data table:

Table.4: Calibration Data Used Standard SLM

Pengukuran ke-	Hasil TI Bunyi Menggunakan SLM Pabrik	Hasil TI Bunyi Menggunakan SLM Rancangan	%error
1	72.4	76.33	0.05149
2	72.9	70.88	-0.0285
3	79.6	73.55	-0.0823
4	74.2	73.02	-0.0162
5	73.7	74.49	0.01061
6	73.7	76.33	0.03446
7	73.4	73.55	0.00204
8	73.4	72.48	-0.0127
9	73.4	78.01	0.05909
10	73.4	75.91	0.03307

(Source: author)

3. The Sample Result of measuring Sound Intensity Level In Sunan Kalijaga Mosque

The Sample result from Measuring Sound Intensity Level in Sunan Kalijaga Mosque is shown below:

Table.5: The Sample result from Measuring Sound Intensity Level in Sunan Kalijaga Mosque

https://dx.doi.org/10.22161/ijaers.4.9.7 *ISSN: 2349-6495(P) | 2456-1908(O)*

The Number of Measure	Sound Intensity Level at d	Sound Intensity Level at night
1	62.2	66.34
2	57.39	68.3
3	69.26	59.43
4	66.23	57.13
5	61.05	71.19
6	74.12	66.34
7	58.54	57.39
8	62.37	64.15
9	63.09	66.18
10	74.85	67.57
11	78.7	63.57
12	66.23	63.26
13	69.11	62.37
14	62.37	61.47
15	63.71	77.08
16	77.55	73.37
17	78.74	74.96
18	63.26	69.65
19	75.36	73.34
20	63.99	64.6
21	62.37	71.33
22	76.97	74.85
23	59.43	70.07
24	67.57	86.56
25	66.79	76.19
26	68.84	57.39
27	66.87	71.25
28	73.34	61.47
29	71.87	64.88
30	74.23	77.08
AVERAGE	67.88	67.95866667

(Source: author)

Graph of the Sample result from measuring sound intensity level in Sunan Kalijaga Mosque at day and

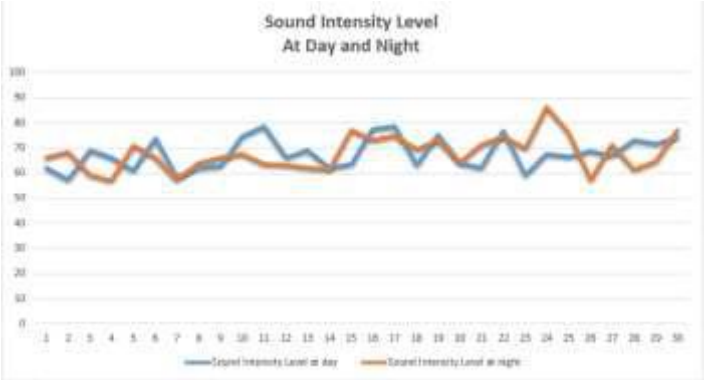

Fig.15: Graph of sample data from measuring sound intensity level

(Source: author)

V. CONCLUSION

Based on the data obtained from the calibration, it can be concluded the output data from SLM that made by the researcher are near by the output data from SLM standart that produced by factory. This is verify that SLM that made by the researcher has been successfully performed as a sound intensity level measuring devices.

In the data at the second table, we found that the intensity level in the Sunan Kalijaga mosque in the morning and the evening have a fluctuating value, depending on the number of sound sources. In this research, the source of sound is a vehicle that passes on the highway. Results can be seen on the graph. In addition, it can

be concluded also to increase the average in the Sunan Kalijaga mosque in the morning and evening exceed the standard level for places of worship set by the government, which is 55 dB[34].

https://dx.doi.org/10.22161/ijaers.4.9.7 *ISSN: 2349-6495(P) | 2456-1908(O)*

REFERENCES

[1] Djalante, S. 2010. Analisis Tingkat Kebisingan di Jalan Raya yang Menggunakan Alat Pemberi Isyarat Lalu Lintas (Apil) (Studi kasus: Simpang Ade Swalayan). *SMARTek*. 8(4): 280-300.

[2] Gabriel, J. F. 1996. *Fisika Kedokteran*. Jakarta: EGC.

[3] Satwiko, P. 2005. *Fisika Bangunan 1*. Edisi 2. Yogyakarta: Penerbit ANDI.

[4] Giancoli, D. C. 2001. *Physics: Principles with Applications*. 5th ed. United States: Prentice-Hall, Inc. Terjemahan Oleh Y. Hanum. 2001. *Fisika*. Edisi Kelima. Jakarta: Erlangga.

[5] Giancoli, D. C. 2001. *Physics: Principles with Applications*. 5th ed. United States: Prentice-Hall, Inc.
Terjemahan Oleh Y. Hanum. 2001. *Fisika*. Edisi Kelima. Jakarta: Erlangga.

[6] Young, H. D. dan R. A. Freedman. 2012. *Sears and Zemansky's University Physics: with Modern Physics*. 13th ed. United States. Pearson Education, Inc.

[7] Feidihal. 2007. Tingkat Kebisingan dan Pengaruhnya Terhadap Mahasiswa di Bengkel Teknik Mesin Politeknik Negeri Padang. *Jurnal Teknik Mesin*. 4(1): 31-41.

[8] Wafiroh, A. H. 2013. Pengukuran Tingkat Kebisingan di Lingkungan SMPN 2 Jember. *Skripsi*. Jember:
Fakultas Matematika dan Ilmu Pengetahuan Alam Universitas Jember.

[9] Setiawan, M. F. 2010. Tingkat Kebisingan pada Perumahan di Perkotaan. *Jurnal Teknik Sipil & Perencanaan*. 12(2): 191-200.

[10] Rossing, T. D. 1990. *The Science of Sound*. 2nd ed. USA: Addison-Wesley Publishing Company, Inc.

[11] Toolstop. Ltd. 2017. http://www.toolstop.co.uk/sealey-ta060-sound-level-meter-p58476. [Diakses pada 23 Januari 2017].

[12] Tuwaidan, Y. A. 2015. Rancang Bangun Alat Ukur Desibel (dB) Meter Berbasis Mikrokontroler Arduino Uno R3. *E-journal Teknik Elektro dan Komputer*. 4(1): 37-43.

[13] Adi, A. N. 2010. *Mekatronika*. 2010. Edisi Pertama. Yogyakarta: Graha Ilmu.

[14] Arduino. 2017. https://www.arduino.cc/. [Diakses pada 02 Januari 2017].

[15] DFRobot. 2017. https://www.dfrobot.com/. [Diakses pada 11 Januari 2017].

[16] Anonymous. http://www.goodluckbuy.com/keyes-diy-high-sensitivity-microphone-sensor-modules-ky-037.html. [Accessed at April 29th, 2017].

[17] Elektronika Dasar. 2013. http://elektronika-dasar.web.id/konsep-dasar-diode/. [Diakses pada 23 Februari 2017].

[18] Sparkfun. 2017. https://www.sparkfun.com/products/11372. [Diakses pada 11 Januari 2017].

[19] Ariyanto, L. 2016. Sistem Data *Logger* Kincir Angin Propeler Berbahan Kayu. *Skripsi*. Yogyakarta: Program Studi Teknik Elektro Universitas Sanata Dharma.

[20] Fitriandi, A., E. Komalasari, dan H.Gusmedi. 2016. Rancang bangun alat monitoring arus dan tegangan berbasis mikrokontroler dngan SMS gateway. *ELECTRICIAN-Jurnal Rekayasa dan Teknologi Elektro*.
10(2):93.

[21] Hartono, R. 2013. Perancangan Sistem Data Logger Temperatur Baterai Berbasis Arduino Uno Duemilanove.
Proyek Akhir. Jember: Fakultas Teknik Universitas Jember.

[22] Sparkfun. 2017. https://www.sparkfun.com/products/11372. [Diakses pada 11 Januari 2017].

[23] Hartono, R. 2013. Perancangan Sistem Data Logger Temperatur Baterai Berbasis Arduino Uno Duemilanove.
Proyek Akhir. Jember: Fakultas Teknik Universitas Jember.

[24] DFRobot. 2017. https://www.dfrobot.com/. [Diakses pada 11 Januari 2017].

[25] Anonymous. http://www.dx.com/p/spi-micro-sd-tf-card-adapter-v1-1-module-for-arduino-blue-works-with- official-arduino-board-316412#.WQbd3TclHIU. [Accessed at April 29th, 2017].

[26] Earl, B. 2017. Adafruit Data Logger Shield. https://cdn-learn.adafruit.com/downloads/pdf/adafruit-data-logger-shield.pdf. [Diakses pada 27 Februari 2017].

[27] Amazon. com. 2017. http://www.amazon.in/Sandisk-Class-MicroSDHC-Memory-SDSDQM-008G-B35/dp/B001D0ROGO. [Diakses pada 11 Januari 2017].

[28] Adi, A. N. 2010. *Mekatronika*. 2010. Edisi Pertama. Yogyakarta: Graha Ilmu.

[29] Circuit diagram. 2014. http://www.circuitdiagram.org/simple-basic-led-circuit.html. [Diakses pada 11 Januari 2017].

[30] Adi, A. N. 2010. *Mekatronika*. 2010. Edisi

https://dx.doi.org/10.22161/ijaers.4.9.7 *ISSN: 2349-6495(P) | 2456-1908(O)*

Pertama. Yogyakarta: Graha Ilmu.

[31] Fritzing. 2016. http://fritzing.org/download/. [Diakses pada 11 November 2016].

[32] Keputusan Menteri Negara Lingkungan Hidup Nomor: KEP-48/MENLH/11 Tahun 1996. *Baku Tingkat Kebisingan*. 25 Nopember 1996. Jakarta. (the definition of sound intensity level) (2)

https://dx.doi.org/10.22161/ijaers.4.9.8 ISSN: 2349-6495(P) | 2456-1908(O)

Study on Impact of Microstructure and Hardness of Aluminium Alloy After Friction Stir Welding

Gosula Suresh

Assistant Professor, Ace Engineering College, Hyderabad, India

***Abstract*—** *The effects of friction stir welding (FSW) on the microstructure and hardness of rolled pure aluminium 6061 were investigated. The weld was obtained by varying its tilt angle (2°) and Pin diameter (6mm). Tensile strength & % Elongation was carried out to evaluate the strength of the weld. Optical microscope study was carried out to study the uniform stirring of materials. The stir zone (SZ) contains fine, equiaxed and fully recrystallized grains. Thermo mechanically- affected zone (TMAZ), heat-affected zone (HAZ), and base material (BM) were different. Hardness test indicated that the minimum and maximum hardness values were obtained in the HAZ and BM, respectively.*

***Keywords*—** *FSW; Aluminium alloy, Mechanical properties, Microstructures, SEM.*

I. INTRODUCTION

FSW is becoming more popular for joining a wide range of aluminium alloys for numerous applications. One advantage of FSW is that there is far lower heat input during the process compared with conventional welding methods such as TIG or MIG. Therefore, this solid-state process results in to minimal microstructural changes and better hardness and tensile tests than conventional welding [1-3]. The FSW process generates three distinct microstructural zones: the nugget zone (NZ), the thermomechanically affected zone (TMAZ) and the heat-affected zone (HAZ) [4]. The HAZ is only affected by heat, without plastic deformation. The TMAZ adjacent to the nugget is plastically deformed and heated. The nugget is affected by the highest temperature and the highest plastic deformation, which generally consists of fine equixed grains due to the fully dynamic recrystallization.

A relationship between microstructure and microhardness of each FSW weld zone has been discovered [5].Changes in microharness along the FSW joint are directly related to the precipitation state.

II. EXPERIMENTAL DETAILS

AA 6061 (0.4 % Si, 0.7% Fe, 0.4% Cu, 0.15% Mn, 1.2% Mg, .35% Cr, 0.25% Zn, 0.15% Ti balance Al) plates of 6mm thickwere friction stir welded vertical to the rolling direction with a travel speed, a rotational speed and a shoulder diameter of 20mm/min, 1000 rpm and 25mm.

The friction stir pin had a diameter of 4mm height of 4.8mm. A simultaneous rotation and translation motion of the FSW tool generates the formation of an symmetric weld [6].

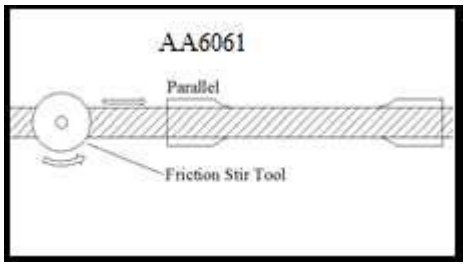

Fig.1: Schematic of the locations from where tensile test specimens were cut from (P-AA6061 (Longitudinal))

Welded cross-sections were ground, polished, and etched with Beaker's reagent for optical metallography. Instrumental (digital) Vickers micro hardness measurements were also made throughout the weld zone and into the initial aluminium alloy plate using a 50gf load. Tensile specimens were machined from NZ in parallel (longitudinal) direction from the weld. The tensile properties of the joints were evaluated using three tensile specimens cut from the same joint.

https://dx.doi.org/10.22161/ijaers.4.9.8 *ISSN: 2349-6495(P) | 2456-1908(O)*

III. RESULTS AND DISCUSSIONS

3.1 Mechanical properties

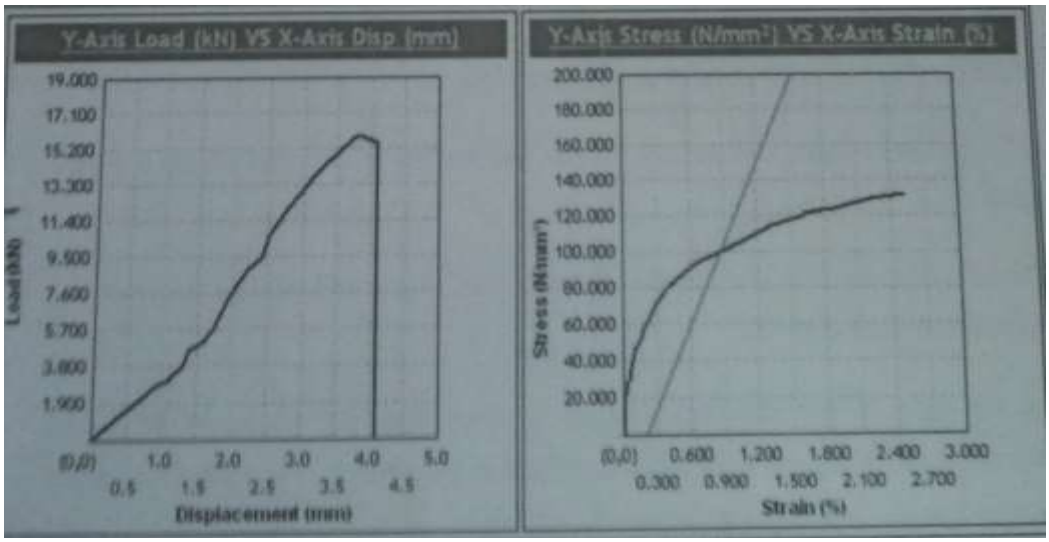

Fig.3: Tensile properties of AA6061-AA6061

As shown in fig 3 the elongation, yield strength, and tensile strength of the BM AA6061 were 2.70%, 136.77 MPa, and102.21MPa, respectively. By comparison, the two FSW specimens showed a significant decrease in both tensile and yield strength. Fig 3 also shows that the ductility for tensile specimen P-AA6061 significantly increased. Fig 1, the tensile specimen P-AA6061 contained only recrystallized grains from the NZ. From the hardness results, we know that the hardness values of the NZ were lower than that of the BM, possibly explaining why the longitudinal tensile specimen P-AA6061 exhibited both tensile and yield strength values. When a tensile load was applied to the joint, failure occurred in the weakest regions of the joint [7], which is the HAZ in this work.

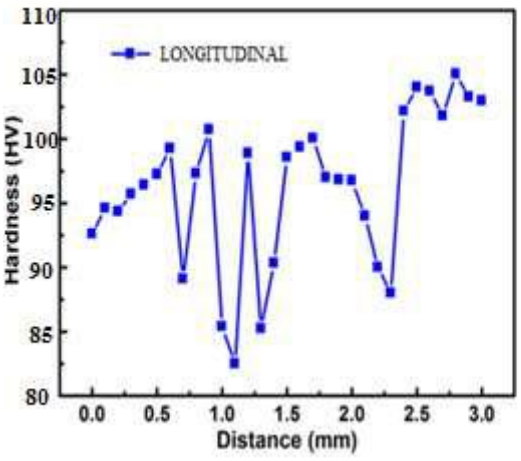

Fig.4: Microharness distribution across the top surface of FSW AA6061-AA6061 measured with a 2mm step

Fig 4 shows the typical microhardness distribution across the top surface of FSW AA 6061-AA6061. The hardness curve is a symmetrical with respect to the weld centreline because the plastic flow field in the two sides of the weld centre is not uniform [8]. The larger distorted grains and distortion energy causes the strain-hardness to increase, resulting in the symmetrical microhardness distribution. The minimum hardness of 83.03HV was obtained in the HAZ region. The maximum value 106.34HV was present in the BM. The hardness of the TMAZ was higher than that of the NZ.

3.2 Microstructure:

The microstructure of the different regions of the welded similar material is shown in fig . The NZ consists of fine equixed grains due to dynamic recrystallization. The grains in NZ are much smaller than those in other regions. The average grain size in the four zones in follows the order of BM>HAZ>TMAZ>NZ. In the TMAZ which is adjacent to the NZ, the strain and the temperature were lower than in the NZ and the effect of welding on the microstructure was correspondingly smaller. Unlike NZ, the microstructure was recognizably that of the parent material, although significantly deformed and rotated. The grain size of the HAZ was similar to that of the BM. The HAZ was common to all welding processes subjected to a thermal cycle, but it was not deformed during welding.

3.3 SEM With EDX analysis:

Elemental analysis of the macro regions in weld zone was performed using a scanning electron microscope (SEM) equipped with an EDX system. This analysis was conducted to gauge the distribution of alloying elements in the FSW zone. SEM image was analyzed at a magnification of 50X, 250X, 500X, 1.50KX

https://dx.doi.org/10.22161/ijaers.4.9.8 ISSN: 2349-6495(P) | 2456-1908(O)

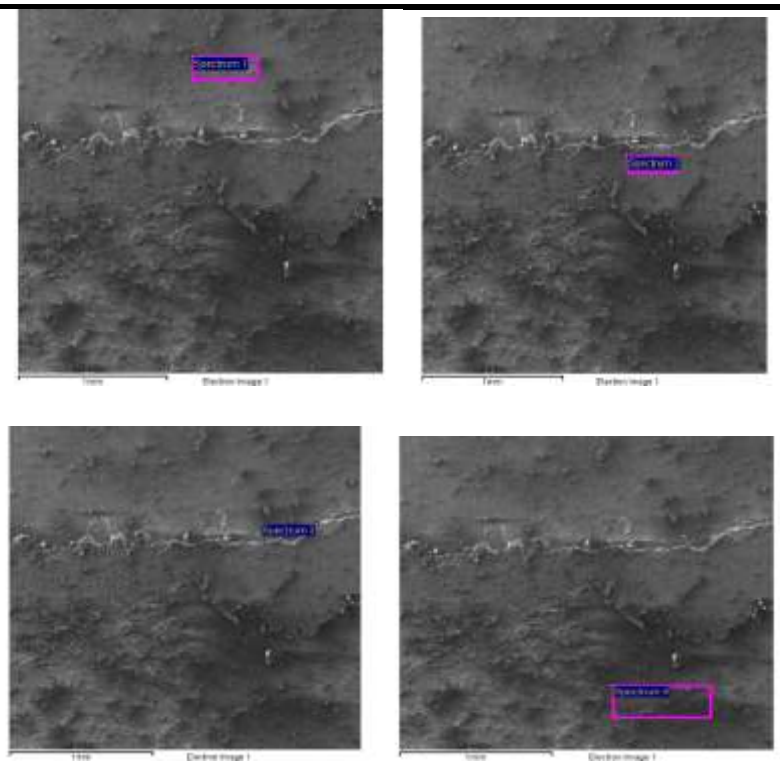

Fig.8: SEM images of FSW AA6061-AA6061 spectrum-1- HAZ, Spectrum-2 –TMAZ, Spectrum-3-NZ, Spectrum-4-BM

Table.1: EDAX quantification results of four points in fig

Element [at. %]	C	O	Al	Si	Cu
Spectrum 1(HAZ)	40.88	10.03	49.09	-----	-----
Spectrum 2 (TMAZ)	32.28	6.14	60.04	1.54	-----
Spectrum 3(NZ)	27.21	4.42	64.28	-----	4.09
Spectrum 4 (BM)	33.76	8.66	57.58	------	-----

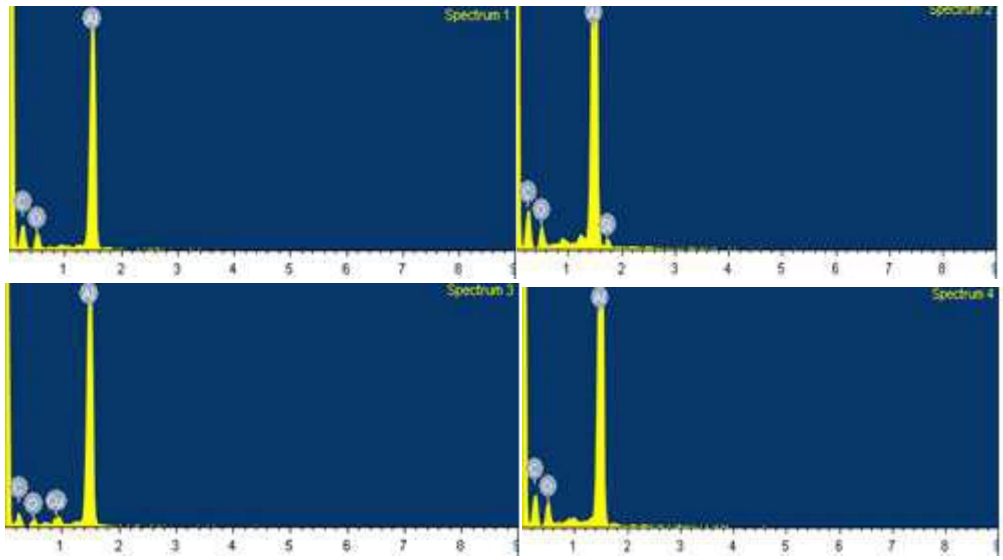

Fig.5: EDAX analysis of FSW AA6061-AA6061 spectrum-1- HAZ, Spectrum-2 –TMAZ,Spectrum-3-NZ, Spectrum-4-BM

The EDAX analysis depicted in Table 1 revealed that high contents of oxygen and aluminium are present.

https://dx.doi.org/10.22161/ijaers.4.9.8 *ISSN: 2349-6495(P) | 2456-1908(O)*

IV. CONCLUSION

An approach of the microstructure, mechanical propertiesof FSW AA6061-AA6061 aluminium alloys had been made. The order of average grain size in different weld zones was as follows: BM> HAZ> TMAZ>NZ. The minimum hardness of 80.2 HV wasobtained in the HAZ region, and the max value of 106.32 HV was present in the BM. The tensile and yield strengths of the weld zones were less than that of the BM tensile specimens. In to the properties of the BM, the ductility increased in the longitudinal tensile test specimens (that consist of the NZ).Fracture occurred in the HAZ region, which had the lowest hardness of all of the weld zones.The EDAX analysis depicted in Table 1 revealed that high contents of oxygen and aluminium are present.

REFERENCES

[1] M.Ericssson, R. Sandstrom, influence of welding speed on the fatigue of friction stir welds, and comparision with MIG and TIG, international Journal of Fatigue, 25 (2003) 1379-1387.

[2] S. Benavides, Y.Li, L.E Murr, D. Brown, J.C. McClure, Low-temperature friction stir welding of 2024 aluminium, ScriptaMeterialia, 41 (1999) 809-815.

[3] J.Q. Su, T.w. Nelson, R. Mishra, M.Mahoney, Microstructural investigation friction stir welded 7050-T651 aluminium, ActaMaterialia, 51 (2003) 713-729.

[4] M.J. Jones, P.Heurtier, C. Desrayaud, F. Montheillet, D.Allehaux, J.H. Driver, Correlation between microstructures and microhardness in a friction stir welded 2024 alumunium alloy, ScriptaMaterialia, 52(2005) 693-697.

[5] M. Sivashanmugam, S. Ravikumar, T. Kumar, V. SeshagiriRao, D. Muruganandam, "A Review on Friction Stir Welding for Aluminium Alloys", 978-1-4244-9082- 0/10/$26.00 ©2010 IEEE, pp. 216 – 221

[6] Mandeep Singh Sidhu, Sukhpal Singh Chatha "Friction Stir Welding – Process and its Variables: A Review" IJETAE Volume 2, issue 12, 2012.

[7] T.R. Mc Nelley, S.Swaminatham, J.Q. Su, Recrystallization mechanisms during friction stir welding/processing of aluminium alloys, ScriptaMaterialia, 58 (2008) 349-354.

[8] M.A. Sutton, B.Yang, A.P.Reynolds, R. Taylor, Microstructural studies of friction stir welds in 2024-T3 aluminium, Materials Science and Engineering: A, 323 (2002) 160-166.

https://dx.doi.org/10.22161/ijaers.4.9.9 ISSN: 2349-6495(P) | 2456-1908(O)

Experimental Research on Performances of Air Turbines for a Fixed Oscillating Water Column-Type Wave Energy Converter

Tengen Murakami[1], Yasutaka Imai[1], Shuichi Nagata[1], Manabu Takao[2], Toshiaki Setoguchi[1]

[1]Institue of Ocean Energy, Saga University, Japan
[2]Department of Mechanical Engineering, National Institute of Technology, Matsue College, Japan

Abstract*—A fixed oscillating water column (OWC)-type wave energy converter is composed of an air chamber for primary conversion and an air turbine for secondary conversion. In the optimal design method of a fixed OWC-type wave energy converter, it is necessary to develop a design method which can consider the characteristics of incident wave motion, the motion of the internal free surface affected in the structure such as a partly submerged wall, the fluctuation of air pressure in an air chamber, the rotation of the air turbine. In this paper, the 2-dimensional wave tank tests in regular waves for the performance evaluation of the air turbines in a fixed OWC-type wave energy converter were conducted to obtain the data needed to make this design method. As the results, the effects of the impulse turbine specification such as the rotor inlet/outlet angle, the guide vane's number and the vane's setting angle on the primary and secondary conversion efficiencies are clarified experimentally. Furthermore, the performances of the Wells turbines with different number of blade are presented for comparison of the operating condition.*

***Keywords*— Wave energy converter, Oscillating water column, Primary and secondary conversion efficiencies, Impulse turbine, Wells turbine.**

I. INTRODUCTION

As for renewable energy resources in the world, we can newly exploit the mini-/micro-hydro, the wind, the solar and the ocean energy, etc. Wave energy which is one of the renewable energies attracts attention as a promising resource that can reduce CO_2 emissions. Wave energy converter (WEC) which converts wave power into electric power has been developed all over the world and many types of WECs [1] such as the movable body type [2,3] and the overtopping wave type [4] were proposed.

There is an oscillating water column (OWC)-type wave energy converter as one of the WECs. This device is composed of an air chamber, an air turbine and a generator and is expected to be safe even under storm conditions. Many studies on this device have been performed experimentally and theoretically since the early 1970s.

In the performance evaluation of the OWC-type WEC, it is necessary to consider the characteristics of the incident wave motion, the motion of the internal free surface affected in the structure such as a partly submerged wall, the fluctuation of air pressure in an air chamber, and the rotation of the air turbine. However, most of the past studies were carried out by dividing into two steps of the primary conversion and the secondary conversion.

To estimate the primary conversion performance, the many researches [5,6] on the air chamber with the nozzle as the substitute of the turbine were conducted. Wilbert et al. [7] carried out the wave flume tests to evaluate the hydrodynamic performance of Double Chamber Oscillating Water Column (DCOWC). Ning et al. [8] investigated the hydrodynamic performance of a fixed OWC wave energy device under various wave conditions and geometric parameters in a wave flume. In this study, the power take-off was implemented through a nozzle situated on the roof of the chamber. Though, the effects of the turbine are unclear in the above studies.

As concerns the secondary conversion, by means of the test rig having a piston-cylinder to generate the oscillating air flow, the performance of the air turbine was evaluated in a series of studies. Setoguchi et al. [9,10] reviewed a variety of experimental results concerning the performances of the Wells turbine and the impulse turbine. Besides, Takao et al. [11] showed that the impulse turbine was superior to the Wells turbine in a wide flow rate range.

On the other hand, there are the studies about the performance of the OWC with the turbine [12], but the most studies make mention of the performance of the OWC with the Wells turbine. Besides, the influences of the turbine geometry on the primary conversion and secondary conversion performances were not clarified.

https://dx.doi.org/10.22161/ijaers.4.9.9 *ISSN: 2349-6495(P) | 2456-1908(O)*

This paper discusses the geometry effects of the impulse turbine on the primary and secondary conversion efficiencies in the fixed OWC-type WEC based on the experimental data needed to make this design method. Additionally, the performance of the Wells turbine is compared with the one of the impulse turbine.

II. EXPERIMENTAL APPARATUS

Fig. 1 shows the arrangement of the experimental devices in the 2-dimensional wave tank. This tank is 18.5 m long, 0.8 m wide and contains 0.8 m water depth. An absorbing wave generator was installed at the end of the tank and the model turbine was located at the other end of the tank. Four wave height gauges (TS-DWG) produced by TECHNO SERVICE Co., Ltd. were arranged to measure the amplitudes of the incident wave accurately [13]. The wave data is fed into the computer through the analog-to-digital converter (PCI-3165) from the Interface Corporation. The incident wave height was configured as high as possible in this wave tank, and the value was 0.1 m.

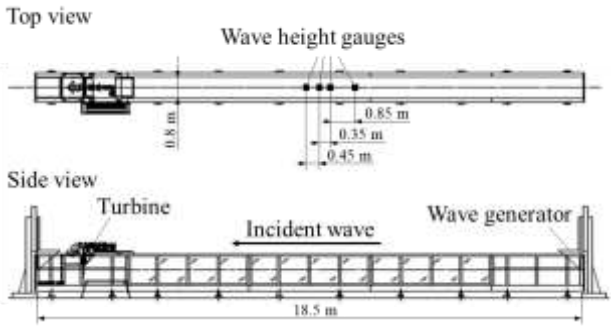

Fig. 1: Arrangements of model turbine and wave height gauges in 2-D wave tank

Fig. 2 shows the model of OWC-type wave energy converter with the impulse turbine. In the experiments, the turbine is rotated by the alternating-current synchronous motor (HG-JR73) manufactured by the Mitsubishi Electric Corporation. The torque transducer (SS-005) and the electromagnetic rotation detector (MP-981) produced by ONO SOKKI Co., Ltd. were located at the end of the turbine shaft. The air chamber length is 0.7 m, the curtain wall depth is 0.1 m and the thickness of the curtain wall is 0.005 m. The schematic design of the air chamber was conducted in a series of numerical studies [14].

Fig. 3 indicates the location of the pressure gauge (AP-10S) and the wave height gauges (FW-H07 and UD320) made by KEYENCE CORPORATION at the top of the air chamber. The rectangular orifice of the air chamber is located at the center. The data of waves, the turbine rotational speed, the torque, the pressure and the water surface elevation in the air chamber were measured simultaneously. The sampling frequency is 50 Hz and the data collection was started after the lapse of 30 seconds from the start of the wave generator.

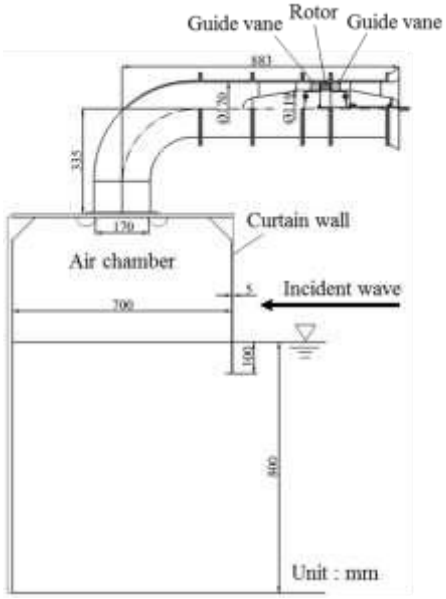

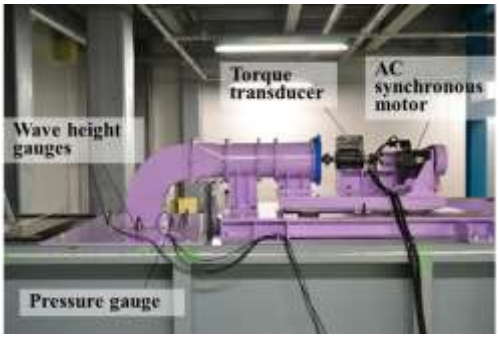

Fig. 2: Model OWC with impulse turbine

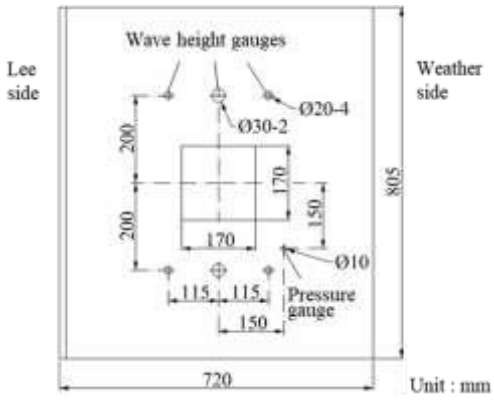

Fig. 3: Positions of pressure gauge and wave height gauges at top of air chamber

Fig. 4 shows the basic configuration of the rotor and the fixed guide vanes. This turbine configuration was adopted on the basis of the air turbine test results [9]. The numbers of the rotor blades and the single-stage guide vanes are 30

https://dx.doi.org/10.22161/ijaers.4.9.9 *ISSN: 2349-6495(P) | 2456-1908(O)*

and 26, respectively. The inlet/outlet angle γ of rotor is 60 degrees and the setting angle θ of guide vane is 30 degrees. The inner diameter D of turbine casing is 170 mm, the hub ratio ν is 0.7 and the clearance between the rotor blade tip and the casing is 0.3 mm. The inner diameter D of the turbine casing was determined based on the condition that the total pressure drop at the turbine is equal to the total pressure difference at the nozzle which the ratio of cross-section between the nozzle and the air chamber is 1/100.

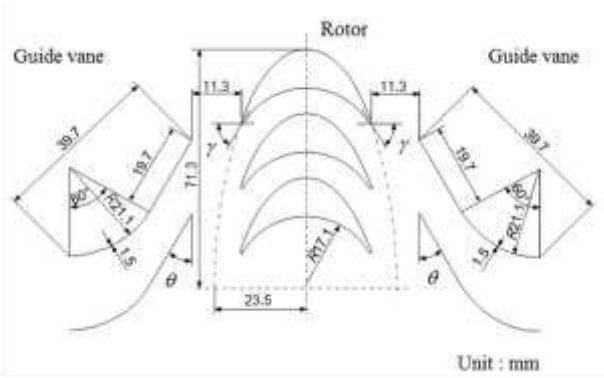

Fig. 4: Configuration of rotor and guide vane

Besides, we conducted the steady flow turbine test. In this test without waves, the bottom of the air chamber was closed by an acrylic board as shown in fig. 5 and the steady flow was generated by a centrifugal fan.

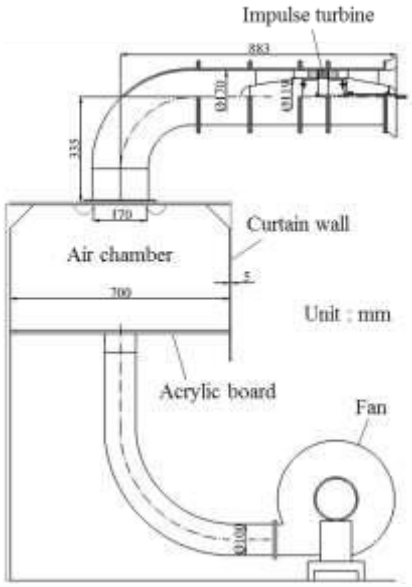

Fig. 5: Model for steady flow test

III. EXPERIMENTAL RESULTS

3.1 Impulse Turbine

3.1.1 Effect of number of guide vanes

Fig. 6 shows a comparison of the efficiencies between the three cases with different number Z_g of guide vanes. The abscissa is the ratio between the wave length λ and the air chamber length L. In this experiment, the wave length λ was changed while keeping the time-averaged rotational speed of turbine N = 700 rpm. The wave periods are T = 1.00 sec., 1.15 sec., 1.30 sec., 1.41 sec., 1.50 sec., 1.56 sec., 1.65 sec., 1.73 sec., 1.87 sec., 2.03 sec., 2.30 sec. and 2.63 sec. The primary conversion efficiency η_1, the secondary conversion efficiency η_2 and the generating efficiency η are defined as:

$$\eta_1 = \frac{P_{air}}{P_{wave}} \tag{1}$$

$$\eta_2 = \frac{P_{torque}}{P_{air}} \tag{2}$$

$$\eta = \frac{P_{torque}}{P_{wave}} \tag{3}$$

where P_{air} is the time-averaged power of the air, P_{wave} is the time-averaged power of the incident wave and P_{torque} is the turbine output. The definitions of these parameters are as follows:

$$P_{air} = \frac{S}{T}\int_0^T p(t)\frac{\partial \zeta}{\partial t}dt \tag{4}$$

$$P_{wave} = \frac{1}{2}\rho_w g \zeta_i^2 C_g W \tag{5}$$

$$P_{torque} = \frac{1}{T}\int_0^T T_0 \omega dt \tag{6}$$

where S, p, ζ, ρ_w, g, ζ_i, C_g, W, T_0 and ω denote the cross-section area of air chamber, the pressure, the six averaged water level in the air chamber, the water density, the gravitational acceleration, the incident wave amplitude, the group velocity, the chamber width, the turbine output torque and the angular velocity of turbine, respectively.

As shown in fig. 6, the maximum generating efficiency η is achieved at around λ/L = 6.3 in all three cases Z_g = 32, 26 and 20.

Next, the rotational speed N was changed while keeping the ratio λ/L = 6.3 as shown in fig. 7. The maximum generating efficiency η was achieved at about N = 700 rpm in all three cases Z_g = 32, 26 and 20. Meanwhile, the high generating efficiency of about 0.28 was obtained in two cases of Z_g = 32 and 26. On the other hand, the maximum value of η decreased in the case of Z_g = 20. The remarkable difference of η appeared at higher speed than 1000 rpm according to the η_2. It seems that the decrease of the η_2 was caused by the reduction of the whirl velocity of flow from the upstream guide vane based on the flow separation in the case of Z_g = 20.

https://dx.doi.org/10.22161/ijaers.4.9.9 *ISSN: 2349-6495(P) | 2456-1908(O)*

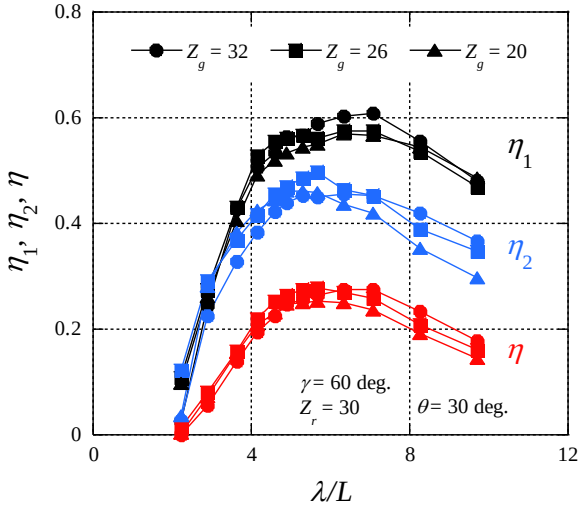

Fig. 6: Change in efficiencies due to number of guide vane at time-averaged rotational speed N = 700 rpm

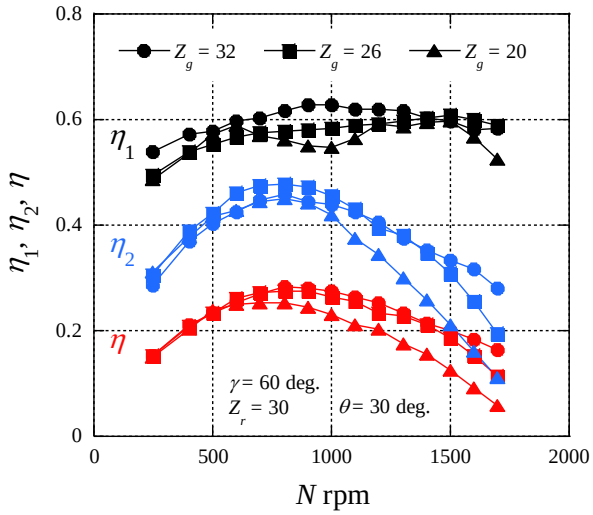

Fig. 7: Change in efficiencies due to number of guide vane at λ/L = 6.3

3.1.2 Effect of setting angle of guide vane

To know the effects of the setting angle θ of guide vane on the primary and secondary conversion efficiencies, the θ was varied from the base case of 30.0 degrees to 37.5 degrees and 22.5 degrees. In fig. 8, the efficiencies are compared between the above three cases. The number of guide vanes is Z_g = 26 giving the high efficiency. The ratio λ/L was kept constant at 6.3. As shown in fig. 8, the effect of the θ on the η_1 is small at about N = 700 rpm giving the maximum η. Besides, the maximum value of the η is highest at θ = 30.0 degrees.

Figs. 9 and 10 show the amplitudes of the pressure and the water surface elevation in the air chamber. It is found that the pressure increases at smaller θ. Meanwhile, the amplitude of the water surface elevation decreases inversely with the pressure rise. Therefore, the difference of the η_1 due to the θ is small in fig. 8.

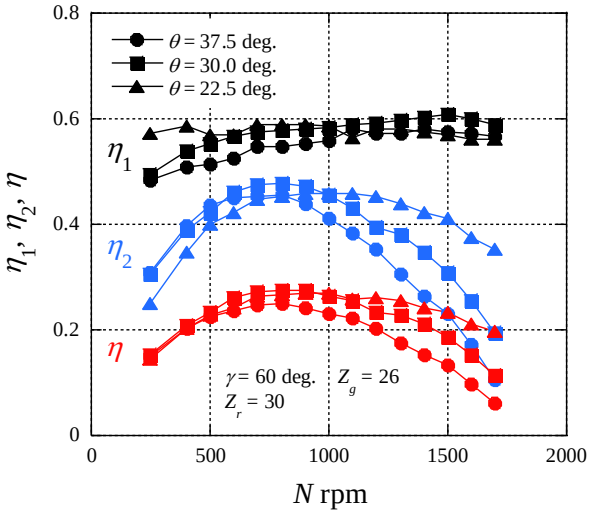

Fig. 8: Change in efficiencies due to setting angle of guide vane at λ/L = 6.3

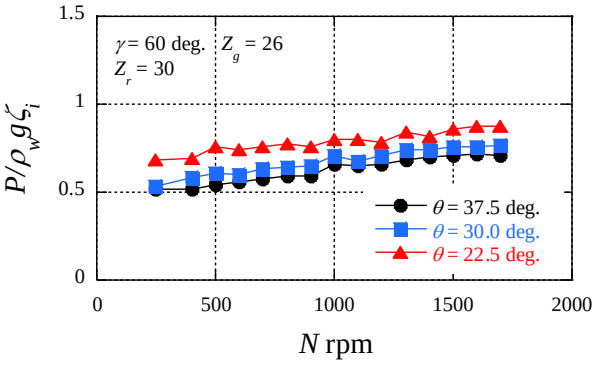

Fig. 9: Pressure amplitude in air chamber

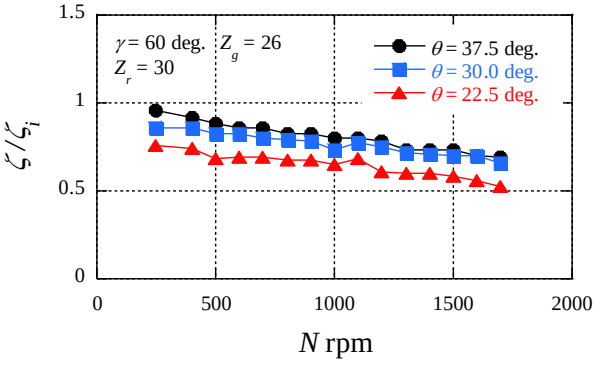

Fig. 10: Water surface elevation in air chamber

Fig. 11 shows the turbine performances in three cases of the above different θ in waves and the result of the steady flow test in fig. 5, where C_T is the torque coefficient, C_A is

https://dx.doi.org/10.22161/ijaers.4.9.9 *ISSN: 2349-6495(P) | 2456-1908(O)*

the input coefficient and the abscissa ϕ is the flow coefficient. The definitions of these parameters are as follows:

$$C_T = \frac{T_0}{\rho(v_a^2 + U^2)S_T r / 2} \quad (7)$$

$$C_A = \frac{\Delta p}{\rho(v_a^2 + U^2)/2} \quad (8)$$

$$\phi = \frac{v_a}{U} \quad (9)$$

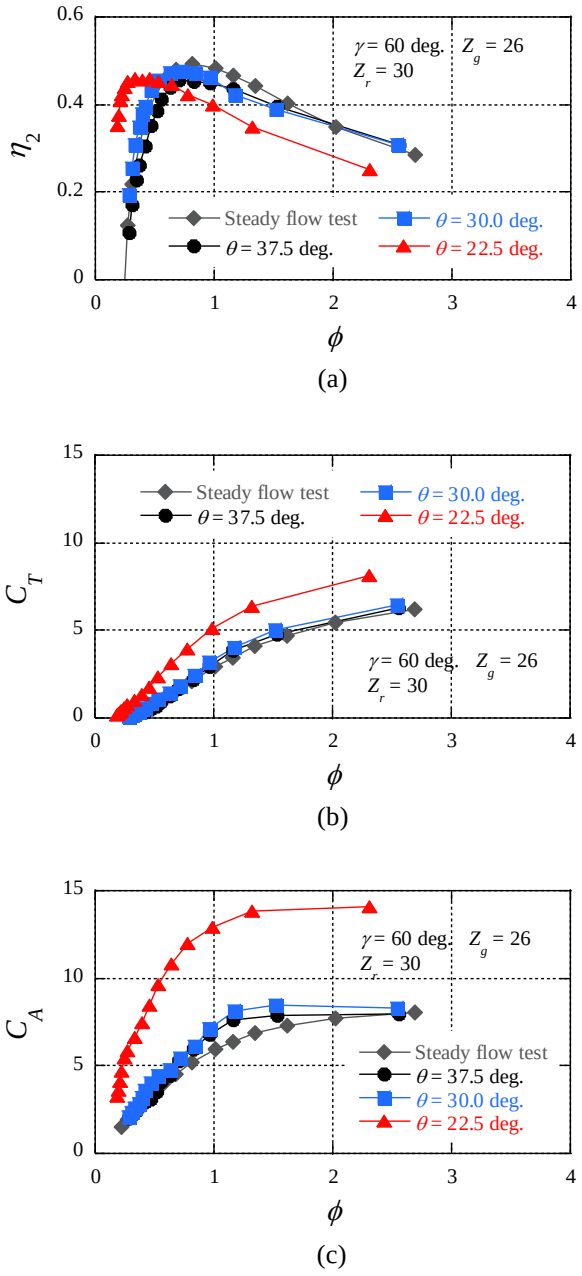

Fig. 11: Turbine performance: (a) secondary conversion efficiency, (b) torque coefficient and (c) input coefficient

where ρ, v_a, U, S_T and Δp are the air density, the axial velocity, the circumferential velocity at mean radius r [= $D(1+\nu)/4$], the flow passage area of turbine and the total pressure drop at the turbine. In the steady flow test, the inlet/outlet angle γ of rotor is 60 degrees, the number Z_g of guide vanes is 26 and the setting angle θ of guide vane is 30 degrees.

In fig. 11(a), the maximum η_2 of about 0.48 was obtained at ϕ = 0.71 in the case of θ = 30.0 degrees in wave test results, and the value is almost the same level as the case of the steady flow test. On the other hand, in both cases θ = 37.5 degrees and 22.5 degrees, the maximum η_2 decreased slightly. In addition, the flow coefficient giving the maximum η_2 became small by reduction of the θ from 30.0 degrees to 22.5 degrees. Furthermore, in the case of θ = 22.5 degrees, the C_A increased markedly at around ϕ = 0.45 of the maximum efficiency point compared with the other cases in fig. 11(c). This fact corresponds to the pressure rise in fig. 9. In the case of θ = 22.5 degrees, along with the pressure rise, the turbine output torque becomes higher at small flow rate due to the increase of the whirl velocity of flow from the upstream guide vane as shown in fig. 11(b). This is the reason why the peak of η_2 appeared in the small flow rate.

3.1.3 Effect of inlet/outlet angle of rotor

The inlet/outlet angle of rotor was changed from γ = 60 degrees to 50 degrees. Fig. 12 shows the variations of the efficiencies due to the rotational speed.

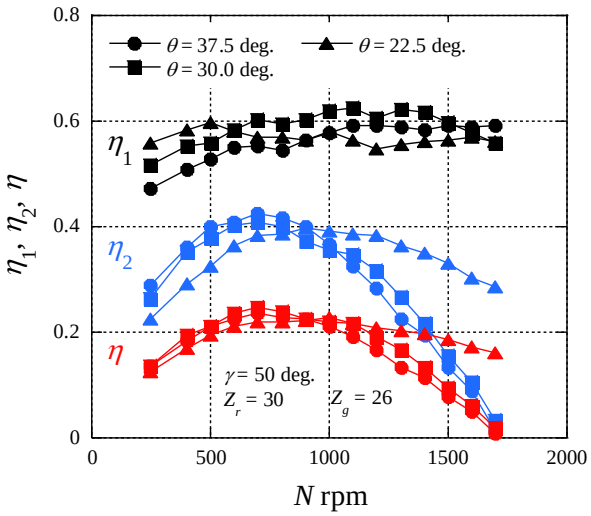

Fig. 12: Efficiencies at γ = 50 degrees

In addition, fig. 13 shows the secondary conversion efficiency as a function of the flow coefficient. The trend shifting the peak of η_2 to the small flow rate region at θ = 22.5 degrees in fig. 13 is similar to the one of the case of γ

https://dx.doi.org/10.22161/ijaers.4.9.9 *ISSN: 2349-6495(P) | 2456-1908(O)*

= 60 degrees in fig. 11(a), although the maximum value of η_2 decreased. This reduction of η_2 causes the deterioration of the η as shown in fig. 12.

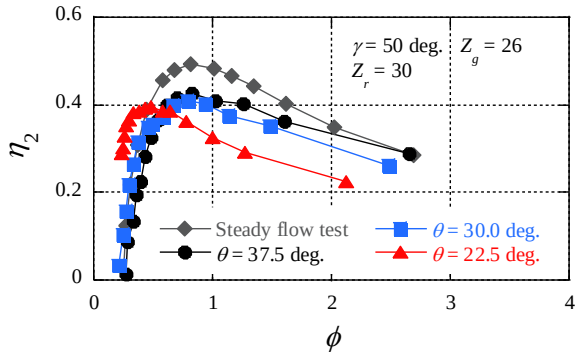

Fig. 13: Change in secondary conversion efficiency due to flow coefficient

Fig. 14 shows a comparison of the efficiency between three cases with different inlet/outlet angle γ of rotor. The setting angle θ of guide vane is 30 degrees. It is noticed that the effect of γ on the η_1 is small at about N = 700 rpm giving the maximum η, and the highest η_2 and η are achieved in the case γ = 60 degrees. As the above results, the recommended impulse turbine consists of the inlet/outlet angle γ = 60 degrees of rotor, the setting angle θ = 30 degrees of guide vane, the number Z_r = 30 of rotor blades and the number Z_g = 26 of guide vanes.

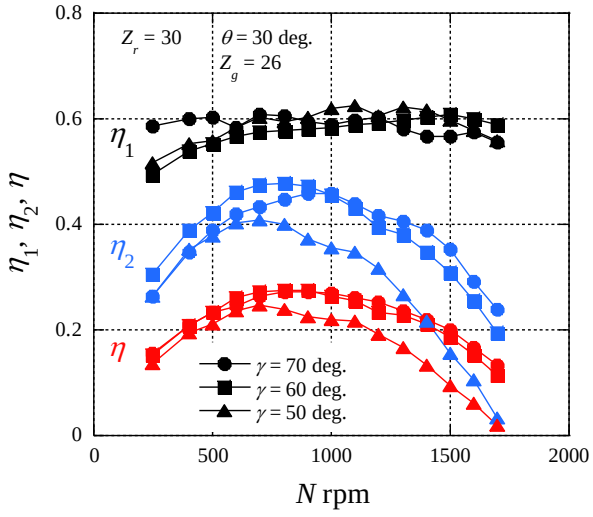

Fig. 14: Comparison of efficiency between three cases with different inlet/outlet angle of rotor

3.2 Wells Turbine

The energy conversion efficiency of the OWC model with the Wells turbine was measured for comparison with the one of the above impulse turbine. In fig. 15, the blades numbers of the Wells turbine without the guide vane are Z_r = 7, 6 and 5. In all three cases, the chord length is 51 mm, blade profile is NACA0020, the aspect ratio is 0.5 and the hub ratio is 0.7. In the case Z_r = 6, the solidity at mean radius is 0.67, and this value was adopted in the previous research on a performance in the steady flow condition [15].

Fig. 15: Wells turbine

Fig. 16 shows the efficiencies at λ/L = 6.3 in three cases Z_r = 7, 6 and 5. It is found that the operating speed range N of the Wells turbine is high compared with the one of the impulse turbine. And, it seems that the N giving the high η_2 and η shifts to the higher speed range with the decrease of the blade number, though the maximum η_2 and η are reduced in the case Z_r = 7. The maximum η_2 of about 0.48 and the maximum η of about 0.28 were achieved in both cases Z_r = 6 and 5. These maximum values are almost the same level as the ones of the impulse turbine in fig. 14.

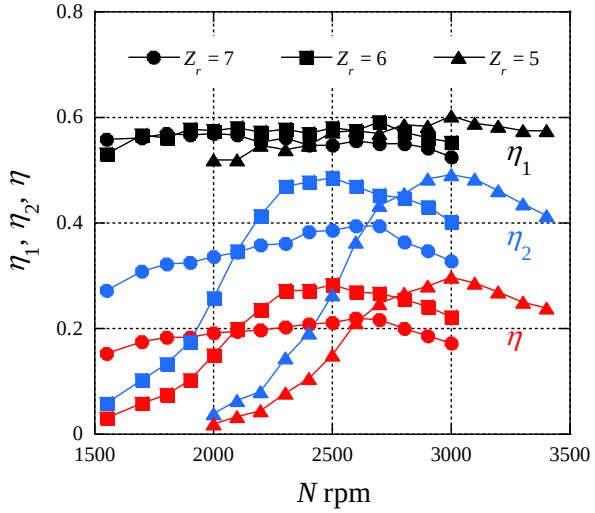

Fig. 16: Efficiencies in model OWC with Wells turbine

Figs. 17 and 18 are the amplitudes of the pressure and the water surface elevation in the air chamber. The pressure increased at the larger Z_r, and the amplitude of the water surface elevation decreased inversely with the pressure rise.

https://dx.doi.org/10.22161/ijaers.4.9.9 ISSN: 2349-6495(P) | 2456-1908(O)

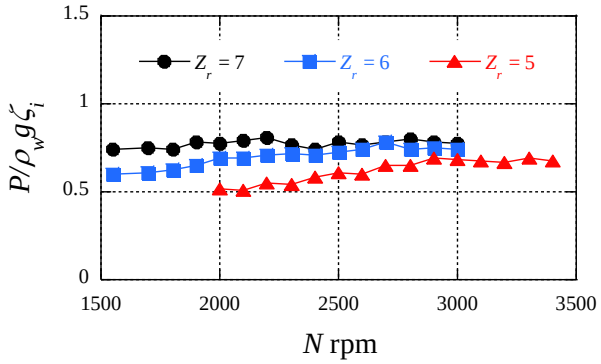

Fig. 17: Pressure amplitude

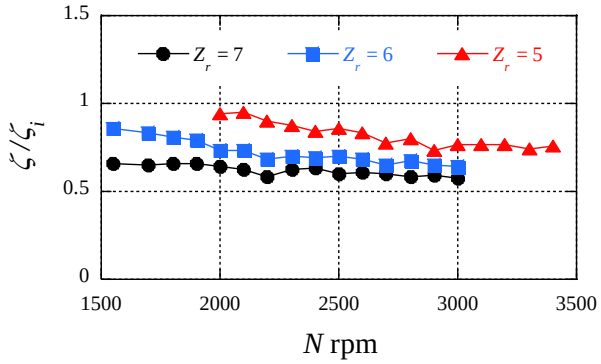

Fig. 18: Water surface elevation

Fig. 19 is a comparison of the turbine performances. The steady flow test results denote the performance of the impulse turbine in fig. 5 and the one of the Wells turbine having the casing diameter D = 300 mm in the previous research [15]. As shown in fig. 19, the maximum η_2 in all three cases Z_r = 7, 6 and 5 are obtained at about ϕ = 0.21, and the C_A increases with the pressure rise in fig. 17. In both cases Z_r = 6 and 5, the same high η_2 as the previous research on the steady flow performance of the Wells turbine is achieved. Meanwhile, the maximum η_2 becomes lower in the case Z_r = 7, because the increase of C_T corresponding to the increase of C_A is not sufficient. This is caused by the fact that the flow passage area at hub side is extremely narrow as shown in fig. 15.

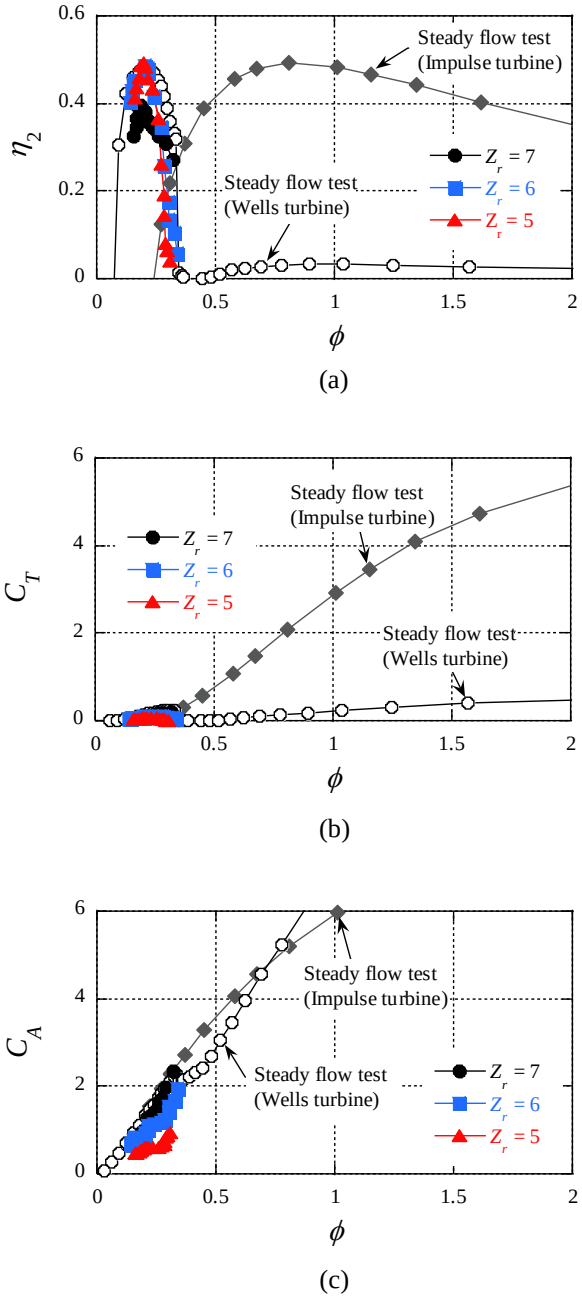

Fig. 19: Wells turbine performance: (a) secondary conversion efficiency, (b) torque coefficient and (c) input coefficient

IV. CONCLUSIONS

This paper discussed the effects of the impulse turbine specification such as the rotor inlet/outlet angle γ, the guide vane's setting angle θ and the guide vane's number Z_g on the primary conversion efficiency η_1, the secondary conversion efficiency η_2 and the generating efficiency η (= $\eta_1\eta_2$) in the fixed OWC-type WEC based on the results of the 2-dimensional wave tank tests.

In the experiments, the rotor inlet/outlet angle was changed between three cases γ = 70 degrees, 60 degrees and 50 degrees, and the guide vane's setting angle was varied from θ = 30.0 degrees to 37.5 degrees and 22.5 degrees. Besides, the single-stage guide vane's number was changed from Z_g = 26 to 32 and 20. Furthermore, the performances of the Wells turbines with different number Z_r of blades were investigated. The following concluding remarks are obtained.

1. The maximum generating efficiency of about 28% is

https://dx.doi.org/10.22161/ijaers.4.9.9 *ISSN: 2349-6495(P) | 2456-1908(O)*

achieved in both cases Z_g = 32 and 26.

2. In the case with γ = 60 degrees and θ = 30 degrees, the maximum secondary conversion efficiency of about 48% as high as the one in the steady flow condition is obtained.
3. The combination of γ = 60 degrees, θ = 30 degrees, Z_g = 26 and the rotor blade number Z_r = 30 is the promising specification of the impulse turbine.
4. As regards this experiment, the maximum secondary conversion efficiency in the OWC with the Wells turbine is almost the same level as the one of the impulse turbine.

ACKNOWLEDGEMENTS

This investigation was carried out under the "Program for the Promotion of New Energy Infrastructure Development", supported by the Mitsubishi Research Institute (MRI)/the Ministry of Economy, Trade and Industry (METI), Japan. It was also supported by a research grant of the Hatakeyama Culture Foundation.

REFERENCES

[1] Mehrangiz, S., Emami, Y., Sadigh, S. H. S., Etemadi, A. (2013). Various technologies for producing energy from Wave: a review, International Journal of Smart Grid and Clean Energy, vol.2, no.2, pp. 289–294.

[2] Watabe, T. (2008). Utilization of the ocean wave energy, Fuji Print Press.

[3] Cameron, L., Doherty, R., Henry, A., Doherty, K., Van't Hoff, J., Kaya, D., Naylor, D., Bourdier, S., Whittaker, T. (2010). Design of the next generation of the oyster wave energy converter, Proceedings of the 3rd International Conference on Ocean Energy, Spain, pp.1–12.

[4] Margheritini, L., Vicinanza, D., Frigaard, P. (2009). SSG wave energy converter: design, reliability and hydraulic performance of an innovative overtopping device, Renewable Energy, vol.34, pp.1371–1380.

[5] Takahashi, S., Ojima, R., Suzumura, S. (1985). Air power pneumatic-type wave power extractors due to irregular wave actions – a study on development of wave power, 3rd report, The Port Harbour Research Institute, vol.24, pp.3–41.

[6] Liu, Z., Hyun, B., Hong, K. (2008). Application of numerical wave tank to OWC air chamber for wave energy conversion, Proceedings of the Eighteenth International Offshore and Polar Engineering Conference, Canada, pp.350–356.

[7] Wilbert, R., Sundar, V., Sannasiraj, S. A. (2013). Wave interaction with a double chamber oscillating water column device, International Journal of Ocean and Climate Systems, vol.4, no.1, pp.21–39.

[8] Ning, D., Wang, R., Zou, Q., Teng, B. (2016). An experimental investigation of hydrodynamics of a fixed OWC wave energy converter, Applied Energy, vol.168, pp.636–648.

[9] Setoguchi, T., Santhakumar, S., Maeda, H., Takao, M., Kaneko, K. (2001). A review of impulse turbines for wave energy conversion, Renewable Energy, vol.23, pp.261–292.

[10] Setoguchi, T., Takao, M. (2006). Current status of self rectifying air turbines for wave energy conversion, Energy Conversion and Management, vol.47, pp.2382–2396.

[11] Takao, M., Setoguchi, T. (2012). Air turbines for wave energy conversion, International Journal of Rotating Machinery, vol.2012, Article ID 717398.

[12] Takahashi, S., Nakada, H., Ohneda, H. (1992). Wave power conversion by a prototype wave power extracting caisson in Sakata port, Coastal Engineering, pp.3440–3453.

[13] Goda, Y., Suzuki, Y. (1976). Estimation of incident and reflected waves in random wave experiments, Coastal Engineering, pp.828–845.

[14] Koirala, P., Nagata, S., Imai, Y., Murakami, T. (2015). A numerical study on multi-chamber oscillating water columns, Journal of Japan Society of Civil Engineers, vol.3, no.1, pp.93–104.

[15] Okuhara, S., Takao, M., Takami, A., Setoguchi, T. (2013). Wells turbine for wave energy conversion, Open Journal of Fluid Dynamics, vol.3, DOI:10.4236/ojfd.201332A006.

https://dx.doi.org/10.22161/ijaers.4.9.10 ISSN: 2349-6495(P) | 2456-1908(O)

On the Schwarzschild Solution: a Review

Carmine Cataldo

Independent Researcher, PhD in Mechanical Engineering, Battipaglia (SA), Italy
Email: catcataldo@hotmail.it

Abstract**—***In this paper the well-known Schwarzschild Solution is discussed. In the first section, by resorting, as usual, to the Einstein Field Equations, a short summary of the conventional derivation is provided. In the second section, we carry out an alternative derivation of the Schwarzschild Metric. The above-mentioned procedure is based upon several noteworthy hypotheses, among which the existence of a further spatial dimension stands out. Initially, we postulate a Universe identifiable with a 4-ball, homogeneously filled with matter, whose radius equates the Schwarzschild Radius. Then, in order to obtain the vacuum field, all the available mass is ideally concentrated in a single point. By imposing a specific condition concerning the measured radius, we deduce a metric that, if subjected to an appropriate parametrization, allows us to finally obtain the Schwarzschild solution.*

Keywords—Vacuum Field, Weak Field Approximation, Schwarzschild Metric, Alternative Derivation.

I. CONVENTIONAL DERIVATION

If we impose a spherical symmetry, the general static solution is represented by the underlying metric:

$$ds^2 = A(r)c^2dt^2 - B(r)dr^2 - r^2d\theta^2 - r^2\sin^2\theta\, d\varphi^2 \quad (1)$$

Obviously, we have already set equal to one, without any loss of generality, the parametric coefficient related to the angular part of the metric. *A* and *B* exclusively depend on the "flat coordinate", denoted by *r*. In particular, coherently with the hypothesized static scenario, whatever time derivatives must necessarily vanish.
As for the metric tensor, from *(1)* we immediately obtain:

$$g_{ij} = \begin{bmatrix} A(r) & 0 & 0 & 0 \\ 0 & -B(r) & 0 & 0 \\ 0 & 0 & -r^2 & 0 \\ 0 & 0 & 0 & -r^2\sin^2\theta \end{bmatrix} \quad (2)$$

$$g^{ij} = \begin{bmatrix} \frac{1}{A(r)} & 0 & 0 & 0 \\ 0 & -\frac{1}{B(r)} & 0 & 0 \\ 0 & 0 & -\frac{1}{r^2} & 0 \\ 0 & 0 & 0 & -\frac{1}{r^2\sin^2\theta} \end{bmatrix} \quad (3)$$

Let's deduce the *Christoffel Symbols*. Generally, we have:

$$\Gamma_{ij}^k = \frac{1}{2}g^{kh}\left(\frac{\partial g_{hi}}{\partial x^j} + \frac{\partial g_{hj}}{\partial x^i} - \frac{\partial g_{ij}}{\partial x^h}\right) \quad (4)$$

The indexes run from *0* to *3*. Clearly, *0* stands for *t*, *1* for *r*, *2* for θ, and *3* for φ.
Setting *k=0*, from *(2)*, *(3)* and *(4)*, we obtain:

$$\Gamma_{01}^0 = \Gamma_{10}^0 = \frac{1}{2A}\frac{dA}{dr} \quad (5)$$

All the other symbols (if *k=0*) vanish.
Setting *k=1*, from *(2)*, *(3)* and *(4)*, we obtain:

$$\Gamma_{00}^1 = \frac{1}{2B}\frac{dA}{dr},\ \Gamma_{11}^1 = \frac{1}{2B}\frac{dB}{dr},\ \Gamma_{12}^1 = -\frac{r}{B},\ \Gamma_{13}^1 = -\frac{r}{B}\sin^2\theta \quad (6)$$

All the other symbols (if *k=1*) vanish.
Setting *k=2*, from *(2)*, *(3)* and *(4)*, we obtain:

$$\Gamma_{12}^2 = \Gamma_{21}^2 = \frac{1}{r},\ \Gamma_{33}^2 = -\sin\theta\cos\theta \quad (7)$$

All the other symbols (if *k=2*) vanish.
Setting *k=3*, from *(2)*, *(3)* and *(4)*, we obtain:

$$\Gamma_{13}^3 = \Gamma_{31}^3 = \frac{1}{r},\ \Gamma_{23}^3 = \Gamma_{23}^3 = \frac{1}{\tan\theta} \quad (8)$$

All the other symbols (if *k=3*) vanish.

Let's now deduce the components of the *Ricci Tensor*. Generally, with obvious meaning of the notation, we have:

$$R_{ij} = \frac{\partial\Gamma_{ik}^k}{\partial x^j} - \frac{\partial\Gamma_{ij}^k}{\partial x^k} + \Gamma_{ik}^l\Gamma_{jl}^k - \Gamma_{ij}^l\Gamma_{kl}^k \quad (9)$$

By means of some simple mathematical passages, omitted for brevity, we obtain all the non-vanishing components:

$$R_{00} = -\frac{1}{2B}\frac{d^2A}{dr^2} + \frac{1}{4B}\frac{dA}{dr}\left(\frac{1}{A}\frac{dA}{dr} + \frac{1}{B}\frac{dB}{dr}\right) - \frac{1}{rB}\frac{dA}{dr} \quad (10)$$

$$R_{11} = \frac{1}{2A}\frac{d^2A}{dr^2} - \frac{1}{4A}\frac{dA}{dr}\left(\frac{1}{A}\frac{dA}{dr} + \frac{1}{B}\frac{dB}{dr}\right) - \frac{1}{rB}\frac{dB}{dr} \quad (11)$$

$$R_{22} = \frac{1}{B} + \frac{r}{2B}\left(\frac{1}{A}\frac{dA}{dr} - \frac{1}{B}\frac{dB}{dr}\right) - 1 \quad (12)$$

$$R_{33} = \sin^2\theta\left[\frac{1}{B} + \frac{r}{2B}\left(\frac{1}{A}\frac{dA}{dr} - \frac{1}{B}\frac{dB}{dr}\right) - 1\right] = \sin^2\theta\, R_{22} \quad (13)$$

https://dx.doi.org/10.22161/ijaers.4.9.10 ISSN: 2349-6495(P) | 2456-1908(O)

If we denote with R the *Ricci Scalar* and with T_{ij} the generic component of the *Stress-Energy Tensor*, the *Einstein Field Equations* [1] can be written as follows:

$$R_{ij} - \frac{1}{2}Rg_{ij} = \frac{8\pi G}{c^4}T_{ij} \tag{14}$$

If we impose that, outside the mass that produces the field, there is the "absolute nothing" (neither matter nor energy), the first member of *(14)*, that represents the so-called *Einstein Tensor*, must vanish. Consequently, we have:

$$R_{ij} - \frac{1}{2}Rg_{ij} = 0 \tag{15}$$

From *(15)*, exploiting the fact that the Einstein Tensor and the Ricci Tensor are trace-reverse of each other, we have:

$$R_{ij} = 0 \tag{16}$$

From *(10)*, *(11)* and *(16)*, we immediately obtain:

$$-\frac{1}{2AB}\frac{d^2A}{dr^2} + \frac{1}{4AB}\frac{dA}{dr}\left(\frac{1}{A}\frac{dA}{dr} + \frac{1}{B}\frac{dB}{dr}\right) - \frac{1}{rAB}\frac{dA}{dr} = 0 \tag{17}$$

$$\frac{1}{2AB}\frac{d^2A}{dr^2} - \frac{1}{4AB}\frac{dA}{dr}\left(\frac{1}{A}\frac{dA}{dr} + \frac{1}{B}\frac{dB}{dr}\right) - \frac{1}{rB^2}\frac{dB}{dr} = 0 \tag{18}$$

From *(17)* and *(18)*, we have:

$$\frac{dB}{B} = -\frac{dA}{A} \tag{19}$$

$$B = \frac{K_1}{A} \tag{20}$$

The value of the constant K_1 can be deduced by imposing that, at infinity, the ordinary flat metric must be recovered. In other terms, we must impose the following condition:

$$\lim_{r\to\infty} A(r) = \lim_{r\to\infty} B(r) = 1 \tag{21}$$

From *(20)*, taking into account *(21)*, we obtain:

$$B = \frac{1}{A} \tag{22}$$

$$g_{00}g_{11} = -1 \tag{23}$$

From *(16)* and *(12)* we have:

$$A + \frac{rA}{2}\left[\frac{1}{A}\frac{dA}{dr} - A\frac{d}{dr}\left(\frac{1}{A}\right)\right] - 1 = 0 \tag{24}$$

$$A + r\frac{dA}{dr} - 1 = \frac{d}{dr}(rA) - 1 = 0 \tag{25}$$

$$A = 1 + \frac{K_2}{r} \tag{26}$$

It is worth highlighting that, at this point, we could already deduce the "original" *Schwarzschild Solution* [2], without assigning any particular value to the constant K_2.

The value of K_2 can be directly deduced by resorting to the so-called *Weak Field Approximation*. If we denote with ϕ the *Gravitational Potential*, we can write:

$$A = g_{00} = \left(1 - \frac{\phi}{c^2}\right)^2 \cong 1 - 2\frac{\phi}{c^2} = 1 - \frac{2MG}{rc^2} \tag{27}$$

From *(26)* and *(27)*, we immediately deduce:

$$K_2 = -\frac{2MG}{c^2} \tag{28}$$

From *(22)* and *(27)*, we have:

$$B = \frac{1}{1 - \frac{2MG}{rc^2}} \tag{29}$$

At this point, the metric can be immediately written. However, in order to directly obtain a more compact form, we can denote with R_s the value of r that makes the metric singular (the so-called *Schwarzschild radius*):

$$\frac{2MG}{c^2} = R_s \tag{30}$$

From *(27)*, *(29)* and *(30)* we finally obtain:

$$ds^2 = \left(1 - \frac{R_s}{r}\right)c^2dt^2 - \frac{dr^2}{1 - \frac{R_s}{r}} - r^2(d\theta^2 - \sin^2\theta\, d\varphi^2) \tag{31}$$

II. ALTERNATIVE DERIVATION

Although the space we are allowed to perceive is curved, since it is identifiable with a hyper-sphere whose radius depends on our state of motion [3] [4], the Universe in its entirety, assimilated to a 4-ball, is considered as being flat [5]. All the points are replaced by straight line segments: in other terms, what we perceive as being a point is actually a straight-line segment crossing the centre of the 4-ball. [4] At the beginning (no singularity), we hypothesize that the Universe, whose radius equates the Schwarzschild Radius, is homogeneously filled with matter [6].

The scenario is qualitatively depicted in *Figure 4*.

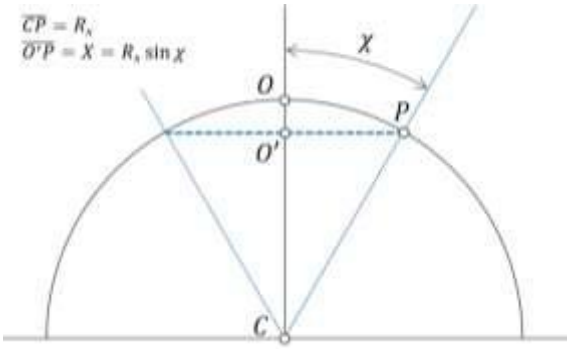

Figure 1. Initial Scenario

https://dx.doi.org/10.22161/ijaers.4.9.10 ISSN: 2349-6495(P) | 2456-1908(O)

If we denote with X the predicted radius (the straight-line segment bordered by O' and P in *Figure 1*), and with χ the angular distance between P and O (as perceived by an ideal observer placed in C), we can write:

$$X = R_s \sin\chi \tag{32}$$

The measure of the corresponding great circumference, denoted by C_X, is provided by the following banal relation:

$$C_X = 2\pi X = 2\pi R_s \sin\chi \tag{33}$$

From *(32)* we immediately deduce:

$$\chi = \arcsin\left(\frac{X}{R_s}\right) \tag{34}$$

If we denote with l the measured radius (the arc bordered by O and P in *Figure 1*), from *(34)* we have:

$$dl = R_s d\chi = \frac{dX}{\sqrt{1-\left(\frac{X}{R_s}\right)^2}} \tag{35}$$

At this point, the *Friedmann–Robertson–Walker* metric can be finally written:

$$ds^2 = c^2dt^2 - \frac{dX^2}{1-\left(\frac{X}{R_s}\right)^2} - X^2(d\theta^2 + \sin^2\theta\, d\varphi^2) \tag{36}$$

Let's now suppose that all the available mass may be concentrated in the origin. According to our model [6], the spatial lattice undergoes a deformation that drags O to C.

The scenario is qualitatively depicted in *Figure 2*.

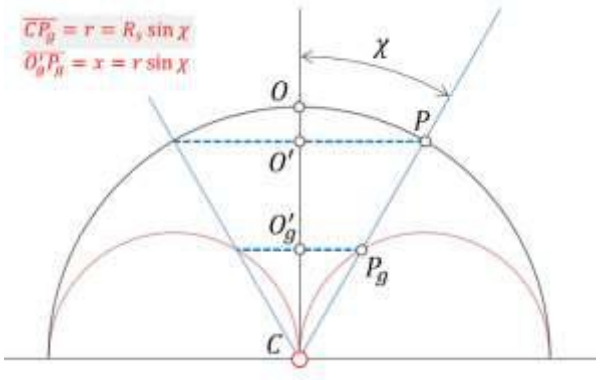

Figure 2. Singularity

We hypothesize that the singularity does not influence the measured distance (the proper radius): in other terms, if the angular distance between whatever couple of points does not undergo any variation, the corresponding measured distance remains the same [6]. In order to satisfy this condition, the radial coordinate (the segment bordered by C and P_g in *Figure 2*) must abide by the following relation:

$$r = R_s \sin\chi \tag{37}$$

In fact, it can be instantly verified that:

$$\sqrt{\left(\frac{dr}{d\chi}\right)^2 + r^2} = R_s \tag{38}$$

The predicted radius (the segment bordered by O'_g and P_g in *Figure 2*), denoted by x, undergoes a reduction. Taking into account *(37)*, we can immediately write:

$$x = r\sin\chi = R_s \sin^2\chi = X\sin\chi = \frac{X^2}{R_s} \tag{39}$$

The measure of the corresponding great circumference, denoted by C_x, is provided by the following banal relation:

$$C_x = 2\pi x = 2\pi X \sin\chi \tag{40}$$

We can now write the following metric:

$$ds^2 = c^2dt^2 - \frac{dX^2}{1-\left(\frac{X}{R_s}\right)^2} - \frac{X^4}{R_s^2}(d\theta^2 + \sin^2\theta\, d\varphi^2) \tag{41}$$

Exploiting *(39)*, the angular distance can be evidently expressed as follows:

$$\chi = \arcsin\left(\sqrt{\frac{x}{R_s}}\right) \tag{42}$$

Consequently, we have:

$$dl = R_s d\chi = R_s d\left[\arcsin\left(\sqrt{\frac{x}{R_s}}\right)\right] = R_s \frac{d\left(\sqrt{\frac{x}{R_s}}\right)}{\sqrt{1-\left(\sqrt{\frac{x}{R_s}}\right)^2}} \tag{43}$$

$$dl = \frac{1}{2}\frac{\sqrt{\frac{R_s}{x}}dx}{\sqrt{1-\frac{x}{R_s}}} \tag{44}$$

Taking into account *(44)*, we can write the metric in *(41)* as a function of x:

$$ds^2 = c^2dt^2 - \frac{1}{4}\frac{\frac{R_s}{x}dx^2}{1-\frac{x}{R_s}} - x^2(d\theta^2 + \sin^2\theta\, d\varphi^2) \tag{45}$$

According to our model [6], once again, the proper radius remains the same, notwithstanding the singularity: on the contrary, the predicted radius, as well as the corresponding great circumference, undergoes a contraction [6] [7].

Let's now suppose that we want to "warp" (not parameterize) the previous metric. If we impose that the measure of the predicted radius must remain the same (if

https://dx.doi.org/10.22161/ijaers.4.9.10 ISSN: 2349-6495(P) | 2456-1908(O)

we assign a greater value to the "quantum of space"), we have to consequently increase the value of the proper radius. Obviously, in order to keep the speed of light constant, we are forced to assign a smaller value to the "quantum of time" (in particular, the more we approach the singularity, the more time must flow slowly) [7] [8]. Taking into account the fact that the relation between the initial predicted radius and the reduced one is expressed by *(39)*, we obtain the following metric, in which time, very evidently, is no longer considered as being absolute:

$$ds^2 = \left(\frac{X}{R_s}\right)^2 c^2 dt^2 - \left(\frac{R_s}{X}\right)^2 \frac{dX^2}{1-\left(\frac{X}{R_s}\right)^2} - X^2(d\theta^2 + \sin^2\theta\, d\varphi^2) \tag{46}$$

Obviously, the metric we have just obtained is far different from the Schwarzschild solution. Suffice it to notice that, very evidently, both *X* and *x* cannot tend to infinity.

In order to recover the Schwarzschild solution, we have to carry out a parameterization [6]. On this purpose, we need to find two new coordinates, denoted by $R^*(\chi)$ and $r^*(\chi)$, that may satisfy the following relations:

$$r^* = R^* \sin\chi \tag{47}$$

$$dl_{r^*} = \sqrt{r^{*2} + \left(\frac{dr^*}{d\chi}\right)^2}\, d\chi = \sqrt{R^{*2} + \left(\frac{dR^*}{d\chi}\right)^2}\, d\chi = dl_{R^*} \tag{48}$$

From *(47)* we have:

$$\frac{dr^*}{d\chi} = \frac{dR^*}{d\chi}\sin\chi + R^*\cos\chi \tag{49}$$

$$r^{*2} + \left(\frac{dr^*}{d\chi}\right)^2 = R^{*2} + \left(\frac{dR^*}{d\chi}\right)^2 \sin^2\chi + 2R^*\frac{dR^*}{d\chi}\sin\chi\cos\chi \tag{50}$$

Very evidently, if the derivative of R^* is null, imposing $R^*(0)=R_s$, we instantly recover *(37)*. On the contrary, if the derivative of R^* is not null, from *(50)* we easily deduce:

$$2\tan\chi\, d\chi = \frac{dR^*}{R^*} \tag{51}$$

Imposing $R^*(0)=R_s$, from *(51)* we immediately obtain:

$$R^* = \frac{R_s}{\cos^2\chi} \tag{52}$$

From *(52)*, we have:

$$\sin\chi = \sqrt{1 - \frac{R_s}{R^*}} \tag{53}$$

$$dR^* = 2R_s\frac{\sin\chi}{\cos^3\chi}d\chi \tag{54}$$

From *(48)*, *(52)* and *(54)*, denoting with l^* the parameterized proper radius (we must bear in mind that, according to the model herein proposed, the singularity does not influence the measured distance), we obtain:

$$dl_{R^*} = dl_{r^*} = 2R_s\frac{\sin\chi}{\cos^3\chi}\sqrt{1+\frac{1}{4\tan^2\chi}}\,d\chi = \sqrt{1+\frac{1}{4\tan^2\chi}}\,dR^* = dl^* \tag{55}$$

From *(54)* and *(55)* we have:

$$\lim_{\chi\to\pi/2}\frac{dl^*}{dR^*} = 1 \tag{56}$$

Taking into account *(47)* and *(52)*, the parameterized predicted radius is provided by the following relation:

$$X^* = R^*\sin\chi = R_s\frac{\sin\chi}{\cos^2\chi} = r^* \tag{57}$$

As for the corresponding great circumference, we have:

$$C_{X^*} = 2\pi X^* = 2\pi r^* \tag{58}$$

From *(54)* and *(57)* we have:

$$\lim_{\chi\to\pi/2}\frac{X^*}{R^*} = 1 \tag{59}$$

Taking into account *(47)* and *(52)*, the parameterized reduced predicted radius can be written as follows:

$$x^* = r^*\sin\chi = R_s\tan^2\chi = R^* - R_s \tag{60}$$

As for the corresponding great circumference, we have:

$$C_{x^*} = 2\pi x^* = 2\pi(R^* - R_s) \tag{61}$$

In *Figure 3* a useful comparison between old and new (parameterized) coordinates is qualitatively displayed.

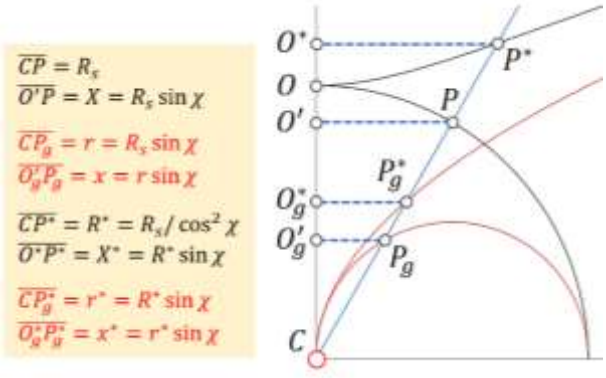

Figure 3. Singularity: Comparison Between Coordinates

https://dx.doi.org/10.22161/ijaers.4.9.10 *ISSN: 2349-6495(P) | 2456-1908(O)*

In *Figure 4*, the very interesting scenario we obtain if $\chi=\pi/4$ is qualitatively depicted.

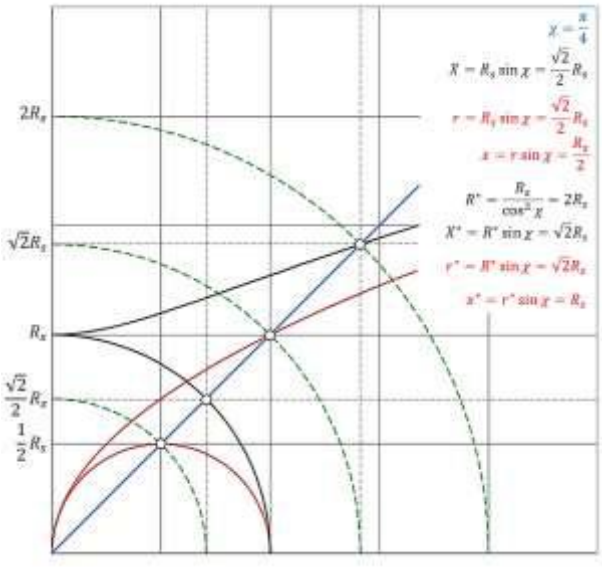

Figure 4. Singularity: particular case ($\chi=\pi/4$)

By virtue of *(55)* and *(57)*, when mass is evenly spread on the hypersphere with which we identify the Universe we are allowed to perceive (actually, when matter homogeneously fills the 4-ball with which we identify the Universe in its entirety), the parameterized distance in *(36)* acquires the underlying compact form:

$$ds^{*2}=c^2dt^{*2}-dl^{*2}-X^{*2}(d\theta^2+\sin^2\theta d\varphi^2) \qquad (62)$$

Obviously, we have replaced *t* with *t**. Time, in fact, shows necessarily trace of the parameterization we have carried out. On this subject, if we consider a null geodesic (a light-like interval) in the equatorial plane, from *(62)* we have:

$$cdt^*=dl^* \qquad (63)$$

The previous banal relation clearly shows that, if space is subjected to a parameterization, being *c* a constant, time must be parameterized too.

Far from the origin (when χ tends to $\pi/2$), taking into account *(56)* and *(59)*, the metric in *(62)* (no singularity) acquires the following "flat" form:

$$ds^{*2}=c^2dt^{*2}-dR^{*2}-R^{*2}(d\theta^2+\sin^2\theta d\varphi^2) \qquad (64)$$

Let's now concentrate in the origin all the available mass. According to our model, once again, the proper radius remains the same, notwithstanding the singularity: on the contrary, the predicted radius, as well as the corresponding great circumference, undergoes a contraction. However, following the same line of reasoning we have exploited in order to deduce *(46)*, imposing that the measure of the predicted radius must remain the same (if we assign a greater value to the "quantum of space"), we have to consequently increase the value of the proper radius. Consequently, in order to keep the speed of light constant, we are forced to assign a smaller value to the "quantum of time" (in particular, the more we approach the singularity, the more time must flow slowly). Since the relation between the initial predicted radius and the reduced one, both parameterized, is expressed by *(47)*, taking into account *(53)*, by "warping" *(65)* we obtain the following metric, that represents a Schwarzschild-like Solution:

$$ds^{*2}=\left(1-\frac{R_s}{R^*}\right)c^2dt^{*2}-\frac{dR^{*2}}{1-\frac{R_s}{R^*}}-R^{*2}(d\theta^2+\sin^2\theta d\varphi^2) \qquad (65)$$

REFERENCES

[1] Einstein, A. (1916). Relativity: The Special and General Theory (translated by R. W. Lawson, 1920). Henry Holt and Company, New York. Retrieved from https://archive.org/details/cu31924011804774

[2] Schwarzschild, K. (1919). Über das Gravitationsfeld eines Massenpunktes nach der Einsteinschen Theorie. Sitzungsber. der Deutschen Akad. der Wiss. zu Berlin, 189-196 (On the Gravitational Field of a Mass Point according to Einstein's Theory, translat. by Antoci and Loinger, 1999). Retrieved from http://zelmanov.ptep-online.com/papers/zj-2008-03.pdf

[3] Cataldo, C. (2016). Faster than Light: again on the Lorentz Transformations. Applied Physics Research, 8(6), 17-24. http://dx.doi.org/10.5539/apr.v8n6p17

[4] Cataldo, C. (2017). From the Oscillating Universe to Relativistic Energy: a Review. Journal of High Energy Physics, Gravitation and Cosmology, 3, 68-77. http://dx.doi.org/10.4236/jhepgc.2017.31010

[5] Cataldo, C. (2017). From General Relativity to A Simple-Harmonically Oscillating Universe, and Vice-Versa: a Review. Applied Physics. Research, 9(1), 86-92. http://dx.doi.org/10.5539/apr.v9n1p86

[6] Cataldo, C. (2017). Gravity and the Absoluteness of Time: a simple qualitative model. App. Phys. Res., 9(2), 42-52. http://dx.doi.org/10.5539/apr.v9n3p46

[7] Cataldo, C. (2017). A short discussion on the Gravitational Redshift in the light of an alleged local variability of the Planck Constant. Journal of Applied Mathematics and Physics, 5, 1001-1008. https://doi.org/10.4236/jamp.2017.55087

[8] Cataldo, C. (2017). On the Absoluteness of Time. Applied Physics Research, 9(3), 46-49. https://doi.org/10.5539/apr.v9n3p46

https://dx.doi.org/10.22161/ijaers.4.9.11 *ISSN: 2349-6495(P) | 2456-1908(O)*

Assessment of Factors Responsible for the Choice of Contractors' Prequalification Criteria for Civil Engineering Project: Consultants' Perspective

Akinmusire Adeleye Ola*, Alabi Olumuyiwa Michael, Olofinsawe Moses Akinloye

Quantity Surveying Department, Faculty of Environmental Studies, Rufus Giwa Polytectnic, Owo, Ondo State, Nigeria.

Abstract— *It is not uncommon, during contractor selection process, for prequalifier's decisions to be informed by certain parameters. In the light of this, the choice of the criteria to be eventually adopted depends on factors that play complimentary role when the contractor is to be selected. Therefore, this study assesses the factors that determine the choice of contractors' prequalification criteria for civil engineering project. The purpose is to bring the unrecognised factors into limelight by establishing the degree of their relevance on the choice of contractor's prequalification criteria as well as ascertaining their importance to meeting stakeholder's objectives. The objectives include identifying the factors which determine the choice of contractors' prequalification criteria for civil engineering project and assess the importance of the factors to meeting stakeholders' expectation. The study employ well-structured questionnaire distributed to various category of respondents comprising Civil/Structural Engineers, Quantity Surveyors and Architects engaging in civil engineering project. It adopts percentile, mean item score (MIS) and relative importance index (RII) in the analysis of the data derived from the retrieved questionnaire. Result indicates that, apart from Civil/Structural Engineers, employment into civil engineering organizations favours Quantity Surveyors than Architects. Construction of building is paramount among civil engineering organizations with little involvement in railway project. The choice of contractors' prequalification criteria for civil engineering project is dictated by a number of factors with project type emerging the most influential. Importance of the factors touches the client, consultants and contractor. It recommends that Quantity Surveyors should embrace continuous professional development. Factors influencing the choice of contractors' prequalification criteria must be duly considered before taking final decision on the criterion/criteria to adopt in choosing the contractor for civil engineering project prioritizing project type.*

Keywords— Contractor's prequalification criteria, civil engineering project, project type.

I. BACKGROUND

Responsibility of the construction industry is multi-dimensional. Part of which include meeting the demands and needs of other industries as well as people in the society through products emanating from different project categories. Its products are actually in form of projects derived from building, civil engineering and heavy/industrial engineering [1]. Actualisation of desire to acquire construction project require the involvement of construction professionals irrespective of the project category. Such professionals include Architects, Quantity surveyors and Civil/Structural engineers who do face many challenges bordering on prequalification, tendering and selecting a contractor in the course of performing their responsibilities of appropriately advising the client. These professionals have been differently described by some authors focusing on their duties based on the training received. For instance, [2] and [3] opined that Quantity Surveyor is professionally trained, qualified and experienced in dealing with problems relating to construction cost management and communication in the construction industry. On the other hand, [4] stated that Architect is a professional who creates and construct building, consultation, analysis and design necessary for creation of building and their environment. According to [5], Civil engineer is professional trained to deal with the design, construction, and maintenance of the physical and naturally built environment, including works like roads, bridges, canals, dams, and buildings. In spite of its existing numerous purposes, prequalification can be adopted at early stages of the bidding process in order to select a group of potential contractors. Adopting bid prequalification process

https://dx.doi.org/10.22161/ijaers.4.9.11 *ISSN: 2349-6495(P) | 2456-1908(O)*

for contractors, project owners can benefit in several ways. If the bid specifications for a contract only require the selection of the lowest-cost bidder, project performance and quality could be jeopardized. Construction projects are risky, and always prone to uncertainties. In view of this, [6] suggested a systematic contractor prequalification process in order to reduce the risks and uncertainties. The process of selecting contractors for a proposed project obviously involve major decision making which may influence the progress and success of any construction project [7]. The work of some authors reveal that contractors can be selected based on some criteria from which client choose for a proposed project [8] and [9]. However, literatures observe that adoption of specific contractor prequalification criterion/criteria demand consideration of some factors. This leads to suggesting that decision makers should consider project characteristics, conditions of the construction market, and project participants in order to enhance the effectiveness of such criterion/criteria. Execution of the decision taken during contractors' prequalification exercise is expected to yield two major results of reducing risk of project failure and increase the chances of project success so as to meet stakeholders' expectations. The effect of project failure, which usually manifest in terms of high initial cost of projects, project inflation, poor quality of works, delay in project delivery and abandonment, has been the principal determinants of the image of Nigeria construction industry. Therefore, chances of achieving a successful construction project may become narrow if client and consultants concentrate on determining the prequalification criteria to be adopted in selecting the contractor for such project. A review of literatures indicate that a lot of research work has been done in the area of prequalification of contractors with much emphasis on the criterion/criteria for selecting the contractor perceived to be the most suitable to undertake the contract for the construction of both building and civil engineering projects [9]; [10]; [8]; and [11]. However, the aspect of factors that influences the choice of the criterion/criteria, which needs proper attention, has not been delved into resulting to dearth of research effort in this area. According to Oforeh (2006) civil engineering projects posses special characteristics demanding peculiar resources for implementation. It is against this background that this research seeks to assess the factors that determine the choice of contractors' prequalification relative to civil engineering project. This work reflects various factors and the degree of their influence in making the choice of contractors' prequalification criterion/criteria focusing civil engineering project. The result is an eye opener to construction industry participants, especially client and consultants saddled with the responsibility of selecting contractors, as it enables them to appreciate the potential ability of the factors that determine the choice of contractors' prequalification for civil engineering project. It also provides data for further studies and an important tool to compare civil engineering project with other category of construction projects in the construction industry.

II. AIM AND OBJECTIVES OF THE STUDY

The aim of the study is to assess the factors responsible for the choice of contractors' prequalification criteria for civil engineering project. However, the specific objectives are as follows:

i. to assess the factors which determine the choice of contractors' prequalification criteria for civil engineering project; and
ii. to evaluate the importance of the factors determining the choice of contractors' prequalification criteria for civil engineering project to meeting stakeholders' expectation

III. REVIEW OF PREVIOUS RELATED STUDIES

3.1 Brief perception on contractors' prequalification criteria and project performance

Construction project development usually witness several decision making exercise. One of such decisions is in respect of selecting the appropriate bidders for a particular project in the face of adversity and uncertainty which must be overcame. No matter how meticulous the development of the contract, poor selection of the contractor(s) to execute the work will surely magnify the problems encountered on the project. In order to overcome these problems, a competent contractor who will be able to complete the project within cost, time and quality is required. This can be achieved through prequalifying contractors prior to the bidding process which is the first stage in the selection process and then through evaluation of tenders. Contractor selection exercise is incomplete without prequalification which is the process of screening construction contractors by project owners or their representatives according to a predetermined set of criteria deemed necessary for successful project performance. The criteria adopted to prequalify contractors are characterized by significant attributes according to [12]. This is often to determine the contractor's competence or ability to participate in the project bid. It implies that there must be a set of principles

https://dx.doi.org/10.22161/ijaers.4.9.11 *ISSN: 2349-6495(P) | 2456-1908(O)*

(criteria) laid down upon which the standard of acceptance and performance are to be measured even though such criteria varies in emphasis according to the characteristics of the project [13]. Performance of a project in the industry is a source of concern to both public and private sector clients whose expectations includes timely project completion within budget, safety and quality standards. These variables constitute overall client's satisfaction ingredients and stakeholders' expectations. [14] defines performance as monitoring and controlling all projects on regular basis. Failure of any construction project in the industry is mainly related to the problems and failure in respect of performance. [15] remarks that performance problems are in large construction industry due to many reasons such as incompetent contractors, poor estimation, change management, social and technological issues, site related issues, and improper techniques. Civil engineering project is very complex having wide range of different clients and contractors which comprises of public and private clients, main contractors, civil engineers and construction professionals operating within the construction industry. Activities in the industry are being carried out on project basis and could be within an organization [16].

3.2 Factors responsible for the choice of contractors' prequalification criteria for civil engineering project

Customariy, evaluation of contractors is often performed by construction industry professionals using their accumulated experience and judgment. Although, there are variations in the amount of effort and time expended in the process, often without an understanding of how such variations influence the project outcome. An important step in evaluation is to examine contractor's system for handling project information relating to work tasks. Contractor's approach to safety and what actions taken to achieve desired results are also usually scrutinized. All these are to ensure the emergency of the most reliable contractor and preventing the contract getting to a wrong hand. Many parameters have been noticed to come to play in an attempt to determine the contractors that would proceed to the financial bid stage of the selection process. Apart from meeting the requirement of predetermined prequalification criteria, there are other factors considered during contractors' screening exercise before final decision is taken. The following are most of the key factors usually considered when making the choice of contractors' prequalification criterion/criteria.

3.2.1 Project size and complexity

Every construction project is characterized by specific size and complexity leading to describing a project as small or big as well as simple or otherwise. Possession of peculiar features or presence of certain elements has been observed as basis for determining whether a construction project is complex or not. For instance, [17] opines that project complexity stemmed from unclear definition of objectives and the type and standard of knowledge/skill needed for its erection. [18] adds that complex projects have a high degree of disorder and instability. They are sensitive to small changes and are typically dynamic. A large and complex project may have some processes that will have to be iterated several times for the purpose of clear define and meeting stakeholders' requirements.

3.2.2 Client type

The construction industry is apparently endowed with different kind of project owners, comprising public and private organizations as well as individuals. The client is extremely important to the extent that no construction project can exist without a client who initiates and plays significant role of financing all activities in the process of achieving any construction project. [19] opine that little work has been done in the aspect of studying the performance of clients in the construction industry in spite of their indispensability and huge responsibilities. It states that construction industry mainly focused on contractors and supply chain neglecting the performance of client which has not been clearly investigated especially in the developing countries.

3.2.3 Experience of consultants

Consultants in the construction industry are many, each performing specific role at preconstruction, during construction and post construction stages of projects. They ensure that project is completed to the right quality as indicated in the technical specification and standards without running afoul of the time and cost. Some of the diverse roles of consultant in the process of acquiring project include reviewing and updating details, monitoring contractor's operations to ensure timely commencement of operations [20]. Bearing in mind that actualisation of construction project involves different developmental stages; consultant is expected to demonstrate a clear understanding of client's objectives, the project, tender process, construction success, and technical requirement of project.

3.2.4 Project cost

https://dx.doi.org/10.22161/ijaers.4.9.11 *ISSN: 2349-6495(P) | 2456-1908(O)*

No construction project exists without corresponding cost which is either pre or post determined in the life of the project. In most cases, construction project cost is determined before construction commences. This is to enable the client to have an idea of the financial implication of the project in addition to the fact that cost is a major aspect of the terms of the agreement between the client and contractor. According to [21] project cost evidently ranks among the important parameters determining the success of a project. In spite of the high degree of importance attached to project cost by client, contractor and consultants, completion of project within estimated cost is very rare. This situation is peculiar to virtually all categories of projects in the construction industry [22]. Project cost, having been determined, is expected to be sufficient to execute the project from start to finish. However, construction project can vary from extremely profitable to barely worth it and sometimes end up costing the contractor more than what he is getting paid to complete it. Evidently, client is happy when paying no extra money on project and the contractor getting paid as at when due. Therefore, cost of a project must be managed so that contractors do not suffer while carrying out different projects because contractor is willing to finish project on time.

3.2.5 Environmental factor

The environment where construction project is located feels the impact of the contractor's activities. According to Youker (1992) cited in [23], construction project is affected by elements that are situated outside the confines of the project. It lists a sizeable number of these elements and note that the elements constitute threat to project success and show different degree of influence on projects. The work of Bennette (1991) referenced in [23] indicate that construction activities cannot take place without interference from environmental factors which are capable of straining a successful completion of construction project. Having identified the various environmental factors confronting construction project, it advised that environmental factors should not be neglected in the process of acquiring a construction project.

3.2.6 Duration of project

How long it will take a construction project to come to reality is one of the important variables the client likes to know and forms part of the terms of agreement between the client and contractor. The period within which a construction project must be achieved or delivered constitute part of the benchmarks for judging the performance of such project [24]. At an early stage in the life of a project, determining the contract duration is one of the critical issues to address because of its importance to assessing the progress and performance of a project as well as the efficiency of the project organization. In spite of the enormity of the research work in the area of construction project duration, [25] submit that construction project still encounter a high degree of uncertainty as far as timely completion is concerned. One of the literatures reviewed in [26] trace the criticism faced by construction industry to failure to complete project on time.

3.2.7 Project type

There are different kinds of construction project delivered by the construction industry according to [27]. They fall into three distinct categories of building, civil and heavy/industrial engineering demanding specific method of construction while execution depends on resource availability, work quantity and complexity of work [1] and [28]. There are obviously different kinds of civil engineering project as listed in [29]. Project type provides a view of the quality the project can be estimated prior to starting of the project or during execution of the project.

3.2.8 Speed of construction

According to Wikipedia, construction is the process of translating designs into reality through involvement of the design team and a contractor selected by means of bidding. In today's fast paced construction environment, clients opt for fast track construction in order to enhance achievement of their intention. To contractors, speed enhances profitability because project is completed without delay and contractor stay on site not more than envisaged. In addition, ability of constructing faster and completing projects on time objectively reflect the capacity of contractor to organize and control site operations, optimally allocate resources and manage the information flow among sub contractors. Construction speed was utilized as a response variable.

3.2.9 Socio-political factor

According to [30] no project exists in a vacuum but it is rather subject to an array of influences from regulatory control to industrial intervention. [31] states that construction project is affected by the social/cultural practices of the people where the project is located. This has to do with the peoples' customs, lifestyles and values believed to be the significant features of a society. Similarly, [32] observe that social/cultural aspect of project

https://dx.doi.org/10.22161/ijaers.4.9.11 *ISSN: 2349-6495(P) | 2456-1908(O)*

environment relate to numerical size, educational standard, beliefs, language and disposition towards social responsibilities of the people. Consequently, the political environment of a project is concerned with the role played by the government as client, national economy and construction environment regulators. This is done via policies, enactment of laws that are capable of dictating the happenings within the construction industry. Every community apparently exhibit peculiarly different socio-political lifestyles which is potentially capable of influencing the operations of organizations carrying out construction activities in the community [23]. Therefore, [30] opine that contractors of construction project will take cognisance of political aspect that can lead to uncertain environment.

3.2.10 Location of project

In the construction industry, project customarily has specific location. This can be on land, sea rock or river bank. Each project location poses different challenges emanating principally from its nature in addition to geographical status leading to demanding different construction method and approach.

IV. RESEARCH METHODOLOGY

For the purpose of this study, 56 organisations dealing in civil engineering projects, spreading across the state capital of the six south west states of Nigeria were visited. These comprise Ikeja, Ibadan, Abeokuta, Oshogbo, Akure and Ado-Ekiti. Data were obtained by means of questionnaire which allowed respondents to choose from the options provided. The questionnaire was designed to elicit information in respect of respondent's area of professionalism and years of experience so as to set the stage for the study. However, respondents were requested to score the listed factors as well as the importance of the factors contributing to the choice of contractors' prequalification criteria relative to civil engineering project. In order to achieve the ordinal data needed, scoring was between 1 and 5 in each case with 1 accorded the least and 5 the highest rating. Percentile was adopted in analyzing the data relating to background information. Mean item score (MIS) was used to analyse the data in respect of the factors determining the choice of contractors' prequalification criteria using the formula stated below.

$$\text{Mean } \frac{\Sigma fx}{\Sigma f} = \frac{f1x1 + f2x2 \ldots\ldots + fnxn}{f1 + x2 \ldots\ldots + fn} \ldots \ldots \ldots (1)$$

Where:

Σ = Summation symbol

X = Class mark

F = Frequency

Moreover, relative importance index (RII) was utilized in case of the importance of the factors to meeting stakeholders' expectations. The formula stated below was adopted.

$$\text{Relative Importance Index (RII)} = \frac{\Sigma 5i=1RWR1RXR1}{\Sigma 5i=1XR1R} \ldots \ldots \ldots (2)$$

Where:

W1 = weight assigned to ith response; w = 1, 2, 3, 4 and 5 for i = 1, 2, 3, 4 and 5 respectively

X1 = frequency of ith response

i = response category index = 1, 2, 3, 4 and 5 for very low, low, moderate, high and very high respectively.

It must be noted that results were ranked in both cases in accordance with their magnitude and presented in tables.

V. RESULTS

5.1 Background information

A total of 107 valid questionnaires were retrieved from target respondents and analysed accordingly. The result of the question posted to identify the area of professional specialization of the consultants is presented in table 1. Over half (53%) are Civil/Structural Engineers while about 33% are Quantity Surveyors. Less than one-quarter (14%) are Architects. This result indicates that Civil/Structural Engineers dominate the organizations visited with reasonable number of Quantity Surveyors and few Architects. However, the presence of Architects in this case may not be unconnected with the likelihood of combining both building and civil engineering projects so as to improve the chances of getting jobs. In order to establish the length of years already spent in the respondents' place of work, table 2 show that majority (49) already spent between 11 and 20 years. Only 22 record between 21 and 30 years of experience while 27 respondents indicate 10 years and below. Few (9) of the respondents have their years of experience established between 31 and 50 years range. The average year of experience of the respondent is about 17 years. This is considered sufficient to acquire relevant experience to justify their competence to provide the reliable data needed in this study.

https://dx.doi.org/10.22161/ijaers.4.9.11 *ISSN: 2349-6495(P) | 2456-1908(O)*

Table.1: Profession of respondents

Consultants	F	%
Quantity surveying	35	32.71
Architecture	15	14.02
Civil/Structural Engineering	57	53.27
Total	**107**	**100.00**

Table.2: Respondents' years of experience

Years	F	X	FX
Less than 10years	27	5	135
11-20years	49	15.5	760
21-30years	22	25.5	561
31-40years	7	35.5	249
41-50years	2	45.5	91
Total	**107**	**127**	**1796**

Mean= $\frac{1796}{107}$ = 16.79 ≈ 17years.

Consequent upon response to the question posted to establish the level of respondents' involvement in some selected civil engineering projects believed to be common in the target towns, table 3 depict that construction of building polls the highest percentage (55%). This is followed by road construction which scored about 27%. Bridge construction accounted for 10% while construction of dam and railway poll approximately 6% and 2% respectively. The result indicates that the respondents mostly involve in building projects probably because contract for other project types are not easy to win. It can be advanced that building project demand the input of an Architect leading to forming the reason for the engagement of Architects by the civil engineering organizations. The level of involvement of the respondents in dam and railway project is low meaning that these are rarely undertaken.

Table.3: Type of project undertaken

Type of project	F	%	Cum %
Road construction	29	27.1	27.1
Building construction	59	55.1	82.2
Dam construction	6	5.6	87.9
Railway construction	2	1.9	89.7
Bridge construction	11	10.3	100
Total	**107**	**100**	

5.2 Factors responsible for the choice of contractors' prequalification for civil engineering project

From table 4, the mean item score of project type is estimated at 4.50 thereby ranking first. This is followed by project type with mean item score of 4.40 leading to ranking second. Consultants' experience and size/complexity of project ranks third and fourth having mean item score of 4.34 and 4.13 respectively. Speed of construction and environmental factor rank fifth and sixth with mean item score of 4.10 and 4.04 respectively. The mean item score of project duration and location is 4.00 and 3.92 leading to ranking seventh and eighth as shown in the table. Client type and socio-political factor has their mean item score estimated at 3.84 and 3.56. These factors came ninth and tenth in the ranking order. The least mean item score from the result is above the mid-point (2.50) of the scale used, meaning that all the listed factors are capable of determining the choice of contractors' prequalification criteria for civil engineering project. In spite of this, a general overview of the result indicate that the mean item score of most (7) of the factors range from 4.00 to 4.50 while that of the remaining three (3), fall between 3.56 and 3.92. This signifies that the factors command different degree of relevance when the choice of contractors' prequalification criteria for civil engineering project is to be made.

Table.4: Factors responsible for the choice of contractors' prequalification criteria

Options	Mean	Rank
project type	4.50	1
Project cost	4.40	2
Experience of consultants	4.34	3
Project size/complexity	4.13	4
Speed of construction	4.10	5
Environmental factor	4.04	6
Duration of project	4.00	7
Location of project	3.92	8
Client type	3.84	9
Socio-political factor	3.56	10

5.3 Importance of factors determining the choice of contractors' prequalification criteria for civil engineering project to meeting stakeholders' expectation

Outcome of the analysis carried out on the data relating to the importance of the factors determining the choice of contractors' prequalification criteria for civil engineering project is presented in table 5. The least and highest relative

https://dx.doi.org/10.22161/ijaers.4.9.11 *ISSN: 2349-6495(P) | 2456-1908(O)*

importance index of the listed options is estimated at 0.72 and 0.89 respectively. These values are considerably high compared to the mid-point (0.50) of the upper limit (1.00) as far as relative importance index is concerned. This shows that high degree of importance is derived from factors determining the criteria to be adopted in the selection of contractor for civil engineering project towards meeting expectations of stakeholders.

Table.5: Importance of factors determining the choice of contractors' prequalification criteria for civil engineering project

Options	RII	Rank
Acquisition of necessary experience by the client that can assist in similar future project and ability to absorb subsequent changes	0.89	1
Enhancement of contractors' ability to select competent subcontractors from a list provided by a client	0.87	2
Assists contractors to rely on previous track record and past experience in similar project	0.87	2
Contractors have opportunity to present recommendation from clients in respect of previously completed work	0.86	4
Creates platform for contractors to present proposed detailed programme of work for the project	0.86	4
Clients have the idea of the challenges the contractor will probably encounter while executing the project	0.85	6
Consultants are allowed to demonstrate the level of their knowledge about the project	0.84	7
Consultants are made to be aware of the likely challenges the contractor may encounter when executing the project	0.81	8
Clients are enabled to establish the level of consultant experience	0.81	8
Clients are enabled to have the idea of the quality the contractor will deliver	0.79	10
Early detection of contractors' weakness and identification of when to advice the client by consultants	0.77	11
Establishment of the team's competence by the client	0.76	12
Assists consultants to recommend contractors based on relevant track record and experience	0.72	13

VI. FINDINGS

Professionals in the field of Civil/Structural Engineering predominates organisations dealing in civil engineering project with considerable number of Quantity Surveyors and few Architects. This may be linked to the nature of the training accorded the professionals and project mostly undertaken by the organizations of employment. Besides, it can be deduced that delivery of civil engineering project demand the involvement of Quantity Surveyors than Architects, hence the degree of their employment into civil engineering organizations. The professionals have spent remarkable length of time in their respective organisation of employment, giving them enough opportunity to be involved in different kind of civil engineering project of different magnitude. This accords them opportunity to acquire relevant experience both in the process of selecting contractors and administration of civil engineering project. Also, the organizations engage mostly in construction of buildings, showing that activities within the organizations tend towards the demands of building projects. In spite of this, the organizations also engage in the delivery of civil engineering products. Therefore, it can be advanced that construction of road is paramount among the professionals compared to construction of bridges, dams and railway. Experience in the construction of bridge may not be unconnected with the road project undertaken by the professionals because of the likelihood of road crossing streams, swampy area and difficult terrains requiring construction of bridges. Furthermore, construction of railway is occasionally undertaken by the professionals. Hence, it can be advanced that railway construction is an uncommon civil engineering project leading to little involvement of the professionals in railway project. This implies that the professional are exposed to slim chances to acquiring experience in railway construction. However, project type is the most important factor to be considered when making the choice of contractors' prequalification criteria for civil engineering project. This signifies that there is possibility of different civil engineering project demanding specific contractors' prequalification criteria. Project cost is also an important yardstick determining the choice of contractors' prequalification criteria as far as civil

https://dx.doi.org/10.22161/ijaers.4.9.11 *ISSN: 2349-6495(P) | 2456-1908(O)*

engineering project is concerned. Hence, the contractors' prequalification criterion/criteria to be adopted for civil engineering project depend on the cost of the project. Experience of the consultants also counts when the choice of contractors' prequalification criteria is to be made for any kind of civil engineering project. This means that the experience acquired by consultants, which may be peculiar to specific civil engineering project type, also determine the choice of contractors' prequalification criteria. Apart from this, magnitude of civil engineering project may vary; therefore, size/complexity proves to be a good determinant of the choice of contractors' prequalification criteria. The choice of contractors' prequalification criteria also depends on the speed at which construction project is to be delivered. This means professionals pay attention to the eagerness of the client to see his/her project completed on or before the scheduled time expires and therefore would consider speed of construction. In addition, it can be inferred that potential users wish to start enjoying the facility as quickly as possible, even ahead the stipulated date. Bearing in mind that construction projects are usually confronted by environmental challenges which can negatively or positively affect their success, environmental factor also influence the choice of contractors' prequalification criteria for civil engineering project. The time allocated to starting and completing a construction project is among the factors agreed to influence the choice of contractors' prequalification criteria for civil engineering project, meaning that consultants place high premium on project duration. This infers that the period within which a project must be delivered forms part of the essential determinants of the choice of contractors' prequalification criteria for civil engineering project. Project location is also prominent among the factors considered as determinant of the choice of contractors' prequalification criteria for civil engineering project. This implies that taken the geographical location of project into account when making the choice of contractors' prequalification criteria is crucial. This may not be unconnected with the need to put into consideration the various pricing ingredients of the project locality when estimating project cost. Client type, which may be private or public, ranks among the important factor believed to influence the choice of contractors' prequalification criteria for civil engineering project. Consideration of client type, in this case may be in respect of client's characteristics which may be in terms of size and popularity. The socio-political nature of the environment where project is located command great relevance when making the choice of contractors' prequalification criteria for civil engineering project. The socio-political factors surrounding a project may differ from one place to another. Therefore, it can be deduced that socio-political factor can negatively or positively affect a project.

Factors determining the choice of contractors' prequalification criteria for civil engineering project showcase series of importance to stakeholders while meeting their expectations. In support of the view that contractors can be selected by either the client or his/her representatives, this study is of the opinion that project owner stands to acquire relevant experience that can assist in similar future project and enhance ability to absorb subsequent changes. Furthermore, ability of contractors to select competent subcontractors from a list provided by a client is also enhanced by factors determining the choice of contractors' prequalification criteria in respect of civil engineering project. Contractors are assisted to rely on previous track record and past experience in similar project in addition to having opportunity to present recommendation from clients in respect of previously completed work. Platform to present proposed detailed programme of work for project is created by factors that determine the choice of contractor selection criteria for civil engineering project. Also, clients are given opportunity to have the idea of the challenges the contractor will probably encounter in the process of project delivery while consultants are allowed to demonstrate the level of their knowledge about the project. Consultants are consequently made to be aware of the likely challenges the contractor may encounter when executing the project. Clients are also enabled to establish the level of consultants' experience which may depend on project type among other factors. This study equally indicates that project owner is enabled to have a prior knowledge of the quality the contractor will deliver at an early stage because contractors' weakness and identification of when to advice the client by consultants can be early detected through factors that determine the choice of contractor selection criteria for civil engineering project. Furthermore, opportunity to establish the team's competence is enjoyed by the client while consultants are assisted to recommend contractors based on relevant track record and experience.

VII. CONCLUSION AND RECOMMENDATIONS

Apart from Civil/Structural Engineers, specially trained in the field of engineering, Quantity Surveyor has greater role to play and more useful in civil engineering inclined organizations than Architects. Involvement and experience of the professionals varies according to project type. There

https://dx.doi.org/10.22161/ijaers.4.9.11 *ISSN: 2349-6495(P) | 2456-1908(O)*

is dearth of railway project leading to corresponding little experience by professionals engaging in civil engineering project. Therefore, it can be submitted that they are vast in construction of buildings and extremely little involvement in railway construction. Professionals are aware of the various factors determining the choice of contractors' prequalification criteria for civil engineering project. In spite of commanding varying degree of relevance, project type emerged the most influential factor as far as civil engineering project is concerned. It should be noted that this is not at the expense of other factors because they show absolutely high degree of influence in determining the choice of contractors' prequalification criteria in this regard. However, factors that determine the choice of contractors' prequalification criteria for civil engineering project are characterized by a number of importance. Scanning the importance of the factors, there is indication that its benefits fall into three dimensions. Hence, it is beneficial to project's key actors comprising owner, consultants and contractor by assisting them to identify appropriate criterion/criteria that can lead to emergence of competent and qualified contractor before awarding any contract. Consequently, it is important to recommend that Quantity Surveyors embrace participation in continuous professional development so as to fortify their relevance in civil engineering project. Also, because of the benefits derivable from the factors influencing the choice of contractors' prequalification criteria, the factors must be considered before making final decision on the choice of the criterion/criteria to be adopted for any civil engineering project. Consideration, in this case, must conform to the ranking order depicted in table 4. This will ultimately give room to balancing such criterion/criteria with attributes of the project and other relevant parameters.

REFERENCES

[1] Oforeh, E. C. (2006). The Cost Management of Heavy capital projects. Vol. 1; *Construction and Management. First editionCosines Nig. Limited*. 2006: 1-10.

[2] Cumingham, T. (2014). The work and skill of the Quantity Surveyor in Ireland – An introduction. Other resources. Available from http//arrowdit.ie/beschreoth. (Accessed 2017, March 17).

[3] Allan, A. and Keith, H. (2002). *Willis's Practice and Procedure for the Quantity Surveyor*, 11th Edition, BSP Professional Books, London.

[4] Massud, A. and Badiru, A. (2004). Project management for executing distance education. *Journal of professional issues in engineering education and practice, 1: 5-6.*

[5] WIKIPEDIA **https://en.wikipedia.org/wiki/Civil_engineering.** Accessed July 27, 2017.

[6] Molla, M. and Asa, E. (2015). Factors influencing contractor prequalification process in developing countries. *International journal of Architecture, Engineering and Construction, 4: 232-245.*

[7] Ajayi, O. M. and Ogunsanmi O. E. (2012). Decision maker's perceptions on contractor prequalification criteria. *Journal of contemporary research in business* 4(6): 174-180.

[8] Arazi, I., Mahmoud, S., and Mohamad, H. (2011). Decision criteria for selecting main contractors in Malaysia. *Research journal of applied engineering and technology*, 3 (12): 1358-1365.

[9] Ogunsemi D. R. and Aje I. O. (2005). A model for contractors Selection in Nigeria. *The Quantity Surveyor* 50(1), 3-7.

[10] Salama, M; Abd, E. A; EL, S. H and El, S. A. (2006, September 4-6). *Investigating the criteria for Contrators' Selection and Bid Evaluation in Egypt.* Conference Proceeding of 22nd Association of Researchers in Construction Management. Bimingham, UK: 531-540.

[11] Huang, X. (2011). An analysis of the selection of project contractor. *International Journal of Business Management*, 6(3): 184-189.

[12] Akinmusire, A. O. (2016). Potential attributes of contractors' prequalification criteria for civil engineering project: Essential tools for project administration. *American journal of construction and building materials*, 1(1): 15-23.

[13] Lam, K.C. Hu, T.S. Ng, S.T. Skitmore, M., and Cheung, S.O. (2005). A fuzzy neutral network approach for contractor prequalification. *Journal of Construction management and economics*,19(2)175-188.

[14] Thomas, G. A. (2002). Civil engineering for buildings. *Journal of San Diego historical society quarterly-winter*, 48 (1).

[15] Long, N. D. (2004). Large construction project in developing countries: A case study from Vietnam. *International journal of project management, 22: 553-561.*

[16] Kolawole, O. (2011). An assessment of housing infrastructural provision. *International journal of civil engineering, construction and management*, 2: 46-61.

https://dx.doi.org/10.22161/ijaers.4.9.11 *ISSN: 2349-6495(P) | 2456-1908(O)*

[17] Paul N. (2011). Is my Project Complex or Simple; That is the Question? Available from http://blog.parallelprojecttraining.com/project-management-articles/is-my-project-complex-or-simple-that-is-the-question/ (Accessed 20 – 07 – 2017).

[18] Dombkins, D. (2008). Contract for complex project: A renaissance of process, Booksurg publishing, Chaleston.

[19] Egbu, C. and Ilozor, B. (2007). Construction client and innovation: An understanding of their roles and impact. *Conference proceeding of CIB World building congress,* 2007: 3259-3267.

[20] Kwame, (2012). Performance of consultants on government project in Ghana. *International journal of business and social 4 research,* 2: 6.

[21] Memon, H. A., Rahman, A. I., Abdullah, R. M., Azis, A. A. and Rakyat, M. A. (2010). Factors affecting construction cost performance in project management projects: Case study of Mara large projects. Proceedings of post graduate seminar on engineering technology and social science, Center for graduate studies & research and innovation center, September, 29 – 30, 2010.

[22] Azhar, N., Farooqui, R. U., and Ahmed, S. M. (2008). Cost overrun factors in construction industry in Pakistan. *First international conference on construction in developing countries (ICCIDCI advancing and integrating construction education, research and practice)*

[23] Akanni, P. O., Oke, A. E. and Akpomiemie, O. A. (2015). Impact of environmental factors on building project performance in Delta State, Nigeria. *Journal of housing and building national research center*, 11: 91-97.

[24] Jha, K. N. (2013). Determinants of construction project success in India. *Topics in safety, risk, reliability and quality,* 23:119-146.

[25] Mohamed, D., Srour, F., Tabra, W. and Zayed, T. (2009). A prediction model for construction project time contingency. *Proceedings of construction research project, sponsored by construction institute of ASCE,* University of Washington, April 5-7, 2009.

[26] Bowen, P. A., Cattel, K. S., Hall, K. A., Edwards, P. J. and Pearl, R. G. Perceptions on time, cost and quality management on building projects. *The Australian journal of construction economics and building,* 2(2): 48-55. Available from http://www.icoste.org/ICMJ%20Papers/AJCEBVol2No2Bowen.pdf. Accessed July, 27, 2017.

[27] Barbara, J. J. (2004). *Construction management jump start.* London: San Francisco.

[28] Civil contractors federation (2010). *Resourcing the future national resources sector employment task force discussion:* 1-15.

[29] Lake, L. (2008). Civil engineering: *Microsoft encanta.*

[30] Thomas, E. U. and Martins, I. (2004). *Essentials of construction project management. First edition.* University of New South Wales press limited, Australia.

[31] Williams, W. (2002). Citizenship questions and environmental crisis in the Niger Delta: A critical reflection. Nordic J. Afr. Stud, 11 (3): 377-382.

[32] Engobo, E. (2009). Social responsibility in practice in the oil producing Niger Delta: Assessing corporations and government's actions. *Journal of sustainable development, Africa,* 11 (2): 113-115.

https://dx.doi.org/10.22161/ijaers.4.9.12 ISSN: 2349-6495(P) | 2456-1908(O)

The Tendency of Development and Application of Service Robots for Defense, Rescue and Security

Isak Karabegović[1] - Milena Dukanović[2]

[1]Department of Technical faculty, University of Bihać, Bosnia and Herzegovina
[2]Department of Electrical Engineering, University of Montenegro, Montenegro

Abstract*—The development of sensor, information and communication technology, or new technology, has contributed to the development of robot technology. A new generation of service robots has been developed, and the highest number of their practical applications is for defense and security. Progress and development of information technology, sensor technology and servo-drive is responsible for the development of over 600 different types or prototype service robots. Service robots are designed for professional jobs and service jobs that are used in everyday life. The rapid development of computer management enabled the rapid development of various service robots that can move independently, autonomously exchange information with their surroundings and act completely autonomously (UV Unmanned Vehicles - vehicles that operate autonomously without human management). They can be used in all operating conditions on land, air and water, which is most important for the development of service robots for defense and security. Different applications of service robots for defense and security have been developed, and some are described in the paper, as well as the tendency of their application in the recent years. A large number of service robots for defense and security were developed, which are used for obtaining information about the vulnerability of human populations during earthquakes, fires or military activities. After obtaining information, we can make proper decisions that will serve the purpose of rescue and assistance to the ones in danger. The tendency of application of service robots for security and defense is constantly rising in the past few years. It is estimated that the development of sophisticated service robots for defense, rescue and security will continue in the future, and the number of applications will increase.*

***Keywords*— Robot, Service Robot, Application of Service Robots, Defense, Rescue, Security.**

I. INTRODUCTION

Robotic technology has a noble objective – for example, to replace the man in performing tedious, monotonous or dangerous and health-endangering jobs. During the 20th century, advances in new technologies, sensors technology, computers and servo-drive enabled the development of hundreds of different types of service robots for non-production applications. Robotic technology is the technical branch, which already has its own rich tradition. Robots, just like people, have passed generation cycles. The development of supporting technologies, such as information and communication and sensor technology, enables each new generation of robots to receive more advanced features than the previous one, which is primarily related to the achieved degree of intelligence, supporting computing power, improved dynamic characteristics, as well as advanced algorithms [1,2,4,13,20]. Service robots for defense, rescue and security are manufactured in different shapes and sizes, from unmanned combat vehicles to groups of insectoid devices that will cooperate in certain task in the near future. The largest operation in their development process is conducted, of course, in the USA, where community sponsors projects involving many different new technologies. In many cases, inspiration for these projects comes directly from nature, because they copy the way the various living organisms perceive and feel their surroundings, determine the course of action, cooperate with other individuals, move and perform some of their tasks. Different remotely control devices are already in use today, mostly in dangerous jobs such as mine clearance and destruction of planted terrorist bombs. Remot-controlled service robots have been introduced in many defense units. They present a transitional step to gather experience for the transition to a new generation of remotely controlled service robots. During operation, remote operator will only occasionally operate service robot, while most of the time the service robot will be autonomous. The ultimate goal of development is for one operator to manage multiple remote-controlled service robots. Such service robots will be reprogrammable, will retain stable behavior even in complex, uncertain and changing conditions, will be able to learn, and will be

https://dx.doi.org/10.22161/ijaers.4.9.12 ISSN: 2349-6495(P) | 2456-1908(O)

safely and reliably used in close proximity to people. For certain operations, they will be so small, so that they can be stored in the military jacket pocket. It is necessary to develop service robots that will operate in risky areas, in order to avoid presence of man. Risky areas include war zones, detection and destruction of landmines, firefighting, inspection of nuclear reactors and steam generators, inspection and analysis of waste water, inspection of pipelines, inspection of power transmission lines [3,4,12,16,19].

II. DISSEMINATION OF SERVICE ROBOTS FOR DEFENSE, RESCUE AND SAFETY IN THE WORLD

According to the classification created and adopted by the UNECE- United National Economic Commission for Europe and IFR- International Federation of Robotic, service robots are divided in two groups: professional service robots and personal/home service robots. The development of new technology such as digital technology, information communication technology, sensor technology, new materials and others, had an enormous impact on the development of robot technology. So far, more than 600 different types of service robots have been developed and applied in different fields [4,14,17]. The need for the development of service robots initiated the development of companies that conduct research and production of service robots. In 2016, IFR – International Federation of Robotic, identified about 620 companies for the production of service robots in the world. The percentage of representation of such companies per continent is shown in Figure 1 [5].

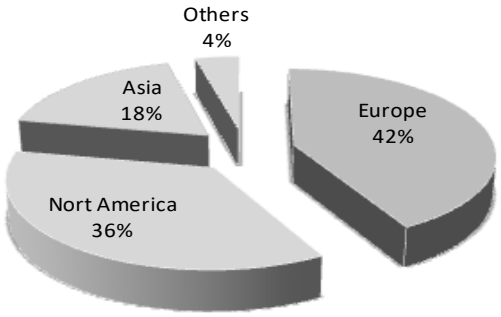

Fig. 1: Percentage of service robot production companies per continent

Based on Figure 1 we can conclude that that IFR- International Federation of Robotic identified the largest number of service robot production companies in Europe, about 258 companies, which presents 42 % of total number of identified companies. The second place is held by North America with about 226 companies, which is about 36 % of the total number of identified companies. The third place is occupied by Asia with 112 identified companies, which presents 18 % of total number of service robot production companies. Other continents have about 4 % of service robot production companies. The tendency of production of service robots in the world per individual countries is shown in Figure 2 [5-15].

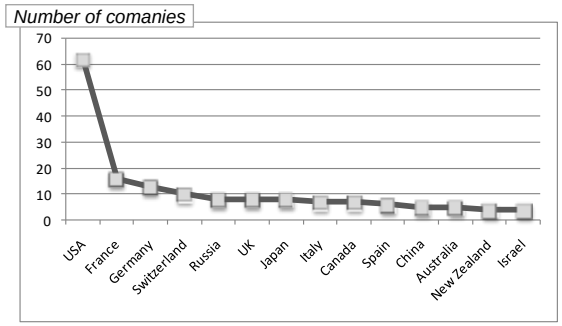

Fig.2: The number of companies for service robot production per countries in the world

Based on Figure 2, we can assert that the united States are in first place by the number of companies for the robot production where the International Federation of Robotics (IFR) has identified around 62 companies. The second place is held by France with 16 companies, followed by Germany with 13 companies and Switzerland with 10 companies for robot production. All other identified countries shown in the Figure 2 have less than 10 companies for robot production. Economic Commission at the United Nations for Europe (UNECE), the Organization for Economic Co-operation and Development (OECD) and the International Federation of Robotics (IFR) adopted the introductory system for the classification of service military robots by categories and types of interaction, so that service robots in defense have the following classification: demining robots, unmanned aerial vehicle, unmanned off-road vehicles and other robots for defense, whereas service robots for security and rescue are separately classified. In order to create a quality tendency of application of service robots in the world, as well as service robots for security and defense, the statistical data is taken from the International Federation of Robotics (IFR), the Economic Commission at the United Nations for Europe (UNECE) and the Organization for Economic Co-operation and development (OECD) [1,2,5-11]. The tendency is shown in Figure 3. Analysis of the chart of the application of service robots for professional services leads to the conclusion that the tendency of application of service robots for professional services during the period 2005-2015 is constantly growing. In 2005, about 5.000 service robot units were applied, with the tendency increasing each year. It is notable that in 2011 about 16.500 robot units were applied, which indicates the linear tendency of increase of the use of service robots for professional

https://dx.doi.org/10.22161/ijaers.4.9.12 *ISSN: 2349-6495(P) | 2456-1908(O)*

services. In the period 2011 – 2015, there was a sudden increase in the application of service robots for professional services, as per exponential function, so that about 41.000 service robots for professional service were used in 2015.

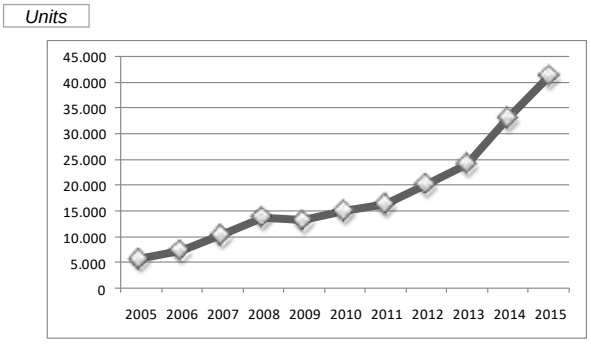

Fig.3: Total annual production of service robots for professional services for the period 2005-2015 [4-11]

This tendency of application of service robots is enabled by the development of new technologies, especially information and sensor technologies that are promoting robotic technology. It is expected that this tendency of the application of service robots for professional services in the world will continue. Service robots for professional services are used in medicine, defense, rescue, security, agriculture, cleaning, construction, underwater systems, household, inspection and maintenance, public relations, space research, or in other words in all segments of society where there is a need to replace the man to perform certain tasks [4,13,18,21-25]. To date, the largest number of service robot units is applied in defense, rescue and security, and therefore the tendency of application of service robots in this area is shown in Figure 4.

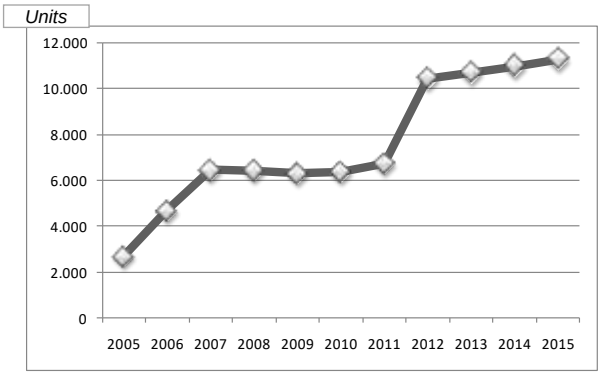

Fig.4: Annual application of service robots for defense, rescue and safety for the period 2005 – 2015

The tendency of annual application of service robots for defense, rescue and security, shown in Figure 4, is linearly increasing, starting with the application of 2.700 robot units in 2005 to the application of 6.400 robot units in 2007. In the period 2007 – 2011 there was little deviation in terms of application of service robots for defense, rescue and security on annual basis, so that the application was approximately 6.500 robot units. In 2012 there was a sudden increase in the application of these robots with 10.000 robot units. The application of robots continued to grow and in 2015, 11.300 robot units were used. It is estimated that this increasing tendency will continue in the future [5]. We can conduct a comparative analysis of the application of service robots for defense, rescue and security with other service robots for professional services in 2015, as shown in Figure 5.

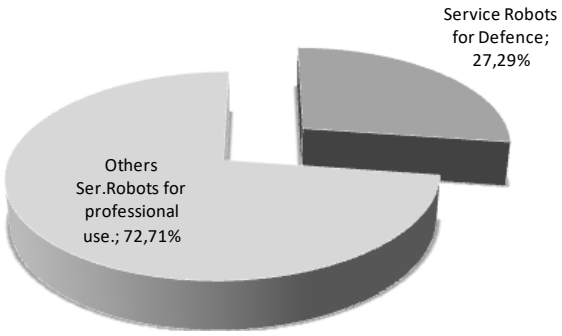

Fig. 5: Percentage of application of service robots for defense, rescue and security in 2015 worldwide

Based on statistical data published in [5], we come to the conclusion that in 2016 total 41.000 service robot units for professional services were applied in the world, of which 11.200 robot units are for defense, rescue and security, which presents 27,29 % of total robots used. All other applications of service robots constitute 72.71 % of robot units. To date, the highest detected application of service robots is for defense, rescue and security. The highest relevant useful factors are: high quality of work and productivity, reduction of manual labor, increased safety and avoiding risk, increase of operational usability, temporary flexibility, new, previously available contents and conditions etc. Table 1 shows the evaluation of the relevance of the factors for service robots that are applied in defense, rescue and security [1,2,4].

Table.1: Assessment of relevance factors for the types of service robots in defense, rescue and security

Defense, Rescue and Security	**Hogh quality work productivity**	**Reduction of manual work**	**Increasing safety avoidance risik**
Demining robot	0	• •	•
Unmanned spacecraft	0	0	• •
Unmanned vehicles	0	•	• •

https://dx.doi.org/10.22161/ijaers.4.9.12 ISSN: 2349-6495(P) | 2456-1908(O)

Rob.for fire and mines	0	• •	•
Security robot	0	0	• •

Table shows the assessment of the relevance of factors for each type of service robot, with the degree of relevance marked from 0 (not relevant) to the two points (high relevance). We can conclude that the best useful factor of the increase of security and risk avoidance is with service robots for defense, rescue and security.

III. APPLICATION OF SERVICE ROBOTS FOR DEFENSE, RESCUE AND SECURITY IN THE WORLD

The complexity, ambiguity and unpredictability of the environment of mobile service robots and certain details of their tasks are far greater than that of stationary robots. Therefore, it is generally impossible to create a detailed plan and program of action of mobile service robots in advance. In order for such service robot to completely independently successfully operate in unstructured natural environment, it must have a complex set of senses (sensors) by means of which will be able to follow actions in the environment. In addition, they have to have power to process and understand information gathered with sensors, followed by artificial intelligence with which to make decisions about their further activities, as well as highly movable and navigated authorities by which they will implement decisions into action. All these very complex systems should ideally be placed inside ofa very small service robot, and use very limited resources of energy during operation. In addition to the above, practical applicability of autonomous robot requires high safety, robustness and resistance to the most diverse failures and unexpected occurrences in the environment. Creating such a service robot is a large initiative whose realization is still a major challenge. The development of new technologies which include digital technology, information and communication technology, sensor technology, and technology of new materials contributed to the development and improvement of service robots for defense, rescue and security. Many applications were developed for demining, unmanned aircrafts, unmanned field vehicle robots, firefighting robots, and robots for security. Unmanned vehicles have proved to be indispensable in carrying out many tasks that would be dangerous for people (mine removal, handling radioactive materials, reconnaissance from the air) or tasks that are located in inaccessible environment for a man (underwater, space). According to the medium through which or by whom service robots move, and according to the basic features of their task, service robots are divided into many classes. Many constructions of unmanned aerial vehicles and service robots for rescuehave been developed. Many companies in the world are working to develop new applications of unmanned aerial vehicles, and service robots for extinguishing fire and rescue. Likewise, there are many solutions for application of service robots for the removal of mines in areas which are a consequence of the war [4,21-28]. Lightweight mobile robots were developed and designed, among other things, for the destruction of explosive devices, for handling hazardous materials, for search and control, to rescue hostages, for handling explosives, and for SWAT (Special Weapons and Tactics Team) teams and military units. They use a mechanical arm that has a full range of audio and video sensors with 8 modulators of user information. Robot weighs less than 24 kg with full equipment, can be carried by hand, can be quickly loaded into a truck and transported to the desired location. In addition, robust robotic systems for demining in war zones were also developed. A series of service robots for surveillance and reconnaissance by day and night were also developed for defense purposes. These service robots are used for observation of the terrain by day and night for safety reasons. Combat versions of these robots have also been developed, which can be armed with long-range missiles, automatic cannon and machine gun. The list of weapons makes it one of the most dangerous robotic platforms. They are still in development, and completed samples should have remarkable AI programs for autonomous action on the ground. These robots are already used by certain armies in the world. In addition, some of these robots are used in police actions, as they are equipped with cameras and night vision devices, as well as other equipment needed by police forces necessary for operations dealing with people safety. Besides mentioned applications of service robots for defense, rescue and safety, many other constructions have been developed, that serve various purposes, including fight service robots, reconnaissance, supply, operation in dangerous areas, construction of service robots for assistance to soldiers in cases of injuries in military operations.

IV. CONCLUSION

Lots of experience collected while using a variety of remotely controlled devices and drones have led researchers to work in the direction of full autonomy. Unmanned platforms should soon take unconditional, dangerous and tedious jobs. Service robots for defense, rescue and security are made in different shapes and sizes, from unmanned combat vehicles to the group of insectoid devices that will cooperate in certain operations in the near future. Most of the companies that produce service robots for defense, rescue and security are based in the

https://dx.doi.org/10.22161/ijaers.4.9.12 *ISSN: 2349-6495(P) | 2456-1908(O)*

USA, where defense community sponsors projects involving many different new technologies. In many cases, the inspiration for these projects comes directly from nature, because they copy the way the various living organisms perceive and feel their surroundings, determine the course of action, cooperate with other individuals, move and perform some of their tasks. Different remote-controlled devices are already in use today, mostly in dangerous jobs such as mine clearance and destruction of planted terrorist bombs. The US military is already using remote-controlled service robots. They present a transitional step to gather experience for the transition to a new generation of remotely controlled service robots. During operation, remote operator will only occasionally operate service robot, while most of the time the service robot will be autonomous. The ultimate goal of the development is for one operator to manage multiple remote-controlled service robots. Such service robots will be reprogrammable, they willretain stable behavior even in complex, uncertain and changeable conditions, they will be able to learn, and could safely and reliably be used in close proximity to people. For certain jobs, they would be so small, so that they can be stored in the military jacket pocket. The objective of the development of these robots is the removal of crew (man) off the weapon system, which reduces the need for armored protection, and reduced the size and perception of the system. This ultimately means greater flexibility and survivability, greater strategic and operational mobility and ease of logistical support. The most likely direction of development is the combination of unmanned and manned platforms, whereas unmanned service robots would be used in most dangerous operations. These two types of platforms should be similar to each other, so that the enemy would not be able to easily identify service robots. Forms of service robots depend on the type of the task for which the service robot was developed. Service robots that must overcome difficult terrains use caterpillar tracks. Some constructions of service robots are the size of a truck, and look quite similar to tractors or bulldozers, as shown in the figures in the paper. Other, smaller service robots have a very low profile to allow the greater mobility. Autonomous service robots use a computer program that allows service robot to process information and make some decisions independently. Instead of autonomous service robots, most military robots are still controlled by humans.

REFERENCES

[1] Karabegović I, Karabegović E, Husak E (2010) Ergonomic integration of service robots with human body, 4th *International ergonomics conference*, Stubičke Toplice, june 30 till july 3: 249-254.

[2] Karabegović I, Karabegović E,Husak H (2013) Application of Service Robots in Rehabilitation and Support of Patients , *Časopis Medicina fluminensis, Vol. 49. No. 2.,juni 2013, Rijeka, Croatia,* : 167-174.

[3] Unmanned Aircraft Systems (UAS), CIR328, (2011) International Civil Aviation Organization, Montreal, Canada:7-20.

[4] Karabegović I, Doleček V (2012) *Servisni roboti*, Tehnički fakultet, Bihać.

[5] World Robotics 2016, IFR, United Nations, New York and Geneva, 2016.

[6] World Robotics 2015, IFR, United Nations, New York and Geneva, 2015.

[7] World Robotics 2013, IFR, United Nations, New York and Geneva, 2013.

[8] World Robotics 2011, IFR, United Nations, New York and Geneva, 2011.

[9] World Robotics 2010, IFR, United Nations, New York and Geneva, 2010.

[10] World Robotics 2008, IFR, United Nations, New York and Geneva, 2008.

[11] World Robotics 2005, IFR, United Nations, New York and Geneva, 2006.

[12] Spencer A, Noah S (2012) Almost 1 In 3 U.S. Warplanes Is a Robot. (https://www.wired.com/2012/01/drone-report/)

[13] Doleček V,Karabegović I (2002) *Robotika*, Tehnički fakultet, Bihać.

[14] Fisher J.M.,Holding the Line in the 21st century,U.S. Costoms and Border protection, 2014 ;8-11. (https://www.cbp.gov/sites/default/files/documents/Holding%20the%20Line_TRILOGY.pdf)

[15] Kennedy, Caroline, Rogers, James I (2015) Virtuous drones, The International Journal of Human Rights. **19** (2) : 211–227 (doi: 10.1080/13642987.2014.991217)

[16] Spencer C, Tucker, Priscilla Mary Roberts (2008) The Encyclopedia of the Arab-Israeli Conflict: A Political, Social, and Military History: A Political, Social, and Military History, ABC-CLIO :1054-1055.

[17] Floreano D, Wood R. J (2015) Science, technology and the future of small autonomous drones, Nature. 521 (7553): 460–466. (doi:10.1038/nature14542.)

[18] Tice Brian P(1993) Unmanned Aerial Vehicles: The Force Multiplier of the 1990s," 5. no. l, Airpower Journal Index 1987-1991, 5. no. l, Air University Press, Alebama, USA, :41-55. (http://www.dtic.mil/dtic/tr/fulltext/u2/a263551.pdf).

[19] Sathurthiiyappan S, Rajkumar G, Sundharavel S (2015) Design and Fabrication of Unmanned Aerial

https://dx.doi.org/10.22161/ijaers.4.9.12 *ISSN: 2349-6495(P) | 2456-1908(O)*

Vehicle,International Journal of Innovative Research in Science, Engineering and Technology, Vol.4.SI.2.:16-21. (www.ijiset.com).

[20] Doleček V (2015) Future of Technology,2nd International Conference "New Technologies NT-2015"Development and Application,Mostar,24-25, april 2015,:1-12.

[21] Davenport C (2015) Watch a step in Navy history: an autonomous drone gets refueled mid-air, The Washington Post. (https://www.washingtonpost.com/news/checkpoint/wp/2015/04/23/watch-a-step-in-aviation-history-an-autonomous-drone-getting-refueled-mid-air/?utm_term=.2bd4389ad27b)

[22] http://www.icao.int/Meetings/UAS/Documents/Circular%20328_en.pdf (30.6.2017.)

[23] http://humanoides42.rssing.com/chan-16169491/all_p2.html (6.7.2017.)

[24] https://www.pinterest.com/pin/458311699562607129/?lp=true (10.7.2017.)

[25] http://www.sener.es/revista-sener/en/up-to-date_development_of_a_robotic_platform_for_military_and_security_applications.html (15.7.2017.)

[26] http://epequip.com/catalogue/counter-iedeod/talon/ (28.7.2017.)

[27] https://www.afcea.org/content/Article-annual-robot-rodeo-challenges-bomb-squads (8.8.2017.)

[28] http://www.lockheedmartin.com/us/what-we-do/emerging/robotics.html (10.8.2017.)

Isak Karabegović Qualification: Doctor of Technical Sciences Professional and academic career: Full professor at University of Bihać.

Competitive research or professional awards received: Author and coauthor of more the 26 books, 80 scientific papers published in international journals, 300 papers published proceedings in international conferences. Editor and coeditor of significant number of conference proceedings. Member in editorial board of 21 international journals. Sketch biography (200 words): Prof. Isak Karabegović is a Full professor at University of Bihać, Technical Faculty in Department of Mechanical engineering. He received doctoral degree from Faculty of Mechanical Engineering, University of Sarajevo in 1989, his Master of Science degree from Faculty of Mechanical engineering and naval architecture Zagreb, University of Zagreb in 1982, and bachelor degree of mechanical engineering from Faculty of Mechanical engineering Sarajevo, University of Sarajevo in 1978. His career as professor started on Technical College and later become Full professor at University of Bihać. In this period of time he was Dean of Technical faculty in several occasions and also rector of University of Bihać in several occasions. His research interest includes domains of Mechanics and Robotics. He also works as reviewer, editorial and technical board member in many reputed national, international journal and conferences. He publishes more then 400 papers of different type in international journals, conference proceedings and book chapters.

Full name : Isak Karabegović
Date of birth : 19.10.1955
Nationality : Bosnian
Department : University of Bihać, Technical faculty
Area of teaching : Mechanics, Robotics
Email : isak1910@hotmail.com
Tel : ++38737226273
Bosnia and Herzegovina

https://dx.doi.org/10.22161/ijaers.4.9.13 ISSN: 2349-6495(P) | 2456-1908(O)

Computational Performances and EM Absorption Analysis of a Monopole Antenna for Portable Wireless Devices

Mohammed Shamsul Alam

Department of Computer Science and Engineering, International Islamic University Chittagong (IIUC), Chittagong, Bangladesh

Abstract**—** *In this paper, a simple inverted L-shaped monopole antenna is presented* for *portable wireless devices. The designed antenna performances and specific absorption analysis is investigated. The antenna can operate at widely used GSM bands 850, 1800, 1900 and LTE 2100MHz. A relatively inexpensive dielectric substrate material FR4 is considered to design the antenna. The Specific absorption rate (SAR) analysis and antenna performances comply the antenna to apply in mobile communication systems.*

Keywords**— Antenna, Mobile Communication, GSM, SAR, Wireless.**

I. INTRODUCTION

Printed microstrip patch antennas have been extensively used in mobile telephony system due to its compactness, cost effectiveness and simplicity characteristics. Several researches have been performed for GSM mobile applications [1-6]. The major lacking these works is covering GSM bands with wide impedance bandwidth. Besides this, Electromagnetic (EM) absorption from the mobile antenna is a major concern to the antenna researchers. Alam et al. proposed a low EM absorption mobile antenna for wireless antenna in [1,3], but the antenna didn't cover lower GSM band. In [2], Zhao et al. proposed segmented loop antenna for mobile applications, but this antenna failed to meet the GSM band requirements. Lee et al. proposed a multiband mobile for wireless communications, but the EM absorption analysis was not performed [4]. In [5], a broadband antenna with SAR analysis has been presented. This antenna also failed to cover lower GSM bands. A quarter-wavelength printed loop antenna is presented in [7], where lower and upper GSM bands has been covered. Moreover, the SAR values of the presented antenna was also investigated, where marginal level of SAR values is observed.

A multiband printed microstrip fed monopole antenna for portable devices has been presented. The proposed antenna has a simple structure and is easy to fabricate using low cost FR4 substrate material. EM absorption in terms of SAR is also investigated. The proposed antenna can operate within the existing wireless GSM standards, such as 850MHz, 1800MHz, 1900MHz and LTE 2100.

II. ANTENNA DESIGN

The proposed antenna is designed using electromagnetic simulation software CST microwave studio. The antenna consists of an inverted L-shaped monopole and a shorted parasitic L-shaped radiating patch, shown in fig. 1. The antenna is designed on available dielectric substrate material FR4. The antenna is fed by 50 Ω microstrip feedline. A partial ground plane is used, which is shorted with parasitic patch.

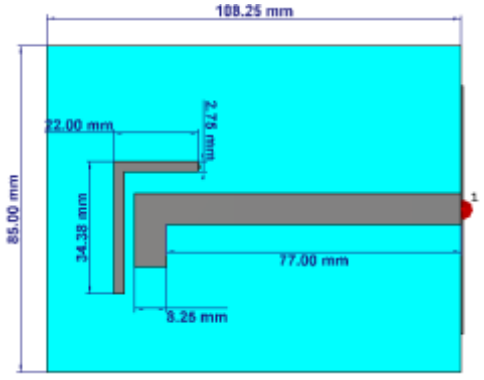

Top View

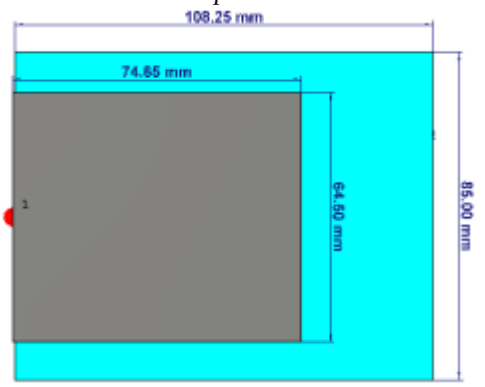

Bottom View

Fig.1: Proposed antenna design layout

https://dx.doi.org/10.22161/ijaers.4.9.13 *ISSN: 2349-6495(P) | 2456-1908(O)*

III. ANTENNA PERFORMANCES ANALYSIS

The reflection coefficient of the proposed antenna is investigated, which is shown in Fig. 1. The reflection coefficient curve shows that the antenna resonates at 850 MHz and 1800MHz, 1900MHz and 2100 MHz.

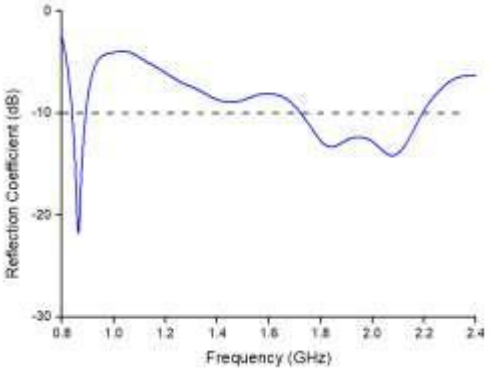

Fig.2: Reflection Coefficient of the proposed antenna

The surface current of the presented antenna is depicted in Fig. 3. Fig. 3 shows that the parasitic inverted L-shaped element is responsible to resonate at 850 MHz. Moreover, the second resonance is created for coupling between two patches. And the third resonance, 2100MHz is created due to third harmonic in microstrip line.

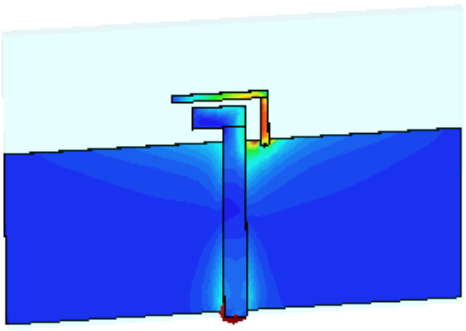

At 800MHz

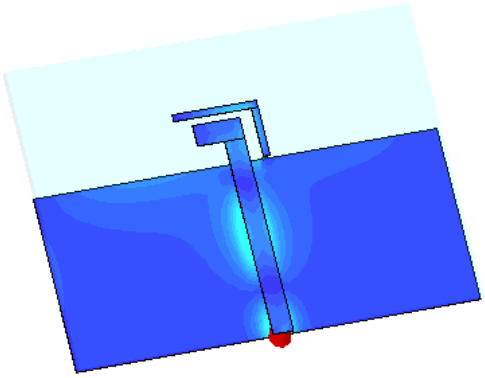

At 1800MHz

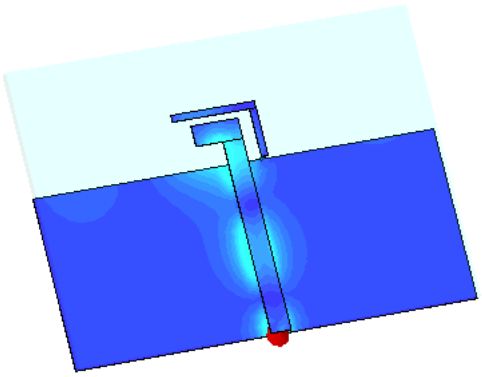

At 2100MHz

Fig. 3: Surface current distribution of the proposed antenna

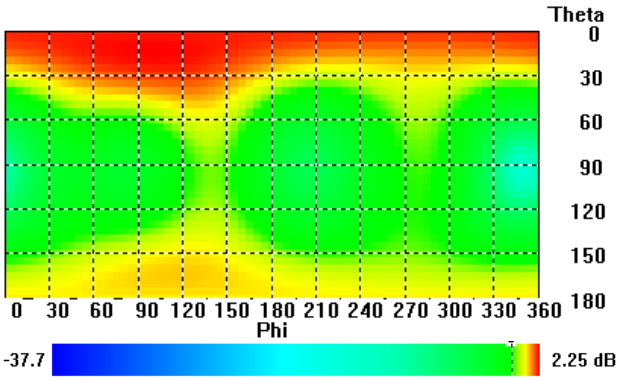

(a) At 850 MHz

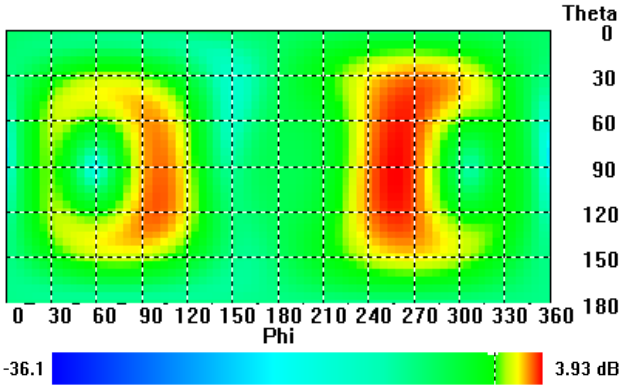

(b). at 1800MHz

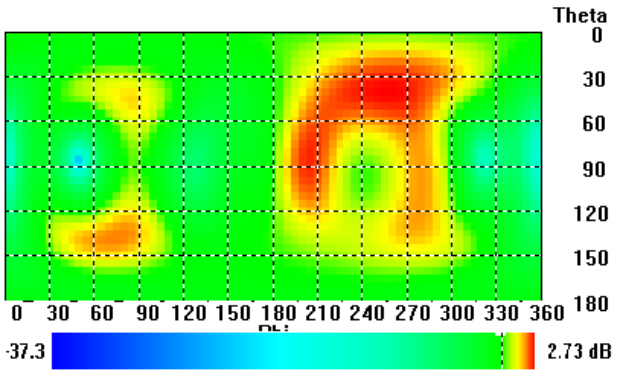

(c). at 2100MHz

Fig. 4: 2D radiation pattern of the proposed antenna

https://dx.doi.org/10.22161/ijaers.4.9.13 *ISSN: 2349-6495(P) | 2456-1908(O)*

The radiatiion pattern of the proposed antenna is analysed, shown in Figure 4. From Fig. 4, it can be observed that the pattern shapes are not as good as a conventional monopole. But the antenna shows about 3.93 dB realized gain at 850 MHz, 2.73 dB at 1800 MHz and 2.729 dB at 2100 MHz. The radiation efficiency of the antenna is presented in Fig. 5. The total efficiency of the proposed antenna at 850, 1800 and 2100 MHz is 84.02%, 88.% and 88.6%, respectively.

Table 1: Antenna performances

Antenna Performances	***Value***
Polarisation	*Linear*
Radiation pattern	*Multipath*
Gain	*Positive realized gain*
Complexity	*Simple*
Impedance	*50 Ω*
Operating frequency bands	*GSM 850, 1800, 2100MHz*
Efficiency (%) at operating frequency	*Above 84%*
Application	*GSM*

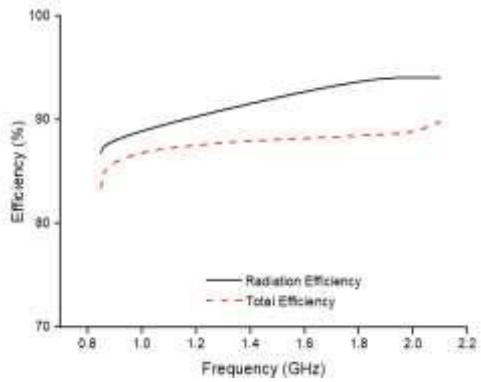

Fig. 5: Efficiency of the proposed antenna

IV. SAR ANALYSIS

The mobile telephony in Bangladesh operated in Global System for Mobile Communication (GSM) network which works in the frequency exposure of 900MHz and 1800MHz. A mobile phone antenna can transmit and receives signal as electromagnetic waves. The EM waves in absorbed by human tissues and tissue temperature increased, which is harmful for human being. The EM absorption is measured in terms of Specific absorption rate (SAR). The SAR values is standardized by some established organizations, like IEEE, International Commission on Non-Ionizing Radiation Protection (ICNIRP), the Federal Communications Commission (FCC) etc. The electromagnetic absorption limit recommended by the ICNIRP and IEEE C95.1:2005 guideline is 1.6 W/kg averaged over 1 gram of tissue volume in the shape of a cube and 2.0 W/kg average over any 10 grams of continuous tissue [8-9]. The SAR value of the proposed antenna has been investigated and presented in Fig. 6. It is shown in Fig.6 that the antenna shows 10 g SAR values at 850 MHz, 1800MHz and 2100MHz of 1.35 W/Kg, 1.26 W/Kg and 1.11 W/Kg, respectively.

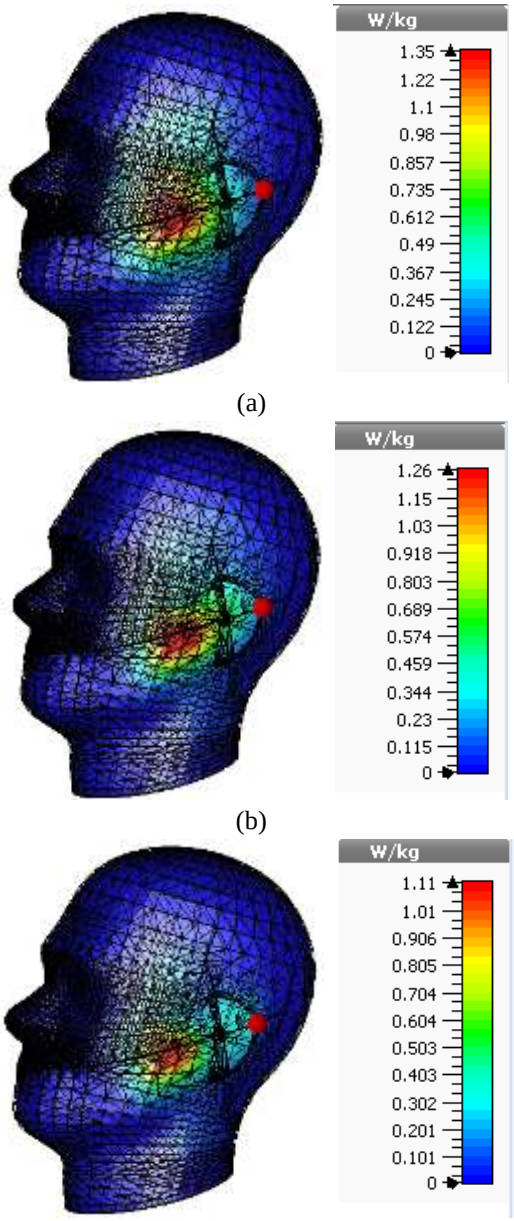

Fig. 6: SAR values of the proposed antenna-(a). at 850MHz, (b). at 1800Mhz and (c). at 2100MHz.

V. CONCLUSION

A compact multifunctional monopole antenna is presented for mobile wireless communication. The proposed antenna is suitable for lower and upper GSM communication systems. In addition, a wide impedance

https://dx.doi.org/10.22161/ijaers.4.9.13 *ISSN: 2349-6495(P) | 2456-1908(O)*

band has also been achieved at about 1800 MHz for GSM, DCS/PCS/UMTS operation. Moreover, the proposed antenna complies the IEEE and ICNIRP requirement, which makes the antenna potential to be applied for wireless mobile telephony systems.

REFERENCES

[1] Alam, T., Faruque, M. R. I., & Islam, M. T. (2016). A corded shape printed wideband antenna design for multi-standard mobile applications. Telecommunication Systems, 62(3), 511-518.

[2] Zhao, X., Tian, B. N., Yeo, S. P., & Ong, L. C. (2017). Wideband Segmented Loop Antenna With Dual-Polarized Omnidirectional Patterns for Mobile Platforms. IEEE Transactions on Antennas and Propagation, 65(2), 883-886.

[3] Alam, T., Faruque, M. R. I., & Islam, M. T. (2015). A double-negative metamaterial-inspired mobile wireless antenna for electromagnetic absorption reduction. Materials, 8(8), 4817-4828.

[4] Lee, Y. C., & Sun, J. S. (2009). A new printed antenna for multiband wireless applications. IEEE Antennas and Wireless Propagation Letters, 8, 402-405.

[5] Alam, Touhidul, Mohammad Rashed Iqbal Faruque, and Mohammad Tariqul Islam. "Specific absorption rate analysis of broadband mobile antenna with negative index metamaterial." Applied Physics A 122.3 (2016): 170.

[6] Ullah, M. A., Ashraf, F. B., Alam, T., Alam, M. S., Kibria, S., & Islam, M. T. (2016, October). A compact triangular shaped microstrip patch antenna with triangular slotted ground for UWB application. In Innovations in Science, Engineering and Technology (ICISET), International Conference on (pp. 1-4). IEEE.

[7] Chi, Y. W., & Wong, K. L. (2009). Quarter-wavelength printed loop antenna with an internal printed matching circuit for GSM/DCS/PCS/UMTS operation in the mobile phone. IEEE Transactions on Antennas and Propagation, 57(9), 2541-2547.

[8] IEEE Standard for Safety Levels with Respect to Human Exposure to Radio Frequency Electromagnetic Fields, 3 KHz to 300 GHz; IEEE Std C95.1–2005 (Revision of IEEE Std C95.1–1991); Institute of Electrical and Electonics Engineers: New York, NY, USA, 2006.

[9] International Non-Ionizing Radiation Committee of the International Radiation Protection Association. Guidelines on limits on exposure to radio frequency electromagnetic fields in the frequency range from 100 KHz to 300 GHz. Health Phy. 1988, 54, 115–123.

https://dx.doi.org/10.22161/ijaers.4.9.14 *ISSN: 2349-6495(P) | 2456-1908(O)*

Nonlinear Dynamic Analysis of Cracked Beam on Elastic Foundation Subjected to Moving Mass

Nguyen Thai Chung, Le Pham Binh

Department of Solid Mechanics, Le Quy Don Technical University, Ha Noi, Viet Nam

Abstract*—This paper presents a finite element algorithm for nonlinear dynamic analysis of cracked beams on an elastic foundation subjected to moving mass. Quantity surveying with parameters of varied cracks, foundation and loads shows their influence levels on the nonlinear dynamic response of the beams. The findings of the paper are the basis for the analysis, evaluation, and diagnosis of damages of beam structures on the elastic foundation subjected to moving loads, in which the common defects of the beams such as cracks are considered in order to improve the system's operational efficiency in a wide range of engineering applications.*

Keywords*—Nonlinear, cracked beam, elastic foundation, moving masses.

I. INTRODUCTION

Beams on the foundations are usually modeled to calculate the structures of railway works and civil engineering. During the use, there are many different causes that can cause weakened defects for beams, one of which is cracks. The appearance of cracks will reduce bearing capacity of the beams, which leads to the risk of damage to the building. Salih N Akour [1] analyzed the nonlinear dynamics of beams on the elastic foundation subjected to evenly distributed moving force by analytical methods. Also using analytical methods, Oni and Awodola [2], Tiwari and Kuppa [3] analyzed the dynamics of Bernoulli - Euler beams on the elastic foundation subjected to moving masses. Haitao Yu and Yong Yuan [4] have focused on the analytical solution of an infinite Euler-Bernoulli beam on a viscoelastic foundation subjected to arbitrary dynamic loads. Şeref Doğuşcan AKBAŞ [5] investigated the free Vibration and Bending of Functionally Graded Beams on Winkler's elastic foundation using Navier method. Nguyen Dinh Kien, Tran Thi Thom [6] studied the influences of dynamic moving forces on the Functionally Graded Porous-Nonuniform beams. D. Froio1, R. Moioli1, E. Rizzi [7] and D. T. Pham, P. H. Hoang and T. P. Nguyen [8] used the nonlinear elastic foundation and New Non-Uniform Dynamic Foundation applied to analyzed response of beam subjected to moving load and the results show that the influence of velocity has effects significantly on dynamic response of structures. N. T. Khiem, P. T. Hang [9] used a spectral method applied to analyzed response of a multiple Cracked Beam subjected to moving load.

Using analytical and finite element methods, Murat. R and Yasar. P [10], Mihir Kumar Sutar [11], Animesh C. and Tanuja S. V [12], Shakti P Jena, Dayal R Parhi, P C Jena [13], A.C.Neves, F.M.F. Simoes, A.Pinto da Costa [14], Hui Ma et al. [15] analyzed the dynamics of cracked beams subjected to moving mass.

Arash Khassetarash, Reza Hassannejad [16] investigated the Energy dissipation caused by fatigue crack in beam-like cracked structures. Erasmo Viola, Alessandro Marzani, Nicholas Fantuzzi [17] used finite element method applied to studied effect of cracks on flutter and divergence instabilities of cracked beams under subtangential forces.

M Attar et al. [18] analyzed the dynamics of cracked beams on the elastic foundation subjected to moving harmonic loads by analytic method, on the basis of using Timoshenko beam model.

So far, there are various researches of beams on elastic foundation under transfer (mass, force, oscillation system). However, for cracked beam on the elastic foundation under moving loads(or masses), most methods reply on analytical approaches which are really applied to simple loading conditions. In this paper, we develop a numerical approach based on finite element method for analyzing the dynamics of beams on elastic foundation under moving masses. We investigate the influence of the elastic foundation, load speeds and location cracks in the dynamic response of the beams. Note that finding analytical solutions of such beam problems under arbitrary loading conditions are really challenging and no research is sufficiently carried out yet. Such a problem will be addressed in this paper.

II. FINITE ELEMENT FORMULATION AND THE GOVERNING EQUATIONS

A damaged beam has an open crack located at the mid-section of the beam at position x = x0. The beam on an elastic foundation described by an elastic spring system to one direction perpendicular to the axis of the beam, which has the stiffness kt subjected to traversing mass 'm' at speed 'v' as in Fig. 1. The dimensions of the damaged

https://dx.doi.org/10.22161/ijaers.4.9.14 *ISSN: 2349-6495(P) | 2456-1908(O)*

beam are as follows, width = b, thickness = h, length = L, crack depth = d.

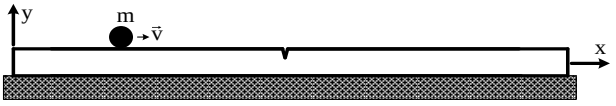

Fig. 1. Cracked beam on the foundation subjected to moving mass

For finite element model formulation the following assumptions are made: Elastic isotropic materials, cracks do not develop, and mass 'm' is always in contact the surface of the beam.

The Timoshenko theory describes the displacement field components (u,v,w) of an arbitrary point (x,y,z) on the beam cross-section can be expressed as

$$\begin{cases} u = u_0(x,t) - y\varphi_z(x,t), \\ v = v_0(x,t), \\ w = 0, \end{cases} \tag{1}$$

where u0, v0 are respectively the x and y components of the total displacement vector of the point (x,0,0) on the beam neutral axis at time t, and φz is the cross-section rotation about the z-axis. The subscript "0" represents axis x (y = 0, z = 0; x contains the cross section centroids of the undeformed beam, that will be often designed as middle line or reference line, in bending it coincides with neutral line). The x-coordinate is defined along the beam length, y-coordinate is along the height and the z-coordinate is along the width. The strain-displacement relations are as

$$\begin{cases} \varepsilon_x = \dfrac{\partial u}{\partial x} + \dfrac{1}{2}\left(\dfrac{\partial v}{\partial x}\right)^2 = \dfrac{\partial u_0}{\partial x} - y\dfrac{\partial \varphi_z}{\partial x} + \dfrac{1}{2}\left(\dfrac{\partial v_0}{\partial x}\right)^2, \\ \gamma_{xy} = \dfrac{\partial u}{\partial y} + \dfrac{\partial v}{\partial x} = \dfrac{\partial v_0}{\partial x} - \varphi_z, \end{cases} \tag{2}$$

$$\{\varepsilon\} = \{\varepsilon^L\} + \{\varepsilon^{NL}\} = \begin{Bmatrix} \varepsilon_x^L \\ \gamma_{xy}^L \end{Bmatrix} + \begin{Bmatrix} \varepsilon_x^N \\ \gamma_{xy}^N \end{Bmatrix}, \tag{3}$$

where $\{\varepsilon^L\}$ is the linear part of the strain and $\{\varepsilon^L\}$ is the nonlinear part given by:

$$\begin{aligned} &\varepsilon_x^L = \frac{\partial u_0}{\partial x} - y\frac{\partial \varphi_z}{\partial x},\ \gamma_{xy}^L = \frac{\partial v_0}{\partial x} - \varphi_z, \\ &\varepsilon_x^{NL} = \frac{1}{2}\left(\frac{\partial v_0}{\partial x}\right)^2,\ \gamma_{xy}^{NL} = 0. \end{aligned} \tag{4}$$

The stresses are related to the strain by Hooke's law:

$$\{\sigma\} = \begin{Bmatrix} \sigma_x \\ \tau_{xy} \end{Bmatrix} = \begin{bmatrix} E & 0 \\ 0 & G \end{bmatrix} \begin{Bmatrix} \varepsilon_x \\ \gamma_{xy} \end{Bmatrix} = [D]\{\varepsilon\} = [D]\{\varepsilon^L\} + [D]\{\varepsilon^{NL}\}, \tag{5}$$

where E is the Young's modulus of the material, G is the shear modulus and [D] is the material matrix.

2.1. Equation of motion of beam element with out crack

The equation of motion is derived by the principle of virtual work [19], [21]:

$$\delta W_V + \delta W_{in} + \delta W_E = 0, \tag{6}$$

where δW_V is the virtual work of internal forces, δW_{in} is the virtual work of inertia forces and δW_E is the vertual work of external forces due to a virtual displacement. They are defined as:

$$\begin{aligned} &\delta W_V = -\int_V \delta\{\varepsilon\}^T\{\sigma\} = -\int_V \delta\{\varepsilon^L\}^T[D]\{\varepsilon^L\}dV - \\ &-\int_V \delta\{\varepsilon^L\}^T[D]\{\varepsilon^{NL}\}dV - \int_V \delta\{\varepsilon^{NL}\}^T[D]\{\varepsilon^L\}dV \\ &-\int_V \delta\{\varepsilon^{NL}\}^T[D]\{\varepsilon^{NL}\}dV = \\ &= -\{\delta q\}^T[K_1]\{q^e\} - \{\delta q\}^T\left[K_2\left(\{q^e\}\right)\right]\{q^e\} - \\ &-\{\delta q\}^T\left[K_3(\{q\})\right]\{q^e\} - \{\delta q\}^T\left[K_4\left(\{q^e\}\right)\right]\{q^e\}, \end{aligned} \tag{7}$$

In this equation [K1] is a matrix of constant terms, [K2({q})] and [K3({q})] are matrices that depend linearly on the generalized displacements and [K4({q})] is a matrix that depends quadratically on the generalized displacements, {qe} is the displacements vector. The linear stiffness matrix [K1], nonlinear stiffness matrices [K2], [K3] and [K4] have the following form:

$$[K_1] = \begin{bmatrix} [K_1]_{11} & [0] & [0] \\ [0] & [K_1]_{22} & [K_1]_{23} \\ [0] & [K_1]_{23}^T & [K_1]_{33} \end{bmatrix}, [K_2] = \begin{bmatrix} [K_2]_{11} & [0] & [0] \\ [0] & [0] & [0] \\ [0] & [0] & [0] \end{bmatrix},$$

$$[K_4] = \begin{bmatrix} [K_4]_{11} & [0] & [0] \\ [0] & [0] & [0] \\ [0] & [0] & [0] \end{bmatrix}, [K_3] = 2[K_2], \tag{8}$$

$$[K_1]_{11} = E\int_V \frac{d\left[N^u\right]^T}{dx}\frac{d\left[N^u\right]}{dx}dV,$$

where (9)

$$[K_1]_{22} = \lambda G\int_V \frac{d\left[N^v\right]^T}{dx}\frac{d\left[N^v\right]}{dx}dV,$$

$$[K_1]_{23} = -\lambda G\int_V \frac{d\left[N^v\right]^T}{dx}\left[N^{\varphi_z}\right]dV,\ [K_1]_{33}$$

$$= \int_V \left(y^2 E\frac{d\left[N^{\varphi_z}\right]^T}{dx}\frac{d\left[N^{\varphi_z}\right]}{dx} + \lambda G\left[N^{\varphi_z}\right]^T\left[N^{\varphi_z}\right]\right)dV, \tag{10}$$

https://dx.doi.org/10.22161/ijaers.4.9.14 *ISSN: 2349-6495(P) | 2456-1908(O)*

$$[K_2]_{11} = \frac{1}{2}E\int_V \frac{d[N^u]^T}{dx}\frac{d[N^v]}{dx}\frac{\partial v_0}{\partial x}dV,$$
$$[K_4]_{11} = \frac{1}{2}E\int_V \frac{d[N^v]^T}{dx}\frac{d[N^v]}{dx}\left(\frac{\partial v_0}{\partial x}\right)^2 dV. \quad (11)$$

$$\delta W_{in} = -\int_V \rho\{\delta d\}^T\{\ddot{d}\} = -\{\delta d\}^T[M^e]\{\ddot{q}^e\}, \quad (12)$$

$$\delta W_E = \int_V \{\delta d_0\}^T\{F_0\}dV = \{\delta d\}^T\{F^e\}, \quad (13)$$

where $[N^u]$, $[N^v]$ and $[N^{\varphi z}]$ are the row vectors of longitudinal, transverse along y and rotational about z shape functions, respectively, $\{\ddot{q}^e\}$ is the acceleration vector, ρ is the density of the beam, $[M^e]$ is the mass matrix, the vector of virtual displacement components will be represented by {δd} and can be written as $\{\delta d\} = \{\delta u \ \ \delta v \ \ 0\}^T$ and $\{\delta d_0\}$ is the vertual displacements on the middle line, $\{F_0\}$ is the external forces on the middle line, $\{F^e\}$ is the generalized external forces.

The mass matrix [M] and vector of generalized external forces {F} have following form:

$$[M^e] = \begin{bmatrix} [M]_{11} & [0] & [0] \\ [0] & [M]_{22} & [0] \\ [0] & [0] & [M]_{33} \end{bmatrix}, \quad (14)$$

where

$$[M]_{11} = \rho\int_V [N^u]^T[N^u]dV, [M]_{22}$$
$$= \rho\int_V [N^v]^T[N^v]dV, [M]_{33} = \rho\int_V y^2[N^{\varphi_z}]^T[N^{\varphi_z}]dV. \quad (15)$$

$$\{F_0\} = \{F_x \ \ F_x \ \ M_z\}^T, \ \{F^e\} = \{F_{u_0} \ \ F_{v_0} \ \ F_{\varphi_z}\}^T, \quad (16)$$

where
$$F_{u_0} = \int_V [N^u]F_x dV, \ F_{v_0} = \int_V [N^v]F_y dV,$$
$$F_{\varphi_z} = \int_V [N^{\varphi_z}]M_z dV. \quad (17)$$

Substituting equations (7), (12) and (13) into (6), the following nonlinear equation of motion of the beam without crack is obtained

$$[M^e]\{\ddot{q}^e\} + [K^e(\{q^e\})]\{q^e\} = \{F^e\}, \quad (18)$$

In case with the damping force $\{f_d^e\} = [C^e]\{\dot{q}^e\}$, equation (18) becomes

$$[M^e]\{\ddot{q}^e\} + [C^e]\{\dot{q}^e\} + [K^e(\{q^e\})]\{q^e\} = \{F^e\}, \quad (19)$$

where

$[K^e(\{q^e\})] = [K_1] + [K_2(\{q^e\})] + [K_3(\{q^e\})] + [K_4(\{q^e\})]$, $[C^e]$ is the damping matrix of element, $\{\dot{q}^e\}$ is velocity vector.

2.2. Beam element with crack

Considering the beam element with crack, stiffness matrix of the element $[K_c^e]$ is identified as [11], [20]

$$[K_c^e(\{q^e\})] = [K^e(\{q^e\})] - [K_c], \quad (20)$$

where $[K_c]$ is the stiffness matrix of weak beam element due to cracks, and the above matrices can be formulated as:

$$[K_c] = \begin{bmatrix} k_{11} & k_{12} & -k_{11} & k_{14} \\ k_{12} & k_{22} & -k_{12} & k_{24} \\ -k_{11} & -k_{12} & k_{11} & -k_{14} \\ k_{14} & k_{24} & -k_{14} & k_{44} \end{bmatrix},$$
$$[K^e] = \frac{EJ_0}{l_e^3}\begin{bmatrix} 12 & 6l_e & -12 & 6l_e \\ 6l_e & 4l_e^2 & -6l_e & 2l_e^2 \\ -12 & -6l_e & 12 & -6l_e \\ 6l_e & 2l_e^2 & -6l_e & 4l_e^2 \end{bmatrix}, \quad (21)$$

with components in equation (21)

$$k_{11} = \frac{12E(J_0 - J_c)}{l_e^4}\left[\frac{2l_c^2}{l_e^2} + 3l_c\left(\frac{2\eta}{l_e^2} - 1\right)^2\right],$$
$$k_{12} = \frac{12E(J_0 - J_c)}{l_e^3}\left[\frac{l_c^3}{l_e^2} + l_c\left(2 - \frac{7\eta}{l_e} + \frac{6\eta^2}{l_e^2}\right)\right],$$
$$k_{14} = \frac{12E(J_0 - J_c)}{l_e^3}\left[\frac{l_c^3}{l_e^2} + l_c\left(2 - \frac{5\eta}{l_e} + \frac{6\eta^2}{l_e^2}\right)\right],$$
$$k_{22} = \frac{12E(J_0 - J_c)}{l_e^2}\left[\frac{3l_c^2}{l_e^2} + 2l_c\left(\frac{3\eta}{l_e} - 2\right)^2\right],$$
$$k_{24} = \frac{12E(J_0 - J_c)}{l_e^2}\left[\frac{3l_c^2}{l_e^2} + 2l_c\left(2 - \frac{9\eta}{l_e} + \frac{9\eta^2}{l_e^2}\right)^2\right],$$
$$k_{44} = \frac{12E(J_0 - J_c)}{l_e^2}\left[\frac{3l_c^2}{l_e^2} + 2l_c\left(\frac{3\eta}{l_e} - 1\right)^2\right]$$

where J_0, J_c , respectively, are the moments of inertia of the beam cross section for Oz axis at non-cracked positions and at the positions of cracks; $l_c = 1{,}5d$ (d is the depth of the crack), l_e is the length of the element, E is the modulus of elasticity, η is the distance from the left end of beam element to the crack.

Considering that the lost mass due to cracks is little compared to the overall mass of the element.

https://dx.doi.org/10.22161/ijaers.4.9.14 *ISSN: 2349-6495(P) | 2456-1908(O)*

2.3. Beam element on elastic foundation

Stiffness matrix of the beam element on elastic foundation $\left[K_{bf}^{e}\right]$ is identified by [3]:

$$\left[K_{bf}^{e}\left(\left\{q^{e}\right\}\right)\right]=\left[K^{e}\left(\left\{q^{e}\right\}\right)\right]+\left[K_{f}^{e}\right], \quad (22)$$

where $\left[K^{e}\left(\left\{q^{e}\right\}\right)\right]=\left[K_{c}^{e}\left(\left\{q^{e}\right\}\right)\right]$ correlates with the cracked beam element, $\left[K_{f}^{e}\right]$ is the stiffness matrix related to an elastic foundation.

2.4. Nodal load vector element beam on elastic foundation under moving mass

According to FEM method, when a moving load is involved in the working of the system, due to the position change property of the load over time, so at each point of time, the moving load acts on one beam element. Considering the beam element on elastic foundation subjected to the moving mass m, the force P(t) acts on m (Fig. 3).

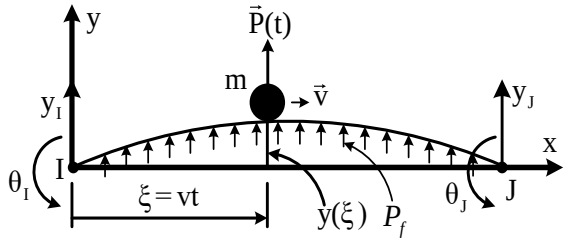

Fig. 3. Beam element on elastic foundation under moving mass.

The force of the moving mass acting on the beam at the coordinate x = ξ = vt is:

$$R(x,t)=P(t)-m\left.\frac{d^{2}y(x,t)}{dt^{2}}\right|_{x=\xi}, \quad (23)$$

where y(x,t) is element deflection, $\frac{d^{2}y}{dt^{2}}$ is the absolute acceleration in the y direction.

After taking the derivative of the deflection function, the expression (23) is rewritten as

$$R(x,t)=P(t)-m\left.\left(\frac{\partial^{2}y}{\partial t^{2}}+2\frac{\partial^{2}y}{\partial x\partial t}v+\frac{\partial^{2}y}{\partial x^{2}}v^{2}\right)\right|_{x=\xi}. \quad (24)$$

The acting force (24) is described by the distributed force p(x,t) as:

$$p(x,t)=R(x,t)\cdot\delta(x-vt). \quad (25)$$

In case, beam on elastic foundation:

$$p(x,t)=R(x,t)\cdot\delta(x-vt)-k_{0}y(x), \quad (26)$$

where δ(x) is denotes the Dirac-Delta function, k0 – foundation modulus.

Therefore, the force vector is:

$$\left\{F^{e}\right\}=\int_{0}^{l_{e}}[N]^{T}\,p(x,t)dx=\int_{0}^{l_{e}}\delta(x-\xi)[N]^{T}\,R(x,t)dx-\int_{0}^{l_{e}}k_{0}[N]^{T}\,y(x)dx, \quad (27)$$

where, $[N]=\begin{bmatrix}\left[N^{u}\right] & [0] & [0]\\ [0] & \left[N^{v}\right] & [0]\\ [0] & [0] & \left[N^{\varphi_{z}}\right]\end{bmatrix}$ is the matrix of shape functions of flexural beam element.

Substituting $y(x)=[N]\left\{q^{e}\right\}$ into Eq. (24) we get

$$R(x,t)=P(t)-m\left.\left([N]\left\{\ddot{q}^{e}\right\}+2v[N']\left\{\dot{q}^{e}\right\}+[N'']\left\{q^{e}\right\}v^{2}\right)\right|_{x=\xi}, \quad (28)$$

where $[N']=\frac{\partial N}{\partial x}$, $[N'']=\frac{\partial^{2}N}{\partial x^{2}}$.

Substituting equations (28) into (26) and paying attention to the nature of the Delta-Dirac function, equation (27) may be rewritten as

$$\left\{F^{e}(t)\right\}=\left\{P^{e}(t)\right\}-\left[M_{p}^{e}\right]\left\{\ddot{q}^{e}\right\}-\left[C_{p}^{e}\right]\left\{\dot{q}^{e}\right\}-\left[K_{p}^{e}\right]\left\{q^{e}\right\}-\left[K_{f}^{e}\right]\left\{q^{e}\right\}, \quad (29)$$

where

$$\left\{P^{e}(t)\right\}=\int_{0}^{l_{e}}[N]^{T}\,\delta(x-\xi)P(t)dx=\left[N(\xi)\right]^{T}P(t), \quad (30)$$

$$\left[M_{P}^{e}\right]=m\int_{0}^{l_{e}}\delta(x-\xi)[N]^{T}[N]dx=m\left[N(\xi)\right]^{T}\left[N(\xi)\right] \quad (31)$$

$$\left[C_{P}^{e}\right]=2vm\int_{0}^{l_{e}}\delta(x-\xi)[N]^{T}[N']dx=2vm\left[N(\xi)\right]^{T}\left[N'(\xi)\right], \quad (32)$$

$$\left[K_{p}^{e}\right]=v^{2}m\int_{0}^{l_{e}}\delta(x-\xi)[N]^{T}[N'']dx=mv^{2}\left[N(\xi)\right]^{T}\left[N''(\xi)\right], \quad (33)$$

$$\left[K_{f}^{e}\right]=\int_{0}^{l_{e}}k_{0}\left[N(x)\right]^{T}\left[N(x)\right]dx. \quad (34)$$

Substituting equation (29) into equation (19), we get the equations of motion governing the nonlinear dynamic response of the beam element on elastic foundation subjected to moving mass

$$\left(\left[M^{e}\right]+\left[M_{p}^{e}\right]\right)\left\{\ddot{q}^{e}\right\}+\left(\left[C^{e}\right]+\left[C_{p}^{e}\right]\right)\left\{\dot{q}^{e}\right\}+\left(\left[K_{bf}^{e}\left(\left\{q^{e}\right\}\right)\right]+\left[K_{p}^{e}\right]\right)\left\{q^{e}\right\}=\left\{P^{e}(t)\right\}, \quad (35)$$

2.5. Governing differential equations for total system

Assembling all elements matrices and nodal force vectors, the governing equations of motions of the cracked beam on elastic foundation subjected to moving mass can be derived as

$$\left(\left[M_{0}\right]+\left[M_{p}\right]\right)\{\ddot{q}\}+\left(\left[C_{0}(\{q\})\right]+\left[C_{p}\right]\right)\{\dot{q}\}+\left(\left[K_{bf}(\{q\})\right]+\left[K_{p}\right]\right)\{q\}=\{P\}, \quad (36)$$

https://dx.doi.org/10.22161/ijaers.4.9.14 *ISSN: 2349-6495(P) | 2456-1908(O)*

where $[M_0]+[M_p]=\sum_e[M^e]+\sum_{e_m}[M_p^e]$,

$[C_0(\{q\})]+[C_p]=\alpha_R[M_0]+\beta_R[K_{bf}(\{q\})]+\sum_{e_m}[C_p^e]$,

$[K_{bf}]=\sum_e[K_{bf}^e]$, e is the number of normal elements, e_m is the number of elements directly subjected to moving mass and α_R, β_R are the Rayleigh damping coefficients.

This is a nonlinear differential equation system with time dependence coefficient that can be solved by using Newmark's direct integration and Newton-Raphson iteration method. A ANSYS program called CBF_Moving_Mass_2017 was conducted to solve equation (36). The code of the calculation program is written in the ANSYS 13.0 environment.

III. NUMERICAL ANALYSIS

Beam's length L = 8m, rectangular cross section with width b = 0.1m, height h = 0.2m; one end is in pinned connection, and the other end is in roller connection. Beam material with elastic modulus E = 2.1×10^{11} N/m^2, Poisson's ratio ν = 0.3; density ρ = 7800 kg/m^3 is used. There is a V-shaped open crack in the center of the beam, and the crack's depth d = 0.1 m. Foundation stiffness k_0 = 2×10^4 N/m^3. The used load is the material point with the mass m = 1000kg, moving along the beam with the velocity v = 36 km/h.

With the established program established, we calculate for 02 cases: Beam with crack (basic problem - BP) and without crack (comparison problem - CP) to see more clearly the impact on the dynamic response of the system when the cracks appear. The response results of deflection y, acceleration $\ddot{y}$, cutting force Q_y and normal stress σ_x at the midpoint of the beam (point A (4,0,0)) are shown in Table 2 and Figures 4, 5, 6, 7. Through this results, we realize that with cracked beam the whole displacement, acceleration of vertical displacements and normal stresses are greater than the beam without crack. This problem showed the dangers of crack to stiffness, stability of cracked beam on elastic foundation under moving loads.

Table 1. Summary of maximum values of calculated quantities

Quantities	y_{max} [cm]	$\ddot{y}_{max}$ [m/s2]	Q_y^{max} [N]	σ_x^{max} [N/m2]
BP (with crack)	0.373	20.994	109.889	3.316×10^7
CP (without crack)	0.191	0.125	119.421	1.079×10^7
Differents	1.95 times	167.95 times	0.92 times	3.07 times

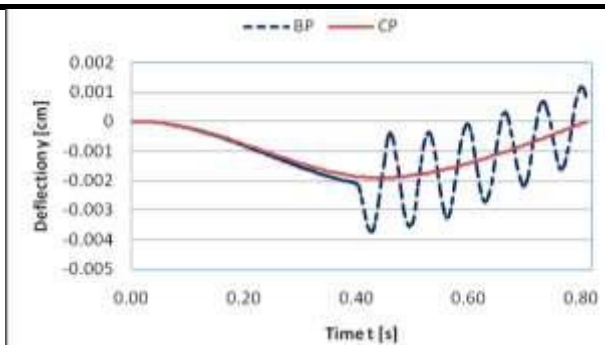

Fig. 4. Response of deflection y over time at the center cross section of the beam

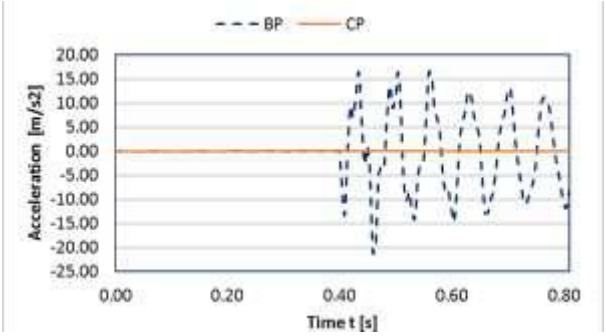

Fig. 5. Response of acceleration $\ddot{y}$ over time at the center cross section of the beam

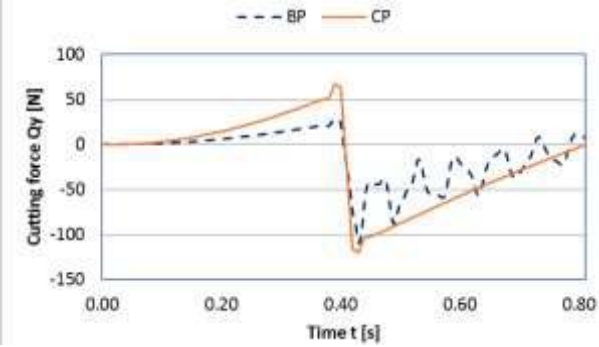

Fig. 6. Response of cutting force Q_y at the center cross section of the beam

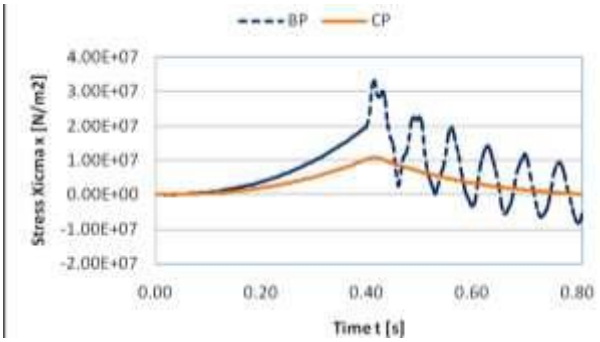

Fig. 7. Response of normal stress σ_x at the center cross section of the beam

The results show that the effect of cracks on the dynamic response of the beam is significant. For cracked beams,

https://dx.doi.org/10.22161/ijaers.4.9.14 *ISSN: 2349-6495(P) | 2456-1908(O)*

vibration of the beams increases after the mass moves through the crack.

3.1. Effect of elastic foundation stiffness

Studying the changes in maximum values of the displacement, internal force and direct stress of the beam under the elastic foundation stiffness, through the stiffness k0 of the spring ranging from 1×104N/m3 to 6×104N/m3. The results of changes in maximum values of the displacement, internal force and direct stress at the center cross section of the beam are shown in Table 3 and graphs in Figures 8 and 9.

Table 3. Summary of maximum values of quantities calculated based on k_0

k_0 [N/m]	1×10^4	2×10^4	4×10^4	6×10^4
y_{max} [cm]	0.459	0.373	0.279	0.228
$\ddot{y}_{max}$ [m/s^2]	17.963	20.994	21.762	21.480
Q_y^{max} [N]	113.220	109.889	104.525	99.085
σ_x^{max} [N/m^2] ($\times10^7$)	3.704	3.316	2.859	2.590

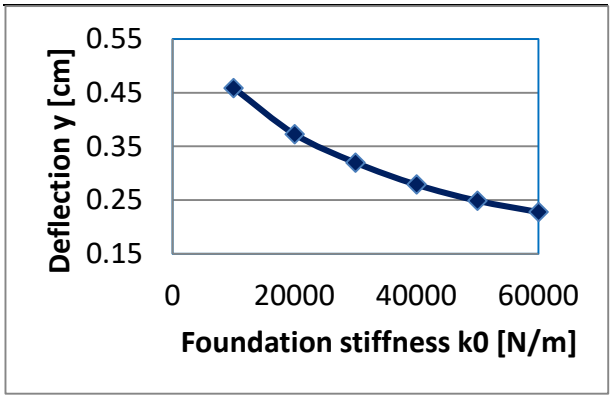

Fig. 8. y_{max} - k_0 relation

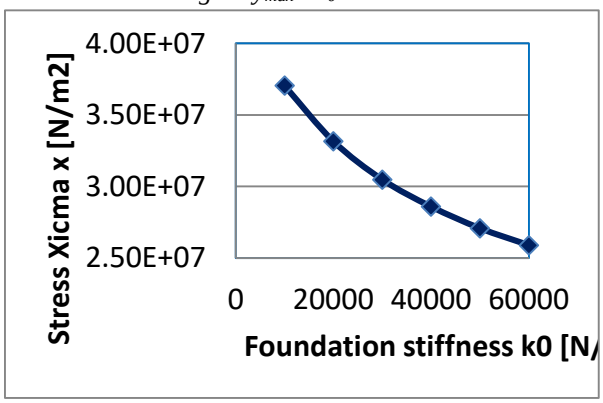

Fig. 9. σ_x^{max} - k_0 relation

It is observed that when the foundation stiffness increases, the maximum values of displacement and flexural moment decrease due to the increase in the system's overall stiffness. The maximum values of displacement and flexural moment decrease sharply when k_0 varies from 1×10^4N/m^3 to 3×10^4N/m^3, then the decreasing rate shall be slower.

3.2. Effect of load speed

Surveying the problem with a load speed v changes from 10m/s (36km/h) to 35m/s (126km/h). The results of the variations of the maximum values of deflection, acceleration, cutting force and stress at the midpoint of the beam based on v are shown in Table 4 and graphs in Figures 10 and 11.

Table 4. Summary of maximum values of quantities calculated based on v

v [km/h]	36	90	126
y_{max} [cm]	0.373	0.290	0.282
$\ddot{y}_{max}$ [m/s^2]	20.994	23.102	27.655
Q_y^{max} [N]	109.889	90.804	82.960
σ_x^{max} [N/m^2] ($\times10^7$)	3.316	2.890	2.797

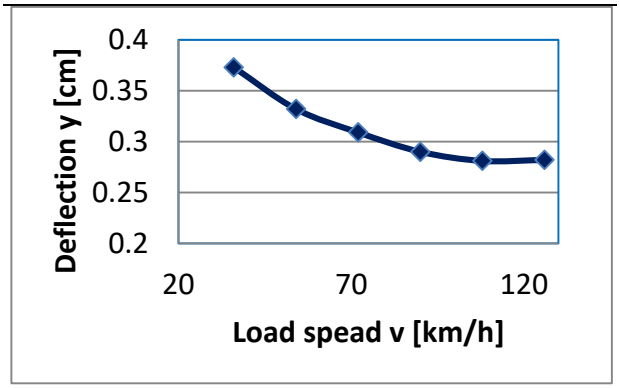

Fig. 10. y_{max} - v relation

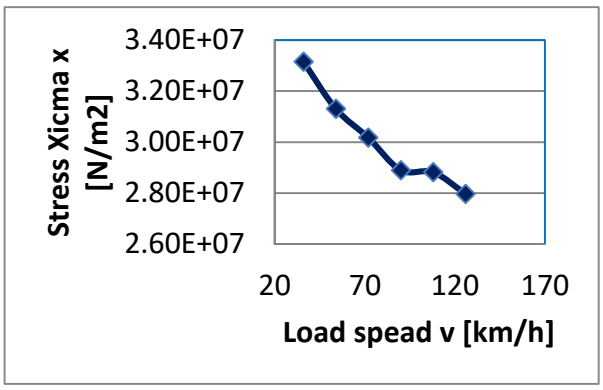

Fig. 11. σ_x^{max} - v relation

It is clear that when the moving speed of the load increases, the maximum values of displacement, internal force and stress in the beam decrease, when the moving speed of the load varies from 90 m/s to 110 m/s, the direct stress does not change much, then decreases sharply.

3.3. Effect of crack location

This example studies the changes in maximum values of displacement and internal force of the beam according to the crack location, giving the cracks located far from the

https://dx.doi.org/10.22161/ijaers.4.9.14 *ISSN: 2349-6495(P) | 2456-1908(O)*

beam's ends the distances L/4, L/2, 3L/4. Results of extreme values of the responses at the calculated points are shown in Tab. 5 and graphs in Figures 12, 13, 14, 15. When mass moving through the crack, the beam vibrates amplitude and frequency, which shows that the stabilization of the beam oscillations during this period decreased.

Table 5. Summary of maximum values of quantities calculated according to the crack location

Crack location (from left end)	L/4	L/2	3L/4
y_{max} [m]	0.257	0.373	0.279
$\ddot{y}_{max}$ [m/s^2]	16.347	20.994	19.855
Q_y^{max} [N]	75.374	109.889	63.418
σ_x^{max} [N/m^2] ($\times 10^7$)	1.453	3.316	1.133

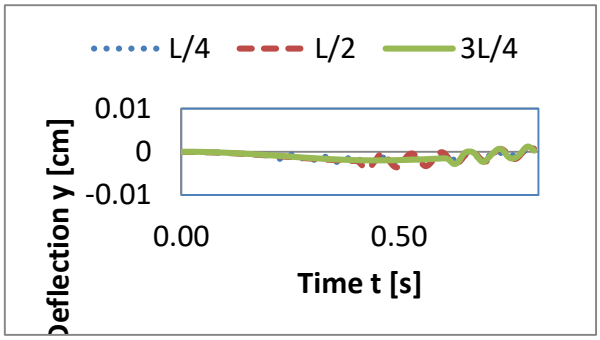

Fig. 12. Response of y according to the crack location

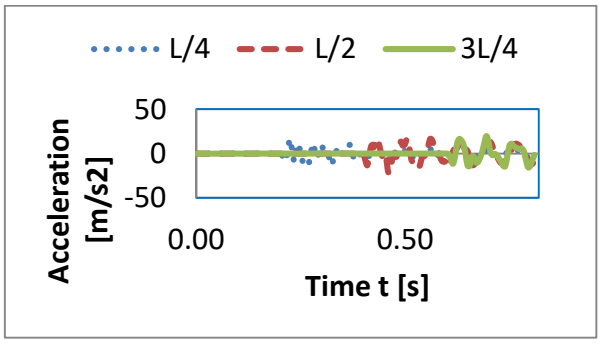

Fig. 13. Response of $\ddot{y}$ according to the crack location

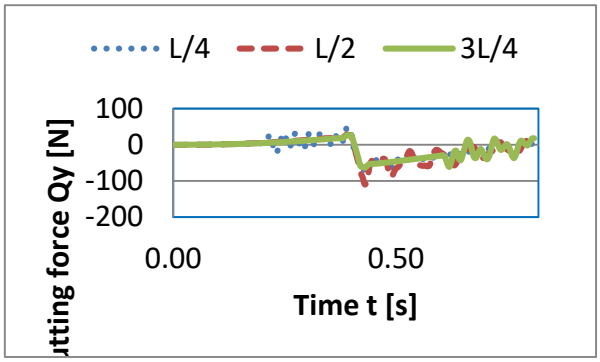

Fig. 14. Response of Q_y according to the crack location

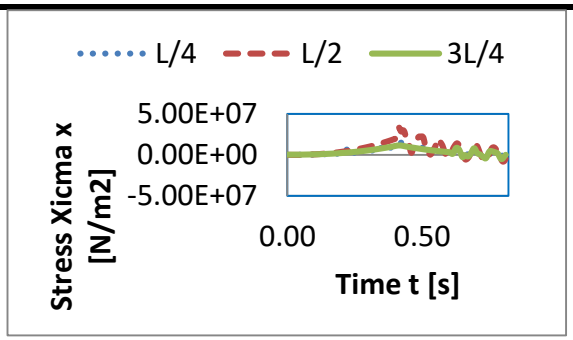

Fig. 15. Response of σ_x according to the crack location

Crack location changes making the maximum responses of displacement, stress and internal force in the beams change significantly; when the crack is in the center of the beam, the above quantities reach the maximum values, so, the beam is most dangerous when there is a crack appearing in this position.

IV. CONCLUSION

A conclusion section must be included and should indicate clearly the advantages, limitations, and possible applications of the paper. Although a conclusion may review the main points of the paper, do not replicate the abstract as the conclusion. A conclusion might elaborate on the importance of the work or suggest applications and extensions.

The nonlinear dynamics analysis of cracked beams resting on a Winkler foundation subjected to a moving mass using the finite element method has been presented. A two-node beam element based on Euler-Bernoulli beam theory, taking the effect of crack and foundation support, was derived and employed in the analysis. The dynamics response of the beams, including the time histories for deflection, acceleration and normal stress, was computed with the aid of Newmark method. The effect of loading parameters, foundation stiffness and crack location on the dynamic response of the beams has been examined and highlighted. The main conclusions can be summarized as follows:

The beam element and computer code developed in the present work are accurate in evaluating the dynamic characteristics of cracked beams subjected to moving masses.

The elastic foundation plays an important role in the dynamic response of the cracked beams under a moving mass. Both the dynamic deflection and normal stress are significaly decreased by the increase of the foundation stiffness.

The dynamic response of the cracked beams, as in case of the uncracked beams, is governed by the moving mass speed. With the moving speeds in the range considered in this paper, both the dynamic deflection and normal stress

https://dx.doi.org/10.22161/ijaers.4.9.14 *ISSN: 2349-6495(P) | 2456-1908(O)*

decreased when increasing the moving speed.

The maximum dynamic deflection and normal stress are significantly influenced by the crack location. The deflection and normal tress attain the largest values when the crack is located at the midpoint of the beam. Thus, from an engineering point of view, the midpoint crack is the most dangerous one.

The results obtained in this paper help to select appropriate parameters, the solution for structural reinforcement cracked beam on elastic foundation under moving load and applications in transportation techniques such as the train rails.

REFERENCES

[1] Salih N Akour, Dynamics of Nonlinear Beam on Elastic Foundation, Proceedings of the World Congress on Engineering 2010 Vol II WCE 2010, June 30 - July 2, 2010, London, U.K., ISBN: 978-988-18210-7-2 ISSN: 2078-0958 (Print); ISSN: 2078-0966 (Online).

[2] S. T. Oni and T. O. Awodola, Dynamic response under a moving load of an elastically supported non-prismatic Bernoulli-Euler beam on variable elastic foundation, Latin American Journal of Solids and Structures 7(2010): 3-20.

[3] Karmvir, Ramakrishna Kuppa, Overview of methods of analysis of beams on elastic foundation, IOSR Journal of Mechanical and Civil Engineering, Volume 11, Issue5.Ver VI (Sep-Oct-2014): 22-29.

[4] Haitao Yu and Yong Yuan, Analytical Solution for an Infinite Euler-Bernoulli Beam on a Viscoelastic Foundation Subjected to Arbitrary Dynamic Loads, Journal of Engineering Mechanics, Vol. 140, No. 3, March 1, 2014, pp.542-551.

[5] Şeref Doğuşcan AKBAŞ, Free Vibration and Bending of Functionally Graded Beams Resting on Elastic Foundation, Akbaş / Journal of Research on Engineering Structures & Materials 1 (2015), pp. 25-37.

[6] Nguyen Dinh Kien, Tran Thi Thom, Buntara Sthenly Gan, Bui Van Tuyen, Influences of Dynamic Moving Forces on the Functionally GradedPorous-Nonuniform Beams, International Journal of Engineering and Technology Innovation, Vol. 6, no. 3, 2016, pp. 173-189.

[7] D. Froio1, R. Moioli1, E. Rizzi, Numerical dynamic analysis of beams on nonlinear elastic foundation under harmonic moving load, VII European Congress on Computational Methods in Applied Sciences and Engineering, Crete Island, Greece, 5–10 June 2016, pp.1-16.

[8] D. T. Pham, P. H. Hoang and T. P. Nguyen, Dynamic Response of Beam on a New Non-Uniform Dynamic Foundation Subjected to a Moving Vehicle Using Finite Element Method, International Journal of Engineering Research & Technology (IJERT), Vol. 6 Issue 03, March-2017, pp.279-285.

[9] N. T. Khiem, P. T. Hang, Spectral Analysis of a multiple Cracked Beam subjected to moving load, Vietnam Journal of Mechanics, VAST, Vol.36, No. 4(2014), pp.245-254.

[10] Murat. R and Yasar. P, Vibration of a Cracked Cantilever Beam under Moving Mass Load, Journal Of Civil Engineering and Management 18(1) 106-113, February 2012, http://dx.doi.org/10.3846/13923730.2011.619330.

[11] Mihir Kumar Sutar, Finite element Analysis of a Cracked cantilever Beam, International Journal of Advanced Engineering Research and Studies, E-ISSN2249-8974/Vol. I/Issue II/January-March, 2012: 285-289.

[12] Animesh C. and Tanuja S. V., Dynamic Analysis of Beam under the moving Mass for Damage Assessment, International Journal of Engineering Research & Technology, Vol. 4 Issue 02, February-2015: 788-796.

[13] Shakti P Jena1, Dayal R Parhi2, P C Jena, Dynamic Response of Damaged Cantilever Beam Subjected to Traversing Mass, International Journal For Technological Research In Engineering, Volume 2, Issue 7, March-2015, pp.860-865.

[14] A.C.Neves, F.M.F. Simoes, A.Pinto da Costa, Vibrations of cracked beams: Discrete mass and stiffness models, Computers and Structures 168 (2016) 68-77, http://dx.doi.org/10.1016/j.compstruc.2016.02.007.

[15] Hui Ma, Jin Zeng, Ziqiang Lang, Long Zhang, Yuzhu Guo, Bangchun Wen, Analysis of the dynamic characteristics of a slant-cracked cantilever beam, Mechanical Systems and Signal Processing 75 (2016) 261-279, http://dx.doi.org/10.1016/j.ymssp.2015.12.009.

[16] Arash Khassetarash, Reza Hassannejad, Energy dissipation caused by fatigue crack in beam-like cracked structures, Journal of Sound and Vibration 363 (2016) 247-257, http://dx.doi.org/10.1016/j.jsv.2015.10.036

[17] Erasmo Viola, Alessandro Marzani, Nicholas Fantuzzi, Interaction effect of cracks on flutter and divergence instabilities of cracked beams under subtangential forces, Engineering Fracture Mechanics 151 (2016) 109-129, http://dx.doi.org/10.1016/j.engfracmech.2015.11.010.

[18] M Attar, A Karrech and K Regenauer-Lieb, Dynamic response of cracked Timoshenko beams on elastic foundation under moving harmonic loads, Journal of

https://dx.doi.org/10.22161/ijaers.4.9.14 *ISSN: 2349-6495(P) | 2456-1908(O)*

Vibration and Control, 2015 1-26, DOI: 10.1177/1077546315580470

[19] Bathe K. J. and Wilson E. L., Numerical Method in Finite Method Analysis, Prentice Hall of India Private Limited, New Delhi, 1978.

[20] Nguyen Thai Chung, Hoang Hai, Shin Sang Hee, Dynamic Analysis of High Building with Cracks in Column Subjected to Earthquake Loading, American Journal of Civil Engineering, 2016; 4(5), ISSN: 2330-8729 (Print); ISSN: 2330-8737 (Online), pp. 233-240.

[21] L. Meirovitch, Methods of Analytical Dynamics, Dover Publications Inc., New York, 2003.

https://dx.doi.org/10.22161/ijaers.4.9.15 *ISSN: 2349-6495(P) | 2456-1908(O)*

Data Acquisition and Processing of Hartha Formation in the east Baghdad oil field, Central of Iraq

Salman Z. Khorshid[1], Falih M. Duaij[2], Hayder H. Majeed[3]

[1]Department of Geology, College of Science, University of Baghdad, Baghdad, Iraq.
[2]Oil Exploration Company, Iraqi Oil Ministry, Baghdad, Iraq.

Abstract*—A three-dimensional survey was carried out to Eastern Baghdad oil field, which consist three parts, the area of (EB South- 2) approximately 179,875 km^2 and (EB South-1) is about (602.03) km^2, while the space segment (EB South-3) is approximately to (419.095) km^2. In this research, was focused on Hartha Formation only. Based on many tests to designation of pre-planning of the survey to get good signal to noise ratio for receivers in addition to the best suit for vibrators distribution and also getting the best signal source where spread of a 60-line impact and the distance between the point of receive and the other are (2 meters), also using (5) vibrators Type (NOMAD 65) with a maximum capacity of (62000 LB) for each shock. Where all processes work such as enhancing signal at the expense of noise, correction CDP gather for Normal Move Out (NMO) and stack them, correction for influence of near-surface time delays (static correction), filtering processes, providing velocity information, increasing resolution and collapsing diffractions and placing dipping events in their correct subsurface locations (migration) This processes are achieved using computers, they include many mathematical processes depend on physical fundamentals. The main processes in seismic data processing include : stacking, deconvolution, and migration. By using the information of EB-1 Well, and making the relationship time-depth curve of EB-1 then following up on getting synthetic to be linked later with seismic data and sections to obtain a real subsurface image.*

Keywords*— *Data Acquisition , Processing of Hartha Formation, upper Cretaceous age-East Baghdad oil field.

I. INTRODUCTION

There are several seismic surveys covered the entire area East of Baghdad, carried out by foreign and Iraqi seismic parties . Oil exploration company in 2009 began planning to survey southern part of east baghdad field by using 3D seismic technique. The study area divided into three parts (S1,S2 and S3) . The second seismic party has carried out the work in two stages: the first stage South-2 (S2) survey in 2010 (O.E.C., 2010) , and the second stage S1 and S3 survey in 2011 [2]. The area of (EB South- 2) is approximately (179.875) km ^{2} and (EB South-1) is about (602.03) km ^{2} , while the space segment (EB South-3) amounted to approximately (419.095) km ^{2}, and this zone which forms part of a flat land interspersed irrigation channels and agricultural areas . The interests in this research are (S1 ,S2).

II. THE PRE-PLANNING OF THE SURVEY

The designation of pre-planning of the survey area was as in (Table 1) (O.E.C., 2010) :-

Table 1 : Shows the designation of pre-planning of the survey area (O.E.C., 2010).

1	The number of recording channels activated	1920 channel spread over 16 registration line by 120 channel / line
2	Number of receiver lines	92 lines
3	The number of source lines	45 lines
4	Distance between receiver lines	300 m.
5	Number of source points in SALVO points .	6
6	Distance between source lines	500 m.
7	Fold	48
8	Bin	25 x 25.
9	Line Roll	4.
10	Receiver Interval	50m.
11	Source Interval	50m.

III. Field tests

Forteen field tests used in the study area to get good signal to noise ratio for receivers in addition to the best suit for vibrators distribution.

https://dx.doi.org/10.22161/ijaers.4.9.15 ISSN: 2349-6495(P) | 2456-1908(O)

3.1 SIGNAL TEST

It has been installed and the spread of a 60-line impact and the distance between the point of receive and the other are (2 meters) as shown in Figure (1) (O.E.C. 2010).

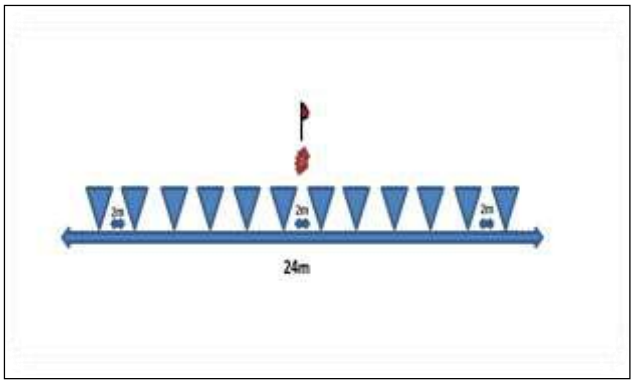

Fig.1: Shows the distribution of receivers.

3.2 Source Test (Vibro pattern)

Several modes for power source test were done using (5) vibrators Type (NOMAD 65) with a maximum capacity (peak force) of (62000 LB) for each shock , four shocks (vibrators) are in work and one vibrators as reserve, and the geometry of the vibrators are shown in Figure (2) , (O.E.C., 2010). The recording below shows on of the seismic record in the field at the study area Figure (3) .

.

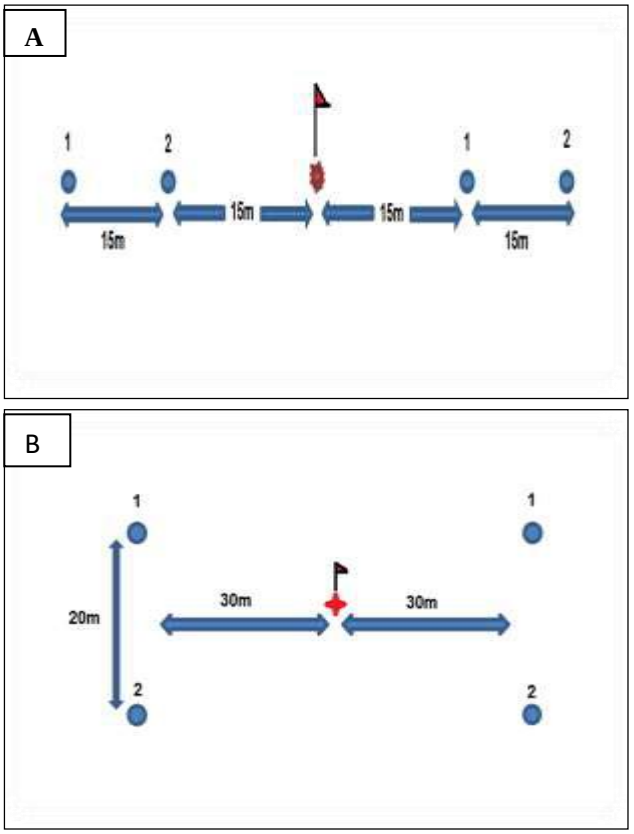

Fig.2: Shows the distribution of vibrators (A) inline and (B) cross line .

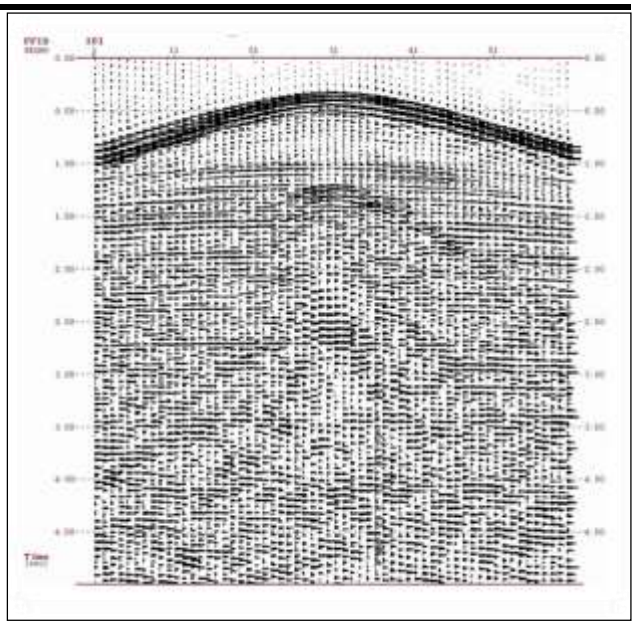

Fig.3: Shows one of the field record in the study area [2].

IV. PROCESSING OF SEISMIC DATA

The seismic data were processed at the processing center of Oil Exploration Company. The primary objective is to enhance the quality of the recorded data with special regard to the 3-D data (O.E.C., 2011). Basically, this improvement is essential to facilate the structural and stratigraphic seismic interpretation. Noise attenuation process leads to improve reflection continuity and enhance our ability to compute seismic attributes. To convert the field recording into a usable seismic section requires a good deal of data manipulation. The purpose of seismic processing is to manipulate the obtained data into an image that can be used to indicate the sub-surface structure and stratigraphy. Only minimal processing would be required if any one had a perfect acquisition system (Yilmaz, 1987) . Processing consists of the application of a sets of computer routines to the acquired data planned by the hand of the processing geophysicist. The interpreter should be interested at all stages to check that processing decisions in order not to take the interpretations of the incorrect direction. Processing routines generally fall into one of the following categories: Enhancing signal at the expense of noise, correction CDP gather for Normal Move Out (NMO) and stack them, correction for influence of near-surface time delays (static correction), filtering processes, providing velocity information, increasing resolution and collapsing diffractions and placing dipping events in their correct subsurface locations (migration). This processes are achieved using computers, they include many mathematical processes depend on physical fundamentals. The main processes in seismic data processing include : stacking, deconvolution, and migration. The processing

https://dx.doi.org/10.22161/ijaers.4.9.15 *ISSN: 2349-6495(P) | 2456-1908(O)*

stages are divided into pre-stack and post-stack processing (Hatton et al., 1986) .

V. LOADING OF 3D SEISMIC DATA

Processed seismic data are loaded in the interacting workstation of interpretation in SEG-Y format and before beginning; special subprograms must be operated to define the required data for loading. This process is called (project creation) for obtaining the interpretation process on an active workstation, loading of 3D seismic data in pre- stack and post stack time migrated format. After that, the base map of the study area is constructed with global coordinate's browser WG 1984 UTM system. This process involves entering the first and last inline number, the first and last cross line number, the divided space between bin size along inline direction and cross line direction is shown in Figure (4).

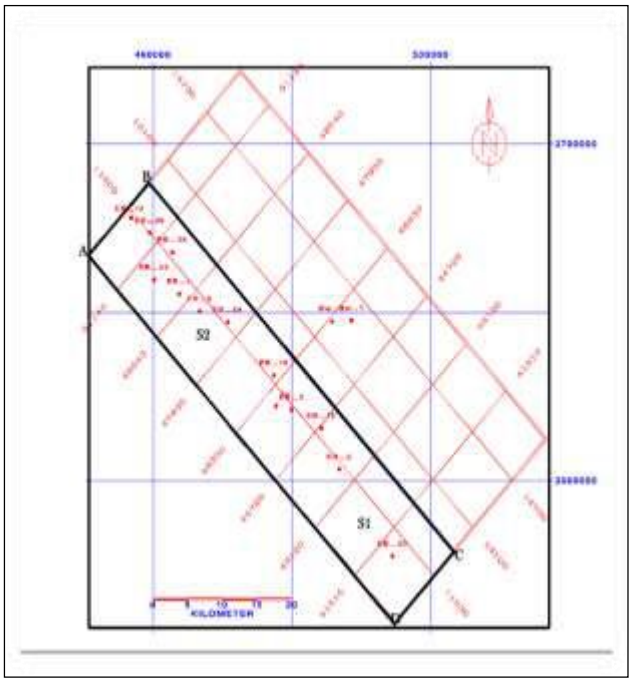

Fig.4: Base map of East Baghdad oil field (south-1 and south-2).

VI. ELEVATION STATIC CORRECTION CALCULATION AND APPLYING

The static correction is so-called because it is a fixed time correction applied to the entire trace (Silvia, and Robinson, 1979). Elevation static was primarily calculated using (elevation information, replacement velocity =2300 m/sec, datum = 0) (O.C.E., 2010) static correction is shown in Figure (5).

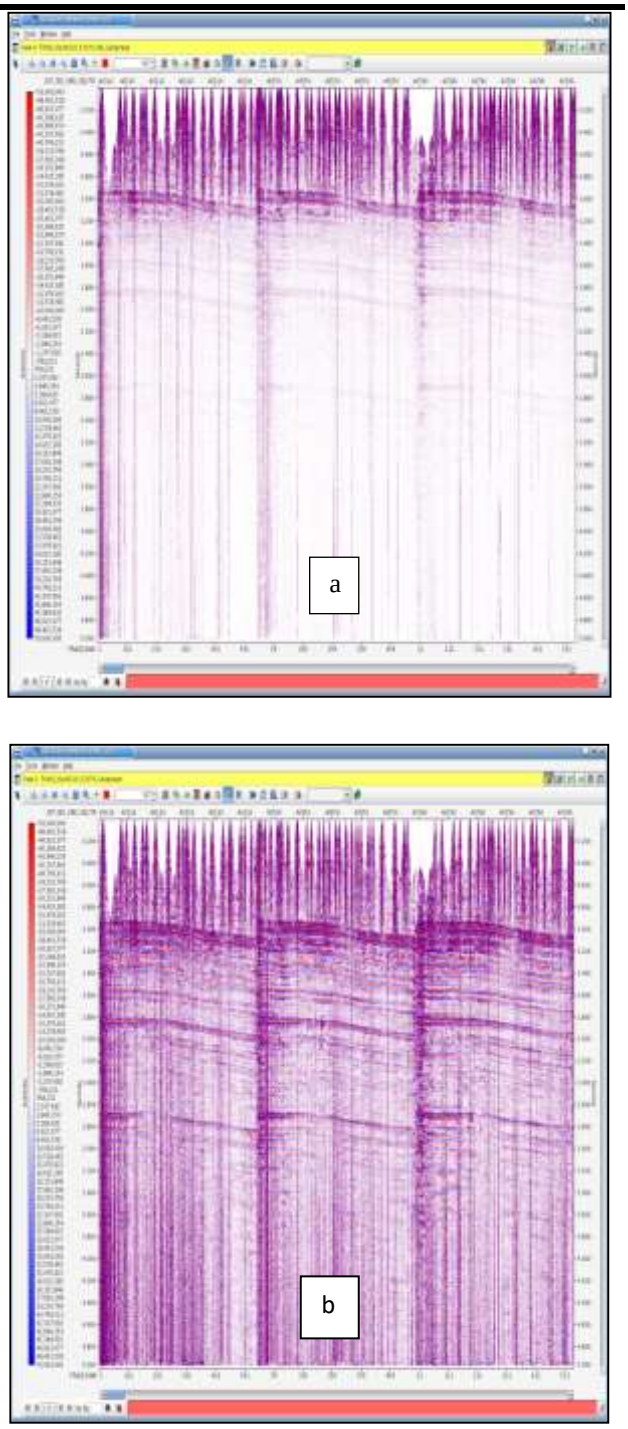

Fig.5: a- before and b- after applying elevation static correction.

VII. DECONVOLUTION

Deconvolution is mathematical processing applied to inverse the effects of convolution on recorded data. Deconvolution improves the temporal resolution of seismic data by compressing the basic seismic wavelet and removes the range character or the reverberating energy. The removal of the frequency-dependant response of the source and the instrument. The instrument response is normally known and can be removed exactly. The

https://dx.doi.org/10.22161/ijaers.4.9.15 *ISSN: 2349-6495(P) | 2456-1908(O)*

source shape can be estimated from the signal itself under certain assumptions. Spiking deconvolution, wavelet deconvolution, gapped deconvolution, signature deconvolution, predictive deconvolution, maximum entropy deconvolution, and surface consistent deconvolution are different appearances of the try to remove the source width from the observed reflections (Deregowski, 1986). The producing reflection sequence always has some smoothing function left, usually called the residual wavelet. Attempting to be too accurate about deconvolution usually conclusions in a very noisy section (Yilmaz, 1987). The effect of deconvolution is shown in Figure(6).

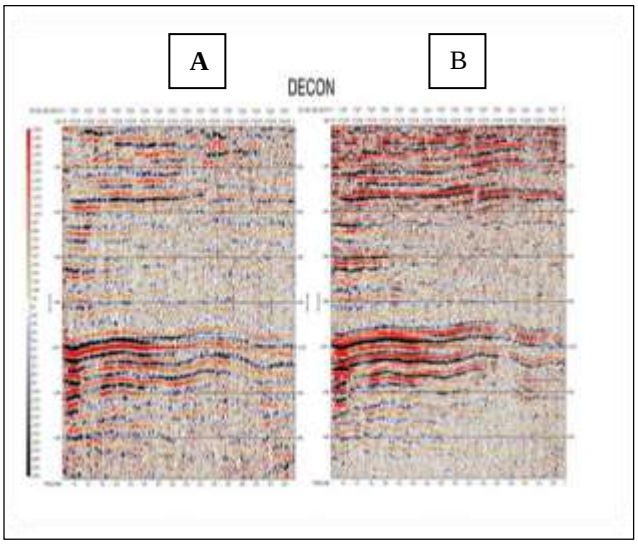

Fig.6: Shows deconvolution A- before deconvolution B- after deconvolution (http:// inter- geo.org /Services /Processing3d /Parameters .php?lang=en) .

VIII. COMMON-MIDPOINT STACKING

CMP stacking is probabiy the most important application of data processing for improving data quality. The component data are sometimes displayed as a gather: a CMP gather has the components for the same midpoint arranged side by side and a common-offset gather has the components for which the offset is the same arranges side by side . after correcting for normal moveout , the data are stacked into single output trace for each midpoint . If reflectors dip , the reflecting point is not common for CMO traces and consequently the stacking result involved smearing and degradation of data quality. The degradation can be avoided by migration before stacking . Somtime partial stacks, each of traces over a limited offset range , are made and migrated to cut down on the amount of data to be migrated. Dip-moveout(DMO) processing transforms a set of pre-stack common-point gathers so that each gather contained events from the same reflecting point (Telford et al., 1990). If the velocity is constant, the locus for equal travel times is an ellipse with the source and receiver locations as foci; all reflectors, dipping as well as horizontal, are tangent to such an ellipse . DMO uses the difference between the mid-point and the points where perpendiculars to the ellipse intercept the surface to create common-reflecting point gathers . These gathers can then be stacked and migrated without reflecting point smear . The constant-velocity assumtion provides a reason ably satisfactory approximation where velocity varies (Stolt and Benson, 1986).

IX. STACKING AND MIGRATION

Migration is one of the main steps in seismic data processing it is the step which try to move the recorded data so that events lie in their right spatial location rather than their recorded location (Bacon and Redshaw , 2003). Once more there are a large number of options ranging from migrating all the pre-stack data to stacking data in a CMP followed by post-stack migration.There is also the issue of whether to use time or depth migration and also the type of algorithm (Kirchoff, implicit finite difference, explicit finite difference, F- K filter, phase shift, etc.). In recent years the choice has become even wider with the ability of some algorithms to incorporate the effects of velocity anisotropy. The option of whether to migrated at a before or after stacking is in general dependent on the velocity regime and the subsurface dips present in the data. An assumed velocity-depth model is used, the data are migrated pre-stack using this model, and the images across the migrated CMP gather are compared. If the velocity model is nearly correct will the events appear flat. Events will only be flat if they have been fully migrated in a 3-D sense and it is expensive to repeat this for the entire section. Since lateral velocity variations also give rise to stacking problems most depth migration benefit is gained from working pre-stack. After the final velocity analysis and Move Out Correction (MOC) the data are stacked. Stacking together traces that include the same reflection information both get better the signal to (random) noise content (by the square root of the number of traces stacked) and reduces any residual coherent noise such as multiples which stack at velocities different from the primary events. During stacking , mutes (zeroing the data within specified zones) are used to the data to ensure that NMO is not a problem and that any residual multiples left on the near-offset traces do not mess the stacked section. There may be some amplitude difference with offset (AVO) effects in the data,which can be inducted as hydrocarbon indicators (Drijkoningen and Verschuur , 2003).

https://dx.doi.org/10.22161/ijaers.4.9.15 *ISSN: 2349-6495(P) | 2456-1908(O)*

X. POST-STACK TIME/DEPTH MIGRATION

In a number of these steps some assumptions have been made that are not valid for general inhomogeneous earth models (Hagedoorn, 1954) such as :

A- **CMP sorting:** If the earth is inhomogeneous and reactors have complex shapes and the reaction events within a CMP gather do not belong to one subsurface reactors point .

B- **NMO correction:** In complex subsurface media the moveout in a CMP gather is not hyperbolic, so a perfect moveout correction cannot be achieved.

C- **DMO:** If strong lateral velocity and/or reactor geometry variations are present, the DMO procedure still will not resolve the reaction point smear within a CMP gather.

D- **Stack:** As the events within a CMP gather do not belong to the same subsurface reaction point, stacking of these events will mix subsurface information.

E- **Poststack time/depth migration:** Given the approximations in the previous steps, a stacked section does not represent a true zero offset section and migration of this stack will therefore not result in an exact image. Furthermore, some poststack migration algorithms have limitations due to the assumed simple velocity field or limitation in the maximum dip that can be handled. Figure (7) shows the Shot gather with MUTE.

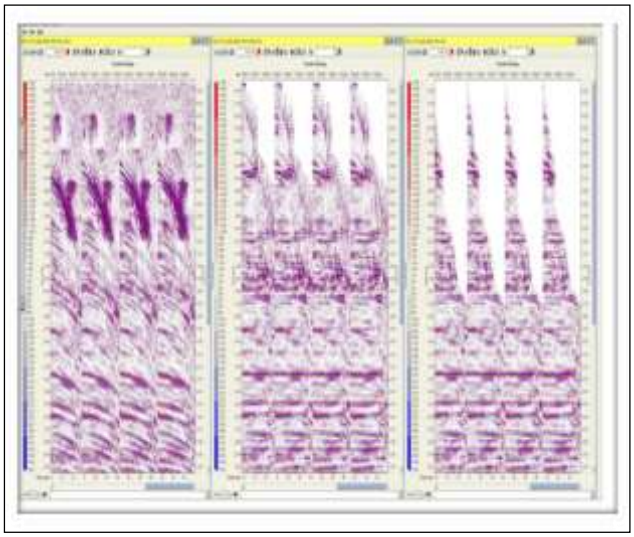

Fig.7: shows the Shot gather with MUTE.

XI. MIGRATION OF SEISMIC DATA

Migration is the process of propagating waves observed on the surface of the ground backward in time into the earth to the subsurface structures. In a geographical region where all the subsurface stratums are quite horizontal, such depropagation would take place on perfectly vertical paths. However, if the undergraond stratums are dipping, the depropagation would take place on curved paths turning away from the vertical. The reason for proceeding migration or depropagation is that it discover the present spatial positions of the subsurface reflection points at depth, where as the unmigrated seismic data observed on the surface of the ground only gives the apparent reflecting positions. Thus migration can be described as the conversion of data observed at the surface to data that would have been observed at depth. That is, migration is the process of mathematically pushing the data back into the ground so as to detect the true spatial locations of the subsurface structure (Stolt , 1978). The common mid-point (CMP) stack record section is works on assembling all the CMP stacked traces along the survey line. The CMP stack section has approximately the properties of a record section in which each trace has the same source and receiver position (Schlumberger. 2004). Recents seismic reflection data possibly processed to approximate closely the reflection coefficient sets of a sedimentary section. Inversion of the groups will result a low-cut filter impedance log. Extension of the technique to involve density relationship and replacement of missing low-frequency components leads to generation of a synthetic sonic log having dimensions and advantages like to a conventional borehole sonic log.

XII. COMPUTER INTERPRETATION AND USED PROGRAMS

The interactive workstation (GeoFrame) available in O.E.C was used to perform interpretation. It is an electronic computer uses (Red hat) as operating system, the later is a copy of UNIX (operating system). There are several specialized programs operating with this interactive workstation such as geology, seismic, reservoir engineering and petrophysics programs (Dobrin and Savit, 1988). The GeoFrame software is a part project database capable of managing tens of thousands of wells, hundreds of 3D seismic surveys, and thousands of 2D seismic lines. Advanced workflow techniques—such as AVO (Amplitude Verses Offset) interpretation, volume interpretation and GIS—give geoscientists an advantage in prospect generation and field development. Coupled with easy arrival to the Petrel E&P software platform, interpretation rise Connected with easy arrival to the Petrel E&P software platform, interpretation dangers are reduced even further (Dobrin and Savit, 1988) The use of workstations for 3D interpretation was therefore welcomed by interpreters. They offered several advantages:

1- The ability to view sections through the data in any orientation.

2- Automatic book-keeping of manually selected horizon: picks made on one line would automatically be ransferred

https://dx.doi.org/10.22161/ijaers.4.9.15 *ISSN: 2349-6495(P) | 2456-1908(O)*

to another lines or to map views.

3- Semi-automated horizon picking.

4- Calculation of pick attributes that can be used to extract additional information.

5- Capability to see the data volume in 3D not just as sections, to obtain all this requires that use of completely powerful workstations (Drijkoningen and Verschuur , 2003).

The GeoFrame software system includes several windows and will be explained windows that have been working out that includes Figure (8) :

12.1 Seismic interpretation: including ((IESX (Interpretation Extracts Seismic Xtrem)) and Charisma)) that work on the interpretation of 2D/3D pre- and post stack seismic interpretation with data versioning for multiple users.

12.2 Mapping and gridding: including (Base map Plus and CPS3 (Control point Sections)) working on quality maps for geological and geophysical interpretation data, and data management functionality in one mapping canvas.

12.3 Depth conversion: Including (in depth and synthetics)

-In depth Domain conversion of 2D/3D seismic and interpretation data by creating velocity models with access to QC (Quality Control) tools.

-Synthetics: Synthetics bridges the gap between geology and geophysics, creates accurate time to depth relationships for the wells in the field.

- Analysis: including (Seismic Attribute ToolKit Bundle) get more detail on the subtle lithological variations of the reservoir.

- LPM (Log Property Mapping) Creates rock property maps guided by seismic attributes (Dobrin, and Savit, 1988).

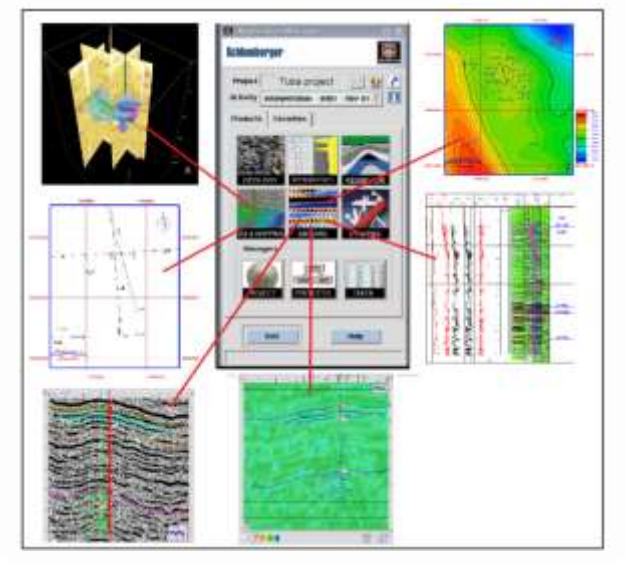

*Fig.8***:** *Shows The GeoFrame software system windows.*

XIII. CHECK – SHOT SURVEY

Is used to determine interval velocities to geologic marker horizons. The typical check shot survey involves lowering a geophone/hydophone into a well to a selected position and measuring the time it takes for an acoustic pulse generated at or near the well head to travel to the receiver. Most often explosive source is used. Unlike it's VSP, the receiver locations are often placed hundreds or thousands of meters apart and the recording windows are only long enough to record the directly arriving signals (Khorshid, 2015). The data can then be correlated to surface seismic data by correcting the sonic log and generating a synthetic seismogram to confirm or modify seismic interpretations (Sheriff and Geldart, 1995). (Table 2) extracted from IESX system shows the dependent depth and time values from upper formation logs, field survey velocity, and the processing of depth field values to the depth of penetrating formations of sea level which considered a reference surface for three dimensional data of the study area. For the purpose of obtaining accurate synthetic seismogram of good matching with seismic data by using available tools and possibilities in the window of creating synthetic seismogram within IESX program of interactive work station (Geoframe) according to the following steps:-

-The process of loading sonic log, velocity log and upper formations of wells.

-A process of calibration of time curve with depth for sonic and velocity logs for the purpose of correcting time values of sonic log according to the field velocity survey. Figures (9) shows the time-depth curve of EB-1 .

- Using of seismic data that cover the well area to extract the wavelet shapes which dependent in the process of convolution to convert reflection coefficient values to seismic signal in amplitude.

https://dx.doi.org/10.22161/ijaers.4.9.15 *ISSN: 2349-6495(P) | 2456-1908(O)*

Table.2: Shows the marker informations of two wells EB-1.

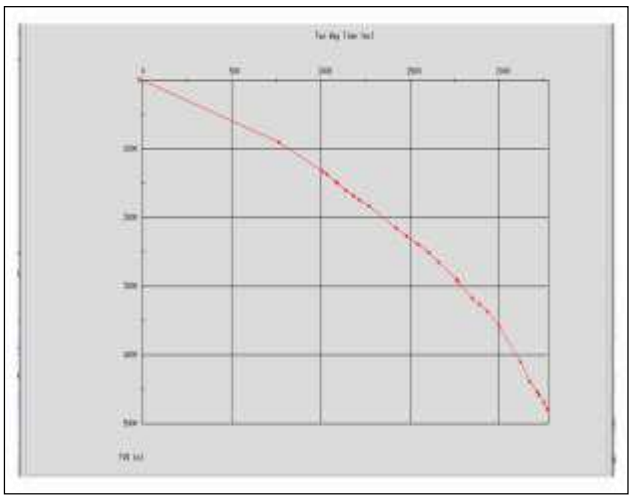

Fig.9: Shows time-depth curves for East Baghdad well-1.

XIV. GENERATION OF SYNTHETIC SEISMOGRAM

Synthetic seismograms was generated for East Baghdad well-1 using GeoFrame software package . (Sheriff and Geldart, 1995) referred to the main steps for generation of the synthetic seismogram which they are :

a- finding the acoustic impedance (= $\rho \times v$)
Where:
v: Is seismic velocity.

ρ: Is density measured from density logs.

b- calculating the reflection coefficients (RC) of the vertical incident wave on reflector separating two groups of time intervals such (i) and (i+1) that have values of acoustic impedance (ρi vi) and (ρi+1, vi+1) respectively (Khorshid, 2015) .

$$RC = \frac{V_2\rho_2 - V_2\rho_2}{V_2\rho_2 + V_2\rho_2} = \frac{A_r}{A_i} \dots\dots\dots\dots\dots\dots\dots (1)$$

Experimentally choice wavelet is made to result the synthetic seismogram. The sonic log data are compared with the wellhole velocity survey which symbolizes the direct method to measure the geological velocity (average velocity) of geological strata. The synthetic seismogram traces of the East Baghdad well for EB-1 were generated using programs within the IESX (synthetic programs). These have ability to extract the relation between the time and depth functions in the well location. This relation is very important in determining the reflection on a time axis of seismic section and synthetic trace against the require bed in the well. The sonic logs were transformed from the depth to the time domain using the check shots that were provided and used to make synthetics from the computed reflectivity series convolved with a Ricker and extraction wavelet to match the dominant frequency of reprocessed 2D seismic data. After that calibration must be done on seismic section of the synthetic as shown in Figure (10).

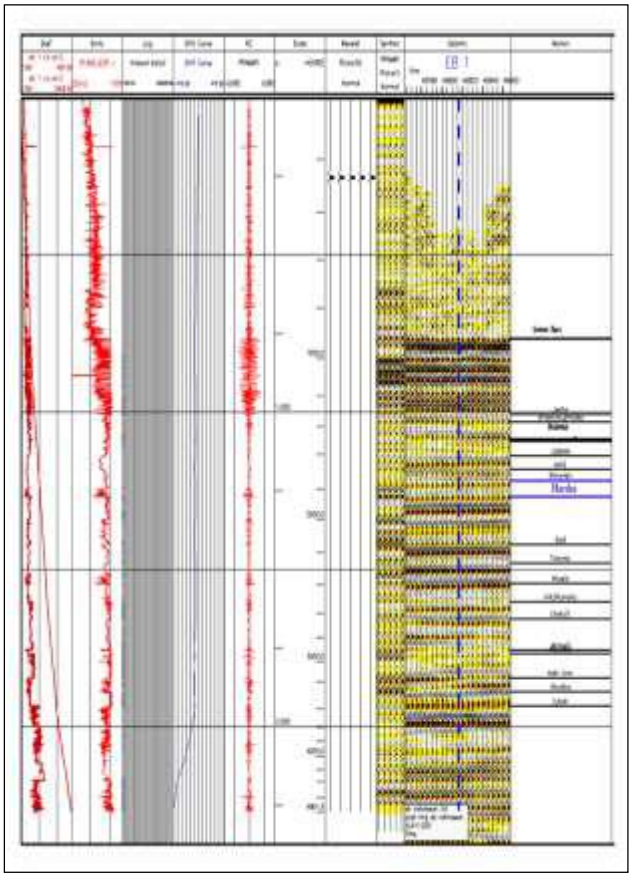

Fig.10: Shows the seismic sections with synthetic seismogram of EB-1.

https://dx.doi.org/10.22161/ijaers.4.9.15 *ISSN: 2349-6495(P) | 2456-1908(O)*

CONCLUSIONS

The following conclusions are the resultant of this research:-

1. Through the implementation of several field tests, a major action plan was adopted as shown in Table -1
2. Best arrangement have been reached through installed and the spread of a 60-line impact and the distance between the point of receive and the other are (2 meters).
3. The best signal source represent by four shocks (vibrators) are in work and one vibrators as reserve Type (NOMAD 65) with a maximum capacity (peak force) of (62000 LB) for each shock.
4. By using the information of EB-1 Well, and making the relationship time-depth curve of EB-1 then following up on getting synthetic to be linked later with seismic data and sections to obtain a real subsurface image
5. Through the use of the interactive workstation (GeoFrame) to get a good applications and interpretation.

ACKNOWLEDGEMENTS

Praise is to Allah, prayer and peace are upon his Messenger Mohammed bin Abdullah and ALLAH of divine good after. Many thanks to the Department of Geology, College of Science, and Baghdad University for providing opportunities and facilities to accomplish this research. I would like to express my appreciation and deep gratitude to my supervisor, Dr. Salman Zain Al-Abdin Khorshid, College of Education, University of Tikrit. My thanks go to the Dr. Faleh Al-Tamimi of the Department interpretation at Oil Exploration Company .

I am terribly grateful to Mr. Jameel R.Kmona at the Oil Exploration Company (O.E.C.) for providing pportunities and facility to accomplish this research, special thanks to Mr. Dhulfiqur Ali of the Department of Geophysical studies at the Oil Exploration Company. Also, I do not forget to present my greatest thanks and gratitude to my family who encouraged and supported me throughout .

REFERENCES

[1] OIL EXPLORATION COMPANY(O.E.C.) (2010). FINAL REPORT OF EAST BAGHDAD PROGRAM, SOUTH-2, IRAQI SEISMIC PARTY NO.2.

[2] Oil Exploration Company(O.E.C.) (2011). report of East Baghdad program, South-1, Iraqi seismic.

[3] Yilmaz, O. (1987). Seismic Data Processing, SEG series: Investigation Geophysics, V. 2, 526 p.

[4] Hatton, C.S.R., Peto, T.E.A., Bunch, C., Pasvol, G., Russell, S.J., Singer, C.R., Edwards, G., & Winstanley, P. (1986) Frequency of severe neutropenia associated with amodiaquine prophylaxis against malaria. Lancet 1, 411-414.Sheriff, R.E. (1976). Encyclopedic Dictionary of Exploration Geophysics, Society of Exploration Geophysicists, 1st edition, 266 p.

[5] Silvia,M.,T., and Robinson,E.,A.(1979). deconvolution of geophysical series in the exploration for oil and natural gas, Elsevier Science, V.10,1st Edition,, 250p.

[6] Deregowski, S. M.(1986) . Seismic reaction data interpolation with differential offset and shot continuation , Published in Geophysics, no 68, pp. 733-744 .

[7] Telford, W.M., Geldart, L.P., Sheriff, R.E.(1990). Applied geophysics, 3rd ed., Cambridge University press, pp.136-229 .

[8] Stolt, R.B., Benson, A.K..(1986). Seismic Migration; Theory and Practice. Geophysical Press, Amsterdam, The Netherlands. 382 p.

[9] Bacon, R. S. and Redshaw T. (2003) 3-D Seismic Interpretation, Printed in United Kingdom at the University press, Cambridge, 212 p.

[10] Drijkoningen, G.G. and Verschuur, D.J. (2003). Seismic Data Processing , Delft University of Technology, 118 p.

[11] Hagedoorn, J.G. (1954). A process of seismic reflection interpretation,Geophysical Prospecting ,Vol 2, No 2, pp. 85-127.

[12] Stolt ,R. H. (1978). Migration by fourier transform,geophysics , GEOPHYSICS. VOL. 43. NO. I ,pp. 23-48.

[13] Schlumberger Information Solution. (2004). GeoFrame Fundamentals, Training and Exercise Guide, Version 4.0.1, 102 p.

[14] Dobrin, M.B. and Savit, C.H.(1988). Introduction to Geophysical Prospecting, 4th ed. McGraw-Hill Co., 865 p.

[15] Khorshid, Salman Z. and Kadhm, Ayat D.(2015). Subsurface Investigation of Oligocene Geologic Formations Age, East Baghdad Oil Field, 2015, Vol. 57, No.1A, pp. 154-162.

[16] Sheriff, Robert E.and Geldart, Lloyd P.(1995). Exploration Seismology, Cambridge University Press . 2nd ed. 628p.

https://dx.doi.org/10.22161/ijaers.4.9.16 *ISSN: 2349-6495(P) | 2456-1908(O)*

Trend Analysis of Landcover/ Landuse Change in Patani L.G.A, Delta State Nigeria

Ojiako, J.C, Igbokwe, E.C

Department of Surveying & Geoinformatics, Nnamdi Azikiwe University Awka, Nigeria

Abstract—*This study examines the use of GIS and Remote Sensing in trend analysis of landcover/landuse change in Patani L.G.A, Delta State Nigeria from 2005 to 2015. Thus the study is to carry out a multi-temporal analysis of development trends, thereby detecting the changes that have taken place between these periods. Two Landsat images, Landsat 7ETM+ (2005) and Landsat 8OLI (2015) were acquired, classified and change detection analysis was performed to determine the multi-temporal landcover/landuse changes between the years. The results showed that vegetation decreased from 16673.73 hectares in 2005 to 15973.9 hectares in 2015 covering 75.45% of landcover/landuse class in the study area, built up area gained from 3684.03 hectares in 2005 to 4346.37 hectares in 2015 covering 20.53 % in the study area, while water bodies also increased from 812.29 hectares in 2005 to 849.78 hectares in 2015 covering 4% of the study area. The study also indicated that the annual growth rate of Built up area has increased at 0.82% from 2005 to 2015, vegetation decreasing significantly at the rate of -0.21% from 2005 to 2015, and water bodies also increasing at a rate of 0.22% from 2005 to 2015. The results from this study can serve as a base for decision making and planning for urban planning and regional developments in Patani L.G.A.*

Keywords— Geographic Information System, Landcover/ Landuse, Remote Sensing, Change detection.

I. INTRODUCTION

Due to anthropogenic activities, the Earth surface is being significantly altered in some manner and man's presence on the Earth and his use of land has had a profound effect upon the natural environment thus resulting into an accelerated growth in settlement expansion (Zubair, 2008). Settlements are products of human activities. They are dynamic and constantly changing with man's changing social and economic needs. Settlements whether informal or formal, require constant monitoring. This is especially true in most developing countries including Nigeria where proper and periodic monitoring of formal settlements is not carried out; there is a very high tendency for informal settlements to develop (Opeyemi et al, 2015). Data on land use/land cover may not be easily obtained except with relevant remote sensing technologies and techniques (Ukor et al, 2016).

Remote sensing and Geographical Information Systems are powerful tools to derive accurate and timely information on the spatial distribution of landcover/landuse changes over large areas. GIS provides a flexible environment for collecting, storing, displaying and analyzing digital data necessary for change detection (Ukor et al, 2016).

Remote sensing imagery is the most important data resource of GIS. The satellite imagery can be used for recognition of synoptic data of earth's surface. The aim of change detection process is to recognize land use on digital images that change features of Interest between two or more dates. There are many change detection techniques such as post classification comparison, conventional image differentiation, using image ratio, image regression, and manual on-screen digitization of Change, principal components analysis and multi date image classification.

Therefore the main aim of this study is to analyze the trend of landcover/landuse changes in Patani Local Government using satellite imageries and GIS with a view to providing recommendations for sustainable development and decision making.

II. STUDY AREA

Patani is a Local Government Area in Delta State, Nigeria. Its headquarters are in the town of Patani. It has an area of 217 km² and a population of 67,707 at the 2006 census. It is located between latitudes $5^0$6' 0" N and $5^0$15'0"N and longitudes $6^0$0'0"E and $6^0$18'0"E see fig 1

https://dx.doi.org/10.22161/ijaers.4.9.16 *ISSN: 2349-6495(P) | 2456-1908(O)*

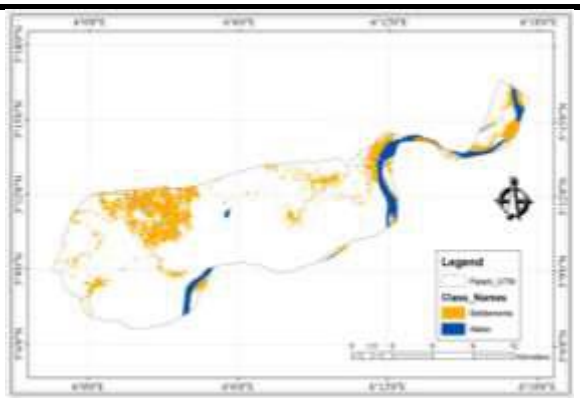

Fig.1: Map of Patani L.G.A

III. METHODOLOGY

For a proper and effective optimization, planning is very important. In this phase of the project, a user requirement analysis was done to focus on what information is presently being used, who is using it and how the source is being collected, stored and maintained. There is ideally a map of existing processes which was improved as well as being replicated by the GIS. The necessary information was obtained through interviews, documentations, reviews and workshops. This also involves the data requirement, hardware and software selections and method to be used.

3.1 Data Requirement

Data used in this research includes;

I. Landsat 7 ETM+ and Landsat 8 OLI Imagery of the study area
II. Co-ordinates of control points and other points of interest
III. Attribute Data of points of interest.
IV. Administrative map of Delta State showing Local Government boundaries
V. Materials available in Academic journals, conference papers, relevant texts, brochures, internet and statistical files of government offices.

3.2 Methods and Techniques

The method used in this study involves image subset, image classification techniques as well as multi-temporal image analysis. Image subset was done on the two multi-temporal sets of images obtained (Landsat7 ETM+, Landsat8 OLI) in order to cut out the study area from the image set, after which land cover maps of the study area were produced using the supervised maximum likelihood classification algorithm in ERDAS Imagine. Trend analysis was also performed to determine the trend of change in the time period between 2005 and 2015.

IV. RESULTS

The results of image analysis as obtained from the hard classification procedure of supervised classification, change detection and trend analysis are presented. Most of the discussions are supported by maps, tables and illustrative graphs.

4.1 Land cover / Land use Distribution of Patani L.G.A of 2005

In mapping landcover/land use, three different classes of interest were identified to include Built up area, Water, and Vegetation. The classified image of Patani L.G.A is shown in figure 4.1

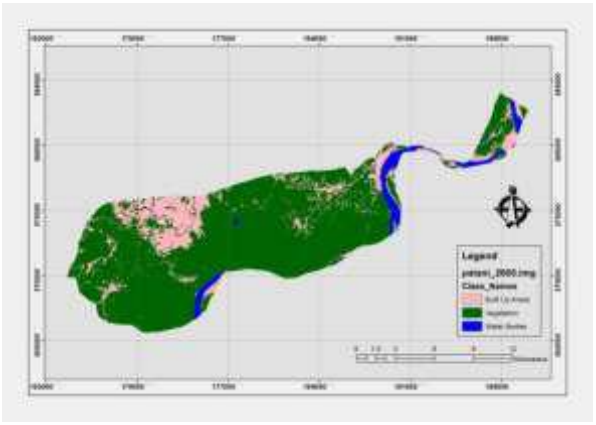

Fig.1: Landcover/Landuse of Patani L.G.A in 2005

The land cover/land use distribution of Patani in 2005 as shown in table 4.1 and fig 4.2 indicates that vegetation accounted for the largest land cover/use class in the study area with about 78.76% of the landcover/landuse class covering 16673.73 hectares in area, built up areas had 17.40% covering at total area of 3684.03 hectares while water body had 3.84% covering a total area of 812.29 hectares.

Table.4.1: 2 Landcover/Landuse distribution of Patani L.G.A in 2005

Class Type	2005	
	Area (Hectares)	Percentage %
Built Up Areas	3684.03	17.40
Vegetation	16673.73	78.76
Water Bodies	812.29	3.84
Total	21170.05	100

https://dx.doi.org/10.22161/ijaers.4.9.16 *ISSN: 2349-6495(P) | 2456-1908(O)*

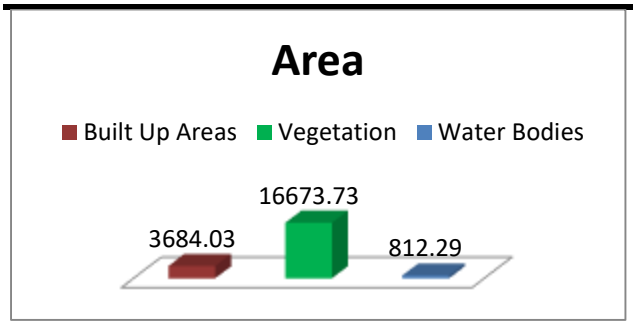

Fig.4.2: Histogram of Landcover/Landuse of Patani L.G.A in 2005

4.2 Land cover / Land use Distribution of Patani L.G.A in 2015

The land cover/land use distribution of Patani L.G.A in 2015 as shown in figure 4.3, 4.4 and table 4.2 indicate that vegetation decreased from 16673.73 hectares in 2005 to 15973.9 hectares in 2015 covering 75.45% of landcover/landuse class in the study area, built up area gained from 3684.03 hectares in 2005 to 4346.37 hectares in 2015 covering 20.53 % in the study area, while water bodies also increased from 812.29 hectares in 2005 to 849.78 hectares in 2015 covering 4% of the study area.

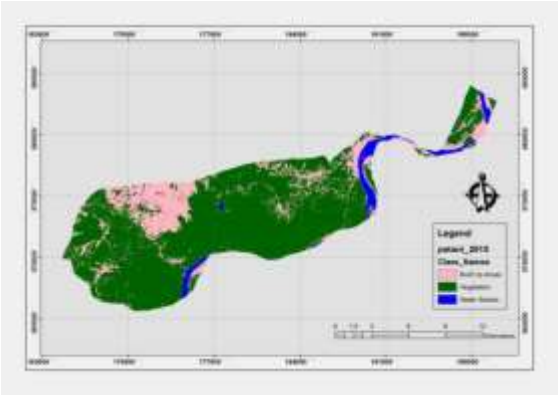

Fig.4.3: Landcover/Landuse of Patani L.G.A in 2015

Table.4.2: Landcover/Landuse distribution of Patani L.G.A in 2015

Class Type	2015	
	Area (Hectares)	Percentage %
Built Up Areas	4346.37	20.53
Vegetation	15973.9	75.45
Water Bodies	849.78	4.014
Total	21170.05	100

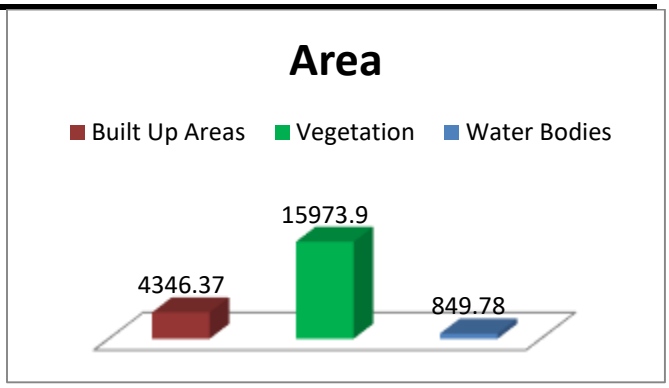

Fig.4.4: Histogram of Landcover/Landuse of Patani L.G.A in 2015

4.3 Trend Analysis

The results of the trend analysis are presented in table 4.3 and figure 4.5. A trend percentage with a value greater than zero means that the land use type has increased over the period of years while a value less than zero shows a decrease in the land cover/land use type over a period of time (long et al, 2007) .

The results indicate that the annual growth rate of Built up area increased at at 0.82% from 2005 to 2015, this is significant as this indicates a trend of urban expansion in the study area from 2005 to 2015. Vegetation decreased significantly at the rate of -0.21% from 2005 to 2015, this is by far the most significant decrease in the study area, and this loss is attributed to urban expansion and flooding events in the study area, due to rapid urbanization and anthropogenic activities in the study area. This activity gives rise to vegetation encroachment thereby resulting in the decrease of vegetation from 2005 to 2015. Water bodies also increased at a rate of 0.22% from 2005 to 2015.

Table.4.3: Trend of change of landcover/landuse of Patani L.G.A from 2005 to 2015

Class Type	Annual Rate (%)
	2005-2015
Built Up Areas	0.82
Vegetation	-0.21
Water Bodies	0.22

https://dx.doi.org/10.22161/ijaers.4.9.16 *ISSN: 2349-6495(P) | 2456-1908(O)*

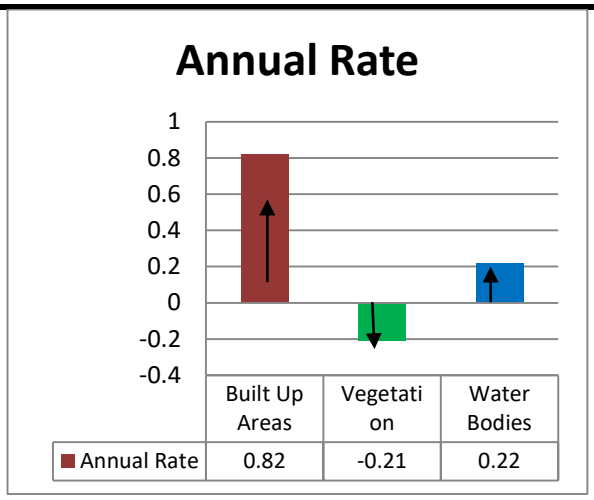

Fig.4.5: Trend of change of landcover/landuse of Patani L.G.A between 2005 and 2015

V. CONCLUSION

This study demonstrates the ability of Remote Sensing and GIS in capturing spatial-temporal data. Attempt was made to capture as accurate as possible the three land use land cover classes as they change through time.

The study indicated that the annual growth rate of Built up area has increased at 0.82% from 2005 to 2015, vegetation decreasing significantly at the rate of -0.21% from 2005 to 2015, and water bodies also increasing at a rate of 0.22% from 2005 to 2015.

This result is significant as it indicates a trend of urban expansion in the study area from 2005 to 2015, this trend can also be said to be responsible for vegetation reduction from 2005 to 2015 due to vegetation encroachment from urbanization.

REFERENCES

[1] Long, H.G., Tang, G., Li, X. and Heilig, G.K. (2007). Socio-economic driving forces of landuse change in Kunshan, the Yangtze river delta economic area of the China. *Journal of Environmental Management*, 83 (3): 351-364

[2] Opeyemi, A. Z., Lazarus, M. O., Richard A. M., (2015), Urbanization: A Catalyst For The Emergence Of Squatter Settlements And Squalor In The Vicinities Of The Federal Capital City Of Nigeria, Journal of Sustainable Development; Vol. 8, No. 2; ISSN 1913-9063 E-ISSN 1913-9071

[3] Ukor, C. D, Ogbole, J., Alaga, A. T. (2016). Analysis of Land Use Land Cover Change in Ikeja, Lagos State, Nigeria. Using Remote Sensing and GIS Techniques, International Journal of Science and Technology Volume 5 No. 10, October, IJST Publications UK

[4] Zubair, A. O. (2008), Monitoring the Growth of Settlements in Ilorin, Nigeria (A GIS and Remote Sensing Approach), The International Archives Of The Photogrammetry, Remote Sensing And Spatial Information Sciences. Vol. Xxxvii. Part B6b. Beijing 2008, Pp 225-232

https://dx.doi.org/10.22161/ijaers.4.9.17 ISSN: 2349-6495(P) | 2456-1908(O)

Characterization of polygalacturonases produced by the endophytic fungus *Penicillium brevicompactum* in solid state fermentation - SSF

Sideney Becker Onofre[1,2], Ivan Carlos Bertoldo[1,2], Dirceu Abatti[2], Douglas Refosco[2], Amarildo A. Tessaro[2] and Alessandra B. Tessaro[3]

[1] Universidade Comunitária da Região de Chapecó - UNOCHAPECÓ - Center of Exact and Environmental Sciences - ACEA - Technology and Innovation Management Posgraduate Program - PPGTI - Av. Senador Attílio Fontana, 591-E EFAPI - 89809-000 - Chapecó - Santa Catarina - Brazil. E-mail: beckerside@unochapeco.edu.br.

[2] União de Ensino do Sudoeste do Paraná - UNISEP - Faculdade Educacional de Dois Vizinhos - FAED - Av. Presidente Kennedy, 2601 - 85660-000 - Dois Vizinhos - Paraná - Brazil. E-mail: amarildo@unisep.edu.br

[3] Federal University of Pelotas – UFPel - Postgraduate Program in Materials Science and Engineering. Rua Flores da Cunha, 809 – Pelotas – Rio Grande do Sul – Brazil. E-mail: alessandrabuss@gmail.com

***Abstract*—** *Polygalacturonases belong to the family of pectinases, enzymes that are in high demand in industry because of their many different applications. This study therefore sought to examine the production of polygalacturonases using an endophytic fungus, Penicilium* brevicompactum, *isolated from Baccharis dracunculifolia D.C. (Asteraceae) through semi solid fermentation using orange peels and citric pectin 2% as base substrate, supplemented with different carbon sources. After the fermentation process, the enzyme was characterized. The results showed that the micro-organism was able to use a wide range of carbon sources, but with polygalacturonase activity varying with each source. The highest yield, however, was achieved after 30 hours of incubation in the presence of 4% of galactose and 2% of pectin. Studies on the characterization of the polygalacturonase revealed that the optimal temperature of this enzyme is 72°C and that it maintains 60 and 15% of its maximum activity when incubated for 2 hours at 40 and 90°C, respectively. The optimal pH for the activity of the enzyme was 4.6. The enzyme retained 65 and 30% of its maximum activity when incubated at pH 3.5 and 9.5, respectively, for 24 hours at ambient temperature. The enzyme activity was stimulated by Mg^{2+} ions. On the other hand, it was inhibited by the ions Cs^{+2}, Hg^{+2}, Li^{+2} and Sr^{+2}. The ions Zn^{+2} and Cu^{+2} inhibited it by 94% and 69%, respectively.*

***Keywords*— Enzymes, pectins, fermentation, polygalacturonase, bioprocess.**

I. INTRODUCTION

Pectins are classes of complex polysaccharides found in the cell walls of plants and they are commonly produced during the early growth stages of the cell wall, corresponding to approximately 1/3 of this wall (Sajjaanatakul; Van-Buren and Downing, 1989; Muralikrishna and Taranathan,1994).

The synthesis of pectin (Figure 1) starts with the UDP-d-galacturonic acid and it is synthesized through the Golgi Complex during the early growth stages of the cell wall. Although galacturonic acid is the main constituent of pectic substances, varying proportions of other sugars, such as D-galactose, L-arabinose, D-xylose, L-rhamnose, L-fucose and traces of 2-O-methyl fucose can also be found (Jarvis, 1984; Leitão *et al.*, 1995).

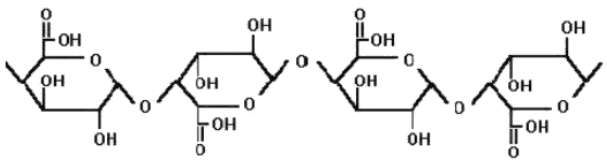

Fig. 1: Chemical Structure of pectin, formed by sub-units of galacturonic acid (Houdert and Muller, 1991).

It has been suggested that the carboxyl groups of pectins are strongly methyl-esterified, but that these esters are cleaved by the PME (pectin methylesterase) present and by the activity of polygalacturonase in tomatoes, resulting in pectins of high molecular weight. Roberts, (1990), Tieman and Handa (1994), described that the decreased activity of PME in tomatoes causes a total loss of integrity of tissues during the senescence of the fruit. PME accelerates the hydrolysis of the ester-methyl bonds in the pectin molecule, forming pectic acid and methanol (Amstalden, 1982).

Although several enzymes called hydrolases of the pectinase type are responsible for the degradation or breaking of this polymer contained in the plant's cell wall, the activity of pectin methylesterase (PME) and polygalacturonase (PG) stands out, which act during the

https://dx.doi.org/10.22161/ijaers.4.9.17 *ISSN: 2349-6495(P) | 2456-1908(O)*

ripening of the fruit and which have been extensively investigated regarding their genetics, biochemistry and levels of gene expression (Fischer; Bennett, 1991).

In Kashyap *et al.*, (2001) and Belafi-Bako *et al.*, (2007), pectinolytic enzymes (Figure 2) are classified according to their mode of action as demethylation pectins, which catalyze the hidrolise of methoxyl groups linked to carboxylic groups of the pectin chain, forming pectic acid, which contains negligible quantities of methoxyl groups (pectinesterase (PE): E.C. 3.1.1.11); depolymerizing pectins, which catalyze hydrolysis reactions (polymethyl-galacturonases (PMG), polygalacturonases (PG): endo-PG (E.C. 3.2.1.15) and exo-PG 1 and 2 (E.C.3.2.1.67, E. C. 3.2.1.82)) and the break up by trans-elimination (polygalacturonatelyase (PGL): endo-PGL (E. C.4.2.2.2) and exo-PGL (E. C.4.2.2.9) and pectin lyase (PL) (4.2.2.10) (Sakai and Okushima, 1982; Ahrens and Huber, 1990; Fischer and Bennett, 1991; Kashyap *et al*., 2001; Belafi-Bako *et al.*, 2007).

Pectinolytic enzymes can be synthesized by bacteria, fungi and yeasts. The production of pectinases by micro-organisms is influenced by growing conditions, and especially by the composition of the culture medium, the type and concentration of the carbon source, pH and temperature of cultivation, in addition to other factors (Fogarty and Ward, 1974; Freitas, 1991; Bravo *et al.*, 2000).

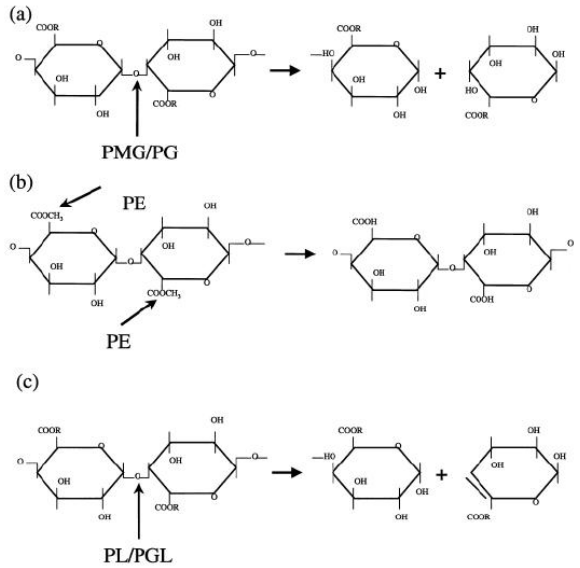

Fig. 2: Different types of pectinases and their modes of action on pectic substances. (a) R = H for PG and CH3 for PMG, (b) PE and (c) R = H for PGL and CH3 for PL. The arrow indicates the place where the pectinases act on the pectic substances. PG: polygalacturonase, PMG: polymetylgalacturonase, PE: pectinesterase, PGL: pectate lyase, PL: pectin lyase (Gummadi and Panda, 2003).

The first step for the industrial use of these enzymes is the selection or development of appropriate strains, followed by an optimization of the cultivation conditions. In other words, one has to learn the various aspects that regulate the synthesis and activity of the enzyme. The micro-organism is, without doubt, the limiting factor of any fermentation process. This fact is commonly corroborated in the literature, as for example in (Maiorano, 1982; Maiorano and Schmidell; Ogaki, 1995; Nogueira, 2003; Collares, 2011).

These enzymes can be obtained through both submerged (SmF) and solid state (SSF) fermentation processes (Fogarty and Ward, 1974; Freitas, 1991; Bravo *et al.*, 2000; Gummadi and Panda, 2003; Collares, 2011). For the specific case of SSF, the supports or substrates consist basically of organic polymers that are characterized by their insolubility in water and their ability to promote microbial growth, even without the addition of additional nutrients. Among the main characteristics of SSF, the following deserve special mention: low quantity of available water, low risk of contamination, use of smaller reactors than those used in SmF for the same amount of substrate, high yields and low costs with respect to the substrate used (Hendges, 2006).

The production of enzymes by micro-organisms through SSF is influenced by several cultivation factors, such as: the micro-organism used in the fermentation process, the availability of water, nutrients, temperature, the applied inoculum, aeration and the presence of inducing substances. The study of these factors is essential for the optimization of a fermentation process (Dartora *et al.*, 2002).

Pectinolytic enzymes are widely employed in various industries. In food, these enzymes are used for the extraction, depectinization and clarification of fruit juices (bananas, papayas, apples) and wine, for the extraction of vegetable oil, and in the production of baby foods (Buenrostro and Lopes-Munguia, 1986; Ghildyal *et al.*, 1994; Kashyap *et al.*, 2001; Nighojkar *et al.*, 2006; Gupta *et al.*, 2007; Ustok, Tari and Gogus, 2007). They can also be used in the industry of fermented products, such as the fermentation of cocoa, coffee and tobacco, and in the degumming of natural fibers (Genari, 1999; Bravo *et al.*, 2000; Fawole and Odunfa, 2003).

The food industry, juice producers in particular, has shown a growing interest in the use of pectinases since their use in various processes results in increased yields, quality improvements of the product and reductions in the operating costs of the process (Wosiacki and Nogueira, 2005). Micro-organisms are a rich source of many enzymes, and pectinases, particularly those produced by fungi, are of great industrial importance (Koch; Nevins, 1989; Ferreira and Castilho; Paiva, 1995; Uenojo and Pastore, 2007).

https://dx.doi.org/10.22161/ijaers.4.9.17 *ISSN: 2349-6495(P) | 2456-1908(O)*

It's in this context that this study observed the production of fungal polygalacturonases by the endophitic fungus *Penicillium brevicompactum*, isolated from *Baccharis dracunculifolia* D.C. (Asteraceae), using Solid State Fermentation (SSF) in a medium made up of dehydrated orange peels, inductor sources and salts.

II. MATERIALS AND METHODS

2.1 Microrganisms

The strain of *Penicilium brevicompactum* used in this work was isolated by Recalcatti *et al*., (2004). The methodology used for isolation has been described by Day, Fincham and Radford, (1979) and Larone, (1985). The conservation of this strain was done in a glycerinated culture medium, following the methodology described by Maiorano, (1982), being maintained through monthly samplings.

2.2 Culture conditions

The culture medium was formulated containing ($g.L^{-1}$) $MgSO_4.7H_2O$ 0.2g, $(NH_4)2SO_4$ 0.2g, KH_2PO_4 0.05 g. This formulation of salts was supplemented with the following carbon sources: citric pectin 2g; galactose 2g, galactose 4g and polygalacturonic acid 4 g in 100 g of orange peels, dried until reaching a humidity of 10%, crushed and sieved to remove particles of smaller size and obtaining fragments with more homogeneous dimensions of approximately 3 mm (Gomes, 1995).

The pH value of the medium was adjusted to 4.5 and the sterilization was performed for 15 min at 120 ºC. The vials, properly capped with cotton stoppers, were sterilized at 120 ºC for 15 minutes and the pressure was maintained at 0.5 atm to avoid caramelization of the culture medium.

Considering the conditions established in the preliminary fermentation, the kinetics of enzyme production were monitored for a period of 96 hours at 35 ºC, taking samples after 0, 20, 40, 60, 80, 100 and 120 hours.

2.3 Enzymatic assay of polygalacturonase

The fermented mass, collected at certain periods of cultivation, was homogenized and macerated (wet) in a mortar. Samples were collected after 0, 20, 40, 60, 80, 100 and 120 hours.

To determine the moisture content, 1g of the sample was submitted to oven drying at 105 °C until reaching a constant weight. After cooling, the sample was weighed again and the moisture content present in the medium was calculated, (AOAC, 1997).

To determine the pH, 10 mL of distilled water was added to the dried samples used for the determination of moisture. After shaking, these were allowed to rest for 10 min, and then the pH reading was performed. The biomass was determined after filtration and the micelles were submitted to heating at 85 ºC until reaching a constant weight.

For the extraction of enzymes, 15 mL of destilled water at pH 4.0 was added to 2.7 g of the previously macerated fermented mass. After 30 min of shaking at 200 rpm, the suspension was centrifuged at 9000 rpm for 20 min. The broth (15 mL) was then used to determine enzyme activity.

Polygalacturonase activity was determined in the filtered cultures of *P. brevicompactum* by determining the content of reducing groups, after reaction with dinitrosalicylic acid (Miller, 1959). The mixture of the reaction contained: 2.4 mL of citrate/phosphate buffer 0.2M, pH 5.0, 0.1 mL of enzyme extract and 2.5 mL of partially methoxylated citric pectin, 0.25% (Sigma, P-9135). The pre-incubation was carried out at 35°C for 10 minutes.

The reaction was initiated by the addition of enzyme extracts and water was added in the control test instead of the substrate (Malvessi, 2000; Malvessi and Silveira, 2004). One unit of activity was considered to be the amount of enzyme capable of generating 1 mol of galacturonic acid, per minute.The content of free reducing sugars (RS) present in the enzymatic extract was determined by the DNS method, using a glucose solution as standard.

To determine the total reducing sugars (TRS) in the fermentation medium, the methodology described by Malvessi, (2000), was used; Malvessi and Silveira, (2004), in which 10 mL of H_2SO_4 1.5 M was added to 0.7 g of homogenized and macerated mass, hydrolyzed at 100°C for 30 min, followed by cooling in an ice bath. After the neutralization, the preparations were deproteinated and filtered, and the reducing sugars obtained through this technique were then quantified through the DNS method (Miller, 1959).

2.4 Characterization of the enzyme

The equivalent of 60% of ammonium sulfate was added to the cell-free supernatant for protein precipitation. After this procedure, the material precipitate was centrifuged at 20.000 revolutions for 10 minutes at 4°C. A minimum quantity of phosphate buffer was added to the precipitate for its re-suspension, after which it was once again centrifuged at 20.000 revolutions per 20 minutes at 4°C. The filtrate was used for determination of the enzyme activity (Malvessi and Silveira, 2004).

2.5 Effect of temperature on the activity and stability of polygalacturonase

The determination of optimal temperature was performed by incubating the reaction mixture (pH 7.0) at temperatures ranging from 40 to 100°C, with intervals of 10°C. After 10 minutes of incubation at each temperature, the enzyme activity was analyzed. The thermal stability was evaluated by incubating the enzyme in temperatures that ranged from

https://dx.doi.org/10.22161/ijaers.4.9.17 *ISSN: 2349-6495(P) | 2456-1908(O)*

30 to 100°C, with intervals of 10°C. After two hours of incubation, the residual activity was examined at the optimal temperature of the enzyme determined above.

2.6 Effect of the pH on the activity and stability of polygalacturonase

The influence of pH on the activity of polygalacturonase was evaluated in the range of 3.5 to 9.5 with an interval of 0.5 units. The substrate preparation used was a buffering mixture containing sodium acetate (pH 5.0 -5.5), phosphate (pH 6.0 - 8.0) and tris (pH 8.5 -10.0), with a final concentration of 50 mM. The pH values of the reaction mixture were adjusted with NaOH or HCl 1N.

The optimal pH was determined by incubation of 0.2 mL of the enzyme and 0.8 mL of citric pectin (0.5%) prepared in buffers with different pH values. After incubation at 70°C for 10 minutes, the enzyme activity was analyzed as described previously. The stability of the polygalacturonase under different pH values was evaluated by incubating the enzyme extract in the buffers described above, without the substrate, for 24 hours at ambient temperature. After this treatment, the residual activity of the polygalacturonase was determined as described previously.

2.7 Effect of ions on the activity and stability of polygalacturonase

The following compounds were added to the reaction mixture, at a final concentration of 1 mM, to study the effect of different metal ions on the activity of polygalacturonase: $CaCl_2$, $BaCl_2$, $AgNO_3$, $HgCl_2$, $CuSO_4$, $ZnSO_4$, CsCl, $CoSO_4$, $NiCl_2$, $C_4H_6O_4Pb$, $FeSO_4$, $MnSO_4$, $MgSO_4$, $SrCl_2$and $LiSO_4$. This method followed that described by Malvessi (2000) and Malvessi and Silveira (2004).

2.8 Statistical analysis

The experiments were carried out in triplicate, and the results were evaluated by analysis of variance (ANOVA) using the SAS software, version 9.4. The effects of the treatments were compared with Tukey's Test.

III. RESULTS AND DISCUSSION

The carbon source in the growth medium of the fungi interferes with the synthesis of extracellular polygalacturonase. The increase in the synthesis of polygalacturonase by adding pectin (Maldonado and Calieri, 1989; Larios, Garcia and Huitron, 1989; Bailey, 1990; Baracat *et al.*, 1991), or galactose (Polizeli, Jorge and Terenzi, 1991), to the growth medium, has been observed with other micro-organisms.

This study was performed using galactose and polygalacturonic acid on pectin 2% as carbon sources in order to analyze the biomass, protein and polygalacturonase activity of *P. brevicompactum*. The highest production of mycelial biomass (6.34 mg/g), polygalacturonase activity (15.25 U/g) and total reducing sugars - TRC (0.84 g/g), was observed in the medium containing 4% galactose and 2% of citric pectin at pH 6.9 (Table 1).

Table 1: Effect of the nature of the carbon source on the accumulation of final biomass, total protein, activity and productivity of polygalacturonase in Penicillium brevicompactum. Time of 60 hours of fermentation.

Carbon[1]	Biomass	PG Activity[2]	TRS[3]	pH	Moisture
A	5.22a*	9.12b	0.33b	4.5a	50a
B	5,56a	8.20b	0.23b	4.6a	60a
S	6,34a	15.25a	0.84a	4.6a	55a
D	5,25a	10.21b	0.35b	4.4a	60a

[1]A= Pectin 2%. B= Pectin 2% + Galactose 2%. C= Pectin 2% + Galactose 4%. D= Pectin 2% + Polygalacturonic Acid * 4%. [2] Polygalacturonase Activity. [3]TRS - Total Reducing Sugars. * Means followed by the same letter vertically, do not differ by Tukey's Test (< 0.05).

In all tests, a drop in pH could be observed during the first 6 hours of incubation of the culture. A decrease in pH from 4.5 to 4.3 of the culture medium could be detected.

This initial drop in the pH of the medium may be due to the production of acids during the fermentation of the carbon source, which is more intense during this period. Subsequently, the pH of the medium increased gradually to 6.8 after 40 hours of incubation of the culture, remaining virtually unchanged until 60 hours, after which it decreased, maintaining itself stable at 4.6 for the medium containing pectin 2% + Galactose 4%. There was no significant difference in the mean pH values of all evaluated media. The increase in pH of the medium may be attributed to the use of organic acids or the production of alkali components during this period.

According to Ming Chu, Lee and Li, (1992), the acidification or alkalinization of the culture medium reflects the consumption of the substrate. When ammonium ions are being used, the environment becomes more acid, and when organic nitrogen (amino acids and peptides) is being assimilated, the environment becomes more alkaline. Due to this relationship between the synthesis of polygalacturonase and the use of nitrogenous compounds, the variation of pH can be used to provide important information about the production of polygalacturonases, such as the beginning and the end of its synthesis.

The effect of incubation time in the polygalacturonase trial was tested in a series of experiments in which the incubation time of the reaction at 30°C varied in the range of 20 to 120 minutes. The activity of the polygalacturonase is at its maximum at 30 minutes of incubation of the reaction (Figure 3).

https://dx.doi.org/10.22161/ijaers.4.9.17 ISSN: 2349-6495(P) | 2456-1908(O)

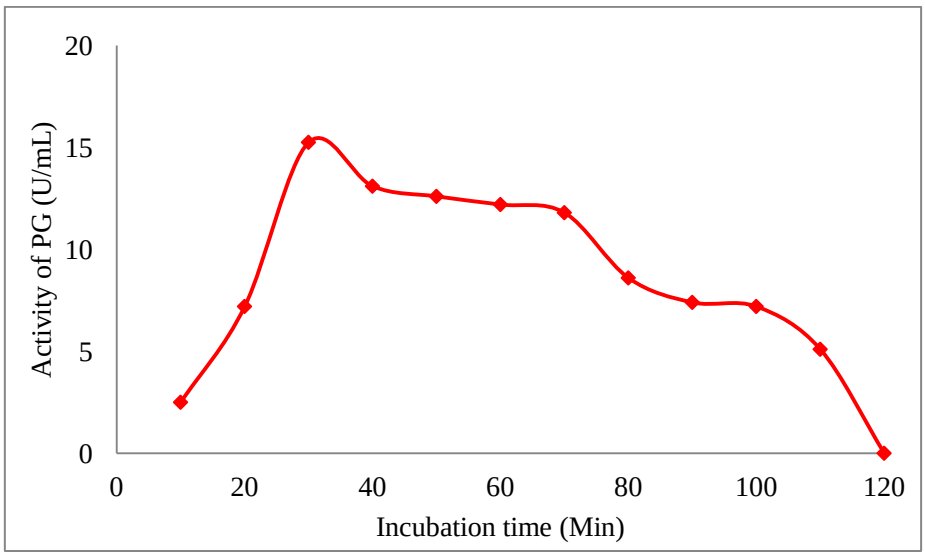

Fig.3: Production of polygalacturonase as a function of time, for Penicillium brevicompactum.

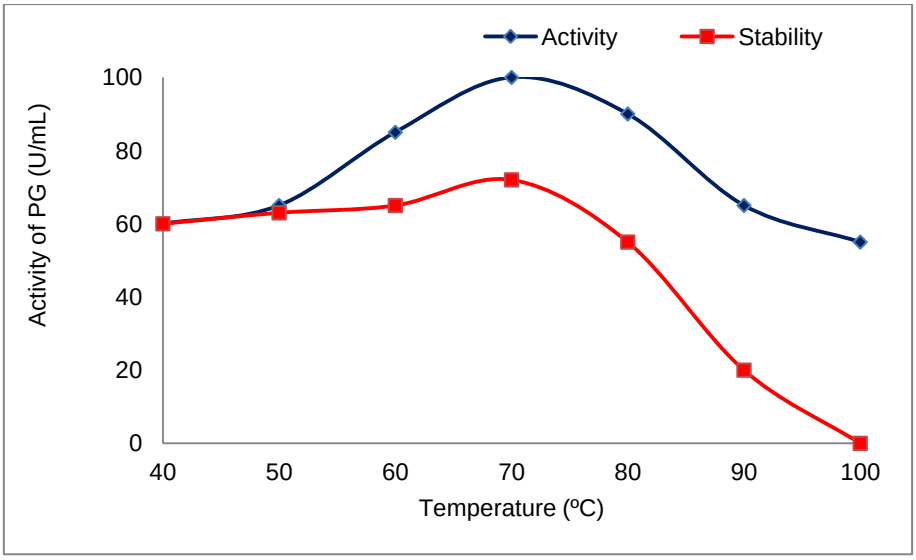

Fig. 4: *Optimal temperature and thermal stability of polygalacturonase secreted by Penicillium brevicompactum.*

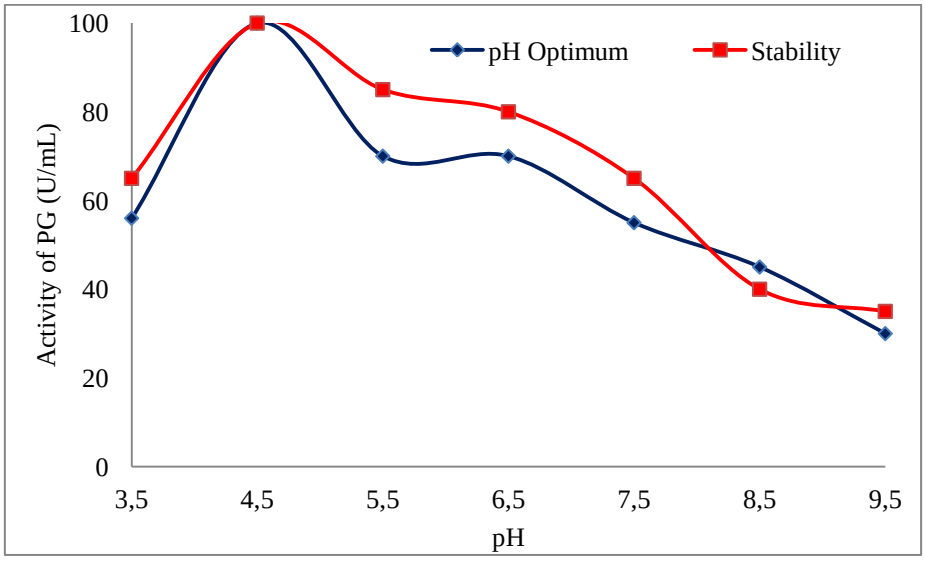

Fig.5: *Influence of pH on the activity and stability of the polygalacturonase secreted by Penicilium brevicompactum.*

https://dx.doi.org/10.22161/ijaers.4.9.17 *ISSN: 2349-6495(P) | 2456-1908(O)*

After 30 minutes of incubation of the reaction, the concentrations of reducing substances decrease as time increases, which means an up to 3-fold drop in the polygalacturonase activity in the fermentation supernatant from the fungus *P. brevicompactum*, with 60 minutes of incubation.

The results obtained in this work show that enzyme activity increased with the addition of galactose to 4% associated with the citric pectin at 2%. This same behavior was observed by Bueno, Peres and Gattas, (2005) who evaluated the behavior of different strains of *Aspergillus* sp. and found that the best results occurred with the association of citric pectin and galactose.

Freitas, (1991) showed that increases in the concentration of citric pectin didn't result in a considerable increase of enzyme activity, showing that the production of polygalacturonase by *Penicillium expansum* initially increased with the rising concentration of pectin in the medium, after which it decreased, because although the fungus continues growing, the polygalacturonase activity varies in response to the carbon source used for the growth of the micro-organism. The activity of the polygalacturonase was significantly higher during the growth of the micro-organism, changing the carbon source, associated with citric pectin.

3.1 Effect of temperature

Polygalacturonase activity increased with the increase in temperature, reaching its maximum value at 72°C, as shown in Figure 4.

The polygalacturonase secreted by *P. brevicompactum* maintained around 72% of its activity when incubated at 70°C for 2 hours and reduced its stability with the increase in temperature. It should be emphasized that this stability with temperatures near 70°C is a good indicator, as thermostable enzymes have a good market acceptance.

Martins *et al.,* (2002) obtained polygalacturonase from *Thermoascus aurantiacus* that retained 100% of its activity when incubated at 60 °C for 2 hours. A 50% reduction in the activity of this enzyme was observed, however, after incubation at 70 °C for 2 hours. These results indicate the production of thermostable polygalacturonase.

3.2 Effect of pH

The polygalacturonase was active in a wide pH range, with maximum activity around pH 4.6, as shown in Figure 5. The lowest enzyme activity was found at the pH values of 3.5 and 9.5, which were the most extreme values studied, with 65 and 40 %, respectively.

Regarding the stability of the pH, the polygalacturonase was stable for 24 hours at pH values between 4.5 and 5.0. When incubated at pH 9.5, the enzyme stability was only 30%.

Similar results were found by Rizatto (1999); Alaña, Llama and Serra, (1991), and Silva *et al*., (2005), who investigated the effect of pH on the polygalacturonase activity of *Penicillium italicum* and *Aspergillus niger* through semi-solid fermentation in industrialized orange bagasse.

According to these authors, these filamentous fungi studied revealed an optimal pH for polygalacturonase activity between 4.5 and 5.5, thus producing acid enzymes. Different Results are observed for cultures with different *Bacillus* strains, which produce enzymes in an optimal pH between 6.5 and 7.0. Kobayashi *et al.,* (2010), found an optimal pH value of 8.0 for a exo-polygalacturonase produced by the *Bacillus sp*. strain KSM-P576, while Devi and Rao, (1996), found an optimal pH of 10 for the polygalacturonase produced by the *Bacillus* sp. MG-cp-2.

3.3 Effect of some metal ions

The activity of the polygalacturonase secreted by *P. brevicompactum* was stimulated by Mg^{+2} ions. In the presence of this ion, a 160% increase in enzyme activity could be observed. The Cs^{+2}, Hg^{+2}, Li^{+2} and Sr^{+2} ions, on the other hand, inhibited enzyme activity. The ions Zn^{+2} and Cu^{+2} inhibited it by 94% and 69%, respectively.

Mg^{+2} also stimulated the activity of polygalacturonase produced by *Aspergillus carbonarius* (Devi and Rao, 1996), but inhibited the activity of polygalacturonase produced by *Bacillus* sp. (Kelly and Fogarty, 1978).

Tomazic, (1991) and Kobayashi; Koike and Yoshimatsu, (2010), highlight that the stabilization of some enzymes can be induced by non-protein additives, especially divalent ions such as Ca^{+2}, Mn^{+2}, Zn^{+2} and Mg^{+2}. If used in low concentrations, these ions can support the tertiary structure of the protein, promoting the formation of cross-links that provide a greater stability to it.

IV. CONCLUSION

After obtaining the results, one can conclude that the endophytic strain of *Penicilium brevicompactum* was able to use a wide range of carbon sources, but with polygalacturonase activity varying with each source. The highest yield, however, was achieved after 30 hours of incubation in the presence of 4% of galactose and 2% of pectin.

The characterization of the polygalacturonase revealed that the optimal temperature of this enzyme is 72 °C and that it maintains 60 and 15% of its maximum activity when incubated for 2 hours at 40 and 90°C, respectively.

The optimal pH for the activity of the enzyme was 4.6. The enzyme retained 65 and 30% of its maximum activity when incubated at pH 3.5 and 9.5, respectively, for 24 hours at ambient temperature.

The enzyme activity was stimulated by the Mg^{2+} ions. On the other hand, it was inhibited by the ions Cs^{+2}, Hg^{+2}, Li^{+2}

https://dx.doi.org/10.22161/ijaers.4.9.17 *ISSN: 2349-6495(P) | 2456-1908(O)*

and Sr^{+2}. The ions Zn^{+2} and Cu^{+2} inhibited it by 94% and 69%, respectively.

REFERENCES

[1] Ahrens M. J. Huber, D. J. (1990). Physiology and firmness determination of ripening tomato fruit. Physiologia Plantarum. 7(8): 8-14.

[2] Alaña A. Llama M. J. Serra J. L. (1991). Purification and some properties of the pectin lyase from *Penicillium italicum*. FEBS Lett. 20(2): 335-340.

[3] Amstalden L. C. (19982). Estudo sobre a ação de pectinesterase em suco de laranja. Campinas, 188p. Dissertação de Mestrado - Faculdade de Engenharia de Alimentos, Universidade Estadual de Campinas. Campinas. São Paulo. Brasil.

[4] AOAC. Association of Official Analytical Chemists. (1997). Official Methods of Analysis. 16th ed. Arlington V.A., USA.

[5] Bailey M. J. (1990). Effect of temperature on polygalacturonase production by *Aspergillus niger*. Enzyme Microb. Technol. 12(2): 622-624.

[6] Baracat M. C. Valentim C. Muchovej J. J. Silva D. O. (1991). Growth condictions of a pectinolytic *Aspergillus fulmigatus* for degumming of natural fibres. Biotechnol. Lett. 13(2): 693-696.

[7] Belafi-Bako K. Ezsterle M. Kiss K. Nemestothy N. Gubicza L. (2007). Hydrolysis of pectin by *Aspergillus niger* polygalacturonase in a membrane bioreactor. Journal of Food Engineering. 78(3): 438-442.

[8] Bravo C. E. C. Carvalho E. P. Schwan R. F. Gómez R. J. H. C. Pilon L. (2000). Determinação de condições ideais para a produção de poligalacturonase por *Kluyveromyces marxianus.* Ciência e Agrotecnologia. 24(1): 137-152.

[9] Bueno M. C. Peres M. F. S. Gattas E. A. L. (2005). Produção de poligalacturonase por três linhagens de *Aspergillus* isolados do solo. Alim. Nutr. 16(3): 253-257.

[10] Buenrostro M. Lopes-Munguia A. (1986). Enzimatic extraction of avocado oil. Biotechnology Letters. 8(4): 505-506.

[11] Collares R. M. (2011). Otimização do processo de hidrólise da mandioca "in natura", com uso de enzimas amilolítica e pectinolítica. 81 p. Dissertação (Mestrado em Engenharia de Processos) – Universidade Federal de Santa Maria, Santa Maria - Rio Grande do Sul. Brasil.

[12] Dartora A. B. Bertolin T. E. Bilibio D. Silveira M. M. E. Costa J. (2002). Evaluation of filamentous fungi and inducers for the production of endo-polygalacturonase by solid state fermentation. Z. Naturforsch. 57: 666-670.

[13] Day P. R. Fincham J. R. S. Radford A. (1979). Fungal Genetics. v.4. 4th ed. Oxford : Blackwell Scientific.

[14] Devi N. A. Rao A. G. A. (1996). Fractionation, purification, and preliminary characterization of polygalacturonases produced by *Aspergillus carbonarius*. Enzyme and Microbial Technology, 18: 59-65.

[15] Fawole O. B. Odunfa S. A. (2003). Some factors affecting production of pectic enzymes by *Aspergillus niger*. International Biodeterior Biodegradation. 52(2): 223-227.

[16] Ferreira J. S. G. Castilho L. R. Paiva S. P. (1995). Produção de pectinases para a indústria de bebidas, Trabalho de Conclusão de Curso - TCC - 56p. 1995. Escola de Química - Universidade Federal do Rio de Janeiro. Brasil.

[17] Fischer R. L. Bennett A. B. (1991). Role of cell wall hydrolases in fruit ripening. Annual Review Physiology Plant Molecular Biology. 42: 675-703.

[18] Fogarty W. M. Ward O. P. (1974). Pectinases and pecticpolysacharides. Progress in Industrial Microbiology. 13: 59-119.

[19] Freitas L. E. (1991). Produção e caracterização parcial de poligalacturonase de *Penicillium expansum*. Viçosa. 66p. Dissertação (Mestrado em Microbiologia Agrícola), Universidade Federal de Viçosa – Viçosa - Minas Gerais. Brasil.

[20] Genari R. (1999). Características de crescimento e produção de pectinases por Klebsiela oxytoca isolada de frutos de café. Viçosa, 90p. Dissertação (Mestrado em Microbiologia Agrícola), Universidade Federal de Viçosa – UFV. Voçosa. Minas Gerais. Brasil.

[21] Ghildyal N. P. Gowthaman M. K. Rao R. K. S. Karanth N. G. (1994). Interaction of transport resistances with biochemical reaction in packed-bed solid-state fermentors: effect of temperature gradients. Enzyme and Microbial Technology. 16(3): 253-257.

[22] GOMES, C. A. O. *Produção de enzimas despolimerizantes porfermentação em meio semi-sólido por Aspergillus niger mutante 3T5B8.* 78p. Dissertação (Mestrado em Ciência e Tecnologia de Alimentos), Universidade Federal Rural do Rio de Janeiro, Seropédica. Rio de Janeiro. Brasil. 1995.

[23] Gummadi S. N. Panda T. (2003). Purification and biochemical properties of microbial pectinases - a review. Process Biochemistry. 38(7): 987-996.

[24] Gupta S. Kapoor M. Sharma K. K. Nair L. M. Kuhad R. C. (2007). Production and recovery of an alkaline exo-polygalacturonase from *Bacillus subtilis* RCK under solid-state fermentation using statistical approach. Bioresource Technology. 98(7): 2969-3180.

[25] HENDGES, D. H. Produção de poligalacturonases por *Aspergillus niger* em processo em estado sólido em

https://dx.doi.org/10.22161/ijaers.4.9.17 *ISSN: 2349-6495(P) | 2456-1908(O)*

biorreator com dupla superfície. 86f. 2006.Dissertação de Mestrado. Universidade de Caxias do Sul - UCS - Caxias do Sul. Rio Grande do Sul. Brasil. 2006.

[26] Houdert D. Muller G. (1991). Solution properties of pectin polysaccharides. Carbohydrate polymers. 16: 409-432.

[27] Jarvis M. C. (1984). Structure and properties of pectin gels in plant cell walls. Plant Cell and Enviromment. 7: 153-164.

[28] Kashyap D. R. Vohra P. K. Chopra S. Tewari R. (2001). Applications of pectinases in the commercial setor: a review. Bioresource Technology. 77(2): 215-227.

[29] Kelly C. Fogarty W. M. (1978). Production and properties of polygalacturonatelyase by an alkalophilic microorganism *Bacillus* sp. RK9. Canadian Journal Microbiology. 24(7): 1164-1172.

[30] Kobayashi T. Koike K. Yoshimatsu T. (2010). Purification and properties of a high-molecular-weight, alkaline exopolygalacturonase from a strain of *Bacillus*. Enzyme and Microbial Technology. 29(1): 70-75.

[31] Koch J. L. Nevins D. J. (1989). Tomato fruit cell wall. I. Use of purified tomato polygalacturonase and pectinmethylesterase to identify developmental changes in pectins. Plant Physiology. 91: 816-822.

[32] Larios G. Garcia J. M. Huitron C. (1989). Endopolygalacturonase production from untreated lemon peel by *Aspergillus* sp. CH-Y-1043. Biotechnol. Lett. 11: 729-734.

[33] Larone D. H. (1985). Medically important fungi: a guide to identification, 3.ed. Washington, P. C. ASM Press, Harper & Row. 240p.

[34] Leitão M. C. A. Silva M. L. A. Januário M. I. N. Azinheira H. G. (1995). Galacturonic acid in pectic substances of sunflower head residues: quantitative determination by HPLC. Carbohydrate Polymers. 26: 165-169.

[35] Maiorano A. E. (1982). Influência da concentração de inóculo e da temperatura na produção de enzimas amilolíticas por cultivo de *Aspergillus oryzae* em meio semi-sólido**.** Dissertação de Mestrado, Escola Politécnica, Universidade de São Paulo. São Paulo. Brasil.

[36] Maiorano A. E. Schmidell W. Ogaki Y. (1995). Determination of the enzymatic activity of pectinases from different microrganisms. World J. of Microb. & Biotechnol. 11: 355-356.

[37] Maldonado M. C. Calieri D. A. S. (1989). Influence of environmental conditions on the production of pectinesterase and polygalacturonase by *Aspergillus niger*. J. Appl. Microbiol. Biotechnol. 5: 327-333.

[38] Malvessi E. (2000). Estudo da produção de poligalacturonases por *Aspergillus oryzae* em processo submerso. Dissertação de Mestrado. 123f. 2000. Universidade de Caxias do Sul - UCS - Rio Grande do Sul. Brasil.

[39] Malvessi E. Silveira M. M. (2004). Influence of Medium Composition and pH on the production of polygalacturonases by *Aspergillus oryzae*. Brazilian Archives of Biology and Technology. 47(5): 693-702.

[40] Martins E. S. Silva D. Silva R. Gomes E. (2002). Solid state of thermostable pectinases from thermophilic*Thermoascus auruntiacus*. Process Biochemistry. 37(6): 949-954.

[41] Miller G. L. (1959). Use of dinitrosalicylic acid reagent for determination of reducing sugar. Anal. Chem. 31: 426.

[42] Ming-Chu I. Lee C. Li T. S. (1992). Production and degradation of alkaline protease in batch cultures of *Bacillus subtilis* ATCC 14416. Enzyme and Microbial Technology. 14(4): 755-761.

[43] Muralikrishna G. Taranathan R. N. (1994). Characterization of pectin polyssaccharides from pulse husks. Food Chem. 50: 87.

[44] Nighojkar S. Phanse Y. Sinha D. Nighojkar A. Kumar A. (2006). Production of polygalacturonase by immobilized cells of *Aspergillus niger* using orange peel as inducer. Process Biochemistry. 41(6): 1136-1140.

[45] Nogueira A. (2003). Tecnologia de processamento sidrícola. Efeitos do oxigênio e do nitrogênio na fermentação lenta da sidra. 210 p. Tese de doutorado em Processos Biotecnológicos Agroindustriais. Setor de Engenharia Química. Universidade Federal do Paraná. Curitiba. Paraná. Brasil.

[46] Polizeli M. L. T. M. Jorge J. A. Terenzi H. F. (1991). Pectinase production by *Neurospora crassa*: purification and biochemical characterization of extracellular polygalacturonase activity. J. Gen. Microbiol. 137: 1815-1823.

[47] Recalcatti J. Oliveira B. F. Araujo L. Onofre S. B. (2004). Isolamento e seleção de fungos produtores de pectinases. Seminário de Iniciação Cientifica da Unipar. Umuarama. Paraná. Brasil. p.63.

[48] Rizzatto, M. L. (1999). Estudo da produção de pectinases por Penicillium italicum IZ 1584 e Aspergillus niger NRRL 3122 por fermentação semi sólida em bagaço de laranja industrializado, Campinas, 89 p. Dissertação de Mestrado em Engenharia de Alimentos, Faculdade de Engenharia de Alimentos, UNICAMP, Universidade Estadual de Campinas. Campinas. São Paulo. Brasil.

[49] Roberts K. (1990). Structure at the plant cell surface. Curr. Opin. Cell. Biol. 2: 920-926.

https://dx.doi.org/10.22161/ijaers.4.9.17 *ISSN: 2349-6495(P) | 2456-1908(O)*

[50] Sajjaanatakul T. Van-Buren J. P. Downing D. L. (1989). Effect of methyl ester content on heat degradation of chelator soluble carrot pectin. J. Food Sci. 54: 1272-1275.

[51] Sakai T. Okushima M. (1982). Purification and crystallisation of a protopectin-solubilizing enzyme from *Trichosporon penicillatum*. Agricultural and Biological Chemistry. 46: 667-776.

[52] Silva D. Tokuioshi K. Martins E. S. Silva, R. Gomes E. (2005). Production of pectinase by solid state fermentation with *Penicillium viridicatum RFC3*. Proc. Biochem. 40: 2885-2889.

[53] Tieman D. M. Handa A. K. (1994). Reduction in pectin methylesterase activity modifies tissue integrity and cation levels in repening tomato fruits. Plant Physiol. 106: 429-433.

[54] Tomazic S. J. (1991). Protein Stabilization. Topic in Applied Chemistry. New York: Ed. Plenum Press. 330p.

[55] Uenojo M. Pastore G. M. (2007). Pectinases: aplicações industriais e perspectivas. Quim. Nova. 30(2): 388-394.

[56] Ustok F. I. Tari C. Gogus N. (2007). Solid-state production of polygalacturonase by *Aspergillus sojae* ATCC 20235. Journal of Biotechnology. 127(2): 322-334.

[57] Wosiacki G. Nogueira A. (2005). Suco de maçã. In: Venturini Filho WG. Tecnologia de bebidas: matéria-prima, processamento - BPF/APPCC - Legislação e mercado. 1.ed. Botucatu: Blücher, p.255-292.

https://dx.doi.org/10.22161/ijaers.4.9.18 ISSN: 2349-6495(P) | 2456-1908(O)

Seismic stratigraphy study of the East Razzaza in Jurassic- Cretaceous succession- Central Iraq

Layalen H. Ali *, Salman Z. khorshid* , Ghazi H.AL.Sharaa**

*Department of Geology, College of Science, University of Baghdad, Iraq.
**Ministry of petroleum, Oil exploration company*

Abstract**—** *This study is deal with seismic structural and stratigraphic interpretation that applied on the East Razzaza (central of Iraq) area, by using 2D seismic data from Oil Exploration Company. Three main seismic reflectors were picked. These reflectors are Zubair, Yamama and Gotnia Formations, which were used to define petrophysical well logs and synthetic seismograms , that are calculated from sonic-logs of the wells of East Baghdad-1 (Eb-1) and West Kifl-1(Wk-1) by Geoframe program, to interpret the Yamama basin and the boundaries of the basin (Zubair and Gotnia Formations), and suggest a stratigraphic model for the study area. Structural maps are prepared for each reflector in addition to analyze stratigraphic features on the seismic sections to obtain the location and direction of the sedimentary basin and shoreline. It is concluded that the basin lies in the east and south east of the area. Seismic stratigraphic interpretation of the area approves the presence of some stratigraphic features in the studied formations. Some distributary buildup mound and carbonate platform are determined. Yamama Formation is interpreted to represent a carbonate platform, and it is divided into three sequences; they represent progradational seismic facies (sigmoid). Maximum flooding surface (MFS) is recognized on top of Yamama Formation and system tracts are determined on the basis of seismic and log data. Seismic attributes technique was used to predict the physical properties distribution of Yamama Formation succession.*

Keyword—Seismic stratigraphy-East Razzaza-Jurassic-Cretaceous succession.

I. INTRODUCTION

Seismic methods are widely applied to exploration problems involving the detection and mapping of subsurface boundaries, they also identify significant physical properties of each subsurface unit, and are therefore widely used in the search for oil and gas [1]. The effectiveness of the seismic method varies for different kinds of stratigraphic features. For example, many types of reefs can be located with consistent success on seismic record sections [2]. The studied area (East Razzaza) is located in the middle parts of Iraq, and belong to three governorates (Baghdad, Karbala and Anbar governorates) on the western side of Mesopotamian basin between Euphrates river and Razazza lake, figure (1). The aim of this study is to interpret a (2-D) seismic data available in Oil Exploration Company for surveys carried out in East Razzaza to determine the seismic stratigraphic architecture and facies changes for the Zubair, Yamama and Gotnia Formations in the area which are covered by two dimensional survey for locating the probable reservoir.

The Geophysical Information of studied area

Gravity Surveys

The Bouguer anomaly map shows increasing of gravity values in NE direction with presence of anomaly as a nose about (-46) milligal in the middle part of the study area, figure (2). Bouguer gravity values is ranged between (-40) to (-53) milligal. This anomaly may be due to difference in rock densities and topography of basement rocks.

The Magnetic Survey

The aeromagnetic map shows that depth of basement rocks in the area ranges between (7-8km). This depth increases towards the S and SW. It was noted the existence of magnetic anomalies with continuous increase in the intensity of the total magnetic field towards the S-SW figure (3).

https://dx.doi.org/10.22161/ijaers.4.9.18 ISSN: 2349-6495(P) | 2456-1908(O)

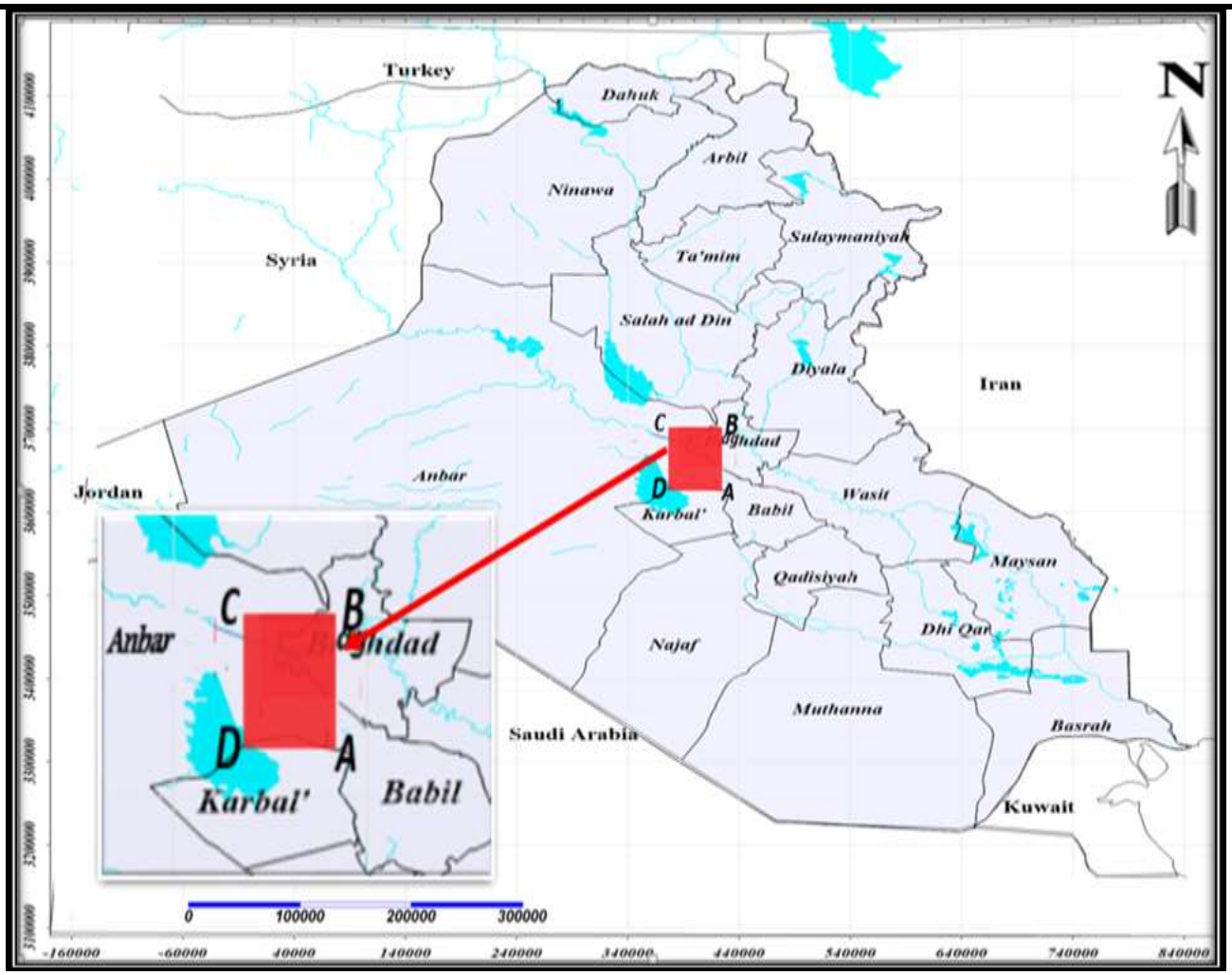

Fig.1: Iraqi map shows the study area.

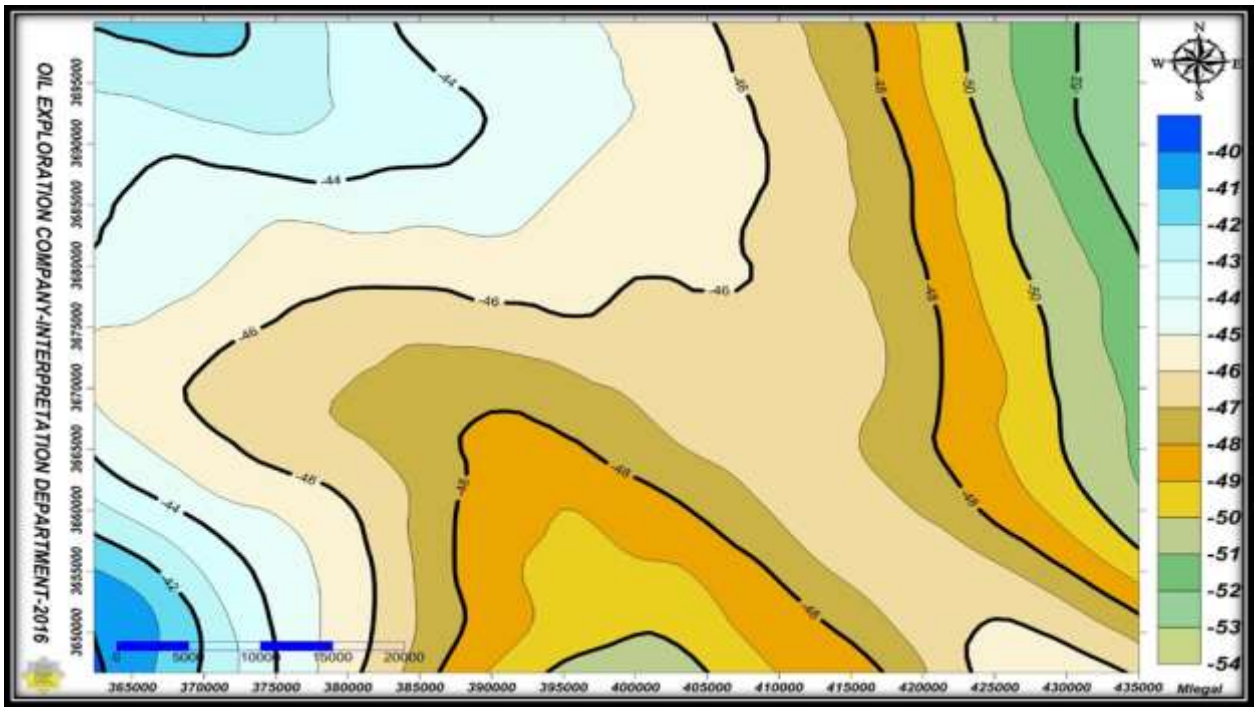

Fig.2: Bouguer anomaly map of the study area.

https://dx.doi.org/10.22161/ijaers.4.9.18 *ISSN: 2349-6495(P) | 2456-1908(O)*

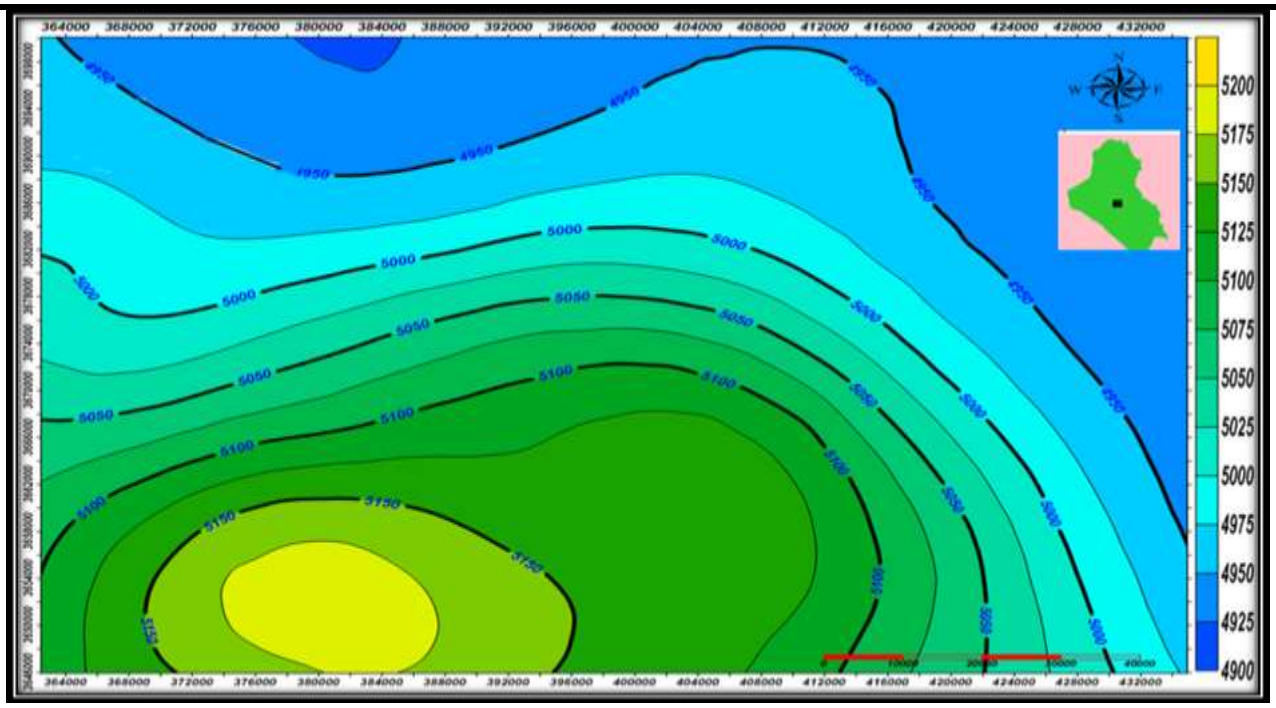

Fig.3: Aeromagnetic map of the study area.

Data Acquisition

Base map preparation

Processed seismic data are loaded in the interactive workstation of interpretation in SEG-Y format and before starting; special subprograms must be operated to define the required data for loading. This process is called (project creation) for achieving the interpretation process on an interactive workstation. After that, the base map of the study area is constructed. This process includes entering strike line and dip line numbers, the separated distance between bin sizes along strike line direction and dip line direction. Base map includes definition of the geographic coordinates in UTM coordinates system of study area, figure (4).

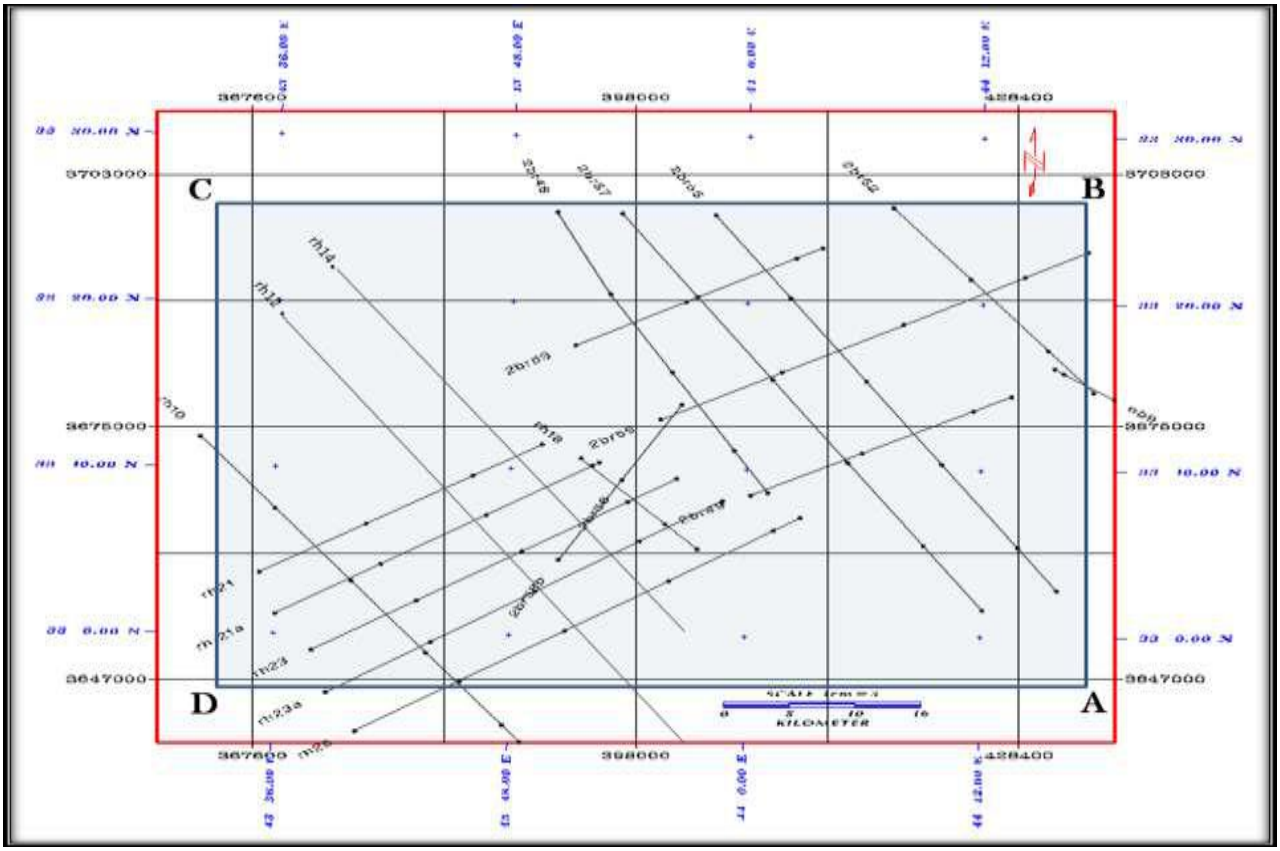

Fig.4: Illustrates a base map of study area (2D survey).

https://dx.doi.org/10.22161/ijaers.4.9.18 *ISSN: 2349-6495(P) | 2456-1908(O)*

Synthetic seismograms and reflectors definition

Synthetic seismograms that is, a theoretical seismic trace, can be made from one or two of the logs in a well [3]. Synthetic seismograms (figures 5,6) are artificial reflection records made from velocity logs by conversion of the velocity log in depth to a reflectivity function in time and by convolution of this function with a presumed appropriate wavelet or source pulse [4]. Synthetic seismograms were generated for Eb-1 and Wk-1 wells using GeoFrame software package. Basically, seismic well tie allows well data, measured in units of depth, to be compared to seismic data, measured in units of time. The sonic and density logs were transformed from depth to time domain. This conversion will permits correlation of horizon tops identified in well with reflections present in the seismic section. The picked reflectors wavelets appeared as peaks on synthetic trace (positive reflection) but in different intensity. The Zubair corresponds to a trough. This is very reasonable because the rocks in Zubair are shale as well as the sandstone was characterized by high porosity and lower density. For this reason, the reflection coefficient of sandstone in this interface is negative (trough). The Gotnia and Yamama corresponds to a (peak) because the rocks in Gotnia is anhydrite and Yamama is limestone which was characterized by low porosity and higher density. For this reason the reflection coefficient of this interface is positive (peak).

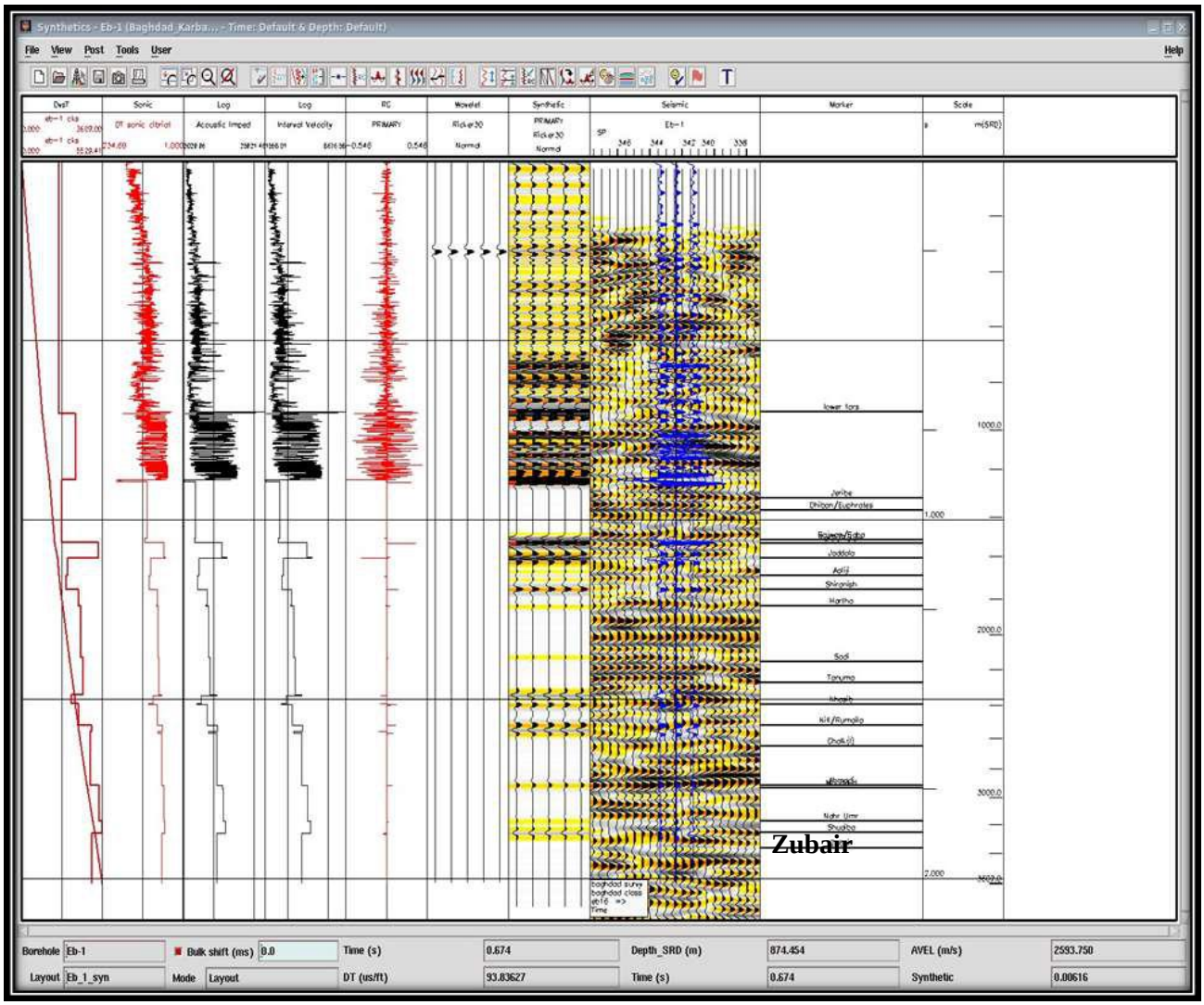

Fig.5: Illustrates the synthetic seismogram of Eb-1 well.

https://dx.doi.org/10.22161/ijaers.4.9.18 *ISSN: 2349-6495(P) | 2456-1908(O)*

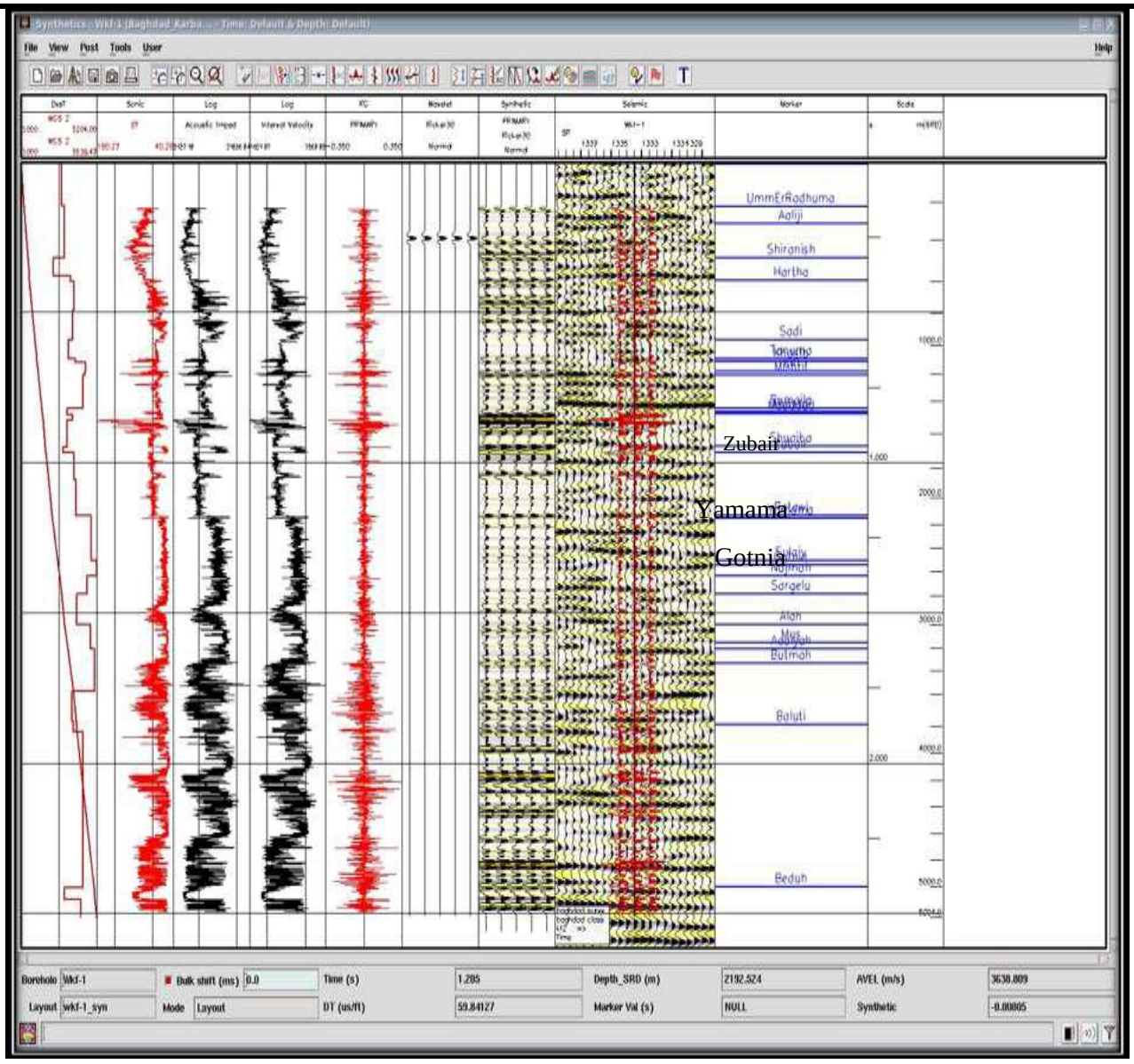

Fig.6: Illustrates the synthetic seismogram of Wk-1 well.

Interpretation of Seismic Data

After completion the process of creating synthetic seismogram and identification of reflection then picking the reflectors is represented by Zubair, Yamama and Gotnia Formations. As previously mentioned, the synthetic seismogram have been created for Eb-1 and Wk-1 wells, in order to identify the reflectors depending on:-

• The well records of sonic logs and integrated velocity survey.

• The well in adjacent area.

• The synthetic seismogram loaded on seismic section in order to matching the seismic signal and the result of matching are very good.

General Specifications of Seismic Reflectors

1- Continuity of reflectors

Continuity of the picked reflector can be described as follows, figure (7):

- Zubair reflector has good continuity.
- Yamama reflector has moderate continuity.
- Gotnia reflector has good continuity.

2- Concordance of reflectors

Concordance of reflectors is good especially at the Upper Jurassic –Lower Cretaceous, it is due to presence of the stratigraphic features.

3- Quality of the reflectors

In general, the quality of the reflectors on the seismic sections of the area is considered good. This is due to the high signal to noise (S/N) ratio of the recorded signal where the resolution is very good. Knowledge of the general specification of the reflector is important because it helps in determining how much and what quality of seismic section involved in achieving the interpretation before using the programs of automatic control. These programs are interpolation, auto picking and they are used to complete of the reflectors picking process.

https://dx.doi.org/10.22161/ijaers.4.9.18 *ISSN: 2349-6495(P) | 2456-1908(O)*

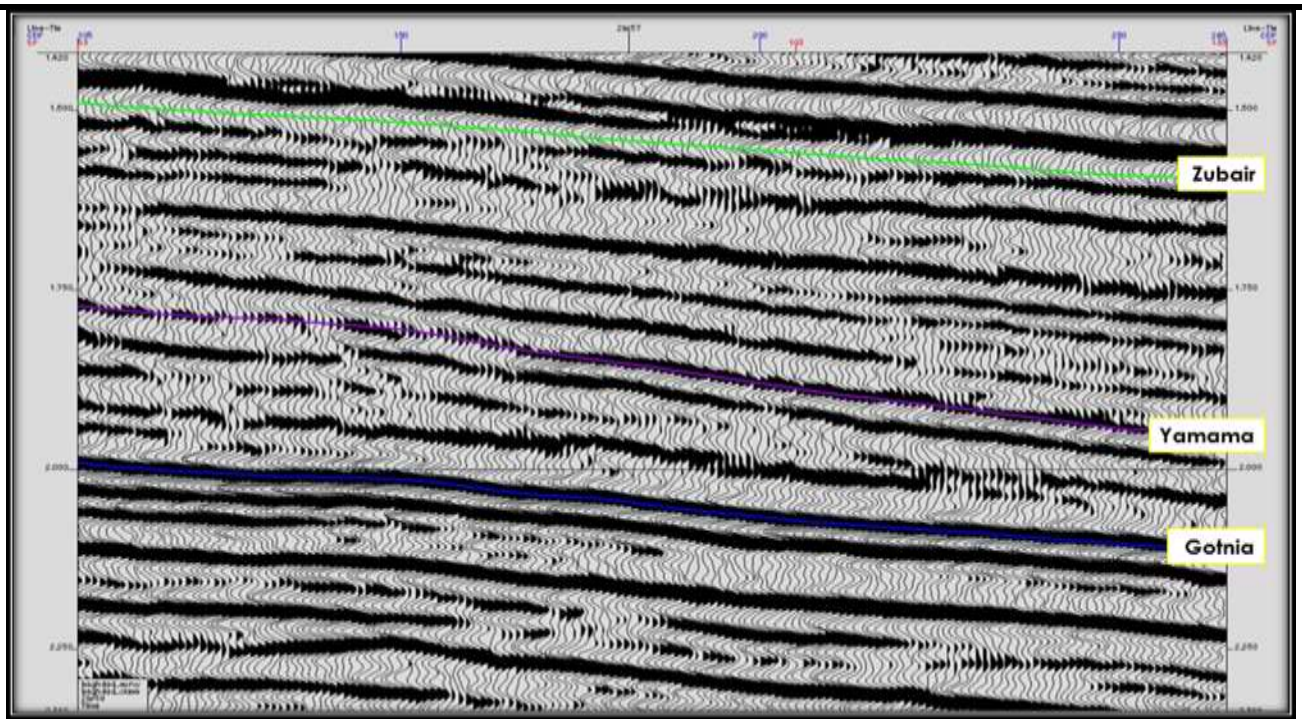

Fig.7: Shows continuity of the picked reflectors (Zubair, Yamama and Gotnia reflector).

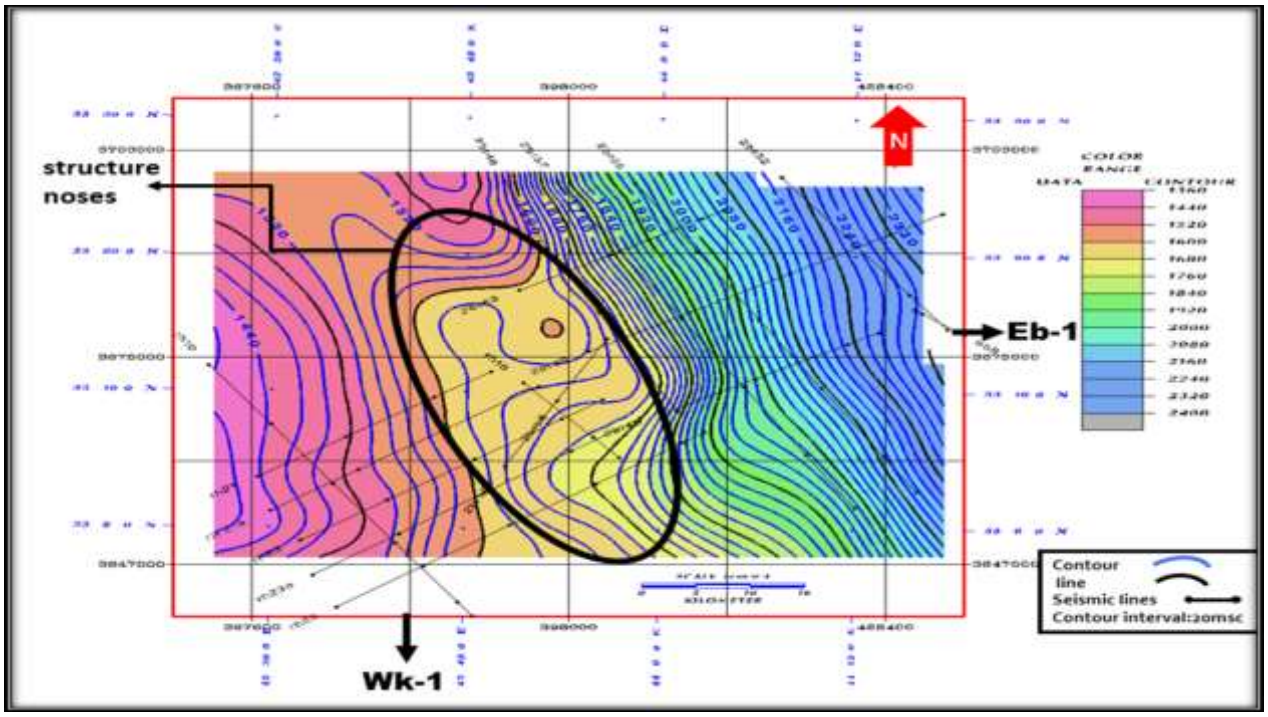

Fig.8: Two way time map of Yamama reflector.

Structural Picture of the picked Horizon

Depending on analysis of the seismic data, synthetic seismogram and well ties, it is easy to recognize and pick three reflectors: Zubair reflector, Yamama reflector and Gotnia reflector. After the definition of studied reflectors using synthetic seismograms in time domain for wells (Eb-1,Wk-1), we picked these reflectors in all area to prepare the time maps which are converted later to structural maps in depth domain by using velocity data of these reflectors, for describe the structural features of selected horizons from two way time(TWT) structure maps.

Time, velocity and depth maps

Time maps

The time maps may carry important information on the subsurface geo-logic features. Zubair, Yamama and Gotnia Formations two way time maps. Figure (8) shows Yamama TWT map as an example which is dominated by NE-SW trending high to the East and drops to the West. The structure rises sharply to the North East. In the middle area,

https://dx.doi.org/10.22161/ijaers.4.9.18 *ISSN: 2349-6495(P) | 2456-1908(O)*

the structure depicts ridges extending NW-SE on the surface, these ridges represent accumulation of sediments that may contain oil, and has nose structure shape (minor structure). Contour interval equals 20 ms.

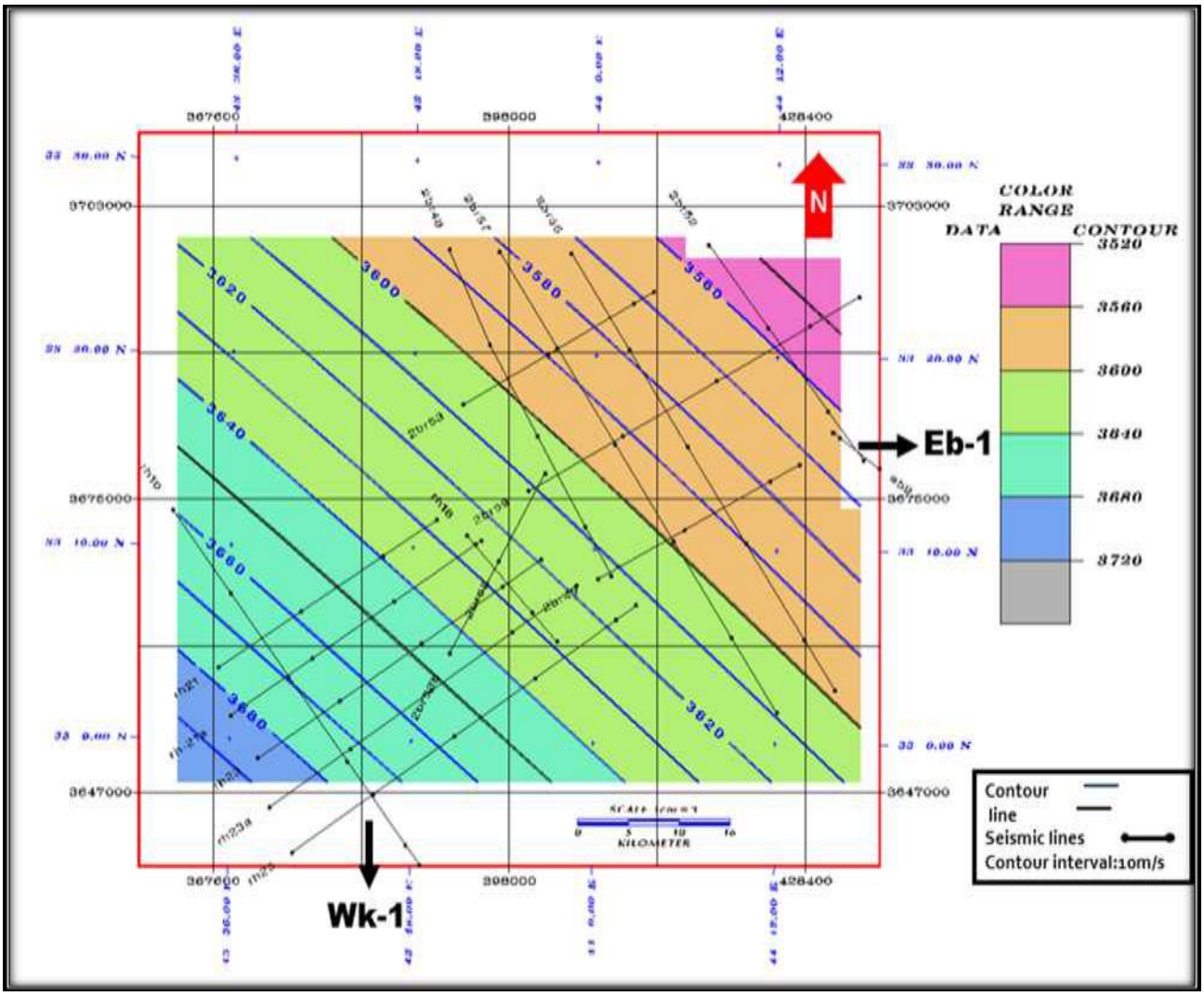

Fig.9: Velocity Map of Gotnia reflector.

Average Velocity maps

To obtain depth maps, the picked time data of any reflector is needed to the velocity data. The more accurate velocity to be used in time to depth conversion is the average velocity, which can be computed directly from well velocity survey (check shot) [5]. For the two wells the area (Eb-1 and Wk-1), check shot data are used to prepare the velocity maps. The velocity map of Gotnia shows the average of velocity increases in SW trend.The magnitude of velocity ranges from (3550-3690) m/s. Velocities in the Gotnia Formation variation and this is indication of variation in lithology and depth from NE to SW trend, figure (9).

Depth Maps

The time map of a given reflector is used with its average velocity map to extract the depth map, as follows:

Depth at any point = (velocity × TWT /2) at this point.

Zubair, Yamama and Gotnia depth maps reveal a structural feature having a general trend in the NW-SE direction. Yamama depth map showsthe minimum depth value of (3000) m is noticed at the W and gradually increase toward the E and NE, and reaches (4240) m towards the basin. Structural noses (minor structure) are observed in the middle part of the area and have NW-SE trend, which represents the direction of buildup carbonate shelf. Contour interval is 40m, figure (10).

https://dx.doi.org/10.22161/ijaers.4.9.18 *ISSN: 2349-6495(P) | 2456-1908(O)*

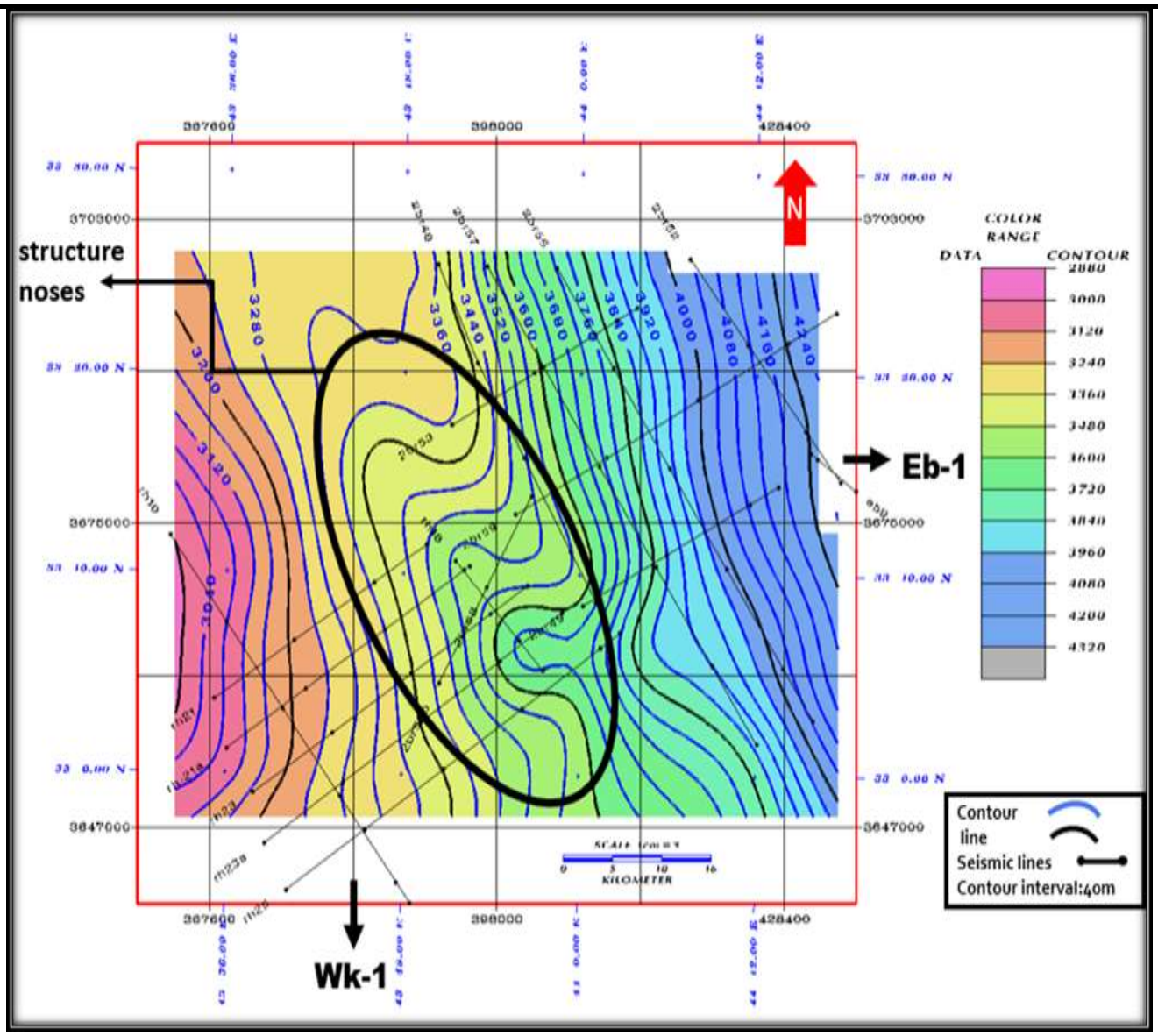

Fig.10: Depth structure map of Yamama Formation.

Stratigraphic Interpretation

Stratigraphic interpretation of seismic data may be simple if there is adequate well control, but in many cases the interpreter has to make inferences from the appearance of observed bodies, these may include both their external form and if the resolution is good enough for it to be visible [6]. Seismic stratigraphy can add important geological information and enhance the understanding of the depositional environments, which may help in the understanding the origin, accumulation, and trapping mechanisms of the hydrocarbon deposits. The seismic traces are trying to tell us the details of the subsurface [7]. The first phase in seismic stratigraphic studies of a basin fill is to delineate genetically related units, which are called depositional sequences [8]. These sequences are of regional importance and are further subdivided into individual system tracts [9]. The system tracts are delineated based on the presence of local unconformities and their laterally equivalent conformities. They contain a grouping of deposits from time-equivalent depositional systems [10]. Sequence stratigraphy analysis is increasingly viewed as an essential methodology for studying carbonate platforms [11].

Sequence Stratigraphy of the Studied Formations

Zubair Formation

The Zubair Formation is interpreted by using the log data for the identification thickness and depositional sequence within Zubair in studied area. Both Eb-1and Wk-1 wells are essentially composed of alternating shales and sandstones with some siltstones. The variation in lithology displays some regularity, towards the shore, in the west the formation is composed mostly of sands only.

Yamama Formation

Yamama Formation is interpreted as three depositional sequence representing the base which is an initial lowstand systems tracts (LST), remaining to top as carbonate package; it represents the highstand systems tracts (HST) and transgressive systems tracts (TST) figure (11).Within

https://dx.doi.org/10.22161/ijaers.4.9.18 *ISSN: 2349-6495(P) | 2456-1908(O)*

the Yamama sequence, three reflection sequences that can be mapped across the entire platform top. The top Yamama was picked from wells parallel to the seismic surface approximately. The Yamama sequence appears to initially backstep and then progrades from SW-NE in the highstand. These latter seismic events can be interpreted as prograding clinoforms. Major environments of deposition are interpreted including three shelves margin, upper slope and inner shelf, and basin. Note that transgressive and highstand system tracts dominate, with transgressive system tracts being associated with major periods of shelves margin aggradations, as build-ups try to keep pace with rising sea level. During highstand, the basin margin progrades basin ward rapidly. Facies have also been interpreted for the individual sequences, figure (12). In terms of petroleum systems we are most likely to encounter source rocks in the deep water basinal settings. Reservoir distribution is harder to predict because of the effects of complex diagenesis associated with carbonate rocks.

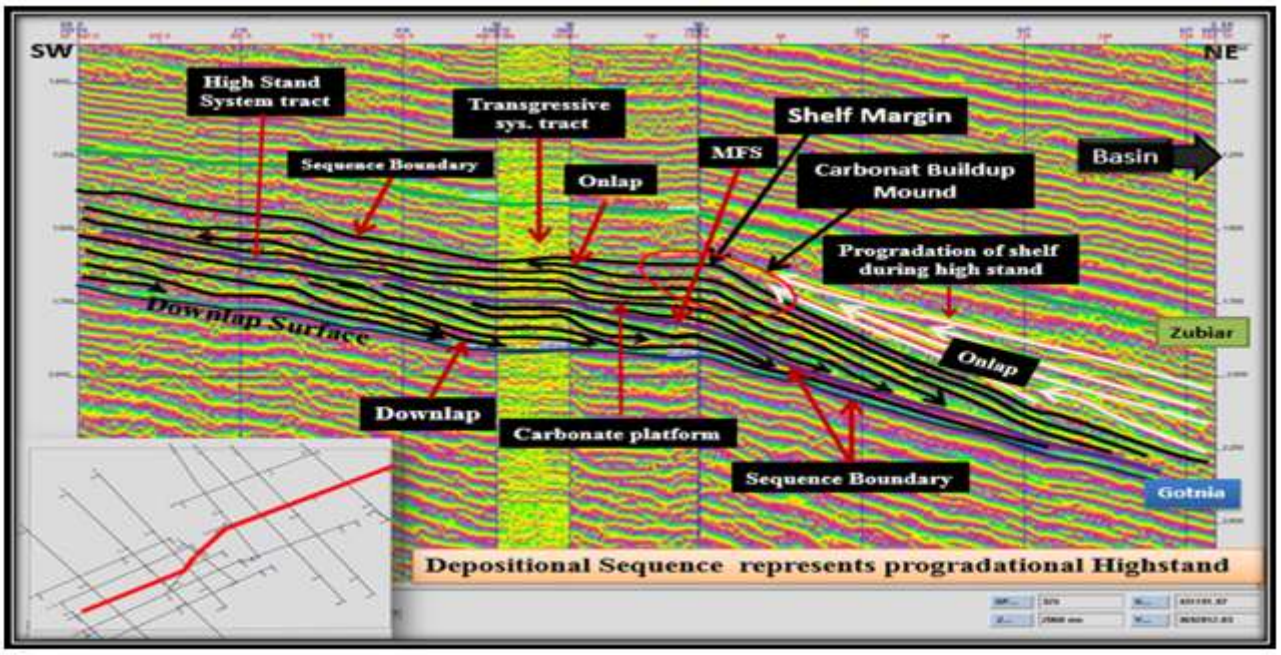

Fig.11: Illustrates architecture of basin ofYamama Formation.

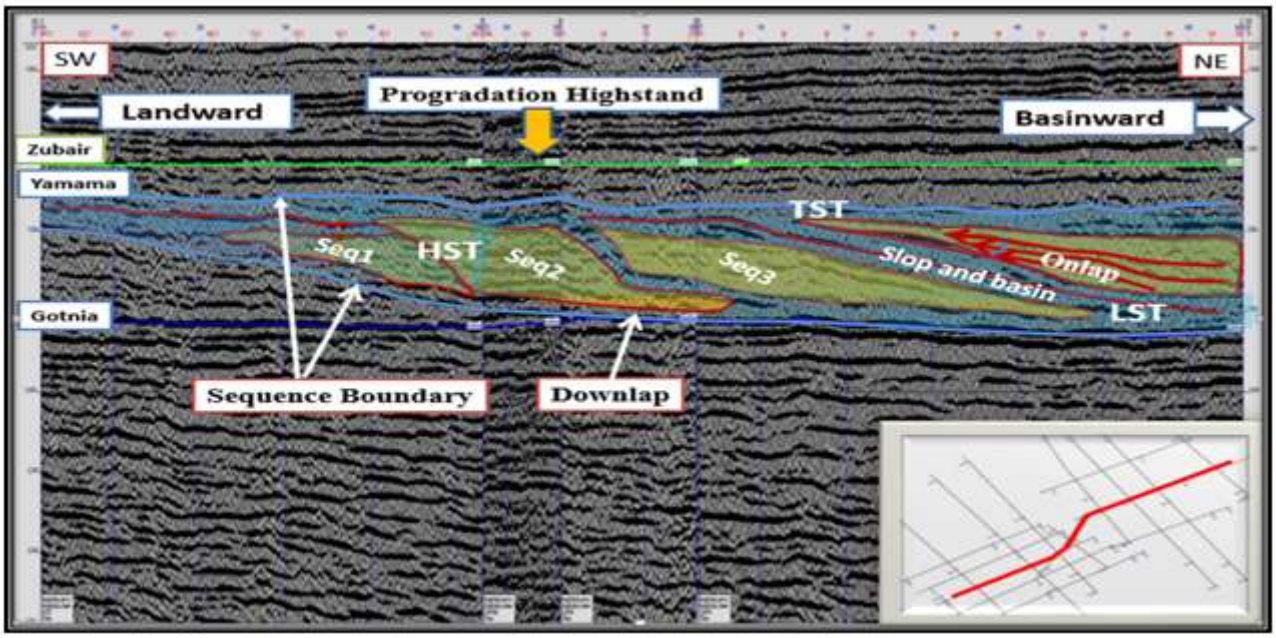

Fig.12: Illustrates sequence stratigraphy of the section.

https://dx.doi.org/10.22161/ijaers.4.9.18 ISSN: 2349-6495(P) | 2456-1908(O)

Gotnia Formation

The Gotnia sequence represents a complete evaporite sequence which was deposited on the basin center and continental slope. It is clear on seismic data and in Wk-1 well. The progradation of Gotnia Formation continued and caused a decrease in the extent of the basin, and therefore created an evaporitic. This interpretation implies that relative sea level needs not to fall, but rather continued progradation further away the basin off from marine circulation and creates an evaporitic basin. Seismic data clearly shows the top of Gotnia to be associated with a dipping event with dip to the north-east direction, and an updip thinning or pinchout onto a prominent shelf edge. The interpretation of deposition is thought to be related to a period of late highstand and associated basin starvation.

Seismic Reflection Configuration

A seismic facies unit is interpreted to express certain lithology, stratification, and depositional features of deposits that generate the reflections in the unit. Seismic facies analysis first involves recognition of distinctive (packages) of reflection within each sequences. Each reflection package exhibits a combination of physical characteristics that distinguish it from adjacent seismic facies [12].

In the studied interval Zubair- Gotnia, These are two main types of seismic reflection configuration are observed.

1- Zubair reflector displaying parallel configuration.

2- Yamama to Gotnia displaying the progradational configuration.

Zubair reflector characterize high to moderate amplitude and continuity. Reflection configurations of Zubair reflector indicate wide, relatively uniform lateral extent in sedimentary basin. The shelf facies consist of neritic shale and generally transgressive. While Zubair Formation represents delta platform facies consisting of shallow-water, high-energy marine (delta- front) sandstone.

The second type of reflection configuration in the studied package which includes Yamama and Gotnia reflectors is progradational, with two fundamentals types of configuration called oblique and sigmoid. The concluded sigmoid model is associated with progradation of shelf system. The depositional energy may be high, and the evidence on that is the reef limestone and predominance of oolites in Yamama, figure (13).

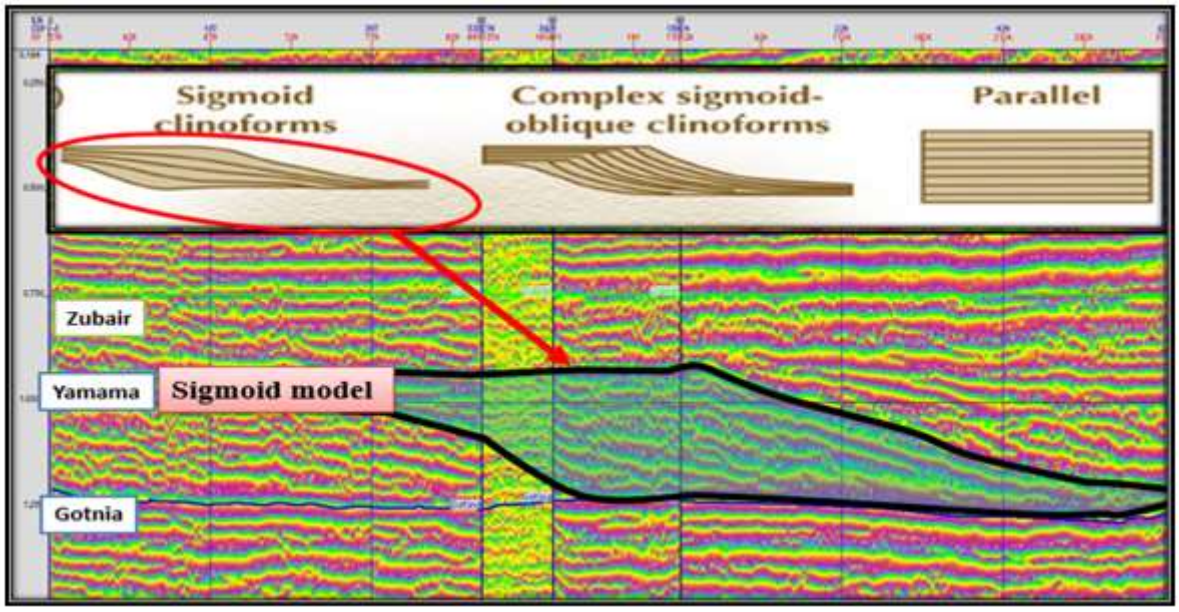

Fig.13: Shows sigmoid model in the study area.

Flattening Procedure

Flattening is transforms a seismic image to make the structural features in the image flat. A flattened seismic image is created by shifting sample in the original image up or down. This means that parts of the original image are stretched in some areas and squeezed in others to flatten the features in the image [13]. Look at a section below, figure (14) one with several good and continuous reflections across it, the up and downs of the reflections are mostly by geological processes that took place after the deposition beds. If we change the section so as to make a reflection flat, then the section more nearly represents the geological situation at the time that bed was deposited.

https://dx.doi.org/10.22161/ijaers.4.9.18 *ISSN: 2349-6495(P) | 2456-1908(O)*

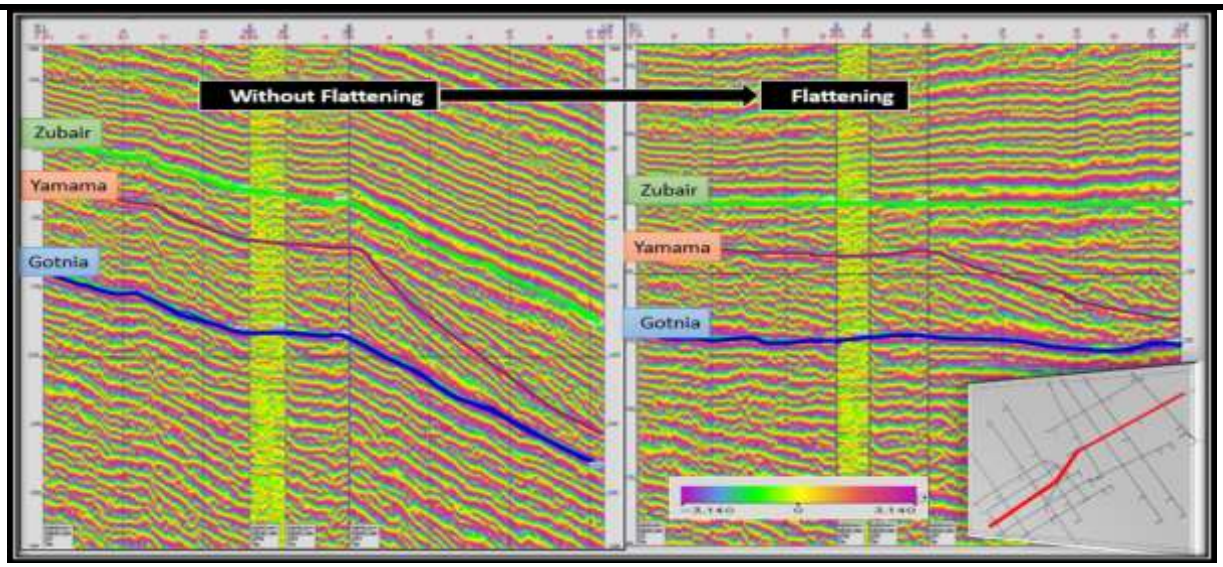

Fig.14: Illustrates Flattening technique applied on 2D section in the study area.

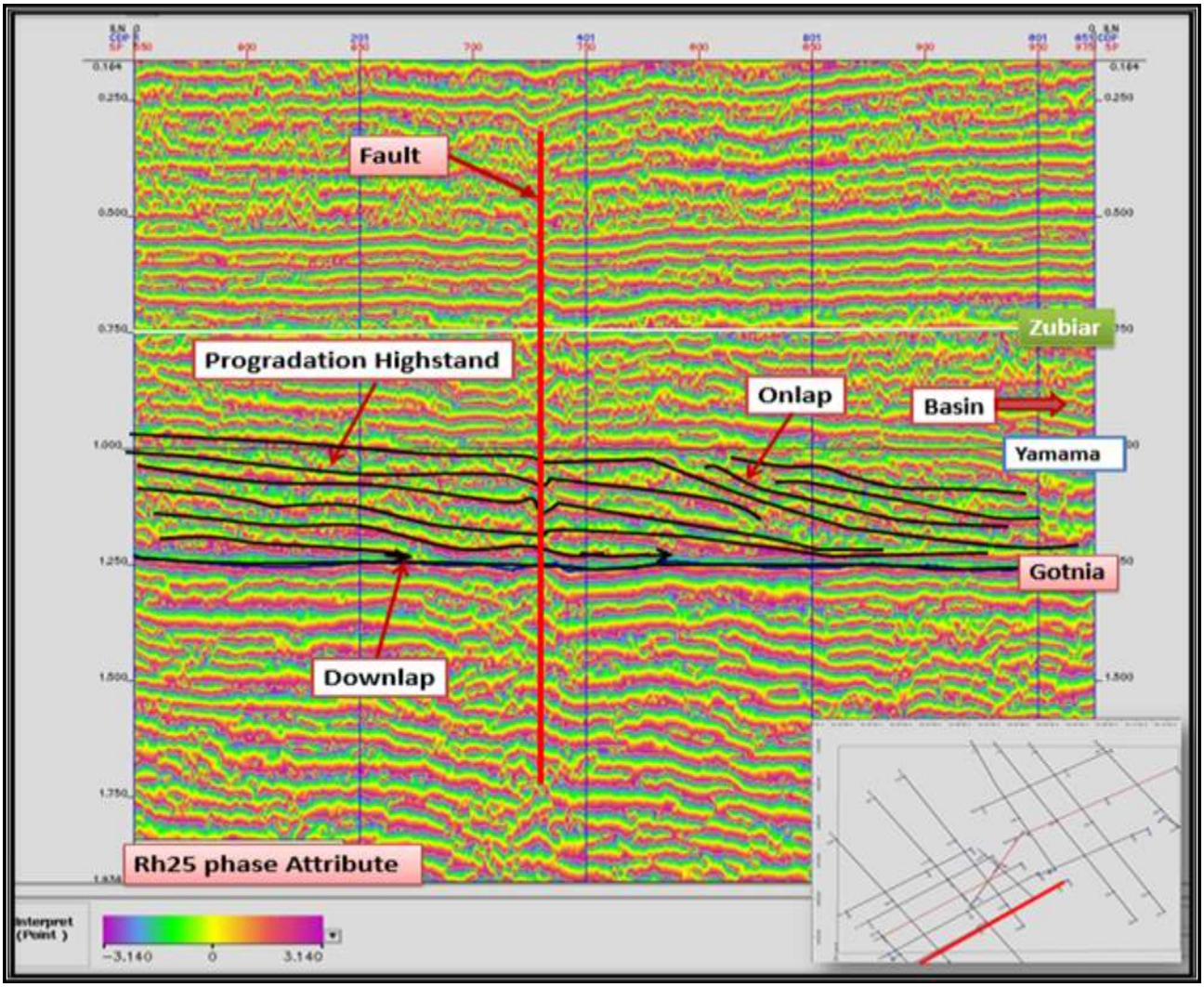

Fig.15: Explain instantaneous phase attribute on the 2D seismic section in the study area.

Seismic Attribute

Seismic attributes is any measure of seismic data that helps us visually enhance or quantify features of interpretation interest [14], and any mathematical transform of the seismic trace data, with or without other accompanying data requirements [15]. The seismic trace represents the variable function between the amplitude and time in the time domain. We can study other characteristics of seismic

https://dx.doi.org/10.22161/ijaers.4.9.18 ISSN: 2349-6495(P) | 2456-1908(O)

wave function by using the Fourier transform, where we get the amplitude change function with the frequency in the frequency domain. The seismic wave is not only a simple time function but, it is a complex function [16].

All instantaneous seismic attributes (amplitude, phase, frequency) can be used in interpretation. In practice, most interpreters use instantaneous amplitude, or some variations of an amplitude attribute, as their primary diagnostic tool. Amplitude is related to reflectivity, which in turn is related to subsurface impedance contrasts. Thus, amplitude attributes provide information about all the rock, fluid, and formation-pressure conditions. Instantaneous phase is useful for tracking reflection continuity and stratal surfaces across low-amplitude areas where it is difficult to see details of reflection waveform character. In general, instantaneous phase is the least used of the seismic attributes. Instantaneous frequency sometimes aids in recognizing changes in bed thickness and bed spacing [17].

Instantaneous phase

Instantaneous phase is measured in degree ($-\pi$, π) it is independent of amplitude and shows continuity and discontinuity of event, also it shows clear bedding, it is best indicator of lateral continuity and useful to show sequence boundaries. Figure (15) illustrates the application Instantaneous phase attribute at the 2D seismic section, where distinguished the end of the continuity of reflective surfaces, and showing the cases of layer termination (onlap, downlap) represented by progradation high stand, add to that the fault was identified at the seismic section.

Instantaneous Amplitude Sections

This attribute is measured in time and primarily used to recognize regional characteristics such as structure, sequence boundaries, thickness and lithology variations. In some cases, mound, bright and dim spots phenomena. Figure (16) illustrates the application Instantaneous phase attribute at the 2D seismic section, where distinguished three mounds with low amplitude coincided with the three shelves margin of Yamama sequences, which represents hydrocarbon content.

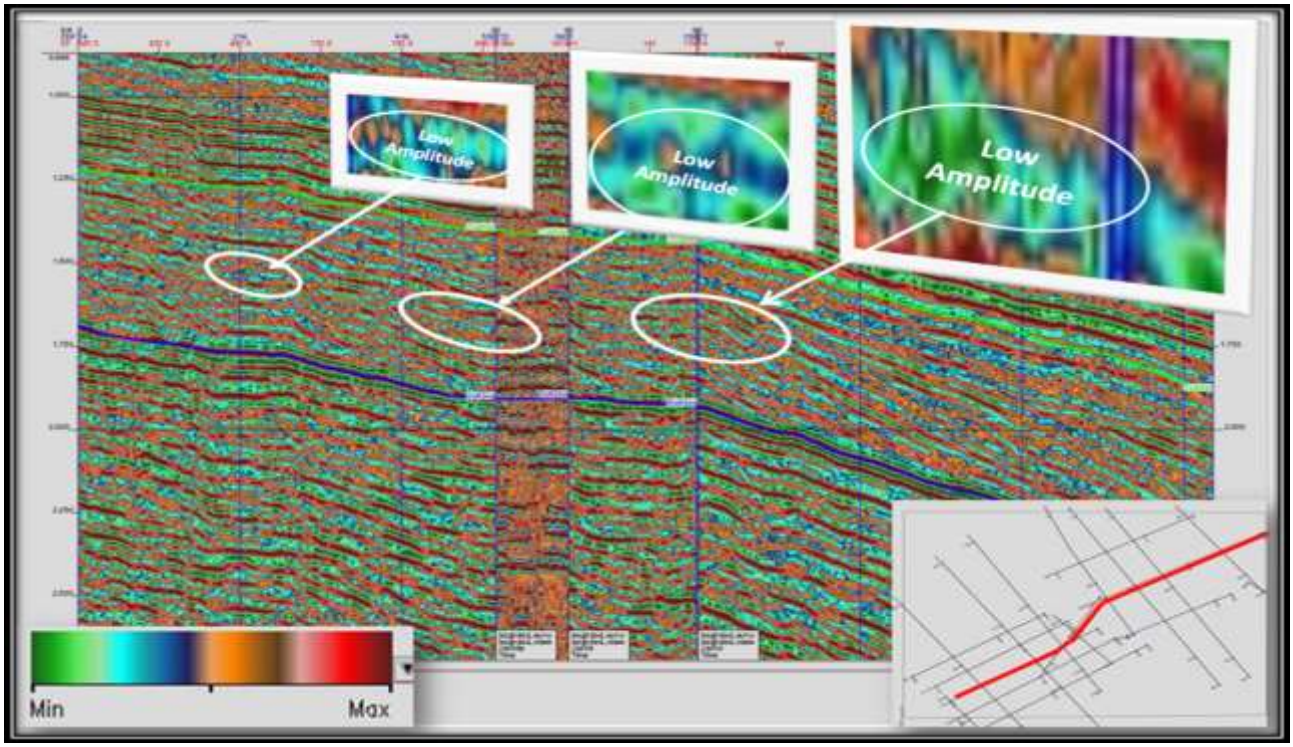

Fig.16: Shows Instantaneous amplitude attribute on the 2D seismic sections (composite).

https://dx.doi.org/10.22161/ijaers.4.9.18 ISSN: 2349-6495(P) | 2456-1908(O)

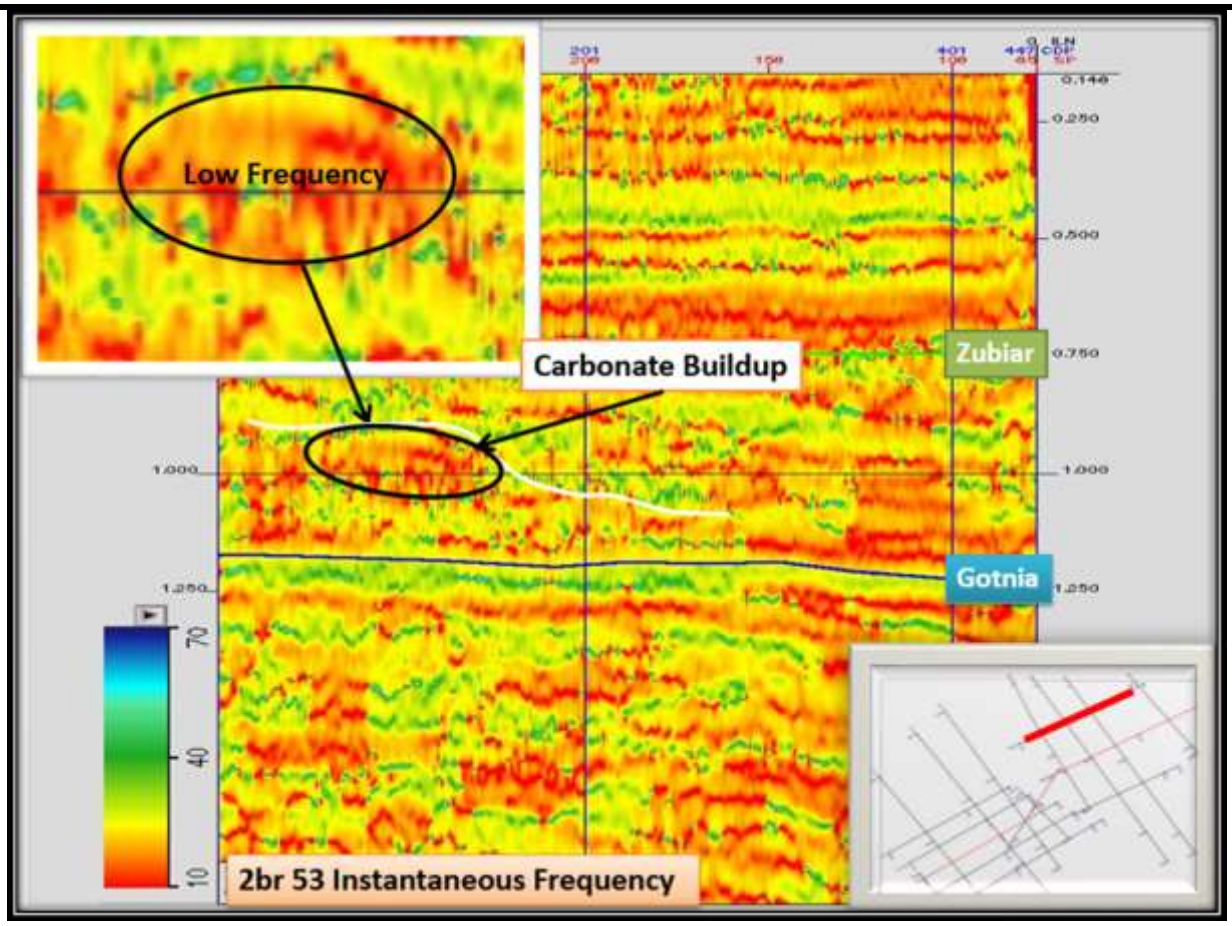

Fig.17: Shows Instantaneous frequency attribute on 2D seismic section of the study area.

Instantaneous Frequency Sections

It is used for visualizing regional depositional patterns. Frequency tuning can indicate changes in bed thickness. The results of the application of attribute assist to determine sites changes Instantaneous frequency and their relationship to changes in petrophysical qualities, is linked frequencies of low-lying areas to zones communities of hydrocarbon.Figure(17) shows a progradation pattern, also a matching is noted between area of low frequency and carbonate buildup which represent the accumulation of hydrocarbon.

Mound

Mound is a seismic reflection configuration interpreted as strata forming an elevation or prominence rising above the general level of the surrounding [8]. They indicate higher energy environments in the basin.

It was Displayed many seismic attributes to explore the stratigraphic phenomena in the area like channel, mound, and unconformity. Figure (18) explains the mound by applied phase attribute photo gray on 2D seismic section. Note that the domes formed through transgressive system tract (TST), where it is deposit during some part of a relative sea level rise cycle can occur progradation and seismic reflection terminate of downlap toward basin. This leads to the accumulation of carbonate material in the shelf margin and be mound.

https://dx.doi.org/10.22161/ijaers.4.9.18 *ISSN: 2349-6495(P) | 2456-1908(O)*

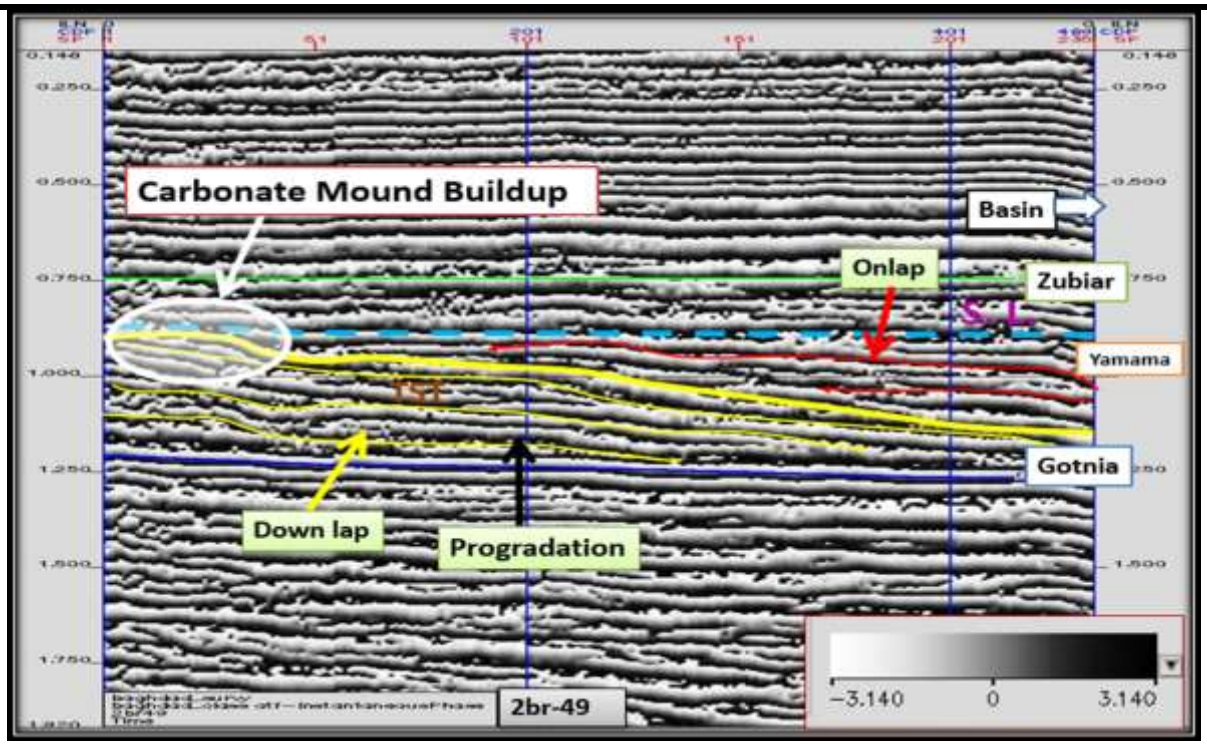

Fig.18: Shows mound on 2D seismic section applied by phase attribute photo Gray in the study area.

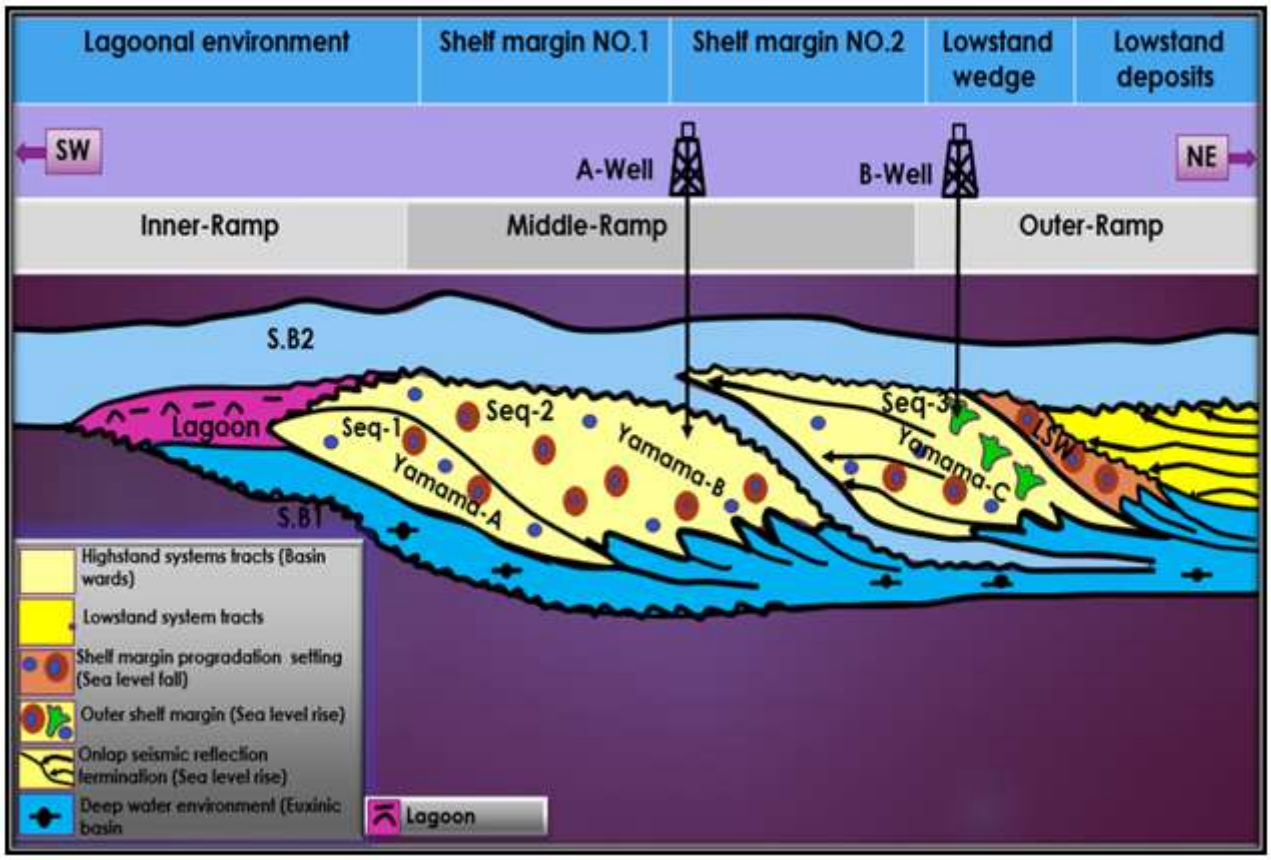

Fig.19: Show the stratigraphy traps and the proposed wells by geological model

Geological model

Geophysical data are best interpreted in tight integration with the geological data. It is combine the most practical and effective geophysical data. 2D geological models are relate with petrophysical properties and 2D seismic section to match the geophysical field data. The structural, formational, and facies modelling software tools ensure that 2D geological models in the context of consistent stratigraphic, and topological framework in addition to

https://dx.doi.org/10.22161/ijaers.4.9.18 *ISSN: 2349-6495(P) | 2456-1908(O)*

ensuring consistency between the geological models and geophysical data.

Working with an extensive set of 2D, exploratory data analysis to data security and enhance interpretational insight. Providing results in common 2D formats for the easy communication of ideas. All required link data that work on it to make the best image to the subsurface. Figure (19) shows the best image for geological model that is correspond with the interpreted seismic data in the previous figure (12). On the basis of the stratigraphic interpretation data we were able to identify two of the stratigraphic traps, which explain by A-Well in the sequence-2 of Yamama Formation and B-Well in the Sequence-3 of Yamama Formation. Which is considered promising hydrocarbon traps. Figure(20) shows the phenomena that have been identified and probable traps at the base map of 2D seismic line.

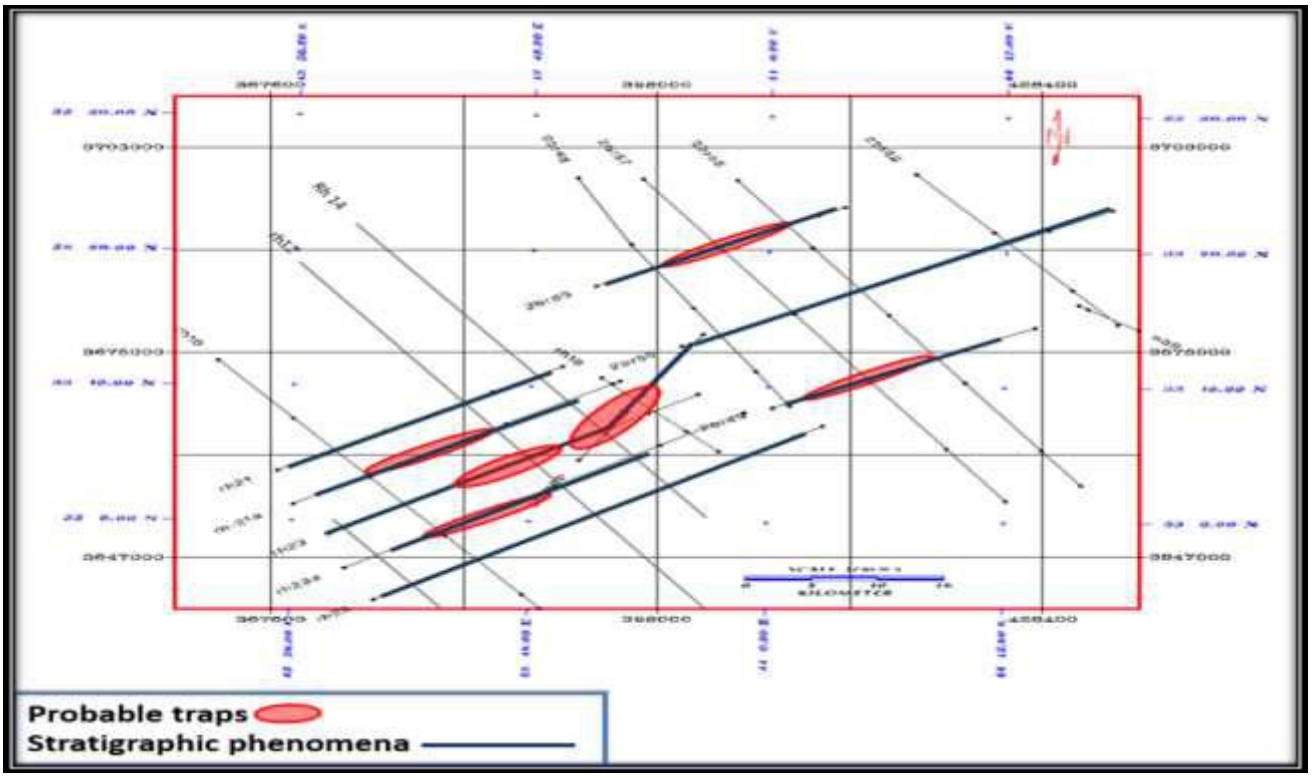

Fig.20: Shows the probable traps that determined from attribute and seismic reflection configuration.

II. CONCLUSIONS AND RECOMMENDATIONS

According to interpretation of 2D seismic data the following are major conclusions of this study:-

1- The TWT, average velocity, depth maps of the studied area interpret the structural picture of East Razazza. The trending of structural noses was toward NW-SE, these noses are compatible with carbonate build up feature, which was identified in the region. Depth maps reveal that the minimum depth values are noticed at the west and gradually increases toward the east and northeast till the middle part of the study area where structural anomalies are observed. The deepening increases from west to northeast, which reflects the transition from the continental slope towards the basin. This is confirmed by the behavior of the TWT and average velocity maps.

2- From studying the seismic section and applying the seismic attributes represented by instantaneous phase, Instantaneous amplitude and instantaneous frequency, discovered locations are considered as carbonate mound build up, which refers to hydrocarbon accumulation.

3- Yamama Formation was interpreted as three depositional sequences representing the base which is an initial lowstand system tracts, remaining to top as carbonate package; it represents the highstand and transgressive systems tracts.Three depositional sequences are identified, which indicate three shelf margin platform due to sea level fall, configured highstand system tracts and terminated by lowstand system tracts, they are regarded promising reservoir.

The geological model that was drawn is the final outcome of the research, where two stratigraphic traps are considered promising exploration targets figure (19).

https://dx.doi.org/10.22161/ijaers.4.9.18 *ISSN: 2349-6495(P) | 2456-1908(O)*

We recommend to use three-dimensional surveys to obtain high resolution power to confirm the stratigraphic features on the time sections, study more wells surrounding the studied area and correlate many wells probes, also drilling exploration well on top of shelf margin, is area requires large scale depositional environmental study in order to recognize depositional facies, reservoir facies and site of hydrocarbon kitchen.

REFERENCES

[1] Kearey, P., Brooks, M. and Lan H., **2002**. *An Introduction to Geophysical Exploration*, 3rd ed., Blackwell Science Ltd., 256p.

[2] Dobrin, M., **1976**, *Introduction to Geophysical Prospecting*, 3rd ed., McGraw Hill. Int. co., International Student Edition 386 p.

[3] Coffen, J.A., 1983, *Interpreting Seismic data, Tulsa, Oklanome, 260 P.*

[4] Dobrin, M.B. and Savit, C.H., **1988**, *Introduction to Geophysical Prospecting*, 4th ed. McGraw-Hill Co. 865*p*.

[5] McQuillin, r., Bacon, M, and Barclay, W., **1984**, *An Introduction to Seismic Interpretation*, Graham and Trotman, 287 p.

[6] Bacon, R.S., and Redshaw, T., 2003, *3D Seismic Interpretation, Printed in Unitrd Kingdom at the University press, Cambridge, 212p.*

[7] Gadallah, M.R., and Fisher, r., **2009**, *Exploration Geophysics* ,Verlag Berlin Heidberg, 292p.

[8] Mitchum Jr., R. M., (1977), *Seismic Stratigraphy and Global Changes of Sea Level: Part 11. Glossary of Terms used in Seismic Stratigraphy: Section 2. Application of Seismic Reflection Configuration to Stratigraphic Interpretation, Memoir 26 Pages 205 - 212.*

[9] Van Wagoner, J.C., Posamentier, H.W., Mitchum, R.M., Vail, P.R., Sarg, J.F., Loutit, T.S., Hardenbol, J., 1988, *An overview of sequence stratigraphy and key definitions. In: Wilgus, C.K., Hastings, B.S., Kendall, C.G.St.C., Posamentier, H.W., Ross, C.A., Van Wagoner, J.C. (Eds.), Sea Level Changes—An Integrated Approach, vol. 42. SEPM Special Publication, pp. 39–45.*

[10] Armentrout, J.M. and B.F. Perkins, 1991, *Sequence stratigraphy as an exploration tool, concepts and practices in the Gulf Coast. SEPM Foundation 11th annual research conference, 417 p.*

[11] Vail, P. R., R. M. Mitchum, Jr., R. G. Todd, J. M. Widmier, s. Thompson, III, J.B. Sangree, J.N. Bubb, W. G. Hatlelied, ,1977, *Seismic stratigraphy and global changes of sea level , in C. E. Payton, ed., Seismic Stratigraphy-Applications to Hydrocarbon Exploration: AAPG Memoir 26, pp.49-212.*

[12] Brown, l. and fisher W., 1984, *Seismic Stratigraphic Interpretation and Petroleum exploration, AAPG, Tulsa Oklahoma, 125 p.*

[13] Parks, D., 2010, *Seismic image flattening as a linear inverse problem, a thesis of master, Colorado school of Mines Golden ,Colorado, CWP-643.*

[14] Chopra, S. and V. Alexeev, 2004, *A new approach to enhancement of frequency bandwidth of surface seismic data. First Break 22 (8), 21–42.*

[15] Hampson, D., Schuelke, J., and Quirein, J. A., 2001, *Use of multiattribute transforms to predict log properties from seismic data: Geophysics ,**66**, 220–236.*

[16] Yilmaz,O., 1987, *seismic data processing, SEG series: Investigation Geophysics, V.2 526 p.*

[17] Hardage, B.A., 1985, *Vertical seismic profiling—a measurement that transfers geology to geophysics. In: O.R. Berg and D.G. Woolverton (Eds), 1985, Seismic Stratigraphy II: An Integrated Approach to Hydrocarbon Exploration,AAPG Memoir No. 39, AAPG, Tulsa, pp. 13–34.*